The Synthesis, Coordination Chemistry and Catalytic Applications of Phosphinite, Phosphonite and Phosphite Ligands Containing Perfluoroalkyl Substituents

Thesis submitted for the degree of

Doctor of Philosophy

at the University of Leicester

by

David Gudmunsen BSc

Department of Chemistry

Faculty of Science

University of Leicester

May 2000

UNIVERSITY OF LEICESTER

UMI Number: U601361

UMI
Dissertation Publishing

ProQuest

Statement

The experimental work described in this thesis has been carried out by the author in the Department of Chemistry at the University of Leicester between October 1996 and May 2000. The work has not been submitted, and is not presently being submitted, for any other degree at this or any other university.

Signed: _____ Date: 6/2/01

Department of Chemistry

University of Leicester

University Road

Leicester

U.K.

LE1 7RH

Abstract

A review is presented of the development and application of liquid-liquid biphase systems in homogeneous catalysis and the concept and application of fluorous biphase systems (FBS) in catalysis. Novel monodentate phosphorus(III) ligands of general formula $Ph_xP(OC_6H_4-4-C_6F_{13})_{3-x}$ and $Ph_xP(OC_2H_4C_6F_{13})_{3-x}$ (x = 0, 1 or 2), and the phosphite ligands $P(OC_6H_4-4-C_8F_{17})_3$, $P(OC_6H_4-4-C_{10}F_{21})_3$, $P(OC_6H_4-3-C_6F_{13})_3$ and $P(OC_6H_4-2-C_6F_{13})_3$ have been synthesised and fully characterised by ^1H, ^{19}F and $^{31}P\{^1H\}$ NMR spectroscopy, mass spectrometry and elemental analysis.

The monodentate phosphinite, phosphonite and phosphite ligands (L) have been reacted with a variety of transition metal complexes to form complexes of the type cis- and trans-[MCl_2L_2] (M = Pt, Pd), cis-[$PtCl_2(PEt_3)L$], [$M(\eta^5-C_5Me_5)Cl_2L$] (M = Ir, Rh) and [$RhClL_3$]. The complexes have been isolated and characterised using analytical techniques including ^1H, ^{19}F and $^{31}P\{^1H\}$ NMR spectroscopy, mass spectrometry, IR spectroscopy, X-ray crystallography and elemental analysis. The steric and electronic influences of the perfluoroalkyl substituents on the chemical and physical properties of the metal complexes have been assessed by comparison of their spectroscopic and structural data with that for their related protio complexes.

Preliminary catalytic studies involving $P(OC_6H_4-4-C_6F_{13})_3$ as a modifying ligand in the rhodium-catalysed hydroformylation of 1-hexene and 1-nonene under FBS conditions have been undertaken. The influence of the perfluoroalkyl substituents on the rate of reaction, product selectivity and catalyst/product separation has been examined.

The synthesis of bidentate phosphonite and phosphite ligands containing perfluoroalkyl substituents has been investigated. The derivatised bidentate phosphonite ligands $(C_6F_{13}-4-C_6H_4O)_2PCH_2CH_2P(OC_6H_4-4-C_6F_{13})_2$ and $\{5,5'-(C_6F_{13})_2-2,2'-O_2C_{12}H_6\}PCH_2CH_2P\{2,2'-O_2C_{12}H_6-5,5'-(C_6F_{13})_2\}$ (L-L) have been reacted with transition metal complexes to form coordination complexes of the type [$PtCl_2(L-L)$] and [$Rh(\mu-Cl)(L-L)$]$_2$.

Contents

Chapter 1: Introduction

Chapter 2: Synthesis and Characterisation of

Chapter 3: Coordination Chemistry

Chapter 4: Fluorous Biphase Catalysis

Chapter 5: Synthesis of Bidentate Ligands

Chapter 6: Experimental

List of Abbreviations

δ	Chemical shift
Δ	Heat
ν	Stretching frequency
δE	Energy difference
acac	Acetylacetonate
AIBN	Azo-isobutyronitrile
Ar	Aryl fragment
atm	Atmosphere
BINAS	bis(disulphonatophenylphosphinomethyl)-tetrasulphonatobinaphthalene
BINAPHOS	2-(diphenylphosphino)-1,1'-binaphthalen-2'-yl-1,1'-binaphthalene-2,2'-diyl phosphite
bipy	2,2'-bipyridine
bs	Broad singlet
COD	1,5-Cyclooctadiene
COSY	Correlated spectroscopy
Cp*	Pentamethylcyclopentadienyl
cq	Consequential quartet
ct	Consequential triplet
Cyclam	1,4,7,11-Tetraazacyclotetradecane
d	Doublet
dd	Doublet of doublets
DMAP	1,3-Dimethylaminopyridine
DMF	N,N-Dimethylformamide
DMSO	Dimethylsulphoxide
dm	Doublet of multiplets
dt	Doublet of triplets
dq	Doublet of quartets
E	Energy
EA	Elemental analysis
ee	Enantiomeric excess

EI	Electron impact
ESR	Electron spin resonance
Et	Ethyl
FAB	Fast atom bombardment
FBS	Fluorous biphase systems
GC	Gas chromatography
HOMO	Highest occupied molecular orbital
Hz	Hertz
IR	Infra red
J	Coupling constant
LUMO	Lowest unoccupied molecular orbital
m	Multiplet
Me	Methyl
MHz	Megahertz
MO	Molecular orbital
mp	Melting point
NMR	Nuclear magnetic resonance
PFC	Perfluorocarbon
Ph	Phenyl
PP3	Perfluoro-1,3-dimethylcyclohexane
ppm	Parts per million
q	Quartet
R	Undefined molecular fragment
R_f	Undefined fluorinated molecular fragment
RCH/RP	Ruhrchemie/Rhône-Poulenc
RT	Room temperature
s	Singlet
SHOP	SHELL higher olefin process
t	Triplet
tm	Triplet of multiplets
tt	Triplet of triplets
TACN	1,4,7-Triazacyclononane
tert	Tertiary
THF	Tetrahydrofuran

THMP	Tris(hydroxymethyl)phosphine
TMS	Tetramethylsilane
TOF	Turnover frequency
TPPMS	Triphenylphosphine monosulphonate
TPPTS	Triphenylphosphine trisulphonate

Acknowledgements

Chapter One

1.1 Homogenous and Heterogeneous Catalysis

Modern homogeneous catalysis has its origins in the discovery made by Roelen in 1938 of the hydroformylation of olefins using a soluble cobalt catalyst.[1] This prompted the application of homogeneous catalysis with organometallic compounds on an industrial scale in processes such as hydroformylation, olefin polymerisation and acetaldehyde synthesis. The growth of homogeneous catalysis over the past 35 years has become increasingly rapid and has made a significant impact on the science of organometallic chemistry. Today the field of homogeneous catalysis covers vast areas of research from simple acid-base catalysis to highly complex metalloenzyme catalysis.[2] New knowledge relating to the reactivity and structure of organometallic compounds has led to the creation of new catalytic processes in industry,[3] and to the improvement of existing catalytic systems through modification of the catalyst and reaction conditions.

A homogeneous reaction is one in which all the components of a reaction are present in the same phase. The most conspicuous feature of homogeneous catalysis is that, in general, the catalyst and all other constituents of the reaction are in a single homogeneous liquid phase, i.e. in solution. The catalyst in this type of system is a discrete entity, and, in the case of transition metal catalysis, is a single transition metal complex or a combination of complexes. The hydrogenation of olefins with Wilkinson's catalyst $[ClRh\{PPh_3\}_3]$[4] is an outstanding example of a transition metal complex catalysing a homogeneous reaction and is one of the most extensively studied.[5-7] The triphenylphosphine ligands coordinated to the transition metal confer solubility in organic solvents and also stabilise the metal centre in a variety of oxidation states throughout the course of the reaction. The olefin substrate is added in either a gaseous or liquid state along with H_2 gas, both of which are taken up into solution, to give the catalyst and the reagents in a single liquid phase. The reaction proceeds stepwise via a series of well-defined intermediates involving the formation and dissociation of bonds at the metal centre accompanied by changes in the metal oxidation state. The active catalytic species is a solvated three coordinate Rh(I) complex formed by the dissociation of a triphenylphosphine ligand from the parent compound. The Rh(I) species is coordination deficient and readily undergoes oxidative addition of H_2 to form a Rh(III) dihydride. The dihydride then coordinates

the olefin leading to the formation of an alkyl rhodium hydride by the migratory insertion of the olefin into a rhodium hydrogen bond. The rapid reductive elimination of alkane follows, regenerating the active Rh(I) species.
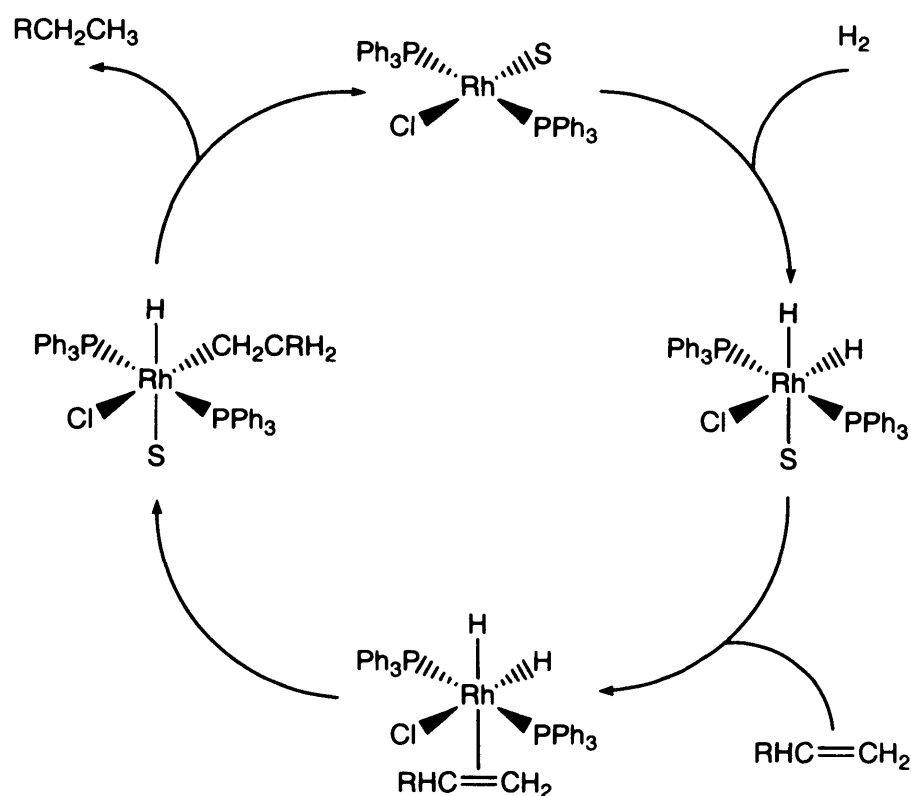
Scheme 1.1 Catalytic cycle for olefin hydrogenation with [ClRh{PPh₃}₃].

The characteristics outlined above differentiate homogeneous catalysis from heterogeneous catalysis in which one or more of the constituents are in different phases. The catalyst is usually present as a solid and the reactants as liquids or, more commonly, as gases for vapour phase reactions. Reactions in heterogeneous catalysis occur at the interface between the two phases, i.e. on the catalyst surface. The majority of industrial heterogeneous catalysts consist of small metal particles ranging from 1-100 nm in size deposited on a porous oxide support with a high surface area, up to 300 m^2 g^{-1}.[8] The catalyst is usually prepared by conventional techniques such as impregnation or coprecipitation from solution which do not give precise control over particle size, shape and inter-particle distance. The hydrogenation of ethylene on a

platinum surface is one of the simplest examples of heterogeneous catalysis.[9] Ethylene and dihydrogen in the gas phase are adsorbed on to the surface of a platinum catalyst where ethylene is hydrogenated stepwise by hydrogen atoms to form ethane. The product of the reaction is then desorbed from the metal surface and enters the gas phase.

Homogeneous catalyst systems can be easily analysed by nuclear magnetic resonance (NMR), electron spin resonance (ESR) and infra-red (IR) spectroscopies, and the structures of the metal complex (pre)catalysts can be determined by the use of X-ray crystallography. In addition, techniques such as NMR and IR spectroscopy can be used *in situ* to trace the course of a catalytic cycle allowing the elucidation of reaction mechanisms.[10,11] Heterogeneous systems are much harder to analyse and, as such, are less well understood in mechanistic terms, although developments in modern surface science have gone some way to bridging this gap by enabling researchers to investigate heterogeneous systems at the molecular level.[12] The ease with which homogeneous systems can be analysed remains a key difference between the two systems, and is the major advantage of homogeneous catalysis. The normally well-defined structures and structural variability of homogeneous catalysts means that tailoring of the steric and electronic properties of catalysts is possible, resulting in catalysts which have a far greater selectivity than heterogeneous catalysts. This flexibility allows catalysts to be designed in a rational manner to give excellent product selectivity making them ideal for the synthesis of fine chemicals and pharmaceuticals.[13]

Homogeneous and heterogeneous catalysis both have their own strengths and weaknesses. The bulk nature of classical heterogeneous catalytic systems gives rise to catalysts with a far higher thermal stability than homogeneous catalysts which tend to undergo decomposition at temperatures greater than 200 °C. Thus, reactions can be run under more forcing thermal conditions giving rise to faster reaction rates, in comparison to that for homogeneous systems, with equal activity. In both heterogeneous and homogeneous catalysis a given reaction is catalysed by a particular site or combination of sites in a catalyst system. In a solid state catalyst there are often many different sites but, possibly, only one type of which catalyses the desired reaction whilst the other sites are either inactive or give rise to undesired catalysed

side reactions. In a homogeneous system there is, in general, only one catalytically active site, resulting in higher activity per metal centre than heterogeneous catalysts.

The solid state nature of heterogeneous catalyst systems is of great advantage in view of the ease with which the catalyst can be recovered after reaction. Assuming that the reaction products are liquids or gases, the catalyst either remains in the solid bed of the reactor, or can be recovered from a suspension by filtration or centrifugation for recycling. These are cheap and efficient processes compared to the expensive and difficult nature of methods employed in the case of homogeneous catalysis, which has relied heavily on advances made in process technology for strategies of catalyst-product separation. The use of transition metals, particularly precious metals, and the employment of increasingly sophisticated and expensive ligands make separation and reuse of the catalyst a necessity.

1.2 Catalyst Immobilisation

Homogeneous catalysis with organometallic catalysts offers great advantages over heterogeneous catalysis through greater activity, chemoselectivity, regioselectivity and stereoselectivity. However, its major disadvantage is the problem of catalyst recovery, which is seen as the "Achilles heel" of homogeneous catalysis. Much research in recent years has involved the design of hybrid catalysts incorporating features of both homogeneous and heterogeneous systems. This has led to the development of catalysts which retain the concept of a well-defined metal complex (incorporating specific ligands) of low-nuclearity which are at the same time immobilised for simple recovery. This "heterogenisation" of homogeneous catalysis has resulted in catalysts tethered to solid supports and those which have been immobilised in a second liquid phase, which have given rise to the aqueous/organic and fluorous/organic biphase approaches to catalysis.

1.3 Supported Catalysts

Since the 1960s, intensive research has focused on achieving industrially competitive homogeneous catalysts by overcoming the problems of catalyst-product separation commonly associated with homogeneous systems. One approach has been the attachment of metal complex catalysts to polymeric, organic or inorganic, supports.[14] Here, metal complexes with well-defined stereoelectronic properties are fixed to a suitably functionalised solid support, with control and knowledge of the immobilised species being retained. Fixation to the support is most commonly achieved via donor ligands anchored to the support, although this can also be achieved through ionic bonding, and by chemisorbtion and physisorbtion. The most frequently used organic supports are polystyrene and styrene-divinylbenzene bearing functional groups such as tertiary phosphines or amines. One of the simplest and most commonly used methods of attaching the metal complex to the support is the displacement of a coordinated ligand by a polymer-bound ligand (Scheme 1.2).

$$\text{P} \cdots \text{—PPh}_2 \quad \xrightarrow[\text{- PPh}_3]{\text{RhCl(PPh}_3)_3} \quad \text{P} \cdots \text{—(PPh}_2)\text{RhCl(PPh}_3)_2$$
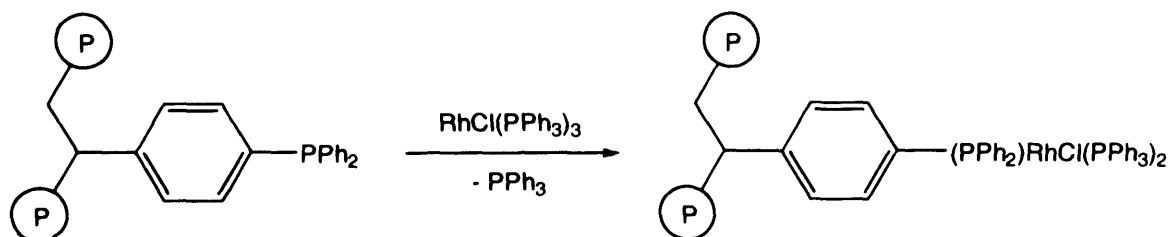
Scheme 1.2 Fixation of metal catalyst to a polymer support.

The catalytic performance of the tethered metal complex can be influenced by the nature of the polymer support, which can be altered by structural changes, variation in the density of the donor groups within the polymer, and changes in the flexibility of the organic chain. The flexibility of the polymer can be limited by the introduction of a cross-linking agent in order to prevent undesired interactions between functional groups. Initial research into catalyst immobilisation using this technique was concerned with insoluble supports in which only the catalytic sites were soluble in the reaction media. Reaction at the metal centre is essentially

homogeneous, however, the insolubility of the polymer support allows recovery of the catalyst by simple filtration. This work was extended to include soluble polymer supports by Bayer et al.[15] and Bergbreiter[16] to overcome problems associated with diffusion limitations. Reactions involving soluble polymer-supported catalysts occur homogeneously and the high molecular-weight complex is separated by membrane filtration or by precipitation, following a change of temperature or the addition of a non-solvent, and subsequent filtration.

Numerous catalytic studies involving supported catalysts have been undertaken, covering in particular hydrogenation, hydroformylation and oligomerisation.[1] Investigations by Pittman et al. with polymer supported hydroformylation catalysts showed greater selectivity towards the linear (n) aldehyde than the branched (i) aldehyde using [RhH(CO)(PPh$_3$)$_3$] bound to a polystyrene support than the homogeneous analogue in the hydroformylation of 1-pentene (Scheme 1.3).[17]
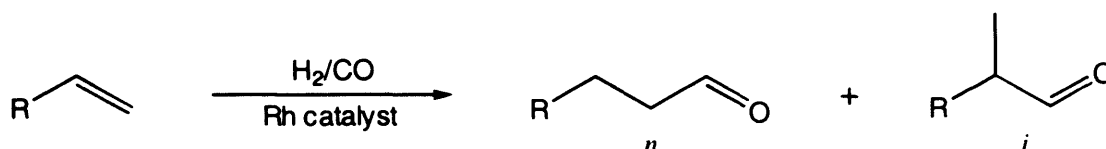
Scheme 1.3 Rhodium catalysed hydroformylation of 1-pentene (R = C$_3$H$_7$).

Ackerman et al. have used rhodium complexes coordinated to resin-anchored chiral phosphines, such as DIOP, for the asymmetric hydroformylation of styrene.[18] Complete selectivity to aldehydes was observed, however, only moderate ee's were obtained and in no case was it possible to duplicate optical yields achieved under homogeneous conditions quoted in the literature. Immobilised palladium catalysts, synthesised by Dinjus et al., have been used to catalyse C-C coupling reactions of carbon dioxide with dienes.[19] The reaction of 1,3-butadiene with CO$_2$ is catalysed by the polymer-supported palladium complex in THF to form the δ-lactone, 2-ethylidene-6-heptene-5-olid, with up to 72% selectivity (Scheme 1.4). The polystyrene support is not soluble in the solvent in which the reaction is carried out and so the catalyst is recovered after reaction by filtration.
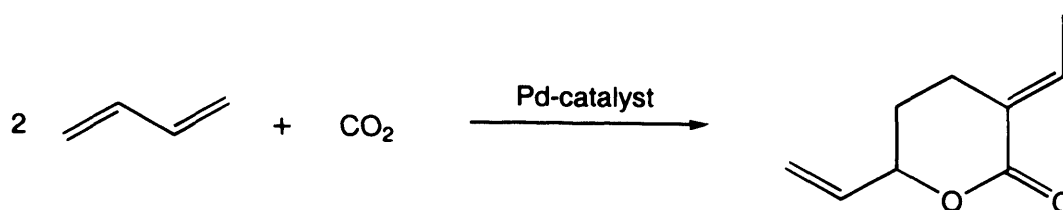
Scheme 1.4 Co-oligomerisation of 1,3-butadiene and CO_2 with an immobilised Pd-catalyst.

In contrast to the work of Dinjus *et al.*, Bergbreiter *et al.* have used a soluble polymer as a support for a rhodium catalyst in the cyclopropanation of functionalised olefins (Scheme 1.5).[20] Reactions were carried out in toluene at 100 °C in which the catalyst support was soluble, whence reactions proceeded in a single homogeneous phase. The solubility of the polymer in toluene was found to be highly temperature dependent, and it precipitated out of solution on cooling the reaction mixture to 25 °C, allowing catalyst/product separation to be achieved by filtration.
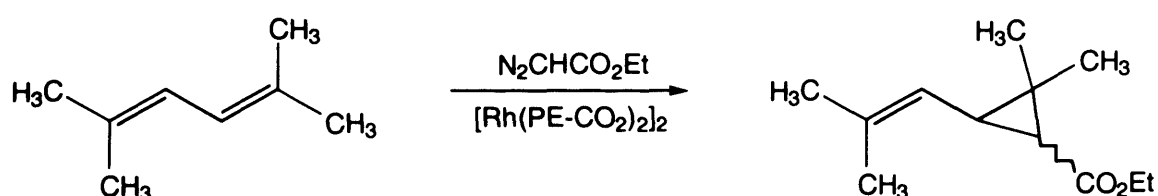
Scheme 1.5 Cyclopropanation of functionalised olefins with a soluble polymer-supported rhodium catalyst.

Recently, Bianchini *et al.* have used tripodal polyphosphine rhodium catalysts immobilised via hydrogen bonding to silica for the hydroformylation of 1-hexene.[21] Reactions were carried out in *i*-octene in which the silica support was completely insoluble, however, the reactions gave only moderate regioselectivity with no appreciable *n/i* ratio.

1.4 Concept of Biphase Catalysis

In a biphasic system employed in homogeneous catalysis two distinct phases exist with the catalyst and the reaction products in different phases, thereby allowing facile catalyst/product separation by decantation. The strict definition of a biphasic system is one in which no additional measures are used to ensure phase separation, such as the introduction of non-solvents or chemical derivatisation of the catalyst or products after reaction. The start of a new catalytic cycle must also be possible without any additional steps. This differentiates biphasic catalysis, in which the catalytic conversion occurs in the biphase from processes which contain biphasic steps, for example the extraction of a catalyst with water subsequent to a homogeneous reaction. A number of variations of the two phase process in which all the starting materials are in solution can be considered. In the simplest case, the catalyst and the reaction substrates and products have such widely differing solubilities that the two liquid phases used provide perfect phase separation. The most technically ideal process would involve a catalyst which formed its own phase in which the substrates and products had no solubility whatsoever. Another possibility is the formation of a biphasic system from a single phase during the course of the reaction as a result of the insolubility of the reaction product in the reaction medium containing the catalyst and substrates, as is the case in the SHELL Higher Olefin Process (SHOP).[22,23]

The SHOP process developed by Keim *et al.* for the polymerisation of olefins, became the first liquid/liquid two-phase catalytic process to be realised industrially. Typically, an organonickel catalyst formed *in situ* from [Ni(1,5-cod)$_2$] and a ligand such as Ph$_2$PCH$_2$COOH (which chelates through phosphorus and oxygen) is used to polymerise ethylene at 80-120 °C and 70-140 bar in a solution of 1,4-butanediol. The reaction products, consisting mainly of linear C$_4$-C$_{20}$ α-olefins, are immiscible with the polar reaction medium and separate as a second liquid phase above the 1,4-butanediol and can be removed by decantation. Traces of catalyst in the product phase are removed by washing with solvent in a second separation step and returned to the oligomerisation reactor.

1.5 Aqueous/Organic Biphasic Catalysis

The introduction of aqueous two-phase catalysis represents one of the most important developments in homogeneous catalysis in recent years. This method employs a well-defined homogeneous catalyst which is exclusively soluble in the aqueous phase, which acts as a mobile phase or mobile support. The catalyst is, therefore, immobilised (although not anchored as in section 1.3) in relation to the reaction products which reside in the organic phase. Thus, the manifold advantages of homogeneous catalysis are combined with the ease of catalyst/product separation which can be achieved by simple phase separation. Costly and inefficient separation techniques such as distillation are avoided, allowing quantitative recovery of the catalyst with no loss of activity through thermal degradation.

Transition metal catalysts can be rendered soluble in the aqueous phase by complexation with water-soluble ligands. These ligands are often phosphine ligands bearing polar substituents, including sulphonate, carboxylate, ammonium, phosphonium and hydroxyl groups. One of the earliest investigations of water-soluble phosphines was undertaken by Mann *et al.* who prepared ligands such as (1.1) containing carboxylic groups.[24] This work was further investigated by Issleib *et al.*[25,26] with the development of new carboxyalkylphosphines and by Podlaha and Podlahová who prepared the ethylenediaminetetraacetic acid derivative (1.2).[27]

(1.1)   (1.2)
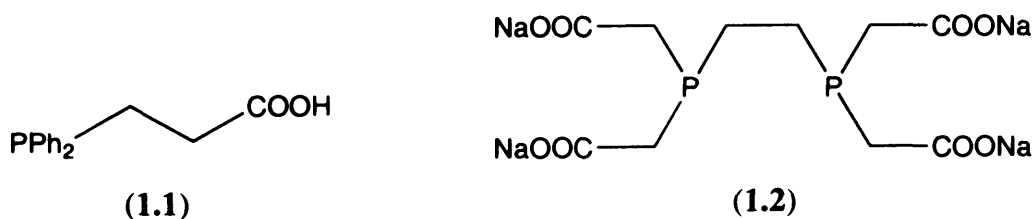
Phosphines bearing hydroxyl functions first investigated by Chatt *et al.*[28] were found to be water-soluble providing the ligand carried several hydroxyl groups, an example being the tris(hydroxymethyl)phosphine, $P(CH_2OH)_3$ (THMP). Recently, the efficiency of THMP complexes of Pt, Pd and Ni in the catalytic hydrophosphination of formaldehyde has been demonstrated by Pringle and co-workers.[29] Water-soluble Ir

and Rh complexes with THMP have been used by Fukuoka et $al.$ for the selective hydrogenation of the C=O bond of cinnamaldehyde and for the hydroformylation of pent-1-ene under biphasic conditions.[30]

Ligands such as (1.3) containing polyether chains in which $n \geq 16$ were found to have excellent water solubility.[31] This approach to water-soluble phosphines was developed further by Iwahara et $al.$ with the synthesis of phosphines substituted with crown ethers.[32] The analogue of (1.1) prepared by Baird and Smith in which the carboxylic function is replaced with a quaternized aminoalkyl group, "amphos" (1.4), was also found to be water-soluble.[33] This class of ligands has been extended by Peiffer et $al.$[34] and Hansen and Tóth[35] to include phosphines containing quaternized aminoaryl groups.

(1.3)   (1.4)
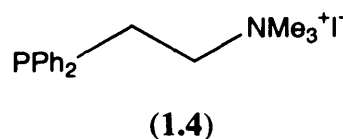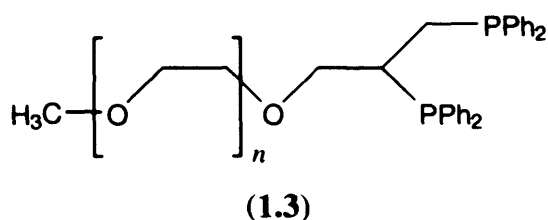
Sulphonated phosphines are presently the most widely used class of ligands in aqueous/organic biphase catalysis and include mono-, bi-dentate, and chiral ligands (Scheme 1.6). In the case of water-soluble ligands of type $R_{3-n}P(C_6H_4\text{-}4\text{-}SO_3K)_n$, the sulphonate group can be introduced during the synthesis of the phosphine by the reaction of the potassium salt of 4-fluorobenzenesulphonate with phosphines of general formula $Ph_{3-n}PH_n$ in DMSO/KOH.[36] Triphenylphosphine monosulphonate (TPPMS) (1.5) and triphenylphosphine trisulphonate (TPPTS) (1.6) are both obtained by direct sulphonation of triphenylphosphine with oleum (20% SO_3 in H_2SO_4) followed by neutralisation with NaOH.[37] The introduction of sulphonate groups is not limited to aryl phosphines, as demonstrated by Feitler et $al.$[38] who synthesised the first phosphines bearing sulphonated side chains. The phosphine $Ph_2PCH_2CH_2SO_3Na$ has since been prepared by Ganguiy et $al.$[39] by the reaction of sodium diphenylphosphide with the sodium salt of 2-bromoethylsulphonic acid.

(1.5)

(1.6)

Ar_2P ～～ PAr_2

(1.7)

(1.8)
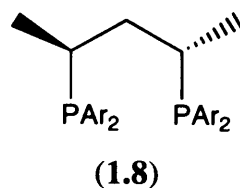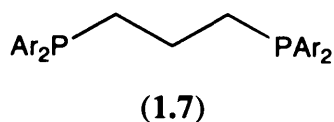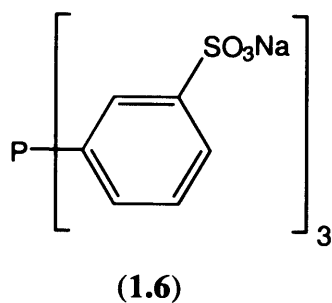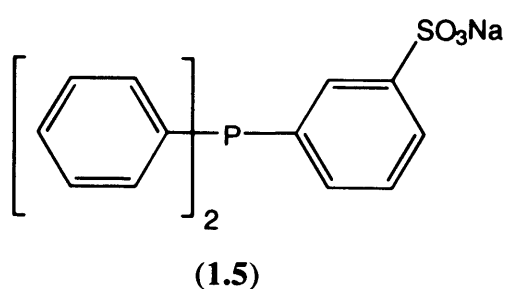
Scheme 1.6 Water-soluble phosphines containing sulphonate functions (Ar = C_6H_4-3-SO_3Na).

The potential of aqueous/organic biphase catalysis was first realised by Kuntz et al.[40] in the development of rhodium complexes with TPPTS ligands as hydroformylation catalysts, a system which was rapidly transformed into a sophisticated industrial process by Ruhrchemie AG.[41] Collaboration between Ruhrchemie and Rhône-Poulenc led to the commercialisation of the process for the hydroformylation of propene which went in to operation in 1984. The current capacity of n-butyraldehyde production using the Ruhrchemie/Rhône-Poulenc (RCH/RP) process is over 300,000 tons per annum with additional units for the production of n-pentanal from n-butene brought onstream in 1995.[42]

The concept of aqueous/organic biphase catalysis has now been applied to a broad range of reactions, one of the earliest being the hydrogenation of CC- and OC-unsaturated compounds with water-soluble rhodium and ruthenium catalysts containing TPPMS ligands.[43,44] The selective reduction of α,β-unsaturated aldehydes to alcohols under biphasic conditions has been demonstrated by Allmang et al.[45] using a ruthenium-TPPMS catalyst to reduce 3-methyl-2-butenal to 3-methyl-2-buten-1-ol with 96 % selectivity (Scheme 1.7). Recently, Mudalige and Rempel employed the novel water-soluble complex [RhCl(Ph₂P(CH₂)₅CO₂Na)₂]₂ as a catalyst for the hydrogenation of polybutadiene, styrene-butadiene, and nitrile-butadiene polymers.[46]
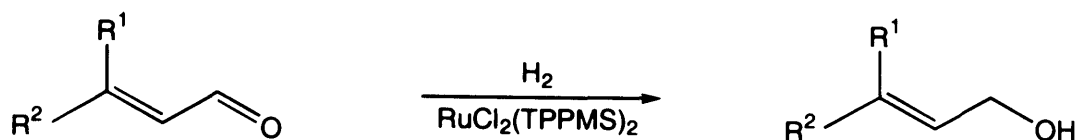
Scheme 1.7 Hydrogenation of an α,β-unsaturated aldehyde ($R^1 = R^2 = CH_3$) with a water-soluble ruthenium catalyst.

Beller and Tafesh[47] disclosed the first selective reduction of aromatic nitro compounds to amines in the presence of other functional groups such as ketone, nitrile and chloride under aqueous biphase conditions. A TPPTS complex of palladium was used as the catalyst for the CO reduction of the nitro group to a nitrene which is converted to an amine by abstracting a proton from water (Scheme 1.8). Good product separation was achieved with this system as the catalyst has a high solubility in water, whereas the product remains in the organic phase.
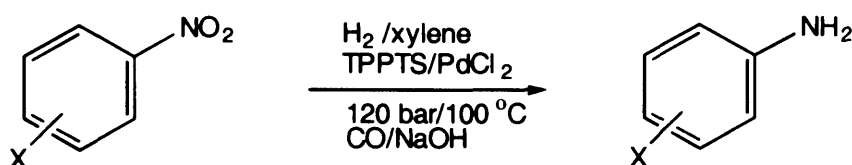
Scheme 1.8 Reduction of aromatic nitro compounds. $X = C=CH_2$, $COCH_3$, CN, Cl.

The aqueous two-phase approach to catalysis has also been applied to a variety of C-C coupling reactions including alkylation of CH-acidic compounds, hydrodimerisation of dienes, carbonylation of allylic compounds and addition reactions to the C=C bond including hydroformylation, hydroamination and hydrocyanation. Suzuki-type cross coupling reactions of boronic acids or esters with alkenyl iodides using a water-soluble palladium catalyst have been investigated by Blart et al.[48] (Scheme 1.9). The advantages offered by this methodology are that reaction occurs under mild conditions allowing the preparation of fragile α,β-unsaturated esters, the reaction exhibits versatility in the substrates which can be coupled, and that the water-soluble catalyst is easily separated after reaction.

B(OH)$_2$

$+$

I

OMe

$\xrightarrow[\text{Pd(OAc)}_2/\text{TPPTS}]{\text{K}_2\text{CO}_3}$

OMe
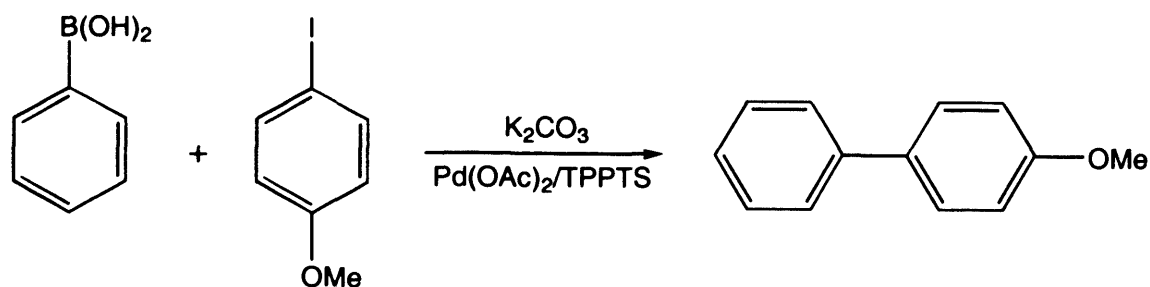
Scheme 1.9 Cross-coupling of phenylboronic acid with 4-iodoanisole.

Catalysis under aqueous/organic biphase conditions undoubtedly offers the advantages of catalyst/product separation found in heterogeneous systems to homogeneous reactions. Undertaking reactions employing a system which includes an aqueous phase is, however, not without its disadvantages in comparison to reactions carried out in an organic monophase. The most obvious drawback is that hydrolytically-sensitive substrates and catalysts are not compatible with this methodology. The hydroformylation of olefins, currently the largest industrial application of aqueous biphase catalysis, has been found to proceed at higher rates and with greater chemo- and regio-selectivity when phosphites are used in place of phosphines as the modifying ligands of the transition-metal catalysts. However, phosphites are notoriously sensitive towards hydrolysis and are, therefore, impractical for use in aqueous/organic biphase systems. Despite the development of water-soluble phosphites such as P[OC$_6$H$_4$-4-SO$_3$\{NH(i-C$_8$H$_{17}$)$_3$\}]$_3$, which have greater resistance towards hydrolysis than triphenyl phosphite, rapid decomposition of the ligand in the presence of water still occurred.[49]

The limited solubility of substrates in the aqueous phase, particularly higher olefins (>C$_8$), can result in a dramatic reduction in the rate of reaction when performed in an aqueous/organic two-phase system. If the reaction occurs in the aqueous phase and the substrate has a low solubility in water then the rate of reaction will be limited by mass transfer.[50] In particular the hydroformylation of higher olefins or functionally-substituted olefins is much more difficult although, ironically, it is these types of reaction which would gain the greatest benefit from the simplification

of reaction sequences and the reduction in costs associated with catalyst recovery offered by biphasic catalysis. Attempts to overcome this problem have involved variation of the organic solvent, the addition of surfactants, and the use of co-solvents to improve the miscibility of the substrate with the aqueous phase. Researchers at Johnson Matthey, investigating the hydroformylation of 1-dodecene under aqueous biphase conditions, found that acceptable reaction rates could only be achieved by the use of amphiphilic additives in high concentrations.[51] Despite this work, and research by Fell *et al.* into catalysts which become soluble in the organic phase only at high temperatures (allowing reaction to occur in the organic phase),[52] no commercial procedure currently exists for the hydroformylation of long-chain olefins using an aqueous/organic biphase process.

Asymmetric catalysis involving the use of expensive chiral reagents is another area of chemistry which would be expected to benefit from a system in which the catalyst could be easily separated from the reaction products and recycled. With this in mind the enantioselective hydrogenation and hydroformylation of prochiral substrates under aqueous/organic biphase conditions have been extensively investigated. The asymmetric hydroformylation of styrene has been studied by Hermann and Kohlpainter using a water-soluble rhodium catalyst bearing bis(disulphonatophenylphosphinomethyl)tetrasulphonatobinaphthene (BINAS) (1.9) as a chiral auxiliary ligand.[53] Limited enantioselectivity was observed using a methanol-water/toluene biphase with an enantiomeric excess (ee) of only 18% obtained. Similarly poor ee's have been observed for the hydrogenation of prochiral olefins under aqueous biphase conditions,[54,55] however, the reduction of prochiral α-acetamidoacrylic esters and α-acetamidocinnamic esters is a notable exception with ee's of up to 91% reported.[56,57]
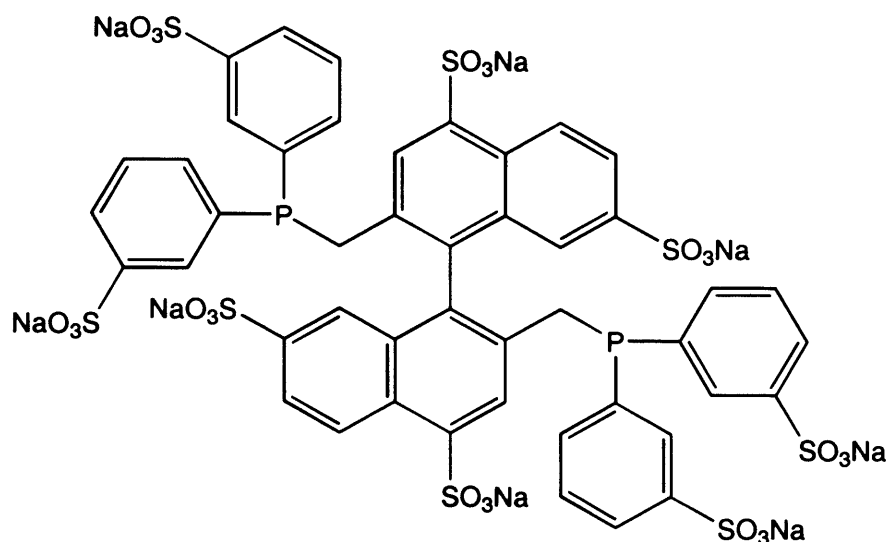
(1.9)

An explanation for the low enantioselectivities observed in the hydrogenation of prochiral substrates under aqueous biphase conditions has been postulated by Amrani and Sinou.[54] The chiral catalyst can form two diastereomeric adducts with the substrate which can then undergo oxidative addition of H_2, the rate of reaction depending upon the energy of the catalyst-substrate adduct. The energy content of these intermediate species and, hence, the energy difference between them can be influenced by solvation, a small energy difference resulting in poor enantioselectivity. It is believed that solvation with water results in a small energy gap and, therefore, low ee's are obtained. The limitations of the aqueous/organic biphase have led researchers to examine the possibilities of immobilising the catalyst in a nonaqueous phase which has sufficiently different intermolecular forces to the organic phase to form a liquid-liquid biphase system. A major advance in this area, which promises to overcome many of the problems associated with catalysis involving an aqueous phase, has been the development of fluorous biphase systems in which water has been replaced with perfluorocarbon solvents.

1.6 Fluorous Biphase Systems

Perfluorinated hydrocarbons are chemically inert compounds which have higher densities and viscosities and lower refractive indexes and surface tensions than their perprotio analogues.[58] Perfluoroalkanes exhibit low tendencies towards van der Waals interactions and, as a result, are exceptionally good at solubilising gases such as dioxygen, carbon dioxide, hydrogen and nitrogen. The non-toxic nature of perfluorocarbons[59] (PFCs) and the ability to solubilise large quantities of oxygen has been exploited in their use as artificial blood substitutes.[60] 3 M Corporation produce a blood substitute which contains FC-47®, which is composed mainly of perfluoro-tri-*n*-butylamine and a polyethylene oxide/polypropylene oxide block polymer called Pluronic F-68® which is used as a surfactant. The solubility of PFCs in common organic solvents is often greatly reduced in comparison to their hydrocarbon analogues and in many cases biphasic systems are generated. Phase diagrams for mixtures of PFCs and organic solvents are characterised by strong deviations from Raoult's law with an abrupt increase in miscibility with increasing temperature.

The use of a fluorous phase for the immobilisation of homogeneous catalysts was first envisaged by Vogt and outlined in his Ph.D. thesis in 1991 with an emphasis on alkene oligomerisation and the hydroformylation of olefins.[61] Horváth and Rábai published the first, archival, paper describing the application of a fluorous phase in biphasic catalysis in 1994 in which they introduced the concept of fluorous biphase systems (FBS).[62] The FBS consists of a fluorous phase containing a dissolved reagent or catalyst and a second phase, organic or aqueous, containing a dissolved substrate, which has limited solubility in the fluorous phase. The fluorocarbon phase is defined as the fluorocarbon rich phase, normally a perfluorinated solvent. The catalyst must be preferentially soluble in the fluorocarbon phase, and can be rendered such by functionalisation with fluorocarbon moieties. Catalysis in FBS can operate either at the interface between the two phases, or in the fluorous phase, depending on the solubility of the substrate in the perfluorinated solvent. Phase transfer agents may also be employed, as is often the case with aqueous biphase catalysis, to facilitate the movement of reactants from the organic phase to the fluorous phase.

In their initial publication, Horváth and Rábai demonstrated the potential of FBS by performing the hydroformylation of 1-octene and 1-decene under fluorous

biphase conditions.[63] The reactions were carried out at 100 °C and 10 bar of H_2/CO in a two-phase system consisting of perfluoromethylcyclohexane as the fluorous phase, containing a fluorous-soluble rhodium catalyst, and toluene as the organic phase, containing the dissolved substrate. The catalyst, in this case $[HRh(CO)\{P(C_2H_4C_6F_{13})_3\}_3]$, generated *in situ* from $[Rh(CO)_2(acac)]$ and $P(C_2H_4C_6F_{13})_3$, is rendered soluble in the fluorous phase by the inclusion of highly fluorophilic perfluoroalkyl groups in the phosphine ligand. A GC analysis of the organic phase from the hydroformylation of 1-octene after 24 hours revealed 85 % conversion to nonanals with an *n/i* ratio of 2.9. A clean autoclave was subsequently charged with the organic phase from this reaction and a solution of 1-octene in toluene and placed under hydroformylation conditions. Only trace amounts of 1-octene conversion were detected, demonstrating that leaching of catalytically active rhodium species into the organic phase had not occurred. The hydroformylation of 1-decene with the same catalyst was further investigated by Horváth and co-workers to elucidate the kinetic parameters of the reaction with the fluorous-derivatised complex in comparison to a homogeneous system with triphenylphosphine as the modifying ligand.[63] Similar selectivities were observed for both systems, however the activity of the fluorous catalyst was found to be an order of magnitude lower than that of the PPh_3 modified complex. The loss of Rh/mol of product(s) due to leaching was determined to be 1.18 ppm over 9 consecutive reaction cycles, as a consequence of the extremely low solubility of the catalyst in the organic phase. The autoclave used by Horváth and Rábai did not contain a window, thus preventing the reaction from being monitored visually. It is believed, however, that the solvent systems used give rise to a single phase under the high temperatures and pressures employed in the catalytic reactions.

Following the success of the FBS approach to hydroformylation, Horváth attempted the rhodium-catalysed hydroboration of alkenes under fluorous biphase conditions using a fluorous analogue of Wilkinson's catalyst, $[RhCl(P[C_2H_4C_6F_{13}]_3)_3]$ (Scheme 1.10).[64] Complexes currently employed in the transition metal catalysed hydroboration of alkenes such as $[RhCl(PPh_3)_3]$, $[PdCl_2(PPh_3)_2]$ and $[Cp_2Ti(CO)_2]$ are destroyed under the conditions used for the subsequent oxidation to the desired alcohol products $(H_2O_2/NaOH)$.[65,66] The advantage of using a fluorous-modified complex in a biphasic system would be the ease with which it could be removed prior

to the oxidation step and, thence, recycled. Reactions were carried out at 40 °C using a solution of perfluoromethylcyclohexane as the fluorous phase, containing the dissolved catalyst, and catecholborane as the second phase. Exploratory runs with solvent mixtures of $CF_3C_6F_{11}$/THF or toluene were successful, however, improved reaction rates were observed in the absence of organic solvent. It was found that [RhCl(PPh$_3$)$_3$] catalysed the reaction of norbornene and catecholborane under homogeneous conditions in C_6D_6 at a faster rate than the fluorous analogue, which may be due to mechanical differences between the two systems. Reaction under fluorous biphase conditions did not proceed homogeneously, therefore, there is some debate as to whether catalysis occurred in the fluorous phase or interfacially, resulting in a reduction in rate. Recent work by the same group concerning the hydroboration of alkenes and alkynes using the same catalyst, in a biphasic system consisting of toluene and perfluoromethylcyclohexane, gave alcohols which were isolated in yields of 77-92%.[67] The fluorous phase was recycled and used in three consecutive reaction cycles without any notable loss of activity. Atomic absorption analyses of the organic phase showed extremely low catalyst losses, corresponding to 2.2-4.5 ppm rhodium per mole of addition product.
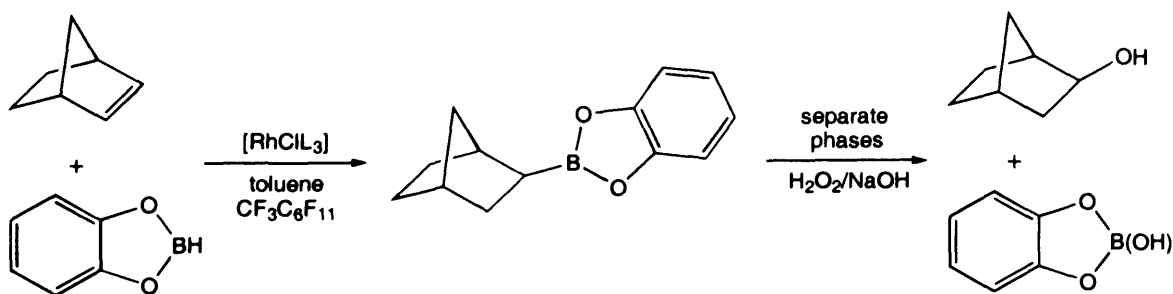
Scheme 1.10   Rhodium catalysed hydroboration in a fluorous biphase system.

Horváth *et al.* have also applied the principle of FBS to the rhodium-catalysed hydrogenation of alkenes.[68] The Wilkinson's analogue [RhCl{P(C$_2$H$_4$C$_6$F$_{13}$)$_3$}$_3$] was used to catalyse the hydrogenation of 2-cyclohexen-1-one, 1-dodecene, cyclododecene and 4-bromostyrene in a toluene/perfluoromethylcyclohexane biphase. Reactions were carried out under 1 atmosphere of H$_2$ at 45°C forming cyclohexanone,

dodecane, cyclododecane and 4-bromoethylbenzene. Overall yields of 87-98% were determined by GC analysis of the separated organic phase combined with toluene extractions of the perfluoromethylcyclohexane phase to remove traces of organics dissolved in the fluorous solvent. No significant loss of catalyst activity was observed over three consecutive reaction cycles. The hydrogenation of alkenes under fluorous biphase conditions has been extensively investigated by Paige *et al.*, who also used fluorous-soluble analogues of Wilkinson's catalyst in the hydrogenation of styrene.[69] The reactions were carried out at 63.5°C under 1 atmosphere of H_2 in a mixture of toluene and hexane as the organic phase, in which the styrene substrate was dissolved, and PP3 as the fluorous phase. The catalysts were prepared *in situ* by the reaction of $[RhCl(C_2H_4)_2]_2$ with the derivatised ligands $P(C_2H_4C_6F_{13})_3$, $P(C_6H_4\text{-}4\text{-}C_6F_{13})_3$ or $P(C_6H_4\text{-}3\text{-}C_6F_{13})_3$. Complete retention of the rhodium complexes in the fluorous phase was observed and no loss of activity occurred on reuse of the recycled catalyst. Reduced rates of reaction were observed when the perfluorinated phosphines were used as modifying ligands in comparison to experiments performed using triethyl- and triphenylphosphine. It was suggested that the lower activity arose from the electron withdrawing effect of the perfluoroalkyl chains lowering the electron-density at the metal centre.

Following the disclosure of the FBS concept by Horváth and Rábai several research groups undertook studies into the synthesis of fluorous-soluble macrocycles compatible with FBS. Pozzi and co-workers investigated the synthesis of perfluoroalkylated metallic complexes of tetraarylporphyrins for the catalysis of a range of oxidation reactions. Fluorophilic C_7F_{15} residues were successfully incorporated by linking the perfluoroalkyl chains, via amido bonds, to a series of amino-tetraarylporphyrins.[70] Ligands (1.10) and (1.11) (Figure 1.1) and their corresponding Mn(III) complexes were prepared using this synthetic strategy. The introduction of four perfluoroalkyl groups resulted in a decrease in the solubility of the porphyrins in organic solvents but was not sufficient to confer solubility in perfluorocarbons. It was hypothesised that the presence of the amido linkages may be inhibiting perfluorocarbon solubility and so porphyrins (1.12-1.15) bearing four C_8F_{17} chains directly bound to the *meso*-aryl ring were synthesised.[71]
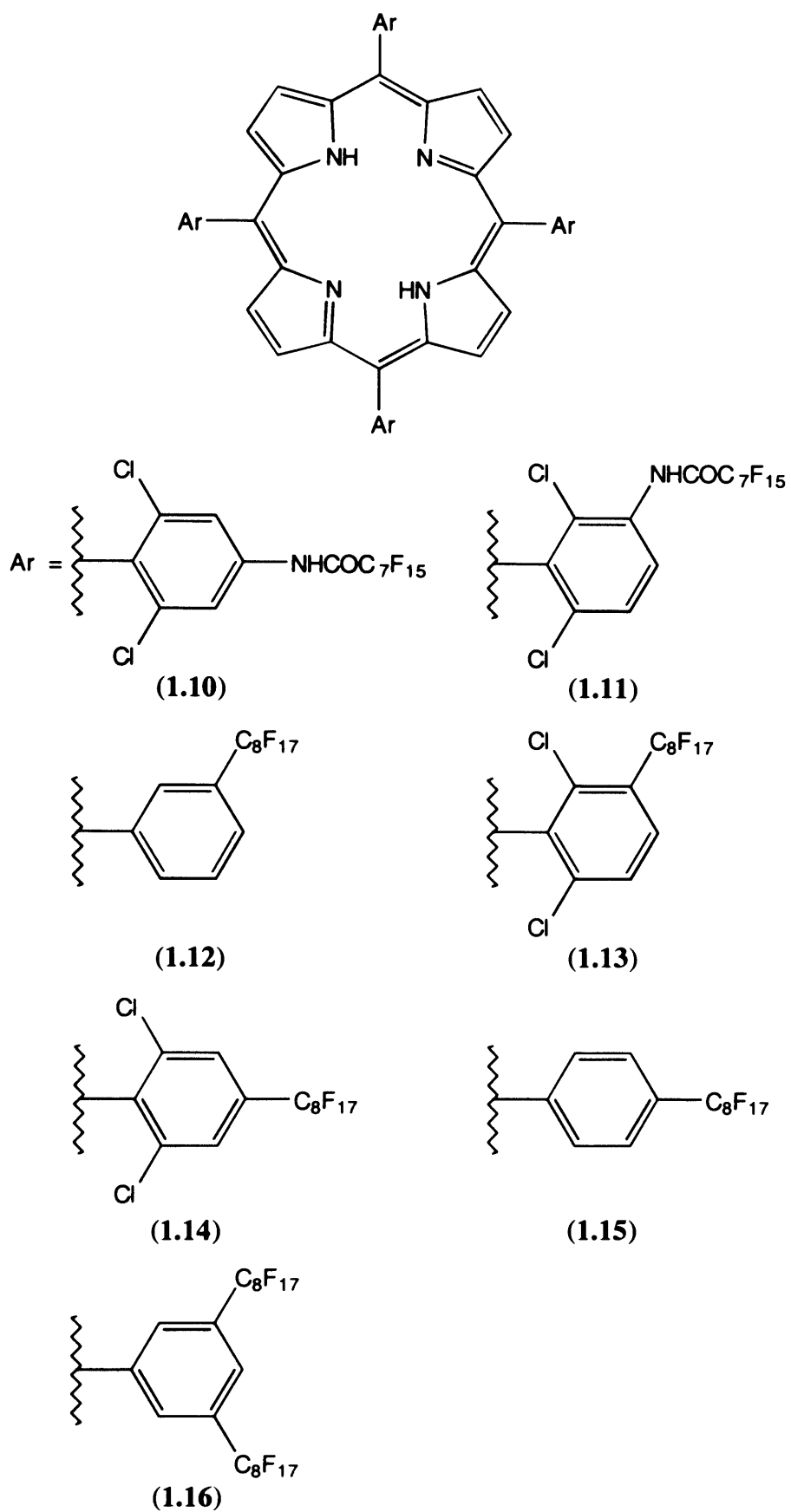
Figure 1.1 Perfluorinated chain derivatised tetraarylporphyrins.

Porphyrins (**1.12-1.15**) shown in Figure 1.1 were also found to be insoluble in perfluorocarbon solvents, demonstrating the difficulty in foreseeing the solubility of molecules containing fluorophilic groups. The introduction of eight C_8F_{17} chains led to the perfluorocarbon solubility of the tetraarylporphyrin (**1.16**),[72] synthesised by the condensation of a fluorous-derivatised pyrrole according to the procedure developed by Kuroda and Ogoshi.[73] The perfluorocarbon-soluble cobalt complex of porphyrin (**1.16**) was found to be an efficient catalyst for the epoxidation of alkenes in a biphasic system consisting of perfluorohexane and acetonitrile in the presence of O_2 and 2-methylpropanal as a reducing agent. The epoxidation of cyclic substrates such as *cis*-cyclooctene at 25 °C was achieved in yields up to 95% at a low catalyst loading of 0.1 mol% with respect to substrate. Recycling of the fluorous phase containing the dissolved catalyst resulted in no discernible decrease in activity.

The scope of macrocyclic ligands compatible with the FBS concept has been widened by the independent synthesis of fluorous-soluble polyazamacrocycles by both Pozzi *et al.*[74] and Fish *et al.*[75] The tetraazacyclotetradecane derivative (**1.17**) prepared by Pozzi *et al.* was synthesised by the reaction of 1,4,8,11-tetraazacyclotetradecane (cyclam) with $R_fCH_2O(CH_2)_2OTs$ in refluxing acetonitrile in the presence of Na_2CO_3. The $CH_2OC_2H_4$ spacer insulates the nitrogen from the electron withdrawing effect of the perfluorooxyalkyl group and prevents elimination reactions from occurring during the reaction of the tosylate with cyclam.

R_f = ——$CF_2(OCFCF_2)_q(OCF_2)_pOCF_3$ p = 3.38
              | q = 0.11
              CF_3
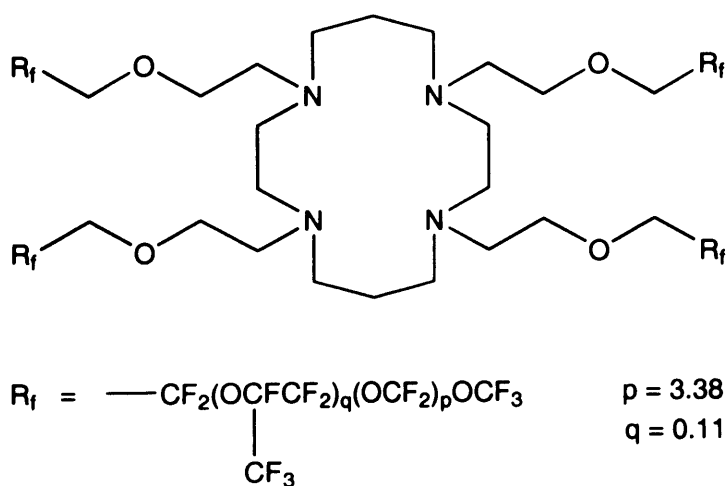
(**1.17**)

The catalytic oxidation of cyclooctane and cyclohexane (Scheme 1.11) were carried out under biphasic conditions with perfluorohexane as the fluorous phase and substrate as the hydrocarbon phase using copper and cobalt complexes of the cyclam derivative. Yields of up to 80% were obtained for the oxidation of cyclooctane with the copper catalyst with 80% selectivity towards the ketone. The fluorous phase was recycled after reaction and used in a second run showing a marginal decrease in the activity of the catalyst.
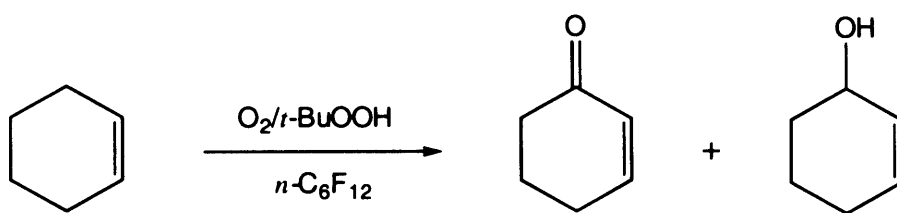
Scheme 1.11   Oxidation of cyclohexane with a fluorous-soluble cyclam complex.

Fish _et al._ synthesised the fluorous derivative of 1,4,7-triazacyclononane (TACN) (**1.18**) in 60% yield by the reaction of TACN and $C_8F_{17}C_3H_6I$ in DMSO in the presence of K_2CO_3. The perfluoroalkyliodide was prepared by the AIBN initiated free radical addition of $C_8F_{17}I$ to allyl alcohol with subsequent reduction to the perfluoroalkylalcohol and conversion of the hydroxyl group to an iodide.
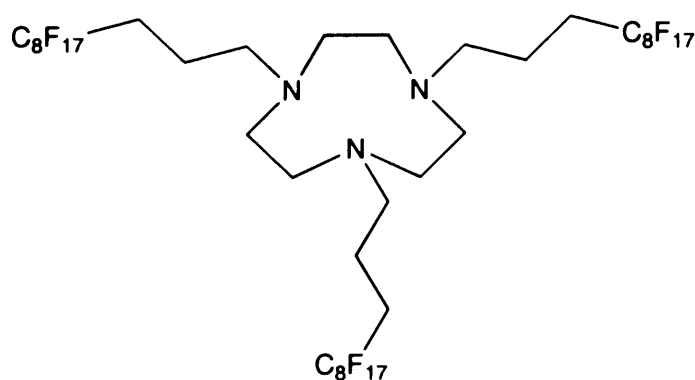
(**1.18**)

In common with the results obtained by Pozzi *et al.*, Fish *et al.* found that a three carbon spacer was necessary to avoid the facile elimination reaction of HI in the reaction of the perfluoroalkyliodide with TACN which dominated when a two carbon spacer was used. The complexes [Mn(O$_2$CC$_2$H$_4$C$_8$F$_{17}$)$_2$] and [Co(O$_2$CC$_2$H$_4$C$_8$F$_{17}$)$_2$] were prepared by the reaction of M(ClO$_4$)$_2$ with two equivalents of the triethylammonium salt of C$_8$F$_{17}$C$_2$H$_4$CO$_2$H. The reaction of these complexes with the fluorous chain derivatised TACN ligand gave complexes of the type [(R$_f$TACN)M(O$_2$CC$_2$H$_4$C$_8$F$_{17}$)$_2$] which were used to catalyse the oxidation of cyclohexane with O$_2$ and *t*-BuOOH under fluorous biphase conditions. At the end of the reaction the organic phase was decanted and the reaction vessel recharged with cyclohexane and *t*-BuOOH for a second run. The substrate was converted at a similar rate to the first run demonstrating that the catalyst had been successfully retained in the fluorous phase.

The oxidation of organometallic compounds, such as organozinc derivatives and the stereoselective oxidation of organoboranes to alcohols using perfluorinated solvents as the reaction media have been studied by Knochel *et al.*[76,77] In both cases reaction rates and selectivities were greater than those obtained when the reactions were carried out in standard organic solvents, as a result of the increased solubility of oxygen in the PFC solvent. Encouraged by these results, Knochel *et al.* investigated the oxidation of alkenes, aldehydes and sulphides under fluorous biphase conditions using fluorous-soluble nickel and ruthenium catalysts.[78] Complexes (1.19) and (1.20) were formed by the reaction of the appropriate metal chloride salt with a perfluoroalkyl chain derivatised acac ligand, prepared by the condensation[79] of a methyl ester functionalised with a C$_7$F$_{15}$ group and a similarly functionalised methyl ketone in the presence of NaOMe. The oxidation of aldehydes with molecular oxygen using the nickel catalyst (1.19) was carried out in perfluorodecalin and toluene which form a monophasic system at the reaction temperature of 64 °C. Aromatic and aliphatic aldehydes were found to be compatible with the reaction which was tolerant of several types of functional groups, forming carboxylic acids in yields of 71-87%. The catalyst was easily recovered by phase separation for use in further catalytic cycles, with no leaching into the organic phase observed.

(1.19)   (1.20)
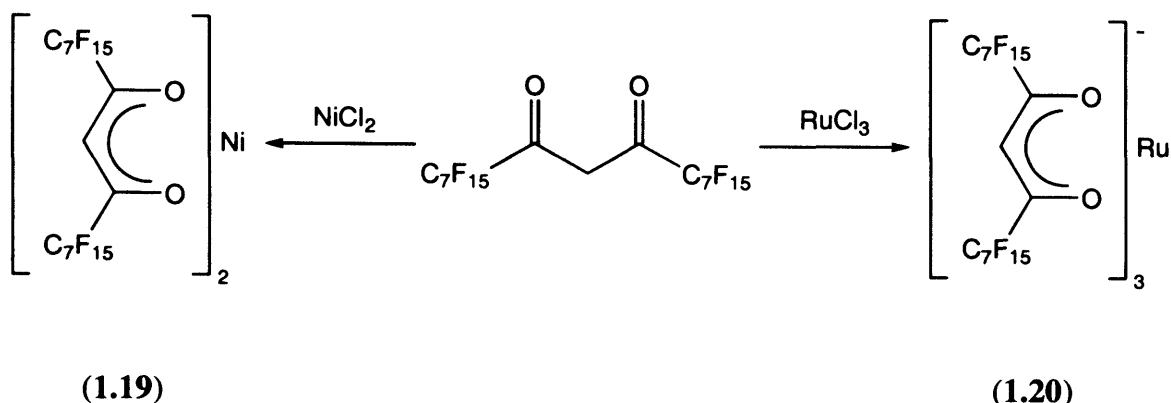
The ruthenium complex (1.20) catalysed the epoxidation of disubstituted olefins in good yields in a mixture of toluene and 1-bromoperfluorooctane (Scheme 1.12). The fluorous phase containing the catalyst was used in several consecutive reaction cycles, although only 95% (by weight) of the catalyst was recovered suggesting partial leaching into the organic phase. Knochel and co-workers went on to investigate the oxidation of alkenes to ketones using t-BuOOH as the oxidant, with a palladium complex of the derivatised acac ligand used previously.[80] Reactions were carried out at 56°C, during which the solvent system of benzene and 1-bromoperfluorooctane formed a single homogeneous phase. Again, facile catalyst/product separation was achieved on cooling allowing subsequent recycling of the catalyst. Begué et $al.$ have also employed the fluorous biphase methodology to the epoxidation of alkenes, using an inexpensive Mn(III) acetate catalyst at 25°C with O_2 and a sacrificial aldehyde.[81]
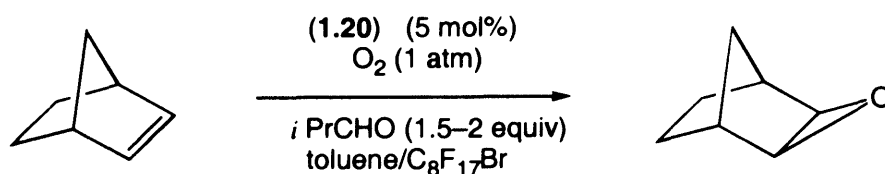
Scheme 1.12 Oxidation of a disubstituted olefin.

The fluorous biphase concept has been adapted by Betzemeier and Knochel to the formation of carbon-carbon bonds by palladium catalysed cross-coupling.[82] Reactions of this type under homogeneous conditions require relatively large quantities of palladium catalyst (1-5 mol %), traces of which are often difficult to remove from the products.[83] A fluorous-soluble palladium(0) complex prepared by the reaction of [Pd(dba)₂] with the perfluoroalkyl derivatised aryl phosphine $P(C_6H_4-4-C_6F_{13})_3$, catalysed the coupling of arylzinc bromides and aryl iodides (Scheme 1.13) in high yields (87-99%) in a mixture of toluene and 1-bromoperfluorooctane. At the reaction temperature of 60°C the solvent mixture is monophasic allowing the reaction to proceed homogeneously and, on cooling, a two phase system is regenerated. The fluorous phase containing the catalyst was reused several times with no significant change in reaction yields. The complex $[Pd\{P(C_6H_4-4-C_6F_{13})_3\}_4]$ was also found to be highly active, with high yields of coupled products obtained with catalyst quantities of only 0.15 mol %.
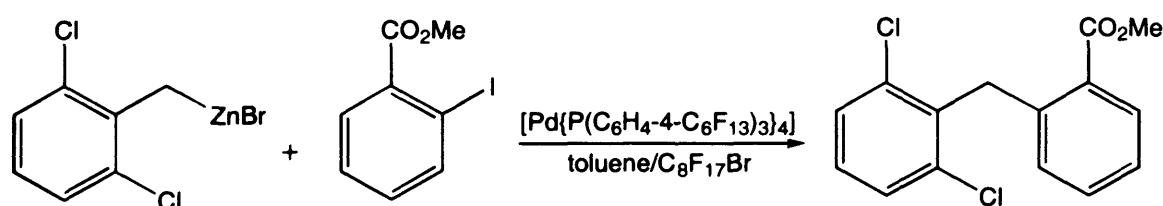
Scheme 1.13 Pd-catalysed cross-coupling of an arylzinc bromide and an aryl iodide.

The application of FBS to enantioselective catalysis is a promising area of research which would offer great advantages over analogous homogeneous systems. Surprisingly, there has been a dearth of research in this area, which would not only bring economic benefits from the recycling of an expensive chiral catalyst, but may also bring about beneficial changes in reaction selectivity due to the unique solvation properties of PFC solvents.[63] The first report of a fluorous-soluble chiral catalyst was made by Pozzi et al. in 1998 and described the synthesis of the C_2 symmetric salen ligands (1.21) and (1.22) bearing four C_8F_{17} chains and the application of their Mn(II) complexes in the aerobic oxidation of alkenes.[84]
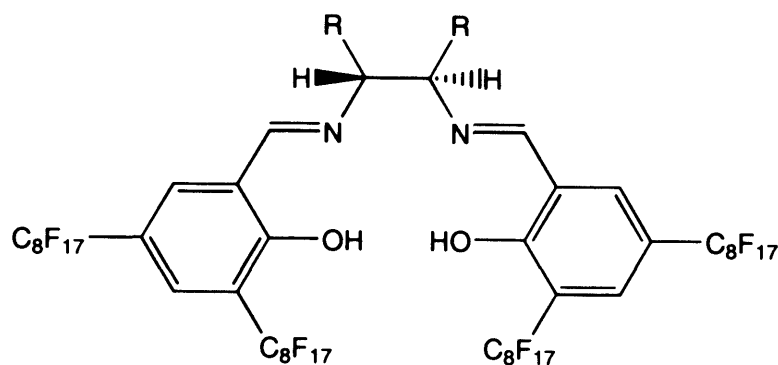
(1.21) R = C$_4$H$_8$ **(1.22)** R = Ph

Smaller quantities of the chiral catalyst were required in comparison to experiments in homogeneous systems, with the catalyst remaining highly active after recycling. Despite the good chemoselectivity of the FBS reaction, poor enantioselectivity was observed for most of the alkenes studied (≤ 15%), the only exception being indene, the epoxidation of which resulted in an ee of 92%. The low enantioselectivity was believed to result from the residual electron withdrawing effect of the perfluoroalkyl chains on the metal centre.[85] Rábai et al. have also turned their attention to enantioselective transformations in perfluorocarbon media having prepared chiral fluorinated amphiphiles.[86] The synthetic precursors to the amphiphiles, the perfluoroalkyl-propyl esters of L-tartaric acid, can also be applied as chelating agents for the formation of fluorous-soluble chiral metal complexes.

1.6 Perfluorocarbons in Organic Synthesis

The unique properties of PFC solvents have been applied to organic synthesis by Zhu,[87] where a non polar and inert reaction medium was required for transesterifications carried out under vigorous conditions. The immiscibility of the PFC solvent with organic solvents allowed the constant removal of water and alcohol formed during the course of the reactions via a modified Dean-Stark trap. The use of PFCs for the recovery and purification of products from organic syntheses has been developed by Curran and co-workers by the insertion of perfluoroalkyl residues into organic reagents.[88-90] Organotin reagents are highly toxic and their separation from homogeneous reaction mixtures is often difficult. In their first publication, Curran et

al. reported the synthesis of a fluorous-soluble tin hydride, which after reaction forms a fluorous-soluble tin halide which could be easily separated from the products after reaction by extraction with a PFC solvent.[86] A stoichiometric amount of the derivatised tin reagent was used in the presence of 10% AIBN for the homogeneous reduction of bromoadamantane to adamantane in benzotrifluoride. After reaction, the solvent is evaporated and the components of the mixture separated by liquid-liquid extraction with dichloromethane and perfluoromethylcyclohexane. The products of the reaction are extracted into the organic phase, while the tin complex is selectively partitioned into the fluorous phase. The perfluoroalkylated tin hydride has also been used as a reagent in the hydroxymethylation of organic halides.[89]

A similar perfluorinated tin reagent has been used by Curran *et al.* in the Stille reaction for the palladium-catalysed cross-coupling of aryl halides and arylstannanes (Scheme 1.14) in high yields (77-98%).[90,91,92] Reactions were carried out in a mixture of DMF and THF which were partially removed by evaporation before extraction with a triphasic mixture of water, dichloromethane and PFC solvent. The tin chloride recovered from the fluorous phase can be recycled for the preparation of perfluoroalkylated organostannanes.
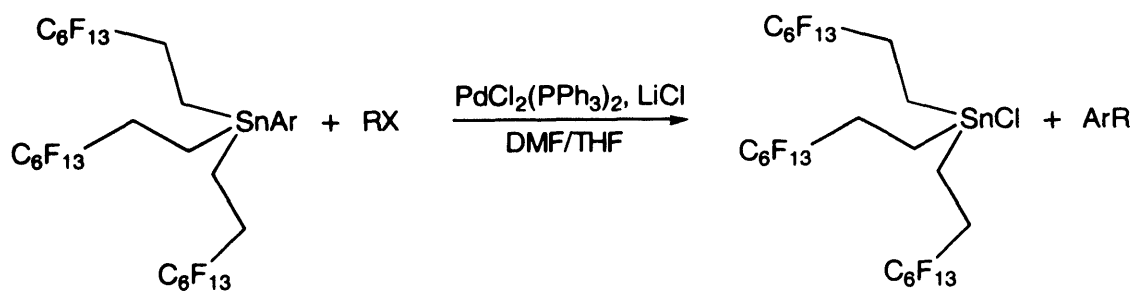
Scheme 1.14 Cross-coupling of perfluoroalkylated stannanes and aryl halides.

The separatory properties of PFC solvents have been applied to liquid-phase organic combinatorial synthesis allowing purification of reaction products derivatised with a fluorous moiety by liquid-liquid extraction.[93,94] The reaction substrate is derivatised with a fluorous group such as $(C_{10}F_{21}C_2H_4)_3Si$ and the liquid phase chemistry carried out using classical methods in an organic solvent. The fluorous substituent on the reaction product renders it preferentially soluble in PFC solvents

and, hence, it can be separated from the reaction mixture by extraction into a fluorous solvent. The fluorous group can then be cleaved from the product and removed by liquid-liquid extraction. This strategy has been applied to the synthesis of isooxazolines and in Ugi and Bignelli multicomponent condensations.[95,96] Recently, Curran *et al.* have reported the synthesis of new perfluoroalkyl tin hydrides[97] and tin azides[98] and their application in radical reactions and the preparation of substituted tetrazoles from nitriles respectively.

1.7 Outline of Thesis

The work contained in this thesis describes the synthesis of novel monodentate and bidentate phosphinite, phosphonite and phosphite ligands bearing long perfluoroalkyl chains, and their application in fluorous biphase systems. The driving force for this work, as outlined above, was the possibility of facile catalyst/product separation following catalysis under FBS conditions. In comparison to the significant body of work concerned with FBS-compatible phosphine ligands, phosphinite, phosphonite and phosphite ligands have received scant attention.[68] The coordination chemistry of the ligands has been investigated to determine the requirements for preferential solubility of metal complexes in perfluorocarbon solvents. The coordination complexes have been fully characterised, and spectroscopic techniques used to probe the impact of the electron-withdrawing perfluoroalkyl moieties on the σ-donor and π-acceptor properties of the phosphorus ligands. The hydroformylation of olefins under fluorous biphase conditions has been performed using rhodium complexes of the fluorous-soluble phosphites. The effect of introducing the perfluoroalkyl groups on the chemoselectivity and regioselectivity of the reaction and the potential for recycling of the catalyst by immobilisation in the fluorous phase have been investigated.

References for Chapter One

[1]   O. Roelen, *Angew. Chem.*, 1948, **62**, 60.

[2]   C. Masters, *Homogeneous Transition-metal Catalysis*, Chapman and Hall, Cambridge, 1981.

[3]   *Chirality in Industry*, Eds. A. N. Collins, G. N. Sheldrake and J. Crosby, John Wiley & Sons, Guildford, 1992.

[4]   J. A. Osborn, F. H. Jardine, J. F. Young and G. J. Wilkinson, *J. Chem. Soc., Chem. Commun.*, 1965, 131.

[5]   C. A. Tolman, P. Z. Meakin, D. L. Lindner, and J.P. Jesson, *J. Am. Chem. Soc.*, 1974, **96**, 2762.

[6]   Y. Ohtani, M. Fujimoto, and A. Yamagishi, *Bull. Chem. Soc. Jpn.*, 1977, **50**, 1453.

[7]   J. Halpern, *Inorg. Chim. Acta*, 1981, **50**, 11.

[8]   *A Molecular View of Heterogeneous Catalysis*, Ed. E. G. Derouane, DeBoeck Université, Paris, 1998.

[9]   M. Aria, S. L. Guo, Y. Nishiyama, M. Shirai and K. Torii, *J. Catal.*, 1996, **161**, 704.

[10]   V. I. Bakhmutov, E. V. Bakhmutova, N. V. Belkova, C. Bianchini, L. M. Epstein, A. V. Ionidis, L. Marvelli, M. Peruzzini, E. S. Shubina and E. V. Vorontsov, *Inorg. Chim. Acta.*, 1998, **280**, 302.

[11]   Y. G. Noskov, E. S. Petrov and M. I. Terekhova, *Kinetics and Catalysis*, 1993, **34**, 898.

[12]   *Catalysis and Surface Characterisation*, Eds. T. J. Dines, C. H. Rochester and J. Thomson, The Royal Society of Chemistry, Cambridge, 1992.

[13]   T. Manimaran, T. -C. Wu, W. D. Klobucar, C. H. Kolich, G. P. Stahly, F. R. Fronczek, and S. E. Watkins, *Organometallics*, 1993, **12**, 1467.

[14]   D. C. Bailey and S. H. Langer, *Chem. Rev.*, 1981, **81**, 109.

[15]   E. Bayer and V. Schurig, *CHEMTECH*, 1976, 212.

[16]   D. E. Bergbreiter, *CHEMTECH*, 1987, 686.

[17]   W. D. Honnick, C. U. Pittman Jr. and J. J. Yang, *J. Org. Chem.*, 1980, **45**, 684.

[18]   J. J. Ackerman, S. J. Fritschel, T. Keyser and J. K. Stille, *J. Org. Chem.*, 1979,

44, 3152.

[19]   E. Dinjus, N. Holzhey and S. Pitter, *J. Organomet. Chem.*, 1997, **541**, 243.

[20]   D. E. Bergbreiter, M. Morvant and B. Chen, *Tetrahedron Lett.*, 1991, **32**, 2731.

[21]   C. Bianchini, D. G. Burnaby, J. Evans, P. Frediani, A. Meli, W. Oberhauser, R. Psaro, L. Sordelli and F. Vizza, *J. Am. Chem. Soc.*, 1999, **121**, 5961.

[22]   W. Keim, T. M. Shryne, R. S. Bauer, H. Chung, P. W. Glockner and H. van Zwet (SHELL Int. Res.), DE-P 2054009, 1969.

[23]   W. Keim, *Chem. Ing. Techn.*, 1984, **56**, 850.

[24]   F. G. Mann and I. T. Millar, *J. Chem. Soc.*, 1952, 4453.

[25]   K. Issleib and G. Thomas, *Chem. Ber.*, 1960, **93**, 803.

[26]   K. Issleib, R. Kümmel and H. Zimmermann, *Angew. Chem., Int. Ed. Engl.*, 1965, **4**, 155.

[27]   J. Podlaha and J. Podlahová, *Collect. Czech. Chem. Commun.*, 1980, **45**, 2049.

[28]   J. Chatt, G. J. Leigh and R. M. Slade, *J. Chem. Soc. Dalton Trans.*, 1973, 2021.

[29]   P. A. T. Hoye, P. G. Pringle, M. B. Smith and K. Worboys, *J. Chem. Soc., Dalton Trans.*, 1993, 269.

[30]   A. Fukuoaka, W. Henderson, M. Hirano, S. Komiya, W. Kosugi and F. Morishita, *Chem. Commun.*, 1999, 489.

[31]   R. G. Nuzzo, M. E. Wilson and G. M. Whitesides, *J. Am. Chem. Soc.*, 1978, **100**, 2269.

[32]   M. Iwahara, J. Kiji, H. Konishi and T. Okano, *J. Organomet. Chem.*, 1988, **346**, 267.

[33]   M. C. Baird and R. T. Smith, *Inorg. Chim. Acta*, 1982, **62**, 135.

[34]   A. Bendayan, S. Chan, G. Peiffer, B. Waegell and J. P. Zahra, *J. Mol. Catal.*, 1990, **59**, 1.

[35]   B. E. Hansen and I. Tóth, *Organometallics*, 1993, **12**, 1506.

[36]   O. Herd, K. P. Langhans, O. Stelzer, W. S. Sheldrick and N. Weferling, *Angew. Chem., Int. Ed. Engl.*, 1993, **32**, 1058.

[37]   Rhône-Poulenc Ind. (E. Kuntz), FR-B 2,314,190 (1975).

[38]   D. Feitler, R. G. Nuzzo and G. M. Whitesides, *J. Am. Chem. Soc.*, 1979, **101**, 3683.

[39]   S. Ganguiy, J. T. Mague and D. M. Roundhill, *Inorg. Chem.*, 1992, **31**, 3500.

[40]   Rhône-Poulenc Recherche (E. Kuntz *et al.*), FR 2,314,910 (1975). Rhône-Poulenc Ind. (E. Kuntz *et al.*), FR 2,338,253 (1976), FR 2,349,562 (1976), FR 2,366,237 (1976), FR 2,473,504 (1979).

[41]   B. Cornils and E. Kuntz, *J. Organomet. Chem.*, 1995, **502**, 177.

[42]   *'Applied Homogeneous Catalysis with Organometallic Compounds'*, Vol. 1, Eds. B. Cornils and W. A. Herrmann, VCH Publishers, New York, 1996.

[43]   M. T. Beack, F. Joó and Z. Tóth, *Inorg. Chim. Acta*, 1977, **25**, L61.

[44]   M. T. Beack, F. Joó and Z. Tóth, *Inorg. Chim. Acta*, 1980, **42**, 153.

[45]   G. Allmang, F. Grass, J. M. Grosselin and C. Mercier, *Organometallics*, 1991, **10**, 2126.

[46]   D. C. Mudalige and G. L. Rempel, *J. Mol. Catal. (A)*, 1997, **123**, 15.

[47]   M. Beller and A. M. Tafesh, *Tetrahedron Lett.*, 1995, **36**, 9305.

[48]   E. Blart, J. P. Genêt, A. Linquist, V. Mouriès, M. Savignac and M. Vaultier, *Tetrahedron Lett.*, 1995, **36**, 1443.

[49]   H. Bahrmann, B. Fell, W. Konkol, G. Papadogianakis and J. Weber, *J. Prakt. Chem.*, 1993, **335**, 75.

[50]   Ruhrchemie AG (B. Cornils, H. Bahrmann, E. Wiebus *et al.*), DE 3,411,034 (1984), EP 0,157,316 (1985), DE 3,447,030 (1984), DE 4,242,723 (1992).

[51]   Johnson Matthey plc (M. J. H. Russel, B. A. Murrer), BE 890,210 (1982), FR 2,489,308 (1982), DE 3,135,127 (1981), NL 81/03989 (1981).

[52]   B. Fell, Z. Jin, Y. Yan and H. Zhuo, *J. Prakt. Chem.*, 1996, **338**, 124.

[53]   W. A. Herrmann and C.W. Kohlpainter, *Angew. Chem., Int. Ed. Engl.*, 1993, **32**, 1524.

[54]   Y. Amrani and D. Sinou, *J. Mol. Catal.*, 1986, **36**, 319.

[55]   J. Bakos, B. Heil, L. Lecomte, D. Sinou and I. Tóth, *J. Organomet. Chem.*, 1989, **370**, 277.

[56]   J. Bakos, B. Heil, M. Laghmari, P. Lhoste, A. Orosz and D. Sinou, *J. Chem. Soc., Chem. Commun.*, 1991, 1684.

[57]   C. Lensink and J. G. de Vries, *Tetrahedron Asymmetry*, 1992, **3**, 235.

[58]   M. Hudlicky, *'Chemistry of Organic Fluorine Compounds'*, Macmillan Co., New York, 1962, 304.

[59]   J. G. Riess and M. LeBlanc, *Pure. Appl. Chem.*, 1982, **54**, 2383.

[60]   R. M. Crowell, D. E. Sakas, K. W. Whittaker and N. T. Zervas, *J. Neurosurgery*, 1996, **85**, 248.

[61]   M. Vogt, *'The Application of Perfluorinated Polyethers for Immobilization of Homogeneous Catalysts'*, Ph.D. Thesis, Rheinisch-Westfälischen Technischen Hochschule, Achen, Germany, 1991.

[62]   I. T. Horváth and J. Rábai, *Science*, 1994, **266**, 72.

[63]   J. E. Bond, R. A. Cook, I. T. Horváth, G. Kiss, E. J. Mozeleski, J. Rábai and P. A. Stevens, *J. Am. Chem. Soc.*, 1998, **120**, 3133.

[64]   J. A. Gladysz, I. T. Horváth and J. J. J. Juliette, *Angew. Chem. Int. Ed. Engl.*, 1997, **36**, 1610.

[65]   D. A. Evans, G. C. Fu and A. H. Hoveyda, *J. Am. Chem. Soc.*, 1992, **114**, 6671.

[66]   K. Burgess and M. J. Ohlmeyer, *Chem. Rev.*, 1991, **91**, 1179.

[67]   J. A. Gladysz, I. T. Horváth, J. J. J. Juliette and D. Rutherford, *J. Am. Chem. Soc.*, 1999, **121**, 2696.

[68]   J. A. Gladysz, I. T. Horváth, J. J. J. Juliette, C. Rocaboy and D. Rutherford, *Catalysis Today*, 1998, **42**, 381.

[69]   D. R. Paige, *'The Synthesis, Co-ordination Chemistry and Catalytic Applications of Phosphine Ligands Containing Long-Chain Perfluoroalkyl Groups'*, Ph.D. Thesis, University of Leicester, 1998.

[70]   S. Banfi, A. Manfredi, F. Montanari, G. Pozzi and S. Quici, *Tetrahedron*, 1996, **52**, 11879.

[71]   I. Colombani, M. Miglioli, F. Montanari, G. Pozzi and S. Quici, *Tetrahedron*, 1997, **53**, 6145.

[72]   F. Montanari, G. Pozzi and S. Quici, *Chem. Commun.*, 1997, 69.

[73]   Y. Kuroda, H. Murase, H. Ogoshi and Y. Suzuki, *Tetrahedron Lett.*, 1989, **30**, 2411.

[74]   M. Cavazzini, S. Fontana, G. Pozzi and S. Quici, *Tetrahedron Lett.*, 1997, **38**, 7605.

[75]   R. H. Fish, A. Rabion, J. –M. Vincent and V. K. Yachandra, *Angew. Chem., Int. Ed. Engl.*, 1997, **36**, 2346.

[76]   I. Klement and P. Knochel, *Synlett*, 1995, 1113.

[77]   I. Klement and P. Knochel, *Synlett*, 1996, 1004.

[78]   I. Klement, P. Knochel and H. Lutjens, *Angew. Chem., Int. Ed. Engl.*, 1997, **36**, 1454.

[79]   A. E. Pedler, R. C. Smith and J. C. Tatlow, *J. Fluorine Chem.*, 1971, **1**, 433.

[80]   B. Betzemeier, F. Lhermitte and P. Knochel, *Tetrahedron Lett.*, 1998, **39**, 6667.

[81]   F. Barbier, J. -P. Begue, D. Bonnetdelpon and K. S. Ravikumar, *Tetrahedron*, 1998, **54**, 7457.

[82]   B. Betzemeier and P. Knochel, *Angew., Chem. Int. Ed. Engl.*, 1997, **36**, 2623.

[83]   M. Beller, C. Brossmer, H. Fischer, W. A. Herrmann, K. Öfele, T. Priermeier and C. -P. Reisinger, *Angew., Chem. Int. Ed. Engl.*, 1995, **35**, 1844.

[84]   F. Cinato, F. Montanari, G. Pozzi and S. Quici, *Chem. Commun.*, 1998, 877.

[85]   M. Cavazzini, F. Montanari, G. Pozzi and S. Quici, *J. Fluorine Chem.*, 1999, **94**, 183.

[86]   J. Rábai, Z. Szlávik and G. Tárkányi, *12th European Symposium on Fluorine Chemistry*, Berlin, 1998.

[87]   D. W. Zhu, *Synthesis*, **1993**, 953.

[88]   D. P. Curran and S. Hadida, *J. Am. Chem. Soc.*, 1996, **118**, 2531.

[89]   D. P. Curran, S. Hadida, M. Komatsu, S. Minakata, T. Niguma and I. Ryu, *Tetrahedron Lett.*, 1997, **38**, 7883.

[90]   D. P. Curran and M. Hoshino, *J. Org. Chem.*, 1996, **61**, 6480.

[91]   D. P. Curran, S. Hadida, A. Hallberg, M. Hoshino and M. Larhed, *J. Org. Chem.*, 1997, **62**, 5583.

[92]   D. P. Curran, P. Degenkolb and M. Hoshino, *J. Org. Chem.*, 1997, **62**, 8341.

[93]   D. P. Curran and A. Studer, *Tetrahedron*, 1997, **53**, 6681.

[94]   D. P. Curran, P. Jeger, A. Struder and P. Wipf, *J. Org. Chem.*, 1997, **62**, 2917.

[95]   C. O. Kappe, *Tetrahedron*, 1993, **49**, 6937.

[96]   I. Ugi, *Angew., Chem. Int. Ed. Engl.*, 1982, **21**, 810.

[97]   D. P. Curran, S. Hadida, S. Y. Kim and Z. Y. Luo, *J. Am. Chem. Soc.*, 1999, **121**, 6607.

[98]   D. P. Curran, S. Hadida and S. Y. Kim, *Tetrahedron*, 1999, **55**, 8997.

Chapter Two

2.1 Monodentate Phosphorus(III) Ligands

Catalysts which are amenable to fluorous biphase systems (FBS) must be preferentially soluble in perfluorocarbon solvents (PFCs). These complexes can be rendered soluble in PFCs by the inclusion of long perfluoroalkyl substituents in the periphery of the modifying ligands. It was, therefore, necessary to synthesise ligands which would be compatible with the FBS approach in order to confer preferential fluorous phase solubility on metal complexes with potential catalytic activity. Trivalent phosphorus donor ligands have been applied to a diverse range of catalytic systems such as hydrogenation,[1] hydroformylation,[2] hydrocyanation,[3,4] and olefin polymerisation[5] on both the laboratory and the industrial scale. This diversity of application is a result of the flexibility of tertiary phosphines and the ease with which the stereoelectronic properties of these ligands can be manipulated to tailor catalysts for a specific purpose. For these reasons phosphine ligands have already been adapted for use in fluorous biphase catalysis. In the initial publication on FBS, Horváth *et al.* employed the alkyl phosphines $P(C_2H_4C_6F_{13})_3$[6] and $P(C_2H_4C_8F_{17})_3$ as modifying ligands for rhodium catalysed hydroformylation.[7] Subsequent work by Paige[8] and Knochel *et al.*[9] has focussed on derivatised aryl phosphines such as $P(C_6H_4-4-C_6F_{13})_3$ as discussed in chapter 1 (section 1.6).

In comparison to phosphines there is a paucity of literature on phosphites, and only recently has much attention turned to this class of ligand despite the advantages that they can offer. Transition metal complexes of phosphites have been found to exhibit superior reactivity and selectivity to phosphines in many catalytic systems, particularly hydroformylation[10] and hydrocyanation.[11] In order to rationalise the observed differences in catalytic activity between metal complexes of phosphines and phosphites it is necessary to understand the nature of the valence orbitals used in bonding with transition metals and the nature of bonding in PR_3 ligands. Phosphines are generally regarded as being good σ-donors but weak π-acceptors, whereas phosphites as a result of the presence of the electronegative oxygen atoms are weaker σ-donors but much better π-acceptors. These subtle differences in σ-basicity and π-acidity between phosphines and phosphites may give rise to variations in the electrophilicity of metal centres resulting in dramatic changes in reactivity and selectivity.

2.2 Bonding in Phosphorus(III) Ligands

The bonding in phosphorus(III) ligands is complex and no model has yet been established which completely fits the varied empirical data obtained on the structures of these ligands. Numerous theoretical studies have been undertaken to explain the bonding in and geometry of tertiary phosphorus ligands, however these involve highly complex molecular orbital calculations.[12,13] Orbital interaction diagrams developed by Walsh are a useful tool for describing the bonding interactions in phosphines.[14] Considering the Walsh MO diagram of the simplest phosphine PH_3 as shown in Figure 2.1, it can be seen that the σ $1a_1$ and $1e$ orbitals correspond to the three σ bonds between the phosphorus and the hydrogens. The $2a_1$ orbital lies above these and is the non-bonding highest occupied molecular orbital (HOMO) composed of a phosphorus sp* hybrid orbital and the σ orbitals of hydrogen, although this latter contribution is small. The lone pair on phosphorus can be regarded as the sp* hybrid orbital and it is through this orbital that phosphine acts as a σ-donor ligand. The lowest unoccupied molecular orbital (LUMO) $2e$ is doubly degenerate and out of phase with the corresponding doubly degenerate $1e$ orbitals. Above the $2e$ set lies the $3a_1$ orbital corresponding to a σ^* interaction between the phosphorus and hydrogens.

The essence of this orbital interaction diagram holds for all PX_3 ligands, despite molecular orbital variances. These ligands contain three low-lying orbitals corresponding to P-X σ-bonds, a non-bonding HOMO which can be regarded as the phosphorus lone pair, and a doubly degenerate LUMO containing P-X σ^* character. Studies by Marynick[15] and Berkovitch-Yellin et al.[16] have shown that the $2e$ set of σ^* orbitals are responsible for the π-acceptor properties of phosphines. As the substituent X becomes more electronegative the energy of the σ^* orbitals decreases, thus increasing their energetic accessibility for π-bonding and leading to the recognised trend in π-acidity $PR_3 < PAr_3 < P(OR)_3 < PF_3$.

Phosphorus   PH₃   Hydrogen
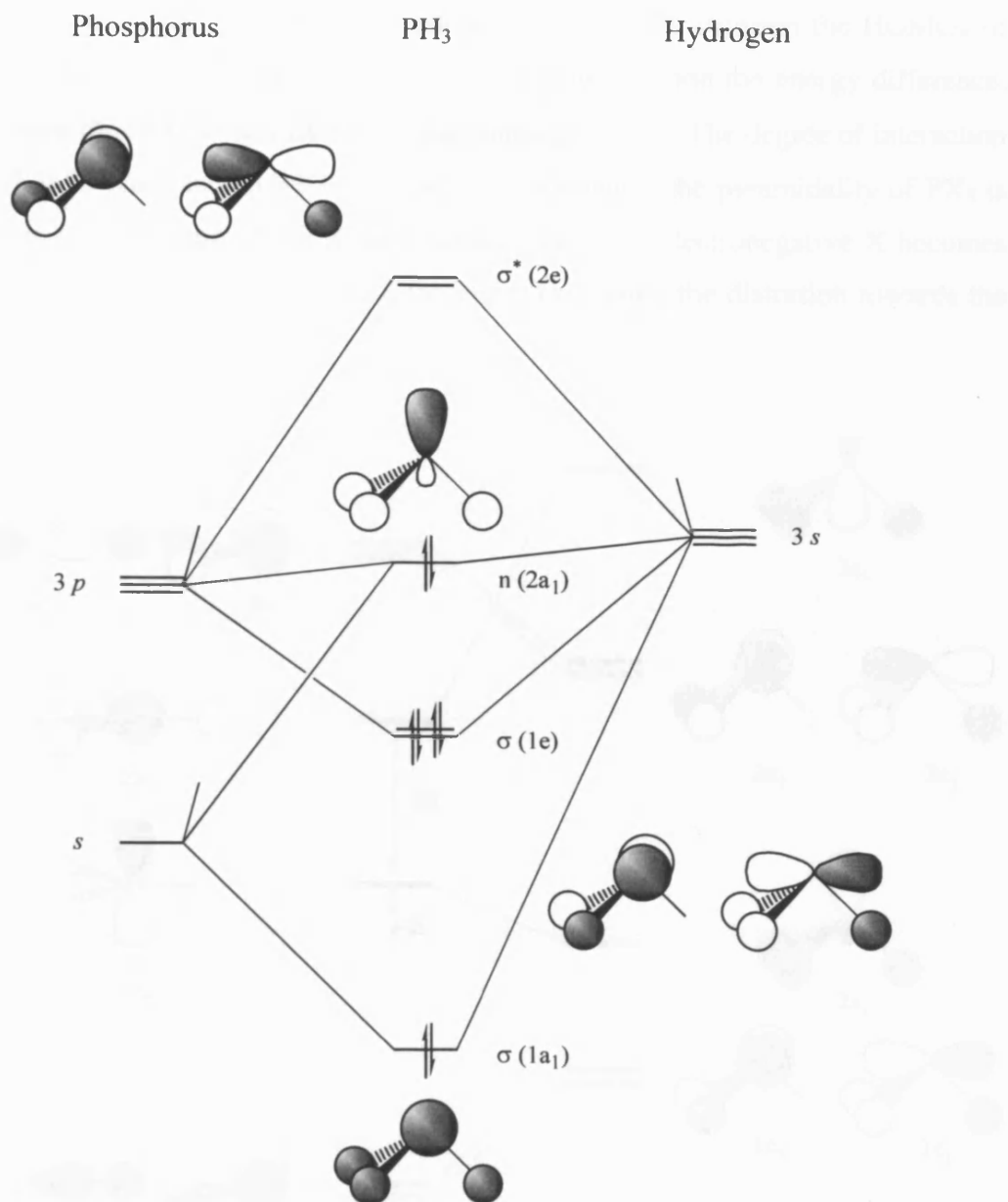
Figure 2.1 Walsh molecular orbital diagram for PH₃.

The geometry of PX_3 ligands has been found to be determined by the degree of interaction between the HOMO and the LUMO[17] as shown in the Walsh correlation diagram for a PX_3 species in the planar and pyramidal geometries (Figure 2.2). The HOMO in the D_{3h} (planar) geometry has a_2'' symmetry and a_1 symmetry in the C_{3v} (pyramidal) geometry. The a_2'' orbital in the D_{3h} geometry is a pure $3p_z$ lone pair, however in the C_{3v} structure the $2a_1$ orbital is an sp* hybrid as a consequence of mixing of phosphorus $3s$ character from the $3a_1$ orbital into the $3p_z$ of $2a_1$. The resulting stabilisation lowers the energy of the C_{3v} HOMO and this pyramidal

36

geometry is, therefore, preferred. The energy difference, E, between the HOMOs of the pyramidal and planar species is inversely dependent upon the energy difference, δE, between the HOMO and LUMO in the planar geometry. The degree of interaction of the HOMO ($2a_1$) and LUMO ($3a_1$) orbitals and, hence, the pyramidality of PX_3 is dependent on the nature of the X substituents. The more electronegative X becomes the greater the degree of mixing and, therefore, increasing the distortion towards the pyramidal geometry.
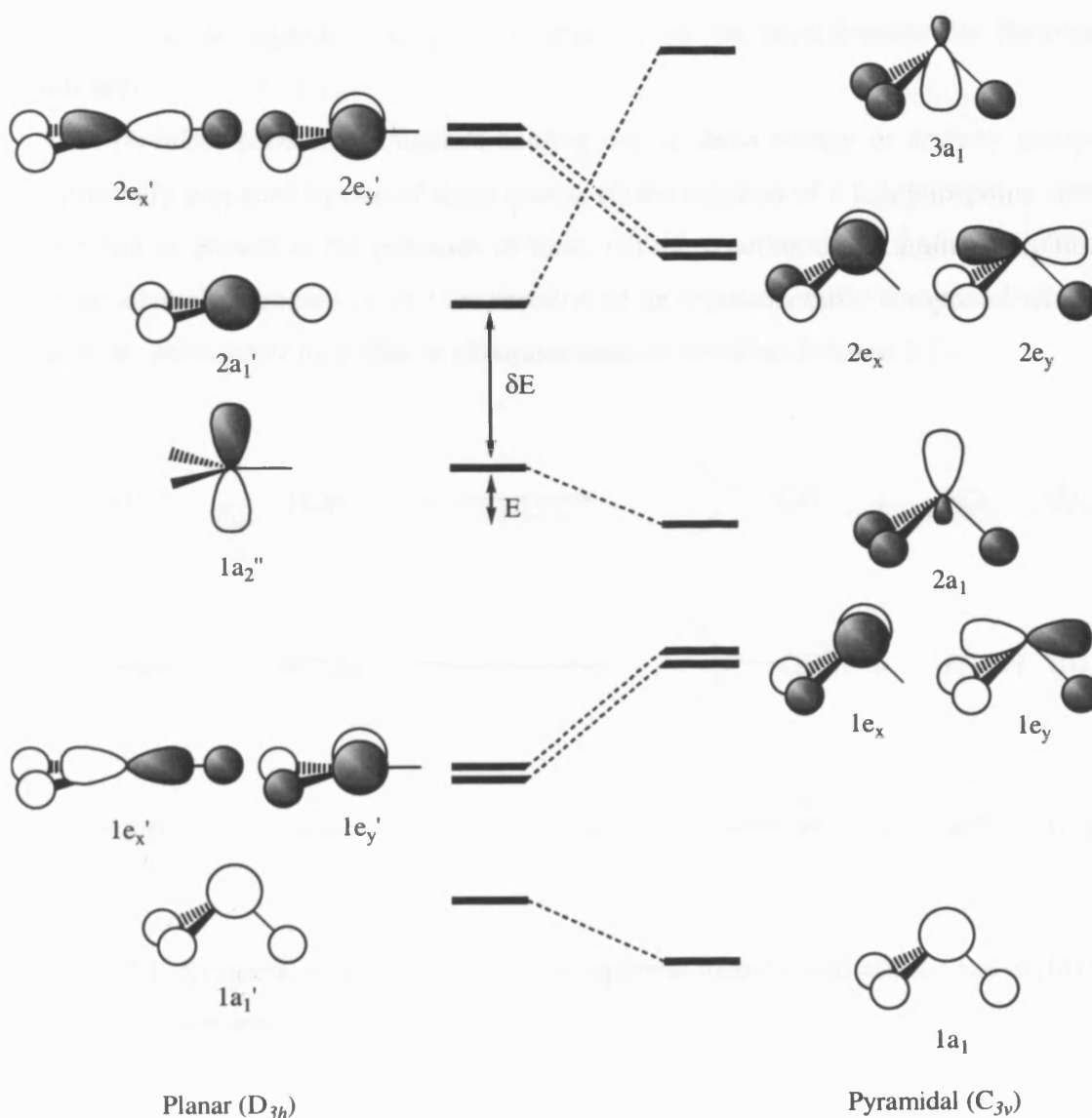
Figure 2.2 Walsh correlation diagram for planar and pyramidal PX_3 molecules.

2.3 Synthesis of Ligands

A series of aryl phosphite, phosphonite and phosphinite ligands of general formula $Ph_xP(OC_6H_4\text{-}4\text{-}C_6F_{13})_{3-x}$ (x = 0, 1 or 2) bearing perfluoro-n-hexyl substituents were synthesised.[18] The rationale behind the synthesis of this series of ligands was that it would allow a comparison of the behaviour and properties of the ligands with one another and with their perprotio congeners. This would give an insight into the influence of the step-wise inclusion of the perfluoroalkyl tails on the stereoelectronic properties of the ligands, and give information on the requirements for fluorous solubility.

Tervalent phosphorus ligands bearing one to three alkoxy or aryloxy groups are generally prepared by one of three routes; (i) the reaction of a halophosphine with an alcohol or phenol in the presence of base, (ii) the reaction of an aminophosphine with an alcohol or phenol or (iii) the reaction of an organometallic compound with a phosphite, phosphorochlorodite or phosphoramidochlorodite (Scheme 2.1).

$$\begin{array}{ccc}
\text{P---Cl} \ + \ \text{ROH} & \longrightarrow & \text{P---OR} \ + \ \text{HCl} \quad \text{(i)}
\end{array}$$

$$\begin{array}{ccc}
\text{P---NR}^1_2 \ + \ \text{R}^2\text{OH} & \longrightarrow & \text{P---OR}^2 \ + \ \text{R}^1_2\text{NH} \quad \text{(ii)}
\end{array}$$

$$\begin{array}{ccc}
\text{Cl---P---OR}^1 \ + \ \text{R}^2\text{M} & \longrightarrow & \text{R}^2\text{---P---OR}^1 \ + \ \text{MCl} \quad \text{(iii)}
\end{array}$$
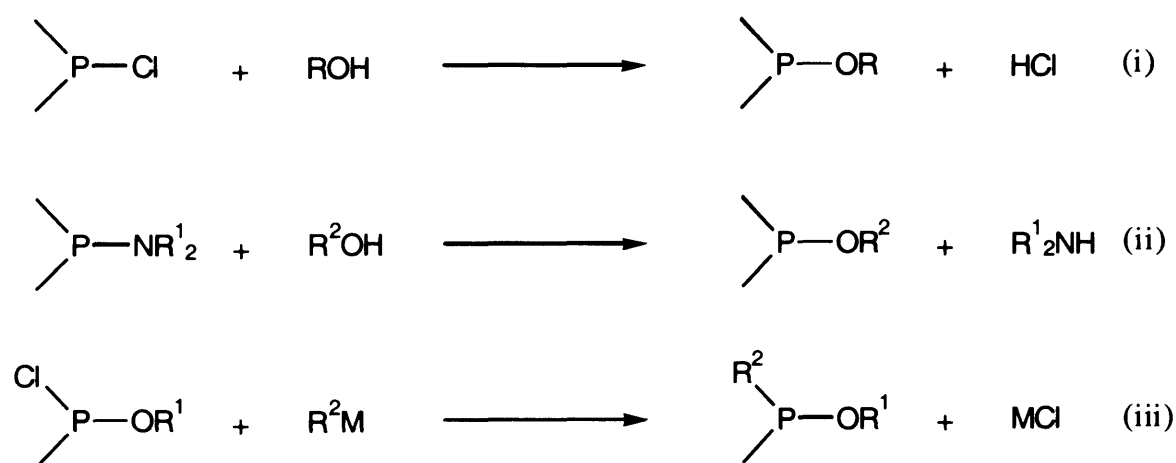
Scheme 2.1 Synthetic routes to tervalent phosphorus ligands with alkoxy and aryloxy groups.

The route involving the use of an organometallic reagent (iii) is the least popular as the yields tend to be much lower than for the other two methods. This is due to difficulties in obtaining pure phosphorochlorodites, phosphorodichlorodites or phosphoroamidochlorodites as starting materials[19] and to the undesired substitution of alkoxy, aryloxy or amino groups in addition to the substitution of the halogen. This

method is useful, however, for the formation of phosphorochloridites of high purity from trialkyl phosphites.[20] The reactions of aminophosphines with alcohols or phenols (ii) generally require the presence of a weak acid to proceed,[21] however, the presence of ammonium halide contaminants in the aminophosphines often result in reaction on heating even in the absence of added acid catalyst. This method has been used for the preparation of butyl diphenylphosphinite and dibutyl phenylphosphonite[22] and dimethyl methylphosphonite.[23]

A variety of other methods have also been employed for the preparation of phosphites, phosphonites and phosphinites. Alkoxy and phenoxy groups are reasonably good leaving groups and can undergo nucleophilic substitution by strong nucleophiles (R⁻). Weaker nucleophiles such as alcohols can also substitute alkoxy or phenoxy groups in base- or acid-catalysed reactions. The transesterification of ligands with higher boiling alcohols or phenols has been used to prepare dibutyl butylphosphonite from diethyl butylphosphonite using sodium as catalyst.[24] Alkylation of dialkoxyphosphines with compounds containing activated C=C bonds such as acrylonitrile give alkyl phosphonites.[25] The reaction of ethylene oxide with phosphorus trichloride generates tris chloroalkyl phosphite without the liberation of HCl. Alkyl phosphites have also been prepared directly from alcohols and elemental phosphorus, although low yields are obtained.[26]

The addition of alcohol to chlorophosphines results in the formation of a phosphorus oxygen bond and the elimination of HCl, the reaction being driven by the high energy of formation of the phosphorus oxygen bond. The addition of alcohols to phosphorus trichloride generates phosphites of general formula P(OR)₃ by a series of consequential and concurrent reactions. These result in the formation of alkyl phosphorodichlorodites, dialkyl phosphorochlorodites, and finally trialkyl phosphites. Addition of phenol and its derivatives to PCl₃ provide the aryl analogues of these compounds. In the absence of a hydrogen halide acceptor, the addition of the alcohol to PCl₃ results in the sequential replacement of chlorine and the rapid formation of alkyl phosphorodichlorodites followed, at a slower rate, by the formation of dialkyl phosphorochloridites. Hydrogen chloride is eliminated during both steps, but not in the third step, due to the dealkylation of the phosphite triester to the dialkyl 'phosphite' being rapid, even at low temperatures. The reactions involved in the synthesis of phosphorus triesters illustrate the electrophilicity of phosphorus. The

reaction between phosphorus halides and alcohols depends on the nature of the halogen, the reactivity of the hydroxyl group, and also the presence of a suitable reagent for the removal of the hydrogen halide liberated in the reaction. The condensation of phenols with chlorophosphines in the presence of base was the route chosen for the preparation of the derivatised aryl ligands in this study.

2.3.1 Synthesis of Para-Substituted Aryl Ligands

In order to prepare the perfluoroalkyl derivatised ligands it was necessary to synthesise a phenol bearing a perfluorohexyl group. The phenol was derivatised in the *para* position in order to minimise any steric effects arising from the inclusion of the fluorous chain. Phenol (**2.1**) was prepared by the copper-mediated cross coupling reaction of 4-iodophenol with perfluoro-n-hexyl iodide. The cross-coupling of iodofluoroalkanes and iodoaromatic compounds with copper in aprotic solvent was first disclosed by McLoughlin and Thrower[27] providing a convenient method for the introduction of perfluoroalkyl groups into an aromatic substrate (Scheme 2.2). The reaction has been extended further by Chen *et al.* to include a variety of functionalised bromoaromatic substrates[28] and perfluorooxaalkyl iodides.[29] Extensive work in this area has been undertaken and fluorocarbon-copper reagents are now one of the most widely studied classes of fluorinated organometallic compounds.[30]

$$R_f I \xrightarrow[L]{Cu} R_f CuL_3 + ICuL_3$$

$$R_f CuL_3 \xrightarrow{ArI} Ar\underset{I}{\overset{R_f}{\diamond}}CuL_2 \longrightarrow ArR_f + ICuL_3$$
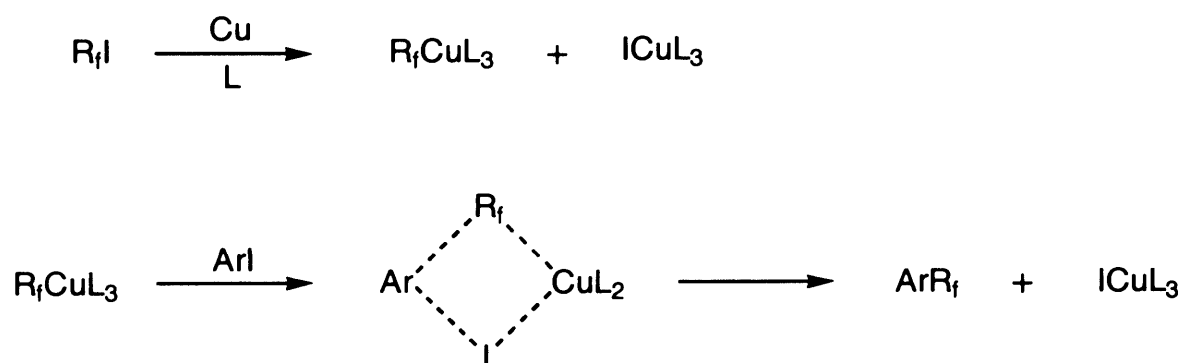
Scheme 2.2 Copper mediated coupling of perfluoroalkyl iodides with aromatic iodides (L = 2,2'-bipyridine).

Due to the electron withdrawing effect of the perfluoroalkyl group the iodine-carbon bond in perfluoroalkyl iodides has a partial positive charge residing at iodine.[31] This allows interaction of the molecule with an electron-donating solvent molecule. The coordinating ability of the solvent is significant in determining the mechanistic direction of the reaction. In solvents such as hexane, benzene, acetonitrile, and acetic anhydride, perfluoroalkyl radicals are produced and can be trapped by alkenes.[32] In solvents such as DMSO, DMF and pyridine the perfluoroalkylcopper reagent is formed and can react with aryl iodides. Aryl iodides have been found to give better yields than aryl bromides, although the difference in many cases is so small that it is often more cost effective to use aryl bromides.[33]

$$HO-\!\!\left\langle\bigcirc\right\rangle\!\!-C_6F_{13}$$

(2.1)
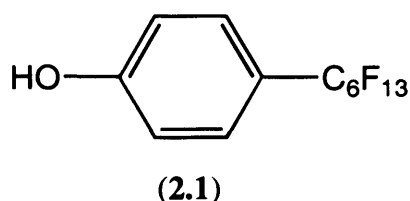
Polar aprotic media are required for this reaction and, therefore, DMSO was used as solvent for the reaction. Fluorobenzene was added as an inert diluent to facilitate the dissolution of the perfluoroalkyl iodide and 2,2'-bipyridine used in a catalytic amount as a complexing ligand for the organocopper intermediate formed in the reaction. The reaction was worked up by the hydrolysis of the reaction mixture followed by filtration to remove any insoluble copper species. The organic phase was then washed repeatedly with water to remove the DMSO which was difficult due to an apparently strong interaction between the solvent and the hydroxy function of the phenol. Extraction of the organic phase with PP3 afforded a crude product which was further purified by distillation *in vacuo* using a Kugelröhr apparatus yielding (2.1) as a white crystalline solid.

The proton NMR of (2.1) exhibits an AA'BB' pattern typical of a *para* disubstituted benzene ring with $^3J_{HH}$ coupling of 7.1 Hz. The doublet resonance for the protons *meta* to the hydroxyl group in 4-iodophenol is shifted to higher frequency on coupling of the perfluoroalkyl chain. This demonstrates the greater negative inductive effect of C_6F_{13} unit in comparison to iodine, resulting in deshielding of the aryl protons. The $^{19}F\{^1H\}$ NMR (Figure 2.3) exhibits six resonances associated with

the C_6F_{13} substituent. The detailed assignment of the resonances is given in the experimental chapter (section 6.5) and follows the arrangement shown in Figure 2.4.
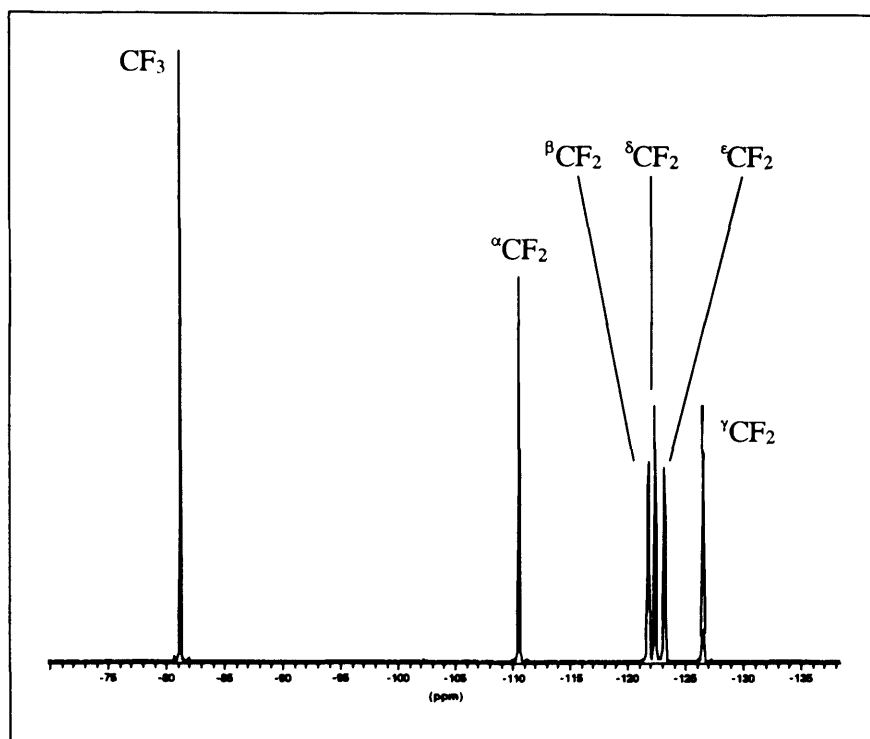
Figure 2.3 $^{19}F\{^1H\}$ NMR spectrum of $HOC_6H_4\text{-}4\text{-}C_6F_{13}$ (2.1).

The resonance of the $^\alpha CF_2$ at -110 ppm in (2.1) is significantly shifted in comparison to the $^\alpha CF_2$ resonance in $C_6F_{13}I$ at -60 ppm whilst the remaining resonances of the perfluoroalkyl chain remain, relatively, unchanged. The terminal CF_3 and $^\alpha CF_2$ resonances were observed as triplets of triplets due to three and four bond fluorine-fluorine couplings. The magnitude of the $^3J_{FF}$ and $^4J_{FF}$ coupling constants for the $^\alpha CF_2$ were found to be 2.5 and 10.0 Hz respectively. The resonances for the rest of the perfluoroalkyl group are highly complex multiplets from which the individual couplings could not be resolved.
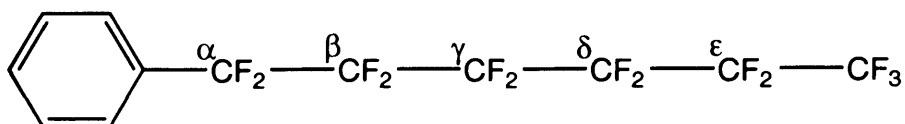
Figure 2.4 Assignment of CF_2 resonances.

4-Tridecafluorohexylphenyldiphenylphosphinite (**2.2**) was prepared by the reaction of chlorodiphenylphosphine with an excess of (**2.1**) in the presence of triethylamine. Chlorodiphenylphosphine and triethylamine were transferred to a three neck flask containing diethyl ether under nitrogen by syringe. An ethereal solution of (**2.1**) was gradually added to the reaction flask via a cannular under nitrogen which was accompanied by the formation of a dense white precipitate of $Et_3NH^+Cl^-$. After the reaction had finished, the mixture was filtered and the solvent removed *in vacuo* to yield the impure product as an off-white solid. Vacuum distillation of the crude product on a Kugelröhr apparatus afforded (**2.2**) as a white solid. The phosphinite was found to be soluble in organic solvents such as dichloromethane and toluene and only sparingly soluble in PP3.
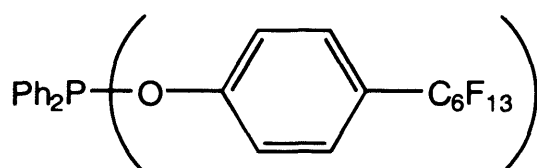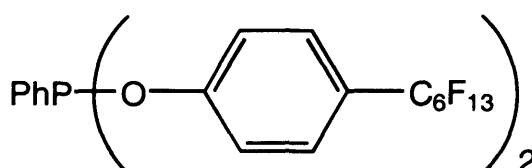
(2.2)   (2.3)

The derivatised phosphonite, bis(4-tridecafluorohexyl) phenylphosphonite (**2.3**), was prepared by the reaction of dichlorophenylphosphine with an excess of derivatised phenol (**2.1**) using the same synthetic route as above. The phosphonite was purified by vacuum distillation and obtained as a white solid. Despite the addition of a second tail the phosphonite was found to exhibit similar solubility behaviour to the mono-derivatised phosphinite and was not preferentially soluble in perfluorinated solvents.

Tris(4-tridecafluorohexyl) phosphite (**2.4**) was prepared using the same procedure used in the synthesis of (**2.2**) by the reaction of phosphorus trichloride with an excess of (**2.1**). The ligand was purified by Kugelröhr distillation and obtained as a clear viscous oil. Phosphite (**2.4**) was found to have a lower solubility in organic solvents than the mono- and bis-derivatised ligands and, most importantly, was readily soluble in PP3 at room temperature. The ligand was found to partition preferentially into the fluorous phase in a biphasic system consisting of equal volumes of dichloromethane and PP3.

$$P \left(O - \left\langle \underset{}{\bigcirc} \right\rangle - C_6F_{13} \right)_3$$

(2.4)
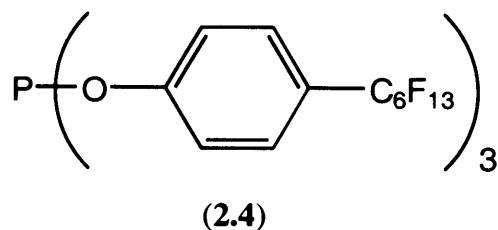
2.3.2 Synthesis of Aryl Phosphites with C_8 and C_{10} Perfluoroalkyl Substituents

Having determined that three perfluoroalkyl tails were necessary to confer preferential fluorous solubility phosphite ligands bearing longer perfluoroalkyl chains were synthesised to determine what effect, if any, this would have on the solubility of the ligands. The derivatised phenols **(2.5)** and **(2.6)** were prepared by the same procedure used to make **(2.1)** by the cross-coupling of 4-iodophenol with $C_8F_{17}I$ and $C_{10}F_{21}I$ respectively and characterised by ^1H, $^{19}F\{^1H\}$ NMR and mass spectrometry. The ^1H NMR spectra of compounds **(2.5)** and **(2.6)** are identical to that for the perfluoro-n-hexyl derivatised phenol **(2.1)**. The $^{19}F\{^1H\}$ NMR spectra are also similar with the exception of the resonances for the additional CF_2 groups which have identical chemical shifts to the $^\delta CF_2$ group which, therefore, overlap and increase the multiplicity of the resonance. Extending the fluorous chain length resulted in a dramatic decrease in the solubility of the phenols in organic solvents in comparison to **(2.1)**. Phenol **(2.6)** was found to have a very low solubility in dichloromethane at room temperature, yet was still readily soluble in diethyl ether.

$$HO - \left\langle \underset{}{\bigcirc} \right\rangle - C_8F_{17} \qquad HO - \left\langle \underset{}{\bigcirc} \right\rangle - C_{10}F_{21}$$

(2.5)   **(2.6)**
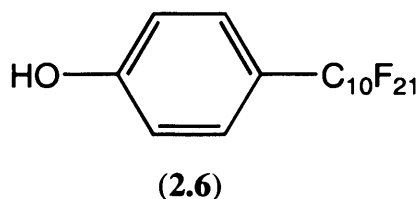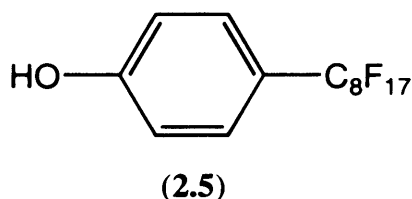
Phosphites **(2.7)** and **(2.8)** were prepared by the same synthetic route as **(2.4)** and obtained as dense white solids. As expected ligand **(2.7)** had a lower solubility than **(2.4)** in dichloromethane and toluene at room temperature and **(2.8)** was found to be insoluble in both. Phosphite **(2.7)**, has recently been reported by Mathivet *et al.*,[34] prepared by an identical procedure and shown to have a solubility of 0.581 Kg/L in $C_8F_{17}I$ at 20 °C. Koch and Leitner have also reported the synthesis of this phosphite

and its application in the rhodium-catalysed hydroformylation of 1-octene in supercritical carbon dioxide.[35]

$$P \left(O - \underset{}{\bigcirc} - C_8F_{17} \right)_3$$ (2.7) $$P \left(O - \underset{}{\bigcirc} - C_{10}F_{21} \right)_3$$ (2.8)
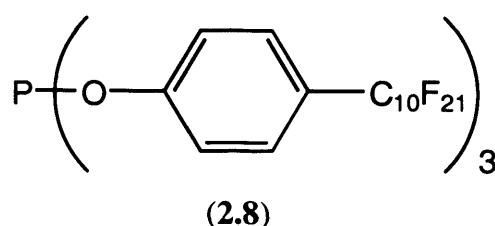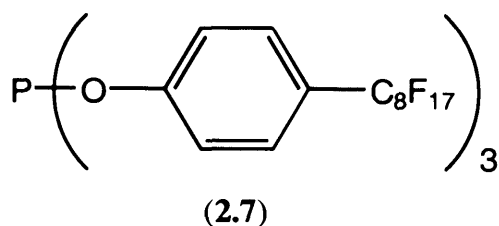
2.3.3 Synthesis of Ortho and Meta Substituted Aryl Phosphites

In addition to the possible modification of the electronic properties of the phosphite ligands arising from the inclusion of the perfluoroalkyl tails, the potential steric influences of derivatisation were also of interest. Therefore, phosphites bearing the perfluoroalkyl substituents in the *meta* and *ortho* positions of the aryl rings were synthesised.

The steric requirements of phosphine and phosphite ligands has been defined by Tolman by measuring the cone angle θ (Figure 2.5). To determine the cone angle, the phosphorus atom is placed 2.28 Å from an apex, a metal atom, and the entire ligand enclosed in a cone generated from the apex. This model works well for symmetrical ligands, however, for unsymmetrical ligands the cone angle measurement is more complex.[36] The modification of Tolman's original methodology to give an indication of ligand shape within the cone has been achieved through the measurement of ligand angular profiles.[37] Recently, work by Smith *et al.* has involved the measurement of cone angle radial profiles to provide an understanding of inter-ligand meshing in systems with two ligands sharing a common apex.[38]
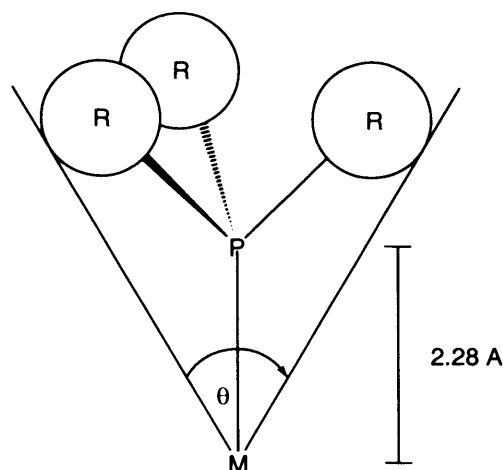
Figure 2.5 Measurement of the Tolman cone angle θ.

To prepare the *ortho-* and *meta-*derivatised phosphites it was necessary to first prepare the derivatised phenols (**2.9**) and (**2.10**) which were synthesised by the same copper-mediated coupling reaction as the *para-*derivatised phenol (**2.1**). Both phenols were obtained in good yields suggesting that the steric and electronic differences in coupling at the *ortho-*, *meta-* or *para-*positions of the aryl ring did not significantly effect the course of the reaction. Interestingly, the resonance of the hydroxyl group in the proton NMR of (**2.10**) is observed as a triplet instead of the expected singlet. This splitting is due to coupling with the two equivalent fluorines of the $^{\alpha}CF_2$ of the perfluoroalkyl chain and has a magnitude of 8.3 Hz. This coupling is believed to be a through space interaction due to the proximity of the OH to the $^{\alpha}CF_2$ as opposed to a $^5J_{HF}$ through bond coupling.

(2.9)   (2.10)   (2.11)

(2.12)   (2.13)
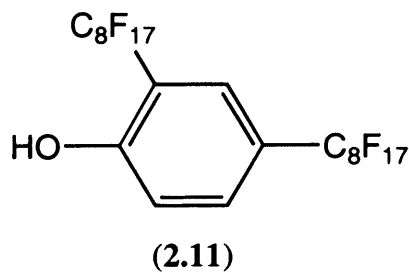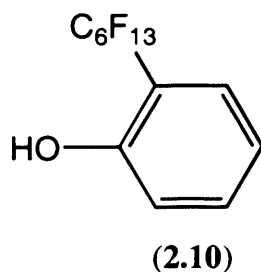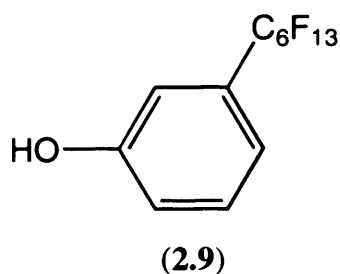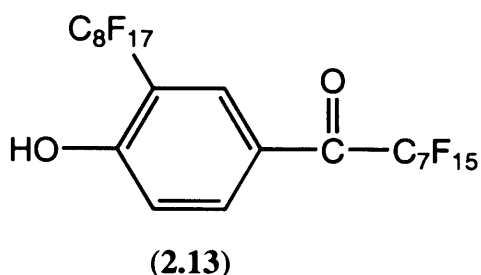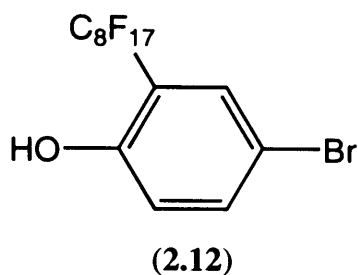
The related derivatised phenol **(2.11)** reported by Mathivet *et al.*[39] was prepared in low yield by the copper-mediated perfluoroalkylation of 2,4-dibromophenol. A complex mixture of reaction products was obtained, composed of 4-bromo-2-perfluorooctylphenol **(2.12)**, bis(perfluorooctyl)phenol **(2.11)** and, preferentially, an unexpected product 4-(1-oxoperfluorooctyl)-2-perfluorooctylphenol **(2.13)**. The absence of 2-bromo-4-perfluorooctylphenol in the reaction mixture suggests that reaction in the *ortho* position is favoured, and that **(2.11)** is formed from 4-bromo-2-perfluorooctylphenol.

Phosphites **(2.14)** and **(2.15)** were synthesised using the same preparative route as the *para*-substituted phosphite **(2.4)**. Both ligands were purified by vacuum distillation on a Kugelröhr apparatus and obtained as clear viscous oils. The *ortho* and *meta* phosphites were found to be far more sensitive towards oxidation and hydrolysis than the *para* phosphites. The initial attempt at the synthesis of ligand **(2.14)** resulted in the formation of the pentavalent phosphate by the addition of oxygen to the phosphite. The phosphate was identified by a characteristically low chemical shift singlet in the ^{31}P NMR spectrum; the absence of a large $^1J_{PH}$ coupling indicated this product did not arise from the usual hydrolysis decomposition pathway from which $O=PH(OC_6H_4\text{-}4\text{-}C_6F_{13})_2$ would have been formed.

(2.14)   (2.15)
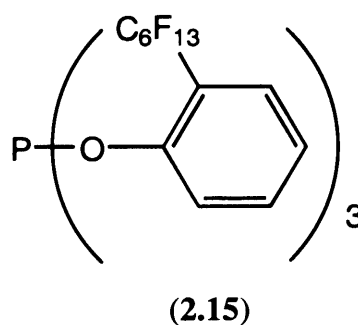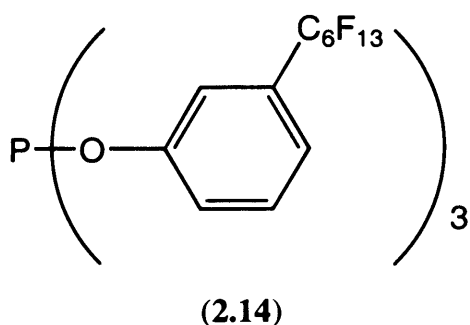
As great care was taken to exclude oxygen from the apparatus it is unlikely that this decomposition arose from atmospheric oxygen. However, a re-examination of the ^{1}H NMR spectra of the *meta*-derivatised phenol indicated that despite distillation, a significant quantity of DMSO was present in the phenol used in the reaction with PCl$_3$. It was thought, therefore, that this may have acted as an oxygen transfer agent, oxidising the phosphite and resulting in the formation of the phosphate and dimethyl sulphide.[40] Studies by Sepiol and Soulen have shown that 1,3-bis(2-hydroxyhexafluoro-2-propyl)-5-(perfluoro-*n*-alkyl)benzenes can form 1:1 molecular complexes with DMSO.[41] These complexes were found to be extremely stable and could be sublimed under reduced pressure without dissociation. The *meta*-derivatised phenol (**2.9**) was freed from DMSO by heating at 80°C with a 5% solution of sodium hydroxide and subsequently precipitated by the addition of hydrochloric acid.

2.4 Synthesis of Alkyl Ligands

It was believed that the aryl group between the oxygen and the perfluoroalkyl chain may act as an insulator, reducing the electron-withdrawing effect of the fluorous moiety on the phosphorus atom.[7] A series of fluorous-derivatised ligands were synthesised in which the aryl 'spacer' is replaced by an ethyl group in order to compare the insulating ability of the two groups.[16] In choosing a suitable insulating group a balance must be made between the solubility of the ligand in fluorous solvents and the degree of insulation offered by the organic spacer, i.e. the relative amounts of fluorous and protio parts in the molecule. The longer the alkyl chain, the greater the insulation offered, however this is accompanied by a decrease in the fluorous solubility of the phosphite. The ethyl group was chosen for comparison as the ligands could readily be prepared by the reaction of the commercially available 1H1H2H2H-perfluorooctan-1-ol with chlorophosphines. The organic bulk of the ethyl unit is significantly less than that of the aromatic ring and the effect of this on the relative solubilities of the ligands and their metal complexes was of interest.

The alkyl phosphinite (**2.16**) was prepared in the same manner as the aryl ligands above by the reaction of an excess of 1H1H2H2H-perfluorooctan-1-ol with chlorodiphenylphosphine. Purification by Kugelröhr distillation afforded the pure

product as a colourless liquid. The phosphonite (2.17) was prepared similarly by the reaction of dichlorophenylphosphine with the fluorous alcohol to afford the pure product as a clear colourless liquid after Kugelröhr distillation.

$Ph_2POCH_2CH_2C_6F_{13}$

(2.16)

$PhP(OCH_2CH_2C_6F_{13})_2$

(2.17)

$P(OCH_2CH_2C_6F_{13})_3$

(2.18)
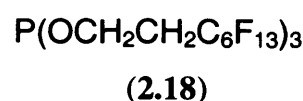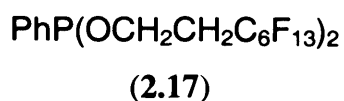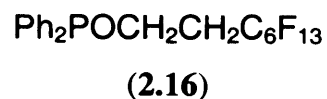
The phosphite (2.18) was obtained by the reaction of phosphorus trichloride with 1H1H2H2H-perfluorooctan-1-ol and purified by Kugelröhr distillation to afford the product as a clear colourless liquid. The alkyl ligands were all found to be soluble in toluene, dichloromethane and hexane. As with the aryl analogues the alkyl ligands were found to be extremely air- and moisture-sensitive. Ligands (2.16) and (2.18) have recently been reported by Haar *et al.*[42] using the same synthetic protocol employed here with the exception of purification of the crude products which were used as obtained. In this work, the ligands were applied to thermochemical studies and the rhodium-catalysed biphasic hydrogenation of 1-hexene under biphasic conditions.

2.5 Characterisation of Derivatised Ligands

Ligands (2.2-2.4), (2.7-2.8), and (2.14-2.18) were characterised by ^1H, ^{19}F and ^{31}P NMR spectroscopy, FAB mass spectrometry and elemental analysis. In all cases the parent ion $[M]^+$ was observed in the FAB mass spectra of the ligands, with evidence of the phosphate $[M+O]^+$ observed in some cases due to oxidation as the mass spectra were run. The $^{19}F\{^1H\}$ NMR spectra for the ligands are almost identical to the free alcohol or phenol as shown in Figure 2.3 and are relatively uninformative. The values of $^3J_{FF}$ and $^4J_{FF}$ coupling are highly consistent and of the same magnitude for both the alkyl and aryl ligands. One notable difference between the spectra of the ligands is the chemical shift of the $^\alpha CF_2$ resonance. In the *para*-derivatised aryl ligands, it is at approximately -110.5 ppm, whereas in the *ortho-* and the *meta*-derivatised phosphites it is at -108.5 and -111.5 ppm respectively. In the case of the alkyl ligands the chemical shift of the $^\alpha CF_2$ resonance is approximately -113.5 ppm.

This variation is expected as the $^{\alpha}CF_2$ is adjacent to the organic spacer unit, therefore, changing this from an alkyl to an aryl group or changing the position of the substituent on the aryl ring is likely to effect the shielding of the CF_2 group.

The $^{31}P\{^1H\}$ NMR spectra of all the ligands exhibited a singlet with a chemical shift indicative of a phosphinite, phosphonite or phosphite (Table 2.1). The chemical shifts of the perfluoroalkyl derivatised aryl ligands are the same as those of their protio analogues. The similarity of the values of δ_P obtained for the *ortho-* and *meta-*derivatised phosphites with that for the *para-*derivatised phosphite suggests that the position of the perfluoroalkyl group on the aryl ring has no significant influence on the environment at phosphorus. The chemical shifts of the derivatised alkyl ligands are slightly lower than those of their protio analogues with the variation diminishing with increasing number of perfluoroalkyl substituents.

Table 2.1 ^{31}P NMR data for perfluoroalkyl chain derivatised phosphinites, phosphonites and phosphites and their protio analogues.

Ligand		δ_P	Ligand		δ_P
$P(OAr\text{-}4\text{-}R_f)_3{}^a$	(2.4)	125	$P(OAr\text{-}3\text{-}R_f)_3{}^a$	(2.14)	126
$P(OPh)_3{}^{b,c}$		128	$P(OAr\text{-}2\text{-}R_f)_3{}^a$	(2.15)	126
$PhP(OAr\text{-}4\text{-}R_f)_2{}^a$	(2.3)	159	$P(OC_2H_4R_f)_3{}^a$	(2.18)	139
$PhP(OPh)_2{}^{b,c}$		159	$P(OEt)_3{}^{b,d}$		137
$Ph_2POAr\text{-}4\text{-}R_f{}^a$	(2.2)	113	$PhP(OC_2H_4R_f)_2{}^a$	(2.17)	157
$Ph_2POPh^{b,c}$		111	$PhP(OEt)_2{}^{b,d}$		153
$P(OAr\text{-}4\text{-}R_f{}')_3{}^a$	(2.7)	125	$Ph_2POC_2H_4R_f{}^a$	(2.16)	116
$P(OAr\text{-}4\text{-}R_f{}'')_3{}^a$	(2.8)	125	$Ph_2POEt^{b,d}$		110

^{a}Recorded in $C_6D_5CD_3$. ^{b}Recorded in $CDCl_3$. ^{c}Ref. 43. ^{d}Ref. 44. $R_f=C_6F_{13}$, $R_f{}'=C_8F_{17}$, $R_f{}''=C_{10}F_{21}$.

Comparison of the data for the aryl and alkyl ligands in Table 2.1 indicates that inclusion of the perfluoroalkyl group in the alkyl ligands has a greater influence on the chemical shift than ligands with an aromatic spacer. Cobley and Pringle[45] have shown that for *para-*substituted triarylphosphites there is a strong correlation between δ_P and the Hammett constant of the substituent. The more electron-withdrawing the

substituent the more the phosphorus is shielded, hence the lower the chemical shift. However, the difference observed in chemical shift between a phosphite with an electron-donating substituent such as a methyl group and an electron-withdrawing substituent such as fluorine was only 0.3 ppm. Triarylphosphine ligands were found to show no clear trend between δ_P and the Hammett constant and it is, therefore, unclear if phosphonites and phosphinites will show a correlation like the phosphites. The interpretation of the chemical shift data for the perfluoroalkyl-derivatised ligands in relation to the electron-withdrawing effect of the fluorous chains has not been attempted as δ_P is not only dependent upon the electronegativity of the substituents, but also upon steric effects and molecular orbital occupancy.[46]

The ^{1}H NMR spectra of the *para*-substituted aryl phosphites are similar to that of the phenol (2.1) exhibiting the familiar AA′XX′ spin system. The doublet resonances are shifted to a lower frequency by approximately 0.2 ppm compared to those for the free phenol accompanied by an increase in $^3J_{HH}$ coupling to 8.5 Hz. The ^{1}H NMR spectra of the *para*-derivatised phosphinite (2.2) and phosphonite (2.3) ligands are more complex exhibiting multiplets for the resonances of the unsubstituted phenyl protons as well as the AA′XX′ pattern for the aryl rings bearing the perfluoroalkyl groups.

The ^{1}H NMR spectra of the alkyl ligands (2.16) and (2.18) are essentially the same as for $C_6F_{13}C_2H_4OH$ exhibiting almost identical chemical shifts and coupling constants. The OCH_2 resonances appear as virtual quartets due to the similar magnitudes of the $^3J_{HH}$ and the $^3J_{PH}$ coupling, collapsing to triplets in the phosphorus decoupled spectra. The CH_2CF_2 resonances are observed as triplets of triplets for both ligands due to $^3J_{HH}$ and $^3J_{HF}$ coupling with no resolvable $^4J_{PH}$ coupling to the phosphorus. The ^{1}H NMR spectra of the alkyl phosphonite (2.17) exhibits the OCH_2 and CH_2CF_2 resonances as complex second-order multiplets. Comparison of the ^{1}H and ^{1}H\{^{19}F\} NMR spectra shows that no $^4J_{HF}$ coupling to the OCH_2 protons exists in the molecule. Therefore, the multiplicity of this resonance must arise from a combination of $^3J_{HH}$ and $^3J_{PH}$ coupling. A decrease in the multiplicity is seen on phosphorus decoupling, however the spectrum remains highly complex rather than giving the expected triplet if only $^3J_{HH}$ coupling is present. Homodecoupling of the protons of the CH_2CF_2 group with phosphorus coupling remaining dramatically changes the OCH_2 resonance. However, the spectrum remains too complex to be

resolved. As the OCH$_2$ protons are coupling to a single phosphorus nucleus the complexity must arise from the chemical inequivalence of the two protons.

In order to test this hypothesis the ^{1}H$\{^{31}$P$\}$ NMR spectrum was simulated using gNMR v4.0, an NMR simulation program. Figure 2.6 shows the simulated spectrum (top) with the actual spectrum (bottom) for comparison. The simulation of the OCH$_2$ resonances is based on a spin system in which the inequivalent protons couple geminally to one another, and vicinally to the protons of the CH$_2$CF$_2$ group. Geminal coupling constants are usually negative. Their magnitudes are dependent mainly on the substituents, but are also affected by the H-C-H bond angle and the hybridisation of the carbon atom. The simulated spectrum gave a value of -10.9 Hz for the $^2J_{HH}$ coupling between the OCH$_2$ protons, almost identical to the value of -10.8 Hz obtained for the $^2J_{HH}$ coupling in CH$_3$OH.[47] The magnitudes of the vicinal coupling of the OCH$_2$ protons, H$_a$ and H$_b$ (Figure 2.7), to the CH$_2$CF$_2$ protons were also found to be inequivalent, $^3J_{HH}$ being 5.85 Hz for H$_a$ and 6.22 Hz for H$_b$.
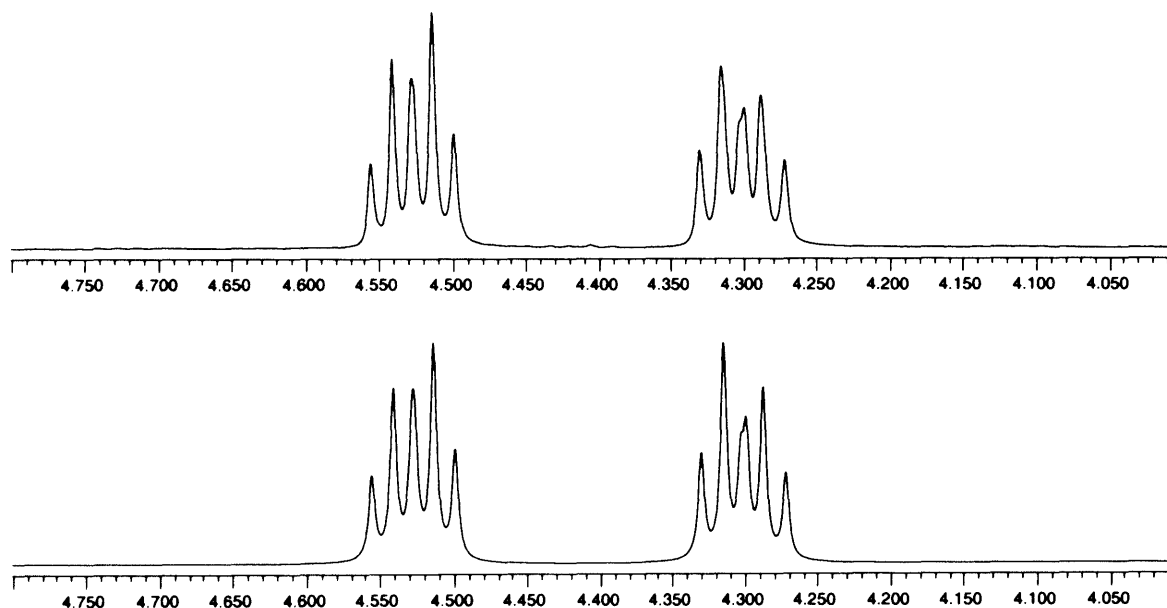
Figure 2.6 Actual (top) and simulated (bottom) ^{1}H$\{^{31}$P$\}$ NMR spectrum of OCH$_2$ resonances of PhP(OC$_2$H$_4$C$_6$F$_{13}$)$_2$ (2.17).

To explain how the inequivalence of the two OCH$_2$ protons arises it is useful to consider the symmetry of the phosphonite ligand (2.17) in comparison to the phosphinite and phosphite ligands (2.16) and (2.18). A plane of symmetry exists in

the phosphinite and phosphite molecules down the carbon backbone of the perfluoroalkyl chains. No such symmetry exists in the phosphonite as can be seen if a mirror plane is placed down one of the perfluoroalkyl chains of the ligand (Figure 2.7). Hence, protons H_a and H_b are chemically inequivalent, as are H_c and H_d. The protons on either side of the alkyl chain backbone are, therefore, chemically and magnetically inequivalent giving an ABXY spin system.
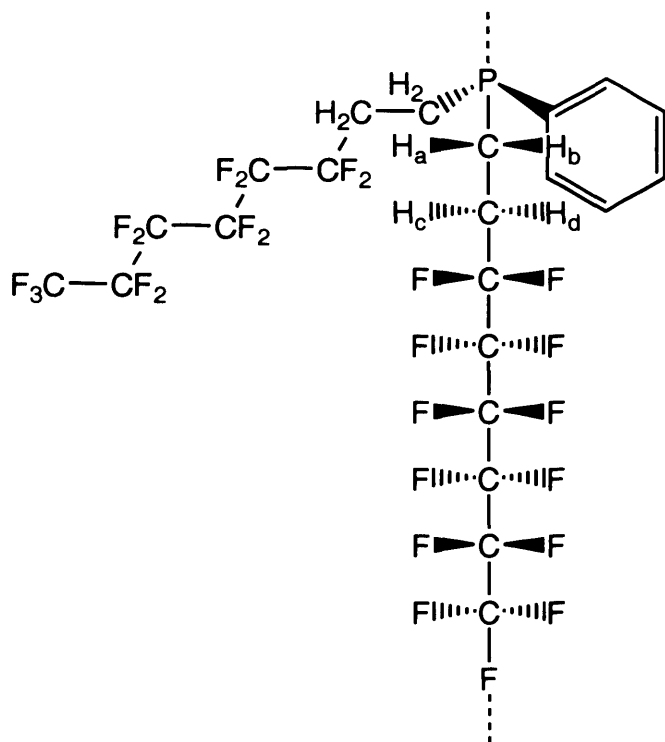
Figure 2.7 Diagram of $PhP(OC_2H_4C_6F_{13})_2$ (2.17) with a mirror plane placed down the backbone of one of the perfluoroalkyl chains.

2.6 Discussion of Ligand Stability

Phosphite triesters are far more stable towards oxidation than phosphines. However, they are intrinsically unstable towards hydrolysis, particularly under mildly acidic or alkaline conditions and hydrolyse to phosphonates (Scheme 2.3).[48] The literature contains conflicting statements relating to the stability of phosphites which is variable and dependent on the nature of the R group, alkyl phosphites being more

reactive than their aryl counterparts. Phosphonates are readily identified using ^{31}P NMR spectroscopy by the marked low frequency shift in comparison to the parent phosphite, and the large $^{1}J_{PH}$ coupling. In the case of the derivatised phosphite (2.4) the chemical shift of the doublet resonance for the hydrolysis product is 0 δ as compared to 125 δ for the phosphite with a $^{1}J_{PH}$ value of 745 Hz.

$$\underset{RO}{\overset{RO}{\diagdown}}P-OR \quad + \quad H_2O \quad \longrightarrow \quad \underset{RO}{\overset{RO}{\diagdown}}\overset{O}{\underset{H}{\diagup\!\!\diagdown}}P \quad + \quad ROH$$
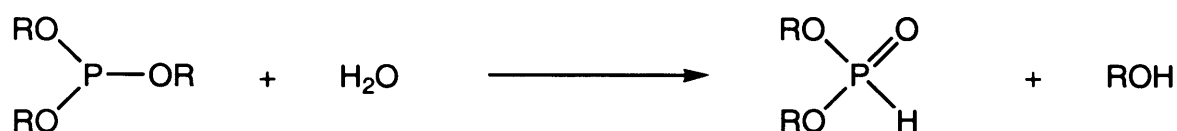
Scheme 2.3 Mechanism of phosphite hydrolysis.

Phosphonites and phosphinites are also susceptible to hydrolysis, although to a lesser extent than phosphites, forming phosphinates (Scheme 2.4) and unsymmetrical phosphine oxides (Scheme 2.5) respectively, the order of reactivity of the ligands being $POR_3 > RP(OR)_2 > R_2POR$.

$$\underset{RO}{\overset{RO}{\diagdown}}P-R \quad + \quad H_2O \quad \longrightarrow \quad \underset{RO}{\overset{R}{\diagdown}}\overset{O}{\underset{H}{\diagup\!\!\diagdown}}P \quad + \quad ROH$$
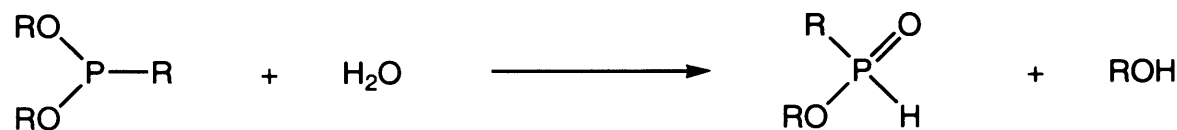
Scheme 2.4 Mechanism of phosphonite hydrolysis.

$$\underset{R}{\overset{R}{\diagdown}}P-OR \quad + \quad H_2O \quad \longrightarrow \quad \underset{R}{\overset{R}{\diagdown}}\overset{O}{\underset{H}{\diagup\!\!\diagdown}}P \quad + \quad ROH$$
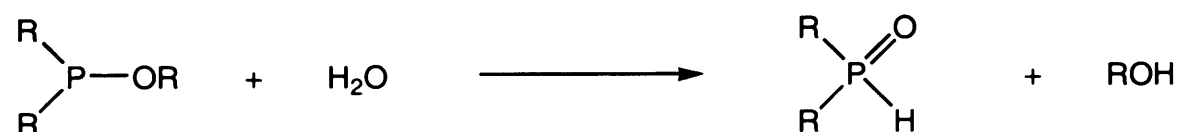
Scheme 2.5 Mechanism of phosphinite hydrolysis.

The *para*-derivatised perfluoroalkylphosphites are relatively stable to oxidation in air unlike the phosphonite and phosphinite ligands, however they do undergo significant hydrolysis in the presence of water. This is in agreement with observations by Mathivet *et al.*[34] that the complete hydrolysis of (2.7) to H_3PO_3 and the corresponding phenol occurs at room temperature in a 50/50 THF-water mixture in 24 hours. The reaction was found to proceed at a much faster rate in the presence of

trace amounts of acid as observed previously with phosphites.[49] The electron-withdrawing effect arising from the inclusion of the perfluoroalkyl chains increases the reactivity of the P-O bond to hydrolysis and results in phosphites with a much lower stability than their non-derivatised protio analogues. Perfluoroalkylation in the *ortho* and *meta* positions of the arene ring dramatically increases the hydrolytic sensitivity of the phosphites. Ligands (2.14) and (2.15) were found to be significantly less stable than (2.4), undergoing rapid hydrolysis when open to atmospheric moisture. Phosphite (2.19) prepared by Mathivet *et al.*[39] was found to have a much lower hydrolytic stability compared to (2.7) although this was attributed to the cumulative electronic influence of the two perfluoroalkyl groups rather than the effect of perfluoroalkylation in the *ortho* position.

(2.19)
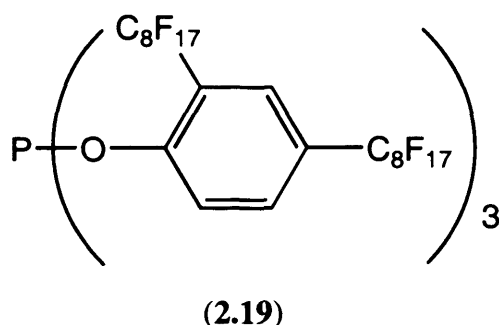
The sensitivity of the derivatised alkyl ligands (2.16-2.18) towards hydrolysis is more pronounced than for the *para*-substituted aryl ligands. The difficulty found in handling the alkyl phosphite is in marked contrast to observations made by Shreeve and Williamson[50] who found that the fluorocarbon-derived phosphite $P(OCH_2CF_3)_3$ allowed for greater experimental ease than its protio analogue $P(OC_2H_5)_3$ due to increased oxygen and moisture stability.

References for Chapter 2

[1]   G. W. Parshall, S. D. Ittel, *Homogeneous Catalysis*, 2nd ed., John Wiley & Sons, 1992. pp. 25-50.

[2]   F. Ungvary, *Coord. Chem. Rev.*, 1999, **188**, 263.

[3]   M. J. Baker, K. N. Harrison, A. G. Orpen, P. G. Pringle and G. Shaw, *J. Chem. Soc., Chem. Commun.*, 1991, 803.

[4]   W. C. Drinkard and R. V. Lindsey, U. S. Patent 3,496,215, 1970.

[5]   K. Nozaki, N. Sato and H. Takaya, *J. Am. Chem. Soc.*, 1995, **117**, 9911.

[6]   S. Benefice-Malouet, H. Blancou and A. Commeyras, *J. Fluorine Chem.*, 1979, **14**, 511.

[7]   I. T. Horváth and J. Rábai, *Science*, 1994, **266**, 72.

[8]   D. R. Paige, *The Synthesis, Coordination Chemistry and Catalytic Applications of Phosphine Ligands Containing Long-Chain Perfluoroalkyl Groups*, Ph.D. Thesis, University of Leicester, 1997.

[9]   B. Betzemeier and P. Knochel, *Angew. Chem., Int. Ed. Engl.*, 1997, **36**, 2623.

[10]   P. W. N. M. van Leeuwen and C. F. Roobeek, *J. Organomet. Chem.*, 1983, **258**, 343.

[11]   C. A. Tolman, W. C. Seidel, J. D. Druliner and P. J. Domaille, *Organometallics*, 1984, **3**, 338.

[12]   L. Fan and T. Ziegler, *J. Chem. Phys.*, 1991, **95**, 7401.

[13]   J. D. Petke and J. L. Whitten, *J. Chem. Phys.*, 1973, **59**, 4855.

[14]   C. C. Levin, *J. Am. Chem. Soc.*, 1975, **97**, 5649.

[15]   D. S. Marynick, *J. Am. Chem. Soc.*, 1984, **106**, 4064.

[16]   Z. Berkovitch-Yellin, D. E. Ellis, W. C. Trogler and S. -X. Xiao, *J. Am. Chem. Soc.*, 1983, **105**, 7033.

[17]   W. Cherry and N. Epiotis, *J. Am. Chem. Soc.*, 1976, **98**, 1135.

[18]   P. Bhattacharya, D. Gudmunsen, E. G. Hope, R. D. W. Kemmitt, D. R. Paige and A. M. Stuart, *J. Chem. Soc., Perkin Trans. 1*, 1997, 3609.

[19]   J. P. Forsman and D. Lipkin, 1953, 3145.

[20]   P. Majewski, *Phosphorus Sulfur*, 1987, **33**, 37.

[21]   E. E. Nifantev, M. K. Gratchev, S. Y. Burmistrov, L. V. Vasyanina, M. Y. Antipin and Y. T. Struchkov, *Tetrahedron*, 1991, **47**, 9839.

[22]   L. Maier, *Helv. Chim. Acta*, 1969, **52**, 858.

[23]   L. Maier, *Helv. Chim. Acta*, 1963, **46**, 2667.

[24]   M. Sander, *Chem Ber.*, 1960, **93**, 1220.

[25]   I. F. Lutsenko, M. V. Proskumia and N. B. Karlstedt, *Phosphorus*, 1973, **3**, 55.

[26]   C. Brown, *Phosphorus Sulfur*, 1979, **6**, 481.

[27]   V. C. R. McLoughlin and J. Thrower, *Tetrahedron*, 1969, **25**, 5921.

[28]   G. J. Chen, L. S. Chen and K. C. Eapen, *J. Fluorine Chem.*, 1993, **65**, 59.

[29]   G. J. Chen and C. Tamborski, *J. Fluorine Chem.*, 1989, **43**, 207.

[30]   *Chemistry of Organic Fluorine Compounds II*, ed by M. Hudlický and A. E. Pavlath, ACS Monograph, Washington, 1995. pp. 699-716.

[31]   P. Calas and A. Commeyras, *J. Electroanal. Chem.*, 1979, **89**, 363.

[32]   Q. -Y. Chen, Z. -Y. Yang and Y. -B. He, *J. Fluorine Chem.*, 1987, **37**, 171.

[33]   G. J. Chen and C. Tamborski, *J. Fluorine Chem.*, 1990, **46**, 137.

[34]   T. Mathivet, E. Monflier, Y. Castanet, A. Mortreux and J. L. Couturier, *Tetrahedron Lett.*, 1998, **39**, 9411.

[35]   D. Koch and W. Leitner, *J. Am. Chem. Soc.*, 1998, **120**, 13398.

[36]   C. A. Tolman, *Chem. Rev.*, 1977, **77**, 33.

[37]   G. Ferguson, P. J. Roberts, E. C. Alyea and M. Khan, *Inorg. Chem.*, 1978, **17**, 2965.

[38]   J. M. Smith, B. C. Taverner and N. J. Coville, *J. Organomet. Chem.*, 1997, **530**, 131.

[39]   T. Mathivet, E. Monflier, Y. Castanet, A. Mortreux and J. L. Couturier, *Tetrahedron Lett.*, 1999, **40**, 3885.

[40]   *The Chemistry of Organophosphorus Compounds*, Volume 4, Ed. F. R. Hartley, John Wiley & Sons, 1996. pp. 25.

[41]   J. Sepiol and R. Soulen, *J. Fluorine Chem.*, 1984, **24**, 61.

[42]   C. M. Haar, J. Huang, S. P. Nolan and J. L. Peterson, *Organometallics*, 1998, **17**, 5018.

[43]   F. H. Allen, A. Pidcock and C. R. Waterhouse, *J. Chem. Soc. A.*, 1970, 2087.

[44]   J. C. Tebby, *CRC Handbook of ^{31}P NMR*, C.R.C. Press, Florida, 1991.

[45]   C. J. Cobley and P. G. Pringle, *Inorg. Chim. Acta*, 1997, **265**, 107.

[46]   S. O. Grim and A. W. Yankowsky, *Phosphorus and Sulphur*, 1977, **3**, 191.

[47]   H. Friebolin, *Basic One- and Two-Dimensional NMR Spectroscopy*, 2nd ed.,

VCH Verlagsgesellschaft, Weinheim, 1993.

[48]   D. E. C. Corbridge, *Phosphorus an Outline of its Chemistry, Biochemistry and*

Technology, Elsevier Science B.V., Netherlands, 1995.

[49]   F. H. Westheimer, S. Huang and F. Covitz, *J. Am. Chem. Soc.*, 1988, **110**, 181.

[50]   J. M. Shreeve and S. M. Williamson, *Organometallics*, 1984, **3**, 1104.

Chapter Three

3.1 Bonding of Phosphorus(III) Ligands to Transition Metals

The bonding in metal phosphine and metal phosphite complexes was traditionally described using the Dewar-Chatt model in which the PX_3 ligand forms a σ-bond with the metal by donating charge through the phosphorus lone pair with concomitant π-back-donation of charge from metal d orbitals into empty phosphorus $3d$ orbitals.[1,2] Critics of this model argued that in many cases molecular orbital calculations showed that phosphorus $3d$ orbitals were of too high an energy to effectively overlap with metal d orbitals.[3] Studies by Marynick[4] and Braga[5] demonstrated that phosphorus ligands could act as π-acceptors in transition metal complexes without the participation of $3d$ orbitals on phosphorus. Marynick proposed that antibonding P-X σ-orbitals were involved in the description of the phosphorus π-acceptor orbitals. Subsequently, Orpen and Connelly undertook the analysis of M-P and P-X bond lengths in transition metal complexes, determined by X-ray crystallography, in which the oxidation state was varied, to compare the theoretical predictions of the participation of P-X σ^* orbitals in M-P π-bonding with experimental observations.[6] In complexes where oxidation was primarily metal based, oxidation resulted in increased M-P bond lengths with concomitant shortening of the P-X bonds. The observed changes in M-P bond lengths indicate an important π-component in the description of the M-P bond, with the accompanying change in P-X bond distances in accordance with the prediction that P-X σ^* orbitals act as π-acceptor orbitals. Molecular orbital calculations carried out by Pacchioni *et al.* including d polarization functions on phosphorus have been shown to increase the interaction between the metal and the phosphorus ligand resulting in improved back-donation to the phosphorus σ^* orbitals.[7] Mixing of P-X σ^* orbitals and P $3d_{xy}$ and $3d_{xz}$ orbitals form orthogonal, doubly degenerate P π-acceptor orbitals of the correct symmetry to overlap with metal d orbitals as shown in Figures 3.1 and 3.2. The lone pair on phosphorus forms a σ-bond with the metal centre by donation of electron-density into unoccupied metal d orbitals, with concomitant back-donation from filled metal d orbitals into hybridized phosphorus $3d\sigma^*$ orbitals forming a π-bond.
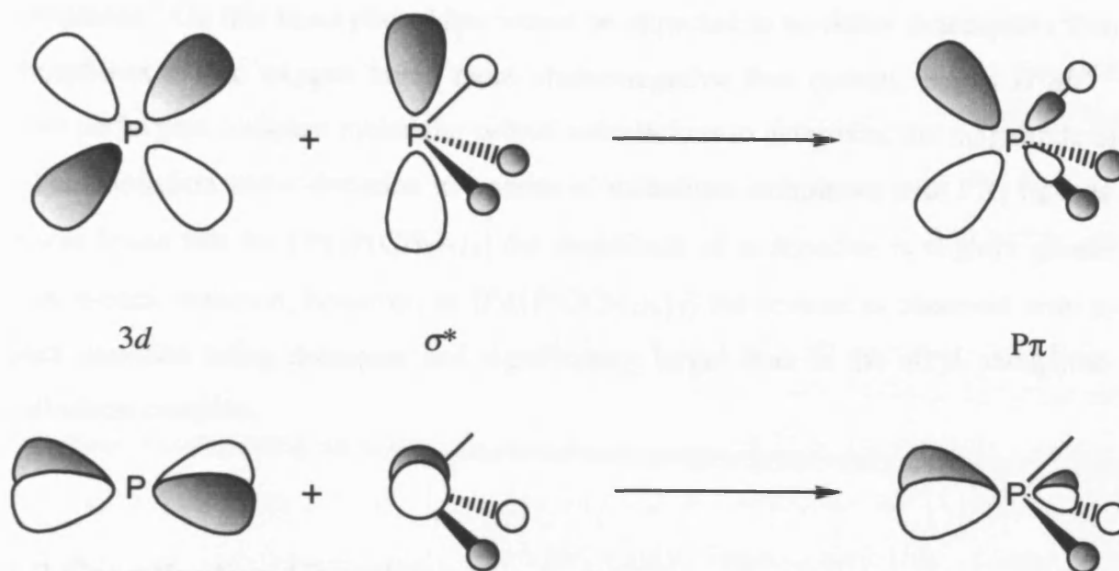
Figure 3.1 Molecular orbital representation of the hybridisation of P σ^* orbitals with P $3d_{xy}$ and $3d_{xz}$ orbitals.
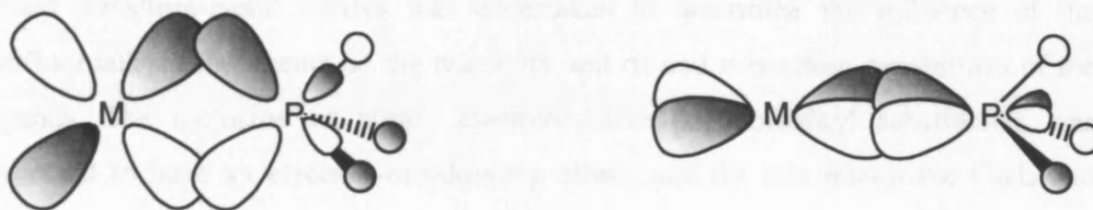
Figure 3.2 Molecular orbital representation of the π-bonding between metal d_{xy} and d_{xz} orbitals with P π-acceptor orbitals.

Lyne *et al.* demonstrated that phosphorus d orbitals are significant in the description of bonding to the metal centre, however, their role is essentially that of polarization functions which favour the formation of hybridized π-orbitals as opposed to that of acceptor orbitals.[8] The involvement of d orbitals considerably reinforces back-bonding causing a shortening and strengthening of the M-P bond, although this effect is more important for alkyl and aryl phosphines than ligands such as PF_3 and phosphites. In accordance with this model the π-accepting ability of PX_3 ligands should increase as X becomes more electronegative due to a decrease in the energy of the P-X σ^* orbitals, thus increasing their energetic accessibility.[4] Indeed, it has been

shown experimentally that PF_3 is a π-acceptor of comparable strength to CO in metal complexes.[5] On this basis phosphites would be expected to be better π-acceptors than phosphines due to oxygen being more electronegative than carbon. Bagus *et al.*[9,10] have performed complex molecular orbital calculations to determine the magnitude of π-back donation and σ-donation in a series of palladium complexes with PX_3 ligands. It was found that for $[Pd\{P(CH_3)_3\}_3]$ the magnitude of σ-donation is slightly greater than π-back donation, however, in $[Pd\{P(OCH_3)_3\}_3]$ the reverse is observed with π-back donation being dominant and significantly larger than in the alkyl phosphine-palladium complex.

3.2 Coordination Chemistry

An investigation into the coordination chemistry of the derivatised phosphinite, phosphonite and phosphite ligands discussed in chapter 2 with platinum group transition-metal centres was undertaken to determine the influence of the perfluoroalkyl substituents on the reactivity and σ- and π-bonding capabilities of the ligands. The inclusion of highly electronegative perfluoroalkyl substituents was expected to have an electron-withdrawing effect, and for this reason the C_2H_4 and C_6H_4 spacer groups have been included to try to insulate the phosphorus atom. Analysis of the coordination complexes would yield information about the efficiency of the insulating group at preventing the perfluoroalkyl group from reducing the electron density at phosphorus. The experiments were also carried out in order to determine the requirements for the synthesis of preferentially fluorous phase soluble metal complexes with the aim of preparing fluorous soluble hydroformylation catalysts.

As discussed in section 3.1 the electronic properties of PX_3 ligands are dependent on the nature of the X substituent. As a result the phosphinite $R_2P(OR)$, phosphonite $RP(OR)_2$ and phosphite ligands $P(OR)_3$ exhibit different physical and chemical properties and therefore form three distinct classes of ligand. Bagus *et al.* have determined that the π-acceptor ability of PX_3 ligands increases with the increasing electronegativity of the X substituent.[10,11] As the electronegativities of alkoxy and aryloxy groups is greater than those of alkyl and aryl groups the π-

acceptor ability of phosphinite and phosphonite ligands are intermediate between those of phosphites and phosphines. The differences in electronic properties between the various classes of ligands therefore give rise to spectroscopic variations between both the free ligands and their respective coordination complexes. Through the interpretation of the spectroscopic analyses of a series of complexes for each class of ligands, Saunders and co-workers have shown that the π-bonding ability of phosphorus ligands follows the order $P(OR)_3 > PR(OR)_2 > PR_2(OR) > PR_3$.[46] To determine the influence of the perfluoroalkyl substituents on the electronic properties of the derivatised alkoxy and aryloxy phosphinite, phosphonite and phosphite ligands it is necessary to make parallels with the protio parent ligands and their complexes. This will require comparison of the spectroscopic data obtained for the derivatised ligands with that for six sets of protio parent ligands and their complexes. Unfortunately, many of the protio ligand complexes either do not exist or the desired spectroscopic data is unavailable. It has, therefore, been necessary to prepare several of these complexes for comparative purposes. Only selected complexes, such as the $[RhCl(CO)L_2]$ complexes, have been prepared as time and interest constraints determined that little information would be gained from the preparation and analysis of all the unavailable protio parent complexes.

The complexes described in this chapter have been characterised using ^1H, ^{19}F and ^{31}P NMR spectroscopy, IR spectroscopy, X-ray crystallography, mass spectrometry and elemental analysis.

3.2.1 Platinum (II) complexes of the type $[PtCl_2L_2]$

The characterisation and structural assignment of coordination complexes with phosphorus ligands is considerably aided when coupling occurs between the metal and the phosphorus nuclei ($^1J_{M-P}$) or between the phosphorus and other donor ligands ($^2J_{P-L}$).[11] The platinum isotope ^{195}Pt (natural abundance 33%, nuclear spin ½) exhibits coupling to phosphorus, thereby providing important information about the geometry of the complex beyond that derived from the symmetry of the spectra. The magnitude of the $^1J_{Pt-P}$ coupling constant also provides information regarding the nature of the M-P bond and the electronic properties of the ligand. Platinum complexes of the

perfluoroalkyl chain derivatised ligands were therefore prepared to investigate the influence of the C_6F_{13} group on the $^1J_{Pt-P}$ coupling constant and hence the M-P bond.

Complexes of the type [PtCl$_2$L$_2$] in which L is a phosphorus(III) ligand are readily prepared from cis-[PtCl$_2$(MeCN)$_2$][12] by the displacement of the MeCN ligands with PX$_3$ ligands under mild conditions (Scheme 3.4). Cis-[PtCl$_2$(MeCN)$_2$] is a convenient starting material in comparison to [PtCl$_2$] as it has greater solubility in common organic solvents. The cis-geometry of the starting material is often retained in the reaction product, although the geometry of the product is dependent on both the steric and electronic properties of the displacing phosphorus ligand. Experimental observations have shown that ligands of the type $R_xP(OR)_{3-x}$ have a tendency to form cis-complexes with platinum(II).[13] This preference can be explained in terms of the stabilisation conferred by M-P π-back-bonding. Due to the symmetry of the metal d orbitals the opportunity for M-P π-back-bonding is increased when the ligands have a cis-disposition as the interaction of the phosphorus π-acceptor orbitals with the metal d orbitals is greater than in the trans-geometry.[14] The flexibility of the P-O bonds in phosphinite, phosphonite and phosphite ligands is also a factor, decreasing steric crowding and hence conformational strain when the ligands are mutually cis.[15] Platinum(II) complexes with tertiary phosphorus ligands are of interest as they homogeneously catalyse a wide range of reactions.[16] Mixtures of platinum(II)/tin(II) chlorides have been extensively investigated due to their ability to catalyse hydrogenation[17], hydroformylation,[18] and carbonylation[19] reactions.
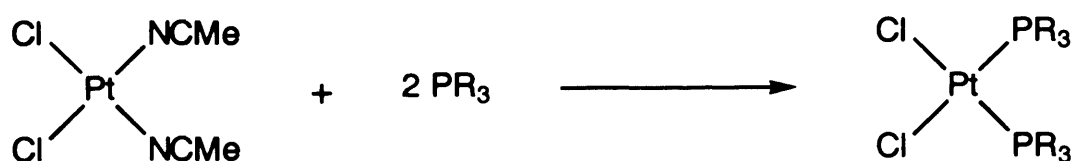
Scheme 3.4 Reaction of tertiary phosphorus ligands with cis-[PtCl$_2$(MeCN)$_2$].

Complexes cis-[PtCl$_2$\{Ph$_2$P(OC$_6$H$_4$-4-C$_6$F$_{13}$)\}$_2$] (3.1), cis-[PtCl$_2$\{PhP(OC$_6$H$_4$-4-C$_6$F$_{13}$)$_2$\}$_2$] (3.2) and cis-[PtCl$_2$\{P(OC$_6$H$_4$-4-C$_6$F$_{13}$)$_3$\}$_2$] (3.3) were synthesised by the reaction of cis-[PtCl$_2$(MeCN)$_2$] with an excess of the respective ligands (2.2-2.4) in

refluxing dichloromethane under nitrogen. Complexes (3.1-3.3) were isolated in approximately 60–70% yield and obtained exclusively as the cis-isomers. All complexes were found to be air- and moisture-stable. Evidence for the formation of complexes (3.1-3.3) was provided by their FAB mass spectra which showed peaks for parent ion fragments [(M-Cl)$^+$] and [(M-2Cl)$^+$] and by elemental analyses. Complexes (3.1) and (3.2) are readily soluble in cold dichloromethane, however, complex (3.3) has only limited solubility, precipitating out of solution as the reaction mixture cooled. Complex (3.3) was found to be insoluble in most common organic and deuterated solvents, and only sparingly soluble in deuterated acetone. It was also found to be insoluble in perfluorinated solvents. Despite the ready solubility of the para-derivatised phosphite (2.4) in perfluorinated solvents, complex (3.3) was found to be insoluble in PP3 and, therefore, incompatible with FBS. Reasonable solubility in Et$_2$O was observed and so the ^{31}P NMR spectrum was obtained by making up an ethereal solution of the complex and using a sealed capillary containing D$_2$O inside the NMR tube.

The ^{31}P NMR spectra of complexes (3.1-3.3) exhibit singlets and accompanying platinum satellites (see Figure 3.1) with $^1J_{Pt-P}$ coupling constants of 4189 Hz, 4859 Hz and 5660 Hz respectively. The complexes were determined to be the cis-isomers by comparison of chemical shift (δ_P) values and $^1J_{PtP}$ coupling constants with values obtained for cis- and trans-isomers of these complexes with a variety of tertiary phosphorus ligands.[20] The δ_P of the ligand in the complex is at a lower frequency than that for the free ligand as the phosphorus atom becomes less shielded on coordination to the metal centre.
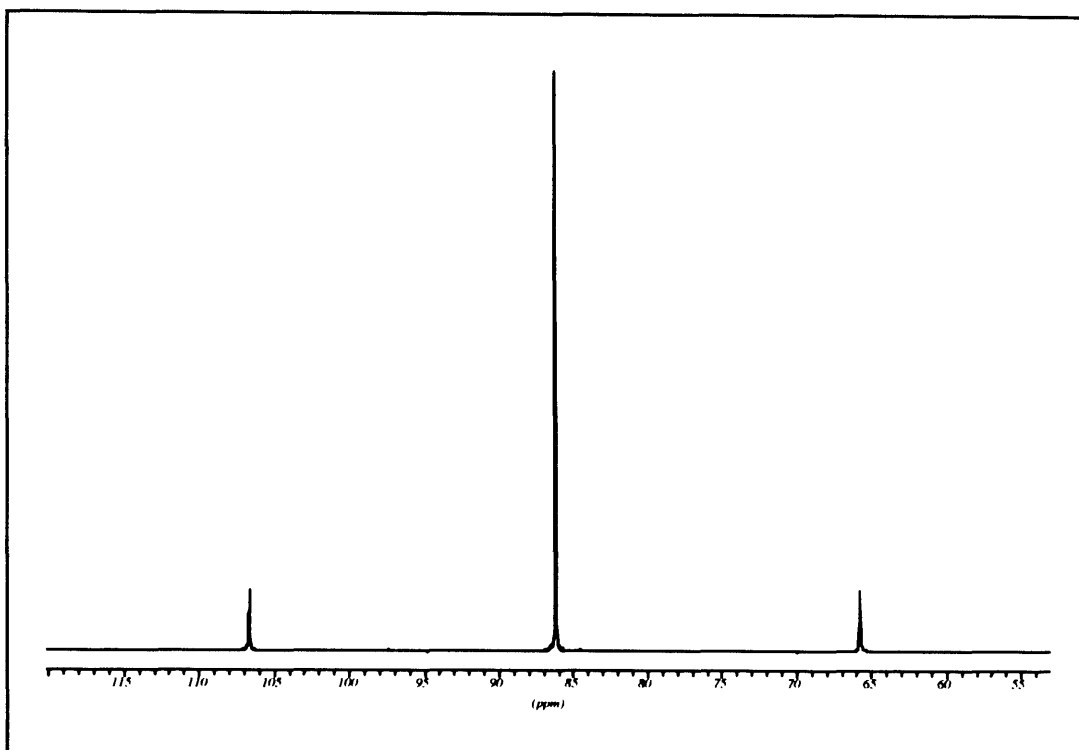
Figure 3.1 ^{31}P{^{1}H} NMR spectrum of PtCl$_2${Ph$_2$P(OC$_6$H$_4$-4-C$_6$F$_{13}$)}$_2$ (3.1).

Structural information can be derived from the coupling constants as the magnitude of $^1J_{PtP}$ coupling for the cis-isomers of [PtCl$_2$L$_2$] complexes of this type are significantly larger than those of the trans-isomers. The $^1J_{PtP}$ values obtained for complexes (3.1) and (3.2) are of similar magnitude to reported coupling constants for cis-[PtCl$_2$L$_2$] complexes with phosphinite[21] and phosphonite[22] ligands providing evidence to support the assigned cis-geometry. Coupling constants for cis-complexes of this type with phosphite ligands generally range from 4000-6000 Hz.[23] Evidence that complex (3.3) is the cis-isomer is provided by the magnitude of the $^1J_{Pt-P}$ coupling constant (5660 Hz) which compares closely to the value of 5800 Hz obtained for cis-[PtCl$_2$P{(OPh)$_3$}$_2$].[24] The ^{1}H and ^{19}F NMR spectra for the complexes are uninformative as they remain essentially unchanged in comparison to those of the free ligand.

PR$_3$ = Ph$_2$P(OC$_6$H$_4$-4-C$_6$F$_{13}$)   (3.1)

PhP(OC$_6$H$_4$-4-C$_6$F$_{13}$)$_2$ (3.2)

P(OC$_6$H$_4$-4-C$_6$F$_{13}$)$_3$ (3.3)
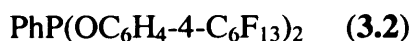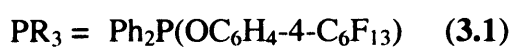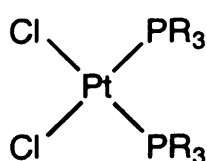
Square planar platinum(II) complexes of the type cis-[PtX$_2$L$_2$] are of the point group C$_{2v}$ and exhibit two bands in their IR spectra attributable to symmetric and antisymmetric vibrations of the PtX$_2$ group. The more symmetrical trans-[PtX$_2$L$_2$] complexes are of the point group D$_{2h}$ and exhibit a single IR active band due to the antisymmetric stretch of the Pt-Cl bond. Complexes (3.1) and (3.2) both exhibit two bands between 280 and 350 cm^{-1} assigned to Pt-Cl vibrations, indicative of a cis-geometry. The far IR spectrum of (3.3) exhibits two bands at 308 and 330 cm^{-1}, indicative of the assigned cis-geometry, and of a slightly lower magnitude than those for [PtCl$_2$P{(OPh)$_3$}$_2$] at 310 and 335 cm^{-1}.[25,26] This small decrease in sym and asym ν (Pt-Cl) suggests that the perfluoroalkyl chain derivatised phosphite competes more effectively than P(OPh)$_3$ for electron density at platinum, thus weakening the trans Pt-Cl bond.
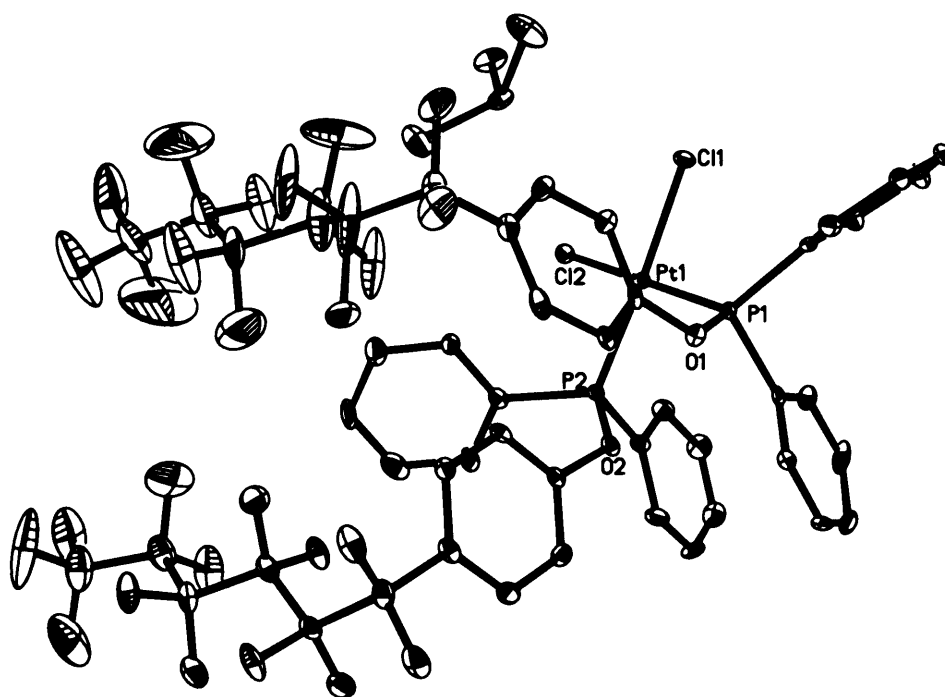
Figure 3.2 Crystal structure of cis-[PtCl$_2${Ph$_2$P(OC$_6$H$_4$-4-C$_6$F$_{13}$)}$_2$] (3.1) showing 30% displacement ellipsoids. H atoms are omitted for clarity.

Crystals of (3.1) suitable for X-ray determination were obtained from an acetone/chloroform solution by slow evaporation. The molecular structure of [PtCl$_2${Ph$_2$P(OC$_6$H$_4$-4-C$_6$F$_{13}$)}$_2$] shown in Figure 3.2 clearly shows the square planar geometry expected for a d^8 platinum complex and the cis-geometry indicated by the

NMR studies. Selected bond lengths and angles are shown in Table 3.1. Angular distortions from ideal values of 90 and 180° are small with *trans* P-Pt-Cl angles of 175° and *cis* P-Pt-Cl angles of 92 and 87° for P(1)-Pt(1)-Cl(1) and P(2)-Pt(1)-Cl(2) respectively. The symmetry about the metal centre is evident in the bond length data as both Pt-P and Pt-Cl bond lengths are the same within experimental error. The Pt-P bond lengths of 2.228(2) Å and 2.230(2) Å are similar in magnitude to those obtained for other *cis*-[PtCl$_2$L$_2$] complexes with phosphinite ligands. For example the molecular structure of *cis*-[PtCl$_2$(Ph$_2$POH)$_2$] exhibits Pt-P bond distances of 2.229 Å and 2.216 Å.[27] Similar coordination geometry about the metal to (**3.1**) is also observed indicating a negligible steric effect of the perfluoroalkyl substituents. The fluorous chains of each ligand spiral in the same manner as fully fluorinated hydrocarbons with both showing high displacement parameters at the chain ends. The crystal packing diagram of complex (**3.1**) indicates a close approach between the terminal CF$_3$ groups of perfluoroalkyl chains of adjacent molecules. The intermolecular F-F distances are in the range 1.8-1.9 Å which are significantly larger than average F-F bond distance of 1.417 Å.[28] The alignment of the molecules is such that the fluorous chains of adjacent molecules are parallel with one another, due in part to these intermolecular interactions.

Table 3.1   Selected bond lengths and angles with estimated standard deviations (e.s.d.s) in parentheses for *cis*-[PtCl$_2$\{Ph$_2$P(OC$_6$H$_4$-4-C$_6$F$_{13}$)\}$_2$] (**3.1**).

Bond Lengths (Å)		Bond Angles (°)	
Pt (1) - P (2)	2.228 (2)	P (2) - Pt (1) - P (1)	92.95 (8)
Pt (1) - Cl (2)	2.343 (2)	P (1) - Pt (1) - Cl (2)	175.73 (7)
P (1) - O (1)	1.622 (5)	P (1) - Pt (1) - Cl (1)	91.99 (7)
O (1) - C (1)	1.380 (9)	P (2) - Pt (1) - Cl (2)	87.11 (7)
Pt (1) - P (1)	2.230 (2)	P (2) - Pt (1) - Cl (1)	175.06 (7)
Pt (1) - Cl (1)	2.347 (2)	Cl (2) - Pt (1) - Cl (1)	87.96 (7)
P (2) - O (2)	1.628 (5)		
O (2) - C (13)	1.396 (8)		

The reaction of cis-[PtCl$_2$(MeCN)$_2$] with an excess of *ortho* and *meta* substituted phosphites (2.14) and (2.15) resulted in the formation of the complexes cis-[PtCl$_2$\{P(OC$_6$H$_4$-3-C$_6$F$_{13}$)$_3$\}$_2$] (3.4) and trans-[PtCl$_2$\{P(OC$_6$H$_4$-2-C$_6$F$_{13}$)$_3$\}$_2$] (3.5). The complex of the *meta* substituted ligand was isolated as a clear, viscous oil, whereas the complex of the *ortho* substituted ligand was obtained as a white solid. Both complexes were found to have limited solubility in dichloromethane and no solubility in perfluorinated solvents. Both complexes exhibit peaks in their FAB mass spectra for the parent ion fragments [(M-Cl)$^+$] and [(M-2Cl)$^+$] at m/z = 2758 and 2723 respectively. Informative near IR spectra for complexes (3.4) and (3.5) could not be obtained, therefore, the structural assignment of the complexes is based on their ^{31}P NMR spectra which exhibit $^1J_{Pt-P}$ coupling constants of 5777 Hz and 4859 Hz respectively. The structure of complex (3.4) has been determined by comparison of its chemical shift and $^1J_{Pt-P}$ coupling constant with that obtained for cis-[PtCl$_2$\{P(OC$_6$H$_4$-4-C$_6$F$_{13}$)$_3$\}$_2$] (3.3). The similarity of δ(^{31}P) values and $^1J_{Pt-P}$ coupling for the two complexes suggests that derivatisation of triphenylphosphite in the *meta* position with the perfluoroalkyl group has no significant impact on the overall geometry of the complex. The magnitude of $^1J_{Pt-P}$ coupling for complex (3.5) bearing triphenylphosphite ligands derivatised in the *ortho* position is significantly lower than the values obtained for complexes (3.3) and (3.4) indicating a trans-geometry for the complex. Robinson and co-workers obtained the analogous platinum(II) complex with tri-*o*-tolyl phosphite ligands as cis-trans-isomer mixtures.[29] Here, this was confirmed by IR spectroscopy for which the mixture exhibits two bands at 315 and 340 cm^{-1} attributable to *sym* and *asym* vibrations of the cis-PtCl$_2$ group, and a third band at 360 cm^{-1} corresponding to the *asym* vibration of the trans-PtCl$_2$ group. Each isomer was found to give rise to a single resonance in the ^{31}P NMR spectrum with a characteristic chemical shift and $^1J_{Pt-P}$ coupling constant. The ^{31}P NMR spectrum for trans-[PtCl$_2$\{P(OC$_6$H$_4$-2-CH$_3$)$_3$\}$_2$] exhibits a singlet with ^{195}Pt satellites at 75 δ and $^1J_{Pt-P}$ coupling of 4405 Hz which is comparable to the ^{31}P NMR spectrum of (3.5) which exhibits a singlet at 77 δ with $^1J_{Pt-P}$ coupling of 4859 Hz. Robinson concluded that the formation of the trans-isomer with tri-*o*-tolyl phosphite was attributable to steric crowding arising from the bulky ligand. It is therefore not surprising that the introduction of a group as sterically demanding as C$_6$F$_{13}$ in the *ortho* position of the aryl ring results in the exclusive formation of complex (3.5) as the trans-isomer.

$$Cl\diagdown_{\diagdown}{}^{Pt}{}_{\diagup}^{\diagup}PR_3$$
$$Cl\diagup{}^{}\diagdown PR_3$$

PR₃ = P(OC₆H₄-3-C₆F₁₃)₃   (3.4)

$$R_3P\diagdown_{\diagdown}{}^{Pt}{}_{\diagup}^{\diagup}Cl$$
$$Cl\diagup{}^{}\diagdown PR_3$$

PR₃ = P(OC₆H₄-2-C₆F₁₃)₃   (3.5)
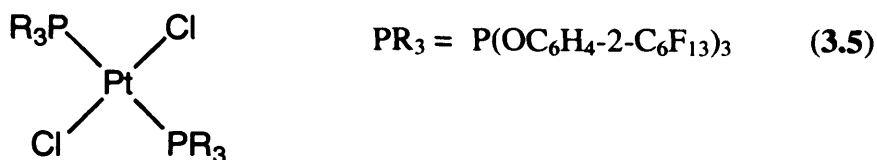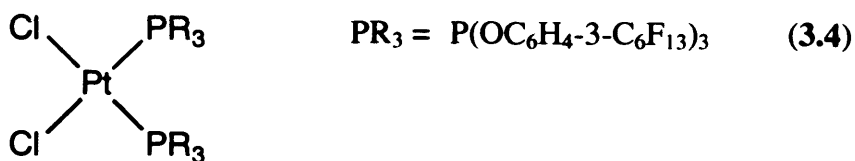
The reaction of ligands (2.16) and (2.17) with cis-[PtCl₂(MeCN)₂] under the same conditions as those used for the aryl ligands produced the complexes cis-[PtCl₂{Ph₂P(OC₂H₄C₆F₁₃)}₂] (3.6) and cis-[PtCl₂{PhP(OC₂H₄C₆F₁₃)₂}₂] (3.7). As with the aryl analogues discussed previously, both complexes were obtained exclusively as the cis-isomers. Elemental analysis and mass spectrometry provided evidence for the formation of (3.6) and (3.7), the FAB mass spectra of the complexes exhibiting characteristic peaks at m/z = 1326 and 1291 for (3.6) and m/z = 1898 and 1863 for (3.7) corresponding to the fragments [(M-Cl)⁺] and [(M-2Cl)⁺] respectively. The cis-geometry of the complexes has been assigned by comparison of δ_P values and $^1J_{Pt-P}$ coupling constants from their ^{31}P NMR spectra with those obtained for the aryl analogues cis-[PtCl₂{Ph₂P(OC₆H₄-4-C₆F₁₃)}₂] (3.1) and cis-[PtCl₂{PhP(OC₆H₄-4-C₆F₁₃)₂}₂] (3.2) and for alkoxy phosphinites and phosphonites.[22,23]

$$Cl\diagdown_{\diagdown}{}^{Pt}{}_{\diagup}^{\diagup}PR_3$$
$$Cl\diagup{}^{}\diagdown PR_3$$

PR₃ = Ph₂P(OC₂H₄C₆F₁₃)   (3.6)
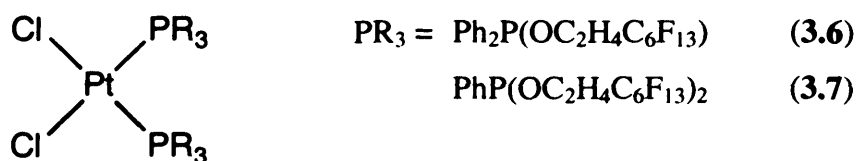
PhP(OC₂H₄C₆F₁₃)₂   (3.7)

The cis-geometry of (3.6) was confirmed by an X-ray crystallographic study of single crystals of cis-[PtCl₂{Ph₂P(OC₂H₄C₆F₁₃)}₂] obtained from a solution of dichloromethane by slow evaporation (Figure 3.3). Complex (3.6) crystallizes with two independent molecules in the unit cell, but the geometry about the metals are very similar. Selected bond lengths and angles for one of the independent molecules of (3.6) are displayed in Table 3.2. The geometry about the metal centre is less symmetrical than observed for the analogous aryl phosphinite complex (3.1) with differing P-Pt-Cl bond angles of 170° and 175°. This asymmetry is not manifested in

the bond distances where the Pt-P and Pt-Cl bond lengths are the same within experimental error. The analogous phosphine complex cis-[PtCl$_2$\{Ph$_2$P(C$_2$H$_4$C$_6$F$_{13}$)\}$_2$] shows considerable variation between the two Pt-P bonds which has been ascribed to the steric effect of the bulky C$_2$H$_4$C$_6$F$_{13}$ groups.[30]
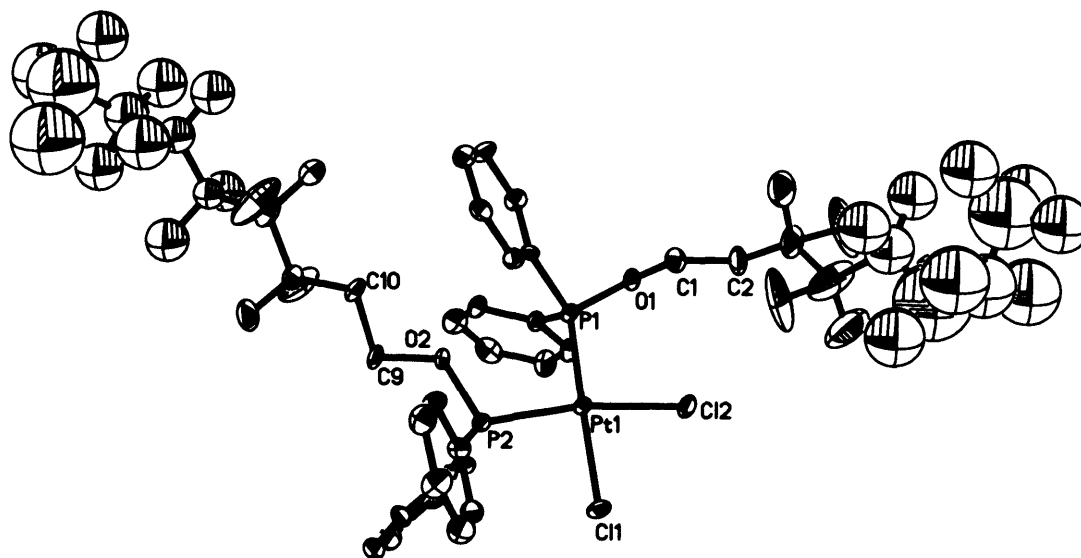
Figure 3.3 Crystal structure of one of the independent molecules of cis-[PtCl$_2$\{Ph$_2$P(OC$_2$H$_4$C$_6$F$_{13}$)\}$_2$] (**3.6**) showing 30% displacement ellipsoids. H atoms are omitted for clarity.

The steric effect of the perfluoroalkyl group in (**3.6**) is reduced in comparison to the phosphine complex due to the oxygen atom distancing the bulky C$_2$H$_4$C$_6$F$_{13}$ group from the metal centre. The flexibility of the P-O-C unit of the phosphinite ligand is also important as potential steric constraints can be alleviated to a greater extent than with the more rigid phosphine ligand. Comparison of the bond lengths of complexes (**3.1**) and (**3.6**) reveals that the Pt-P and P-O distances are the same within experimental error. This is interesting as the difference between the two complexes is that the 'spacer' between the phosphorus and the perfluoroalkyl chain is an aryloxy group in (**3.1**) and an ethoxy group in (**3.6**). The electron-withdrawing effect of the C$_6$F$_{13}$ moiety is believed to reduce electron-density at phosphorus, thereby decreasing the amount available for σ-donation to the metal centre. This in turn would lead to a reduction in the metal-phosphorus and possibly phosphorus-oxygen bond strengths and hence an increase in bond lengths. As there are no significant differences in these

bond lengths between the two complexes it appears that either the alkoxy and aryloxy phosphinites are comparable in terms of their σ-donor and π-acceptor abilities or that X-ray crystallography and bond length data are insensitive to slight variations in the electronic properties of coordinated ligands. As with complex (3.1) the fluorous chains of complex (3.6) show a high degree of disorder towards the end of the chains.

Table 3.2 Selected bond lengths and angles with e.s.d.s in parentheses for one of the independent molecules of cis-[PtCl$_2$\{Ph$_2$P(OC$_2$H$_4$C$_6$F$_{13}$)\}$_2$] (3.6).

Bond Length (Å)		Bond Angle (°)	
Pt (1) - P (2)	2.230 (3)	P (2) - Pt (1) - P (1)	96.25 (10)
Pt (1) - Cl (2)	2.343 (3)	P (1) - Pt (1) - Cl (2)	90.80 (10)
P (1) - O (1)	1.629 (8)	P (1) - Pt (1) - Cl (1)	175.37 (10)
O (1) - C (1)	1.439 (13)	P (2) - Pt (1) - Cl (1)	85.90 (10)
Pt (1) - P (1)	2.227 (3)	P (2) - Pt (1) - Cl (2)	170.14 (10)
Pt (1) - Cl (1)	2.353 (3)	Cl (2) - Pt (1) - Cl (1)	86.59 (11)
P (2) - O (2)	1.617 (8)		
O (2) - C (9)	1.444 (12)		

The ^{19}F\{^{1}H\} NMR spectrum of complex (3.7) shows a significantly different splitting pattern for the $^\alpha$CF$_2$ resonance of the perfluoroalkyl chain (Figure 3.4) in comparison to the spectrum of the free ligand. In the case of the free ligand (2.17) all the protons of the C$_2$H$_4$ group are inequivalent (see chapter 2) leading to a highly complex ^{1}H NMR spectrum. The inequivalence of protons on the same carbon is a result of the symmetry of the phosphonite ligand, and it would, therefore, be expected that similar inequivalence of the fluorine atoms of the perfluoroalkyl groups would be observed. The ^{19}F\{^{1}H\} NMR spectrum of the free ligand, however, exhibits the $^\alpha$CF$_2$ resonance of the perfluoroalkyl chains as a triplet of triplets with $^3J_{F-F}$ coupling of 2.5 Hz and $^4J_{F-F}$ coupling of 13.9 Hz, indicating that the two fluorine atoms are essentially equivalent. Coordination of the ligand to platinum appears to give rise to inequivalence of the fluorine atoms of the $^\alpha$CF$_2$ group, resulting in a complex, highly second order spectrum. It is unclear why coordination of the ligands to platinum increases the inequivalence between geminal atoms along the perfluoroalkyl chain.

The inequivalent fluorine atoms exhibit ^3J and ^4J coupling to the fluorines of the $^\beta CF_2$ and $^\gamma CF_2$ groups respectively as well as coupling geminally to one another. The fluorine atoms of the $^\beta CF_2$ and $^\gamma CF_2$ may also be inequivalent, although no conclusions can be made from the spectral data as the resonances for both groups in the free ligand and complex (3.7) are highly complex, unresolvable, multiplets.
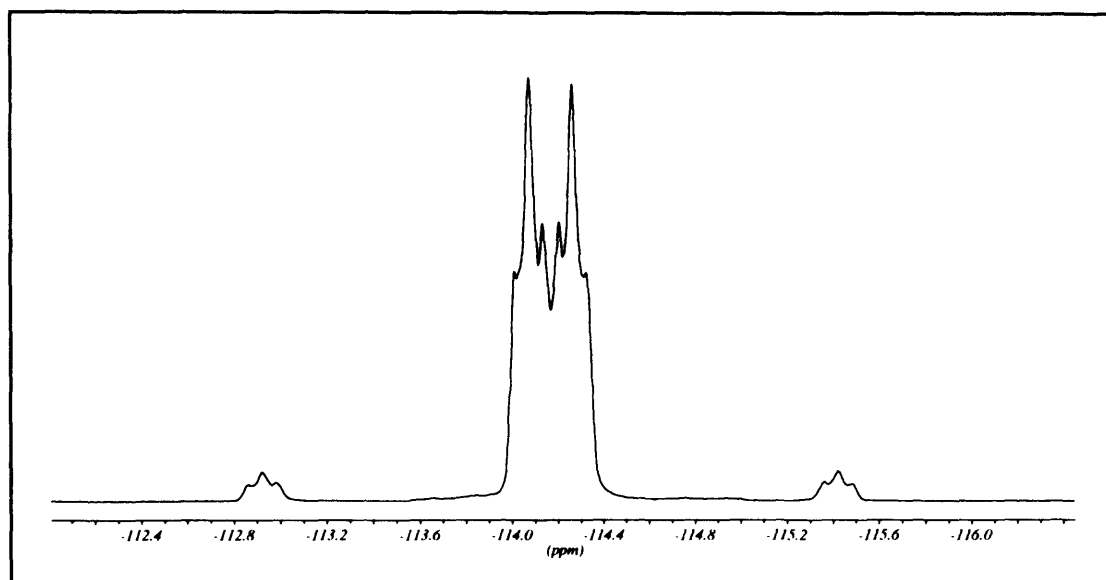
Figure 3.4 $^{19}F\{^1H\}$ NMR the $^\alpha CF_2$ resonance of $PtCl_2\{PhP(OC_2H_4C_6F_{13})_2\}_2$ (3.7).

The complex cis-$[PtCl_2\{P(OC_2H_4C_6F_{13})_3\}$ (3.8) was obtained as a clear viscous oil from the reaction of $P(OC_2H_4C_6F_{13})_3$ (2.18) with cis-$[PtCl_2(MeCN)_2]$. Evidence for the formation of (3.8) was provided by FAB mass spectrometry with characteristic peaks observed for the fragments $[(M-Cl)^+]$ and $[(M-2Cl)^+]$ at m/z = 2470 and 2435. The $^{31}P\{^1H\}$ NMR spectrum of complex (3.8) was found to be highly second order and could, therefore, not be resolved. The solubility of the reaction product in dichloromethane was poor as expected, however good solubility in acetone was achieved. As with complex (3.3) which bears derivatised triphenylphosphite ligands, no solubility in PP3 was observed for (3.8) despite the high solubility of the free ligand in PFC solvents.

$$Cl \diagdown \quad \diagup PR_3$$
$$Pt$$
$$Cl \diagup \quad \diagdown PR_3$$

$PR_3 = P(OC_2H_4C_6F_{13})_3$ (3.8)
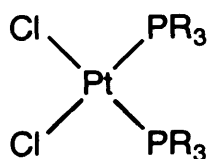
3.2.2 Discussion of $^{31}P\{^1H\}$ NMR data

The magnitudes of $^1J_{Pt-P}$ coupling constants are useful in the assignment of platinum complexes as their values are dependent on the nature of the phosphorus ligand,[31] the *cis* and *trans* ligands,[32] and the metal oxidation state.[33] Interpretation of coupling constants are founded on assumptions made by Ramsey[34] and later by Pople[35] that the coupling derives essentially from the Fermi contact term. The expression for the Fermi term derived by Pople and Santry[36] is such that $^1J_{Pt-P}$ coupling constants must depend strongly on the s-orbital character of the Pt-P bond. Equation 3.1 is a modified form of the molecular orbital expression adapted from Pople and Santry for the Fermi contribution to directly bonded Pt-P coupling constants;

$$^1J_{Pt-P} \propto \gamma_{Pt}\gamma_P(^3\Delta E)^{-1}|S_{Pt}(0)|^2|S_P(0)|^2(P_{PtP})^2 \qquad \text{Equation 3.1.}$$

The terms γ_{Pt} and γ_P are the magnetogyric ratios of the coupled nuclei, $^3\Delta E$ is an approximation of the average excitation energy, $|S_{Pt}(0)|$ and $|S_P(0)|$ are the electron densities at the parent nuclei and P_{PtP} is the molecular orbital bond order between the s-orbitals of the coupled atoms. The s-character of the phosphorus donor orbital (α^2_P) contributes directly to P_{PtP} and $|S_P(0)|$. As the term P_{PtP} increases with α^2_P and with the s-character of the platinum acceptor orbital (α^2_{Pt}), the most important factor in determining the magnitude of $^1J_{Pt-P}$ is the s-character of the Pt-P bond. Variation of the s-character of the Pt-P bond is, therefore, responsible for changes in $^1J_{Pt-P}$ as a function of the σ-donor and π-acceptor properties of the phosphorus ligand.

Table 3.3 ^{31}P{^{1}H} NMR data for [PtCl$_2$L$_2$] complexes (3.1-3.7).

Complex		δ (^{31}P)	$^{1}J_{Pt-P}$ (Hz)
cis-[PtCl$_2${Ph$_2$P(OC$_6$H$_4$-4-C$_6$F$_{13}$)}$_2$]^a	(3.1)	87.6	4189
cis-[PtCl$_2${PhP(OC$_6$H$_4$-4-C$_6$F$_{13}$)$_2$}$_2$]^a	(3.2)	95.0	4859
cis-[PtCl$_2${P(OC$_6$H$_4$-4-C$_6$F$_{13}$)$_3$}$_2$]^c	(3.3)	65.4	5660
cis-[PtCl$_2${P(OPh)$_3$}$_2$]^{a,d}		59.1	5800
cis-[PtCl$_2${P(OC$_6$H$_4$-4-CF$_3$)$_3$}$_2$]^{a,e}		67.9	5669
cis-[PtCl$_2${P(OC$_6$H$_4$-3-C$_6$F$_{13}$)$_3$}$_2$]^b	(3.4)	60.8	5777
trans-[PtCl$_2${P(OC$_6$H$_4$-2-C$_6$F$_{13}$)$_3$}$_2$]^b	(3.5)	77.2	4859
cis-[PtCl$_2${P(OC$_6$H$_4$-2-CH$_3$)$_3$}$_2$]^{a,d}		57.0	5859
trans-[PtCl$_2${P(OC$_6$H$_4$-2-CH$_3$)$_3$}$_2$]^{a,d}		74.9	4405
cis-[PtCl$_2${Ph$_2$P(OC$_2$H$_4$C$_6$F$_{13}$)}$_2$]^a	(3.6)	86.2	4141
cis-[PtCl$_2${PhP(OC$_2$H$_4$C$_6$F$_{13}$)$_2$}$_2$]^a	(3.7)	100.0	4754

^{a} Recorded in CDCl$_3$. ^{b} Recorded in (CD$_3$)$_2$CO. ^{c} Recorded in Et$_2$O with a D$_2$O insert. ^{d} From ref. 28. ^{e} From ref. 39.

The ^{31}P{^{1}H} NMR data for complexes (3.1-3.7) are contained in Table 3.3. The values of δ(^{31}P) for complexes (3.1-3.7) are to lower frequency than those of the free ligands and show the same variation with the number of phenoxy or alkoxy groups. As the magnitude of $^{1}J_{Pt-P}$ coupling constants is related to the s-character of the Pt-P bond they provide information on the geometry of the complexes. In the cis-geometry the displacement of the π-acceptor orbitals on phosphorus is such that they overlap with the d_{xy}, d_{zy}, and d_{xz} orbitals of platinum. The geometry of the phosphorus π-orbitals in the trans-configuration means that only two metal d-orbitals are available for π-bonding.[37] The increased π-bonding in the cis-isomers leads to a synergic increase in the s-character of the Pt-P bond and, hence, a larger $^{1}J_{Pt-P}$ coupling constant relative to the trans-isomer. The lower magnitude of $^{1}J_{Pt-P}$ coupling for trans-isomers can also be discussed in relation to the trans-effect.[38] The trans-influence is defined as the ability of a ligand to weaken bonds in a trans-relationship. In cis-[PtCl$_2${PX$_3$}$_2$] the phosphorus ligand is trans to Cl which has a small trans-

effect and, therefore, does not greatly influence the *trans* Pt-P bond. In the case of *trans*-[PtCl$_2$\{PX$_3$\}$_2$] the phosphorus ligand is *trans* to an identical ligand, which exerts a large *trans*-influence, thereby weakening the Pt-P bond. Although the *trans*-influence theory predicts that a decrease in the Pt-P bond distance should be associated with an increase in the *trans* bond length, it has been observed that when the Pt-P bond is shortened by the introduction of electronegative substituents on phosphorus the *trans* bond length is also shortened. Hitchcock *et al.*[48] hypothesised that this may be a result of changes in the energy of the phosphorus lone pair with an accompanying reduction in the contribution of the metal orbitals to the Pt-P bond. This would allow for a greater contribution from the metal orbital to the orbital binding the *trans*-ligand, which would result in a shorter bond.

The values of the $^1J_{Pt-P}$ coupling constants for complexes (3.1-3.7) increase in the order phosphinite < phosphonite < phosphite. The increase in $^1J_{Pt-P}$ can be ascribed to differences between the ligands in the magnitude of $|S_P(0)|^2$ in the Fermi contact term, representing the 3s-electron density at the phosphorus nucleus.[39] The value of $^1J_{Pt-P}$ for complex (3.3) containing the perfluoroalkyl derivatised aryl phosphite is *ca.* 140 Hz lower than that for *cis*-[PtCl$_2$\{P(OPh)$_3$\}$_2$]. Recent observations by Cobley and Pringle for a series of platinum(II) complexes with sterically similar *para*-substituted phosphite complexes have demonstrated that, in general, the more electronegative the substituent (as measured by the Hammett parameter σ_P), the smaller the $^1J_{Pt-P}$ coupling constant.[40] It was concluded that the reduction in $^1J_{Pt-P}$ was a result of the electron-withdrawing substituents decreasing σ-donation from phosphorus to platinum, thereby weakening the Pt-P bond. The observed reduction in $^1J_{Pt-P}$ for (3.3), therefore, indicates the electron-withdrawing effect of the C$_6$F$_{13}$ group in the *para*-substitution of the phenyl ring results in the reduction of the σ-component of the Pt-P bond. The similarity in the $^1J_{Pt-P}$ values for (3.4) and *cis*-[PtCl$_2$\{P(OPh)$_3$\}$_2$] (5777 Hz and 5800 Hz respectively) suggests that substitution of the phosphite ligand in the *meta* position virtually negates the impact of the electronegative substituents on the Pt-P bond parameters. In contrast, it has been reported that $^1J_{Pt-P}$ for the analogous phosphine complex, *cis*-[PtCl$_2$\{P(C$_6$H$_4$-3-C$_6$F$_{13}$)$_3$\}$_2$], in which the phosphine ligand is derivatised in the *meta* position, is lower than that for *cis*-[PtCl$_2$\{P(C$_6$H$_4$-4-C$_6$F$_{13}$)$_3$\}$_2$], in which the substituents are in the *para* position.[31] Due to the flexible nature of the phosphite ligand,[41] *meta* substitution is likely to be less sterically demanding than for

the more rigid phosphine. Therefore, steric contributions to the magnitude of the $^1J_{Pt-P}$ coupling constant will be greater for the phosphine than for the phosphite. Larger $^1J_{Pt-P}$ coupling constants are observed for the aryloxy phosphinite and phosphonite complexes (3.1) and (3.2) compared to the analogous ethoxy complexes (3.6) and (3.7). This demonstrates that substitution of an aryloxy group with an ethoxy group results in increased π-acceptor ability of the ligands and hence a synergic increase in the σ-component of the Pt-P bond due to increased π-bonding.

3.3 Platinum (II) complexes of the type [PtCl₂(PEt₃)L]

A series of platinum complexes of the type [PtCl₂(PEt₃)L] have been prepared by the reaction of *trans*-[{PtCl(μ-Cl)(PEt₃)}₂] with the perfluoroalkyl chain derivatised phosphinite, phosphonite and phosphite ligands. These complexes are of interest as the phosphorus ligands have different electronic properties. Comparison of the spectral data obtained for these complexes with that for the [PtCl₂L₂] complexes discussed in section 3.2 should yield more information on the effect of the perfluoroalkyl substituents on the coordination chemistry of the derivatised ligands. *Trans*-[{PtCl(μ-Cl)(PEt₃)}₂] is a convenient starting material as it is soluble in most organic solvents and the chlorine bridge is readily cleaved by tertiary phosphorus ligands (Scheme 3.3).
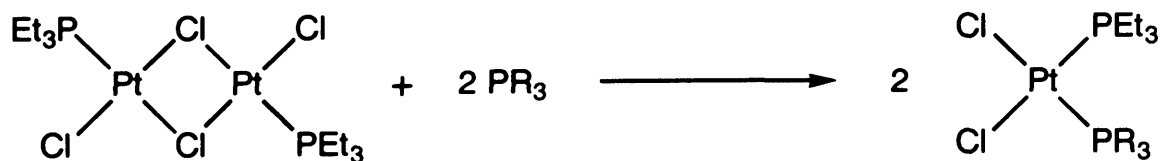
Scheme 3.3 Reaction of tertiary phosphorus ligands with *trans*-[{PtCl(μ-Cl)(PEt₃)}₂].

The reaction of the dinuclear complex [{Pt(μ-Cl)₂(PEt₃)}₂] with the aryloxy phosphinite, phosphonite and phosphite ligands (2.2-2.4) in refluxing dichloromethane gave the complexes *cis*-[PtCl₂(PEt₃){Ph₂P(OC₆H₄-4-C₆F₁₃)}] (3.9), *cis*-[PtCl₂(PEt₃){PhP(OC₆H₄-4-C₆F₁₃)₂}] (3.10) and *cis*-[PtCl₂(PEt₃){P(OC₆H₄-4-

$C_6F_{13})_3$}] **(3.11)**. The reaction of *trans*-[{$Pt(\mu\text{-}Cl)_2(PEt_3)$}$_2$] with the alkoxy phosphinite, phosphonite and phosphite ligands **(2.16-2.18)** under the same conditions as above led to the formation of *cis*-[$PtCl_2(PEt_3)${$Ph_2P(OC_2H_4C_6F_{13})$}] **(3.12)**, *cis*-[$PtCl_2(PEt_3)${$PhP(OC_2H_4C_6F_{13})_2$}] **(3.13)** and *cis*-[$PtCl_2(PEt_3)${$P(OC_6H_2C_6F_{13})_3$}] **(3.14)**. All complexes were obtained as air- and moisture-stable solids. Due to the low number of perfluoroalkyl tails present in the complexes they were found to be highly soluble in common organic solvents such as dichloromethane and insoluble in PFC solvents such as PP3. Evidence for the formation of complexes **(3.9-3.14)** is given by their FAB mass spectra which exhibit characteristic peaks corresponding to the fragments [$(M\text{-}Cl)^+$] and [$(M\text{-}2Cl)^+$]. The ^1H NMR spectra of **(3.9-3.14)** exhibit resonances for the fluorous chain derivatised ligands which are essentially the same as those for the free ligands and a doublet of quartets at *ca.* 2.0 δ and a doublet of triplets at *ca.* 1.0 δ which are assigned to the PEt_3 group. The ^{19}F{^1H} NMR spectra are uninformative, as they remain unchanged in comparison to spectra obtained for the free ligands. All complexes were obtained as a single isomer as evidenced by ^{31}P{^1H} NMR spectroscopy.

$PR_3 =$	$Ph_2P(OC_6H_4\text{-}4\text{-}C_6F_{13})$	**(3.9)**
	$PhP(OC_6H_4\text{-}4\text{-}C_6F_{13})_2$	**(3.10)**
	$P(OC_6H_4\text{-}4\text{-}C_6F_{13})_3$	**(3.11)**
	$Ph_2P(OC_2H_4C_6F_{13})$	**(3.12)**
	$PhP(OC_2H_4C_6F_{13})_2$	**(3.13)**
	$P(OC_2H_4C_6F_{13})_3$	**(3.14)**
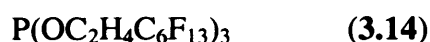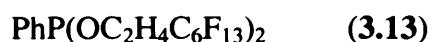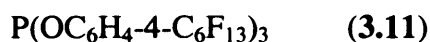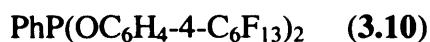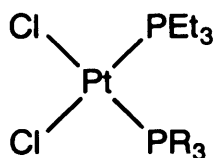
The ^{31}P{^1H} NMR spectra of complexes **(3.9-3.14)** exhibit two characteristic doublet resonances flanked by ^{195}Pt satellites. The resonances at higher frequency have been assigned to the aryloxy ligands on the basis of their characteristic δ_P values and $^1J_{Pt\text{-}P}$ coupling constants and comparison of the ^{31}P NMR parameters with literature values (Table 3.4).[42] The lower frequency resonances are assigned to the PEt_3 ligands which exhibit $^1J_{Pt\text{-}P}$ coupling constants and chemical shift values typical of phosphine ligands in platinum(II) complexes.[43] The complexes were determined to be the *cis*-isomers due to the magnitude of their $^2J_{P\text{-}P}$ coupling which are between 16 and 21 Hz. In complexes of the type [$PtCl_2L_2$] where L is a tertiary phosphorus ligand

$^{2}J_{P-P}$ coupling constants for the cis-complexes are generally in the range 0-80 Hz, whereas values for the trans-complexes are usually in the range 550-830 Hz.[21]

The chemical shift of the $PPh_{x}(OR)_{3-x}$ ligands in the $^{31}P\{^{1}H\}$ NMR spectra of complexes (3.9-3.14) show the same variation with the number of phenoxy or aryloxy groups as those of the free ligands. The $^{1}J_{Pt-P}$ coupling constants for the derivatised $PPh_{x}(OR)_{3-x}$ ligands of the cis-[PtCl$_2$(PEt$_3$)L] complexes are significantly higher than those observed for the cis-[PtCl$_2$L$_2$] complexes (see section 3.2). As the ligands in complexes (3.9-3.11) are functionalized in the para position of the aryl group steric contributions to $^{1}J_{Pt-P}$ due to the perfluoroalkyl chain are minimised. As discussed previously, it is well established that the nature of the trans ligand has a profound effect on the magnitude of $^{1}J_{M-P}$ coupling constants. Changes in the σ-component of the metal-phosphorus bond are mainly responsible for these changes in $^{1}J_{M-P}$ coupling as well as affecting other bonding parameters. The relative importance of σ-bond effects, π-bond effects, and steric contributions to the effects of cis ligands on the magnitude of $^{1}J_{M-P}$ is less understood. Changing the cis ligand in complexes such as [PtCl$_{4-n}$(PR$_3$)$_n$]$^{(n-2)+}$ has very little effect on $^{1}J_{Pt-P}$ coupling or M-P bond lengths,[44] while in complexes of the type cis-[PtCl$_2$(PR$_3$)L] variation of the cis ligand induces considerable change in $^{1}J_{Pt-P}$ coupling.[45] The $^{1}J_{Pt-P}$ coupling constants of the derivatised phosphite ligand in cis-[PtCl$_2$(PEt$_3$){P(OC$_6$H$_4$-4-C$_6$F$_{13}$)$_3$}] (3.11) and cis-[PtCl$_2${P(OC$_6$H$_4$-4-C$_6$F$_{13}$)$_3$}$_2$] (3.3) are 6300 and 5660 Hz respectively. As phosphines are much poorer π-acceptors than phosphites, the derivatised phosphite competes more effectively for π-electron density at platinum when cis to PEt$_3$ in the case of complex (3.11) than when cis to an identical ligand as in complex (3.3). Synergic strengthening of the Pt-P σ-bond through increased π-bonding is responsible for the larger $^{1}J_{Pt-P}$ coupling constants and reflects the dominance of the phosphorus-centred term $|S_P(0)|^2$ in the Fermi contribution to $^{1}J_{Pt-P}$ coupling constants.

Table 3.4 $^{31}P\{^1H\}$ NMR data for platinum derivatives [PtCl$_2$(PEt$_3$)L]^a.

L	$\delta(^{31}P)$	$^1J_{Pt-P}$ (Hz)	$^2J_{P-P}$ (Hz)
Ph$_2$P(OC$_6$H$_4$-4-C$_6$F$_{13}$)^b (3.9)	88.7	4362	16
(cis)	(12.6)	(3356)	
Ph$_2$P(OPh)^{b,c}	87.3	4362	16
(cis)	(12.6)	(3407)	
PhP(OC$_6$H$_4$-4-C$_6$F$_{13}$)$_2$^{b} (3.10)	97.9	5195	16
(cis)	(16.1)	(3276)	
PhP(OPh)$_2$^{b,c}	93.8	5181	16
(cis)	(15.2)	(3348)	
P(OC$_6$H$_4$-4-C$_6$F$_{13}$)$_3$^{b} (3.11)	66.3	6300	20
(cis)	(17.6)	(3106)	
P(OPh)$_3$^{b,c}	62.7	6261	19
(cis)	(16.5)	(3191)	
Ph$_2$P(OC$_2$H$_4$C$_6$F$_{13}$)^b (3.12)	86.6	4342	16
(cis)	(12.9)	(3423)	
PhP(OC$_2$H$_4$C$_6$F$_{13}$)$_2$^{b} (3.13)	100.7	4911	16
(cis)	(15.6)	(3383)	
P(OC$_2$H$_4$C$_6$F$_{13}$)$_3$^{b} (3.14)	75.3	5875	21
(cis)	(16.7)	(3288)	

^{a} Values for the PEt$_3$ ligand are given in brackets. ^{b} Recorded in CDCl$_3$. ^{c} Ref. 35.

Analysis of the $^{31}P\{^1H\}$ NMR data, displayed in Table 3.4, shows that $\delta(^{31}P)$ for the PPh$_x$(OR)$_{3-x}$ ligands of complexes (3.9-3.11) are at higher frequency than those of the respective perprotio analogues. Two further trends regarding $^1J_{Pt-P}$ coupling constants are also apparent. The first is the small increase in $^1J_{Pt-P}$ coupling to the PPh$_x$(OR)$_{3-x}$ ligands in complexes (3.10-3.11) relative to the analogous protio complexes.[46] This increase would be expected if the introduction of electron-withdrawing groups in the periphery of the modified ligands increases their π-acceptor ability. Literature observations demonstrate that $^1J_{Pt-P}$ coupling constants in cis-[PtCl$_2$(PEt$_3$)L] complexes increase with increasing π-acceptor ability of ligand L in the order PR$_3$ < PPh$_3$ < PPh$_2$(OR) < PPh(OR)$_2$ < P(OPh)$_3$ < PF$_3$.[47] As increases in $^1J_{Pt-P}$ are related to increases in the s-character of the Pt-P σ-bond the differences observed for the derivatised complexes can be explained by synergic strengthening of the σ-bond through increased π-bonding. Followingly, changes in Pt-P π-bonding should be reflected in changes in Pt-P bond strengths, and thus Pt-P bond distances.

Evidence for this is provided by X-ray crystallographic studies of cis-[PtCl$_2$(PEt$_3$)L] complexes with ligands which differ in their π-acceptor ability. Hitchcock et al.[48] demonstrated that changing ligand L from PEt$_3$ to the stronger π-acceptor PF$_3$ results in a decrease in the Pt-PX$_3$ bond distance from 2.258(2) Å to 2.141(3) Å. In contrast, the Pt-PEt$_3$ bond is lengthened from 2.258(2) Å to 2.272(2) Å, indicating that variation of L directly influences the Pt-P bond cis to L. It is believed that ligand L may affect the Pt-P bond length cis to L via competition for d_π electron-density at the metal centre. Lengthening of the Pt-PEt$_3$ bond in cis-[PtCl$_2$(PEt$_3$)(PF$_3$)] demonstrates the greater 'cis influence' of PF$_3$ in comparison to PEt$_3$. The cis-influence of a ligand is defined as the power of the ligand to weaken bonds in cis-relationship.[48] The increases in $^1J_{Pt-P}$ coupling observed for the phosphinite, phosphonite and phosphite series of complexes (3.9-3.11) in comparison to their perprotio analogues are small, suggesting limited variation in σ-bonding and π-bonding.

The second trend is a significant change in the size of $^1J_{Pt-P}$ for the cis PEt$_3$ ligands in complexes (3.9-3.11) in comparison to values obtained for the phosphine ligands in the non-derivatised complexes. The trend follows a step-wise decrease in the magnitude of $^1J_{Pt-P}$ coupling to the PEt$_3$ ligand as the number of perfluoroalkyl substituents increases. The decrease in $^1J_{Pt-P}$ reflects the greater cis influence of the, respective, derivatised ligands (2.2-2.4) compared to their perprotio analogues and is consistent with these ligands (2.2-2.4) being stronger π-acceptors, reducing the σ-character of the cis M-PEt$_3$ bond through increased Pt-P π-bonding to the derivatised ligand. The increased π-acceptor ability of the derivatised ligands can be rationalised by the effect of the electronegative C$_6$F$_{13}$ group which lowers the energy of the P-X σ^* orbitals, thus increasing their accessibility for π-bonding.

Comparison of the ^{31}P{^{1}H} NMR data for the aryloxy complexes (3.9-3.11) with that for the related alkoxy complexes (3.12-3.14) indicates a marked decrease in the magnitude of $^1J_{Pt-P}$ coupling to the PPh$_x$(OR)$_{3-x}$ ligand and an increase in $^1J_{Pt-P}$ coupling to the cis PEt$_3$ group when an aryloxy group is substituted for an alkoxy group. The $^1J_{Pt-P}$ coupling to PEt$_3$ in cis-[PtCl$_2$(PEt$_3$){P(OC$_6$H$_4$-4-C$_6$F$_{13}$)$_3$}] (3.11) of 3106 Hz in comparison to 3288 Hz for cis-[PtCl$_2$(PEt$_3$){P(OC$_2$H$_4$C$_6$F$_{13}$)$_3$}] (3.14) suggests that the aryl phosphite exerts a greater cis influence than the alkyl phosphite, thereby weakening the cis Pt-PEt$_3$ bond to a greater extent due to competition for d_π electron-density at the metal centre. This is to be expected as triaryl phosphites are

known to be significantly better π-acceptors than trialkyl phosphites. The larger $^1J_{Pt-P}$ coupling to the phosphite ligand in complex (3.11) can be accounted for by synergic strengthening of the Pt-P σ-bond through greater π-bonding.

Single crystals of complex (3.11) suitable for X-ray crystallographic analysis were obtained from dichloromethane solution. Selected bond distances and angles about the platinum atom for complex (3.11) are given in Table 3.5. Complex (3.11) (Figure 3.6) displays square planar geometry about the metal atom with *trans* P-Pt-Cl angles of 172.2(3) and 177.7(3)° and P-Pt-Cl *cis* angles of 85.5(3) and 91.7(3)°. The Pt-P(OR)$_3$ distance is *ca.* 0.1 Å shorter than the Pt-PEt$_3$ bond distance. The difference in bond lengths can be ascribed to the greater π-bonding ability of phosphite ligands in comparison to phosphines, which is manifested in shorter metal-phosphite bonds.[49] The Pt-Cl bonds are similar in length with bond distances of 2.342(7) Å (*trans* to P(OR)$_3$) and 2.339(6) Å (*trans* to PEt$_3$). Saunders and co-workers found that in complexes of this type the Pt-Cl bond lengths do not show a regular variation. For *cis*-[PtCl$_2$(PEt$_3$){P(OPh)$_3$}] and *cis*-[PtCl$_2$(PEt$_3$){P(OC$_6$H$_4$-2,6-F$_2$)$_3$}] the Pt-Cl bond *trans* to PEt$_3$ is significantly longer than Pt-Cl *trans* to the phosphite, but for *cis*-[PtCl$_2$(PEt$_3$){PhP(OC$_6$H$_4$-2,6-F$_2$)$_2$}] the two bond lengths are essentially identical.[50]
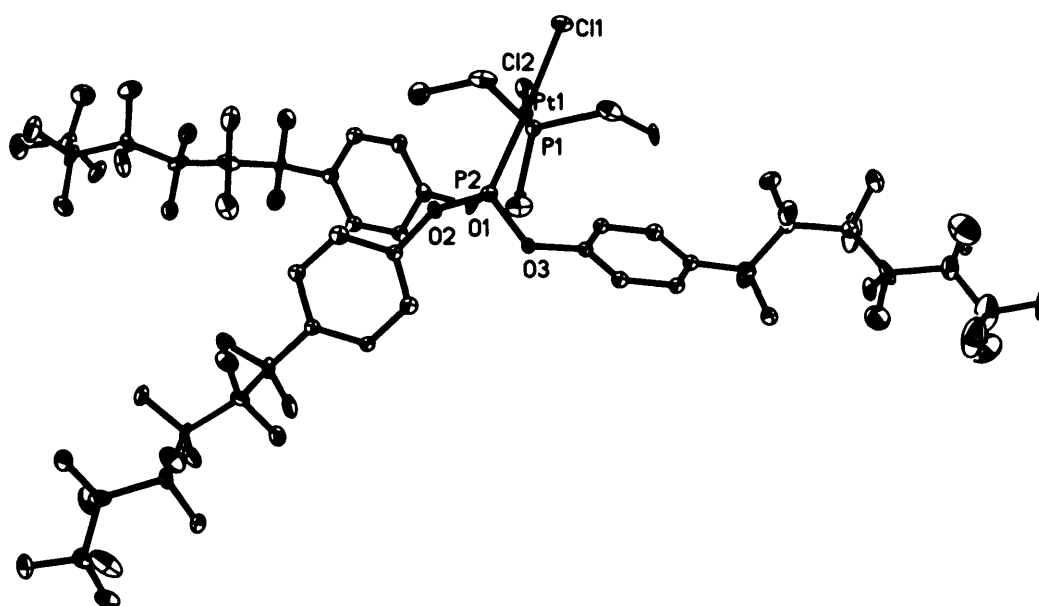
Figure 3.6 Crystal structure of *cis*-[PtCl$_2$(PEt$_3$){P(OC$_6$H$_4$-4-C$_6$F$_{13}$)$_3$}] (3.11) showing 30% displacement ellipsoids. H atoms are omitted for clarity.

Table 3.5 Selected bond distances and angles with e.s.d.s in parentheses for *cis*-[PtCl₂(PEt₃){P(OC₆H₄-4-C₆F₁₃)₃}] (**3.11**).

Bond Length (Å)		Bond Angle (°)	
Pt (1) - P (1)	2.271 (7)	P (1) - Pt (1) - P (2)	95.9 (3)
Pt (1) - P (2)	2.175 (8)	P (1) - Pt (1) - Cl (1)	85.5 (3)
Pt (1) - Cl (1)	2.342 (7)	P (1) - Pt (1) - Cl (2)	172.2 (3)
Pt (1) - Cl (2)	2.339 (6)	P (2) - Pt (1) - Cl (1)	177.7 (3)
P (2) - O (1)	1.59 (2)	P (2) - Pt (1) - Cl (2)	91.7 (3)
P (2) - O (2)	1.58 (2)	Cl (1) - Pt (1) - Cl (2)	86.9 (3)
P (2) - O (3)	1.58 (2)		

Comparison of the Pt-P bond lengths of (**3.11**) with those for *cis*-[PtCl₂(PEt₃){P(OPh)₃}] (Table 3.6) reveals that the Pt-P and P-O bond distances are the same within experimental error. The P-O and P-C bond distances of the phosphite ligands in both complexes are also the same within experimental error, indicating that the σ-donor and π-acceptor abilities of triphenylphosphite in platinum(II) complexes are not significantly modified by the introduction of perfluoroalkyl substituents in the *para* positions of the phenyl rings.

Table 3.6 Selected bond distances and angles with e.s.d.s in parentheses for *cis*-[PtCl₂(PEt₃){P(OPh)₃}].[50]

Bond Length (Å)		Bond Angle (°)	
Pt - PEt₃	2.269 (1)	P - Pt - P	97.9 (1)
Pt - P(OPh)₃	2.182 (2)	Cl - Pt - Cl	87.4 (1)
Pt - Cl (*trans*-PEt₃)	2.355 (2)	Cl - Pt - PEt₃ (*cis*)	86.7 (1)
Pt - Cl (*trans*-P(OPh)₃)	2.344 (2)	Cl - Pt - P(OPh)₃ (*cis*)	88.6 (1)
P - O (1)	1.583 (4)	Cl - Pt - PEt₃ (*trans*)	172.3 (1)
P - O (2)	1.579 (6)	Cl - Pt - P(OPh)₃ (*trans*)	171.6 (1)
P - O (3)	1.595 (4)		

3.4 Palladium(II) complexes of the type [PdCl$_2$L$_2$]

A series of palladium complexes of the type [PdCl$_2$L$_2$] have been prepared by the reaction of trans-[PdCl$_2$(MeCN)$_2$][51] with the perfluoroalkyl chain derivatised phosphinite, phosphonite and phosphite ligands. Trans-[PdCl$_2$(MeCN)$_2$] is a convenient starting material as it readily undergoes substitution of the labile acetonitrile ligands for tertiary phosphorus ligands (Scheme 3.3). Palladium complexes with tertiary phosphorus ligands have been shown to be active catalysts for a variety of homogeneous reactions including carbonylation[52] and C-C bond forming reactions.[53]

$$\text{Cl} \diagdown \underset{\diagup \text{Pd} \diagdown}{\diagup} \text{NCMe} \qquad + \qquad 2\,\text{PR}_3 \qquad \longrightarrow \qquad \text{Cl} \diagdown \underset{\diagup \text{Pd} \diagdown}{\diagup} \text{PR}_3$$
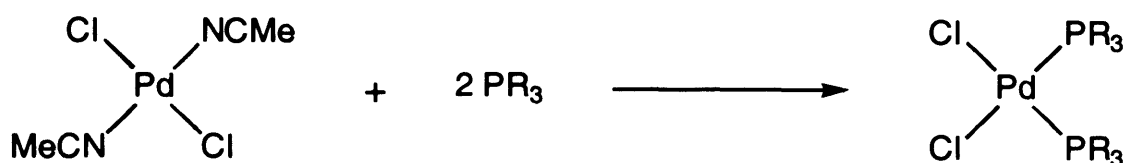
Scheme 3.3 Reaction of tertiary phosphorus ligands with trans-[PdCl$_2$(MeCN)$_2$].

3.4.1 Reaction of the phenoxy ligands PPh$_x$(OR)$_{3-x}$ with trans-[PdCl$_2$(MeCN)$_2$].

The reaction of ligands (2.2-2.4) with trans-[PdCl$_2$(MeCN)$_2$] in refluxing dichloromethane results in the formation of the complexes cis-[PdCl$_2$\{Ph$_2$P(OC$_6$H$_4$-4-C$_6$F$_{13}$)\}$_2$] (3.15), cis-[PdCl$_2$\{PhP(OC$_6$H$_4$-4-C$_6$F$_{13}$)$_2$\}$_2$] (3.16) and cis-[PdCl$_2$\{P(OC$_6$H$_4$-4-C$_6$F$_{13}$)$_3$\}$_2$] (3.17) as air- and moisture-stable off-white solids. Evidence for the formation of the complexes (3.15-3.17) was provided by their FAB mass spectra which exhibit characteristic peaks for the fragments [(M-Cl)$^+$] and [(M-2Cl)$^+$], and by elemental analysis. Complexes (3.15-3.17) have been assigned cis-geometries from their $\delta(^{31}$P) values which are characteristic for cis-isomers of this type. The far IR spectra of the complexes exhibit two bands between 280-340 cm^{-1}, confirming the cis-geometry. In common with the analogous platinum complex of the derivatised triaryl phosphite (3.3), complex (3.17) was found to be insoluble in perfluorinated solvents, however it was found to have a comparatively higher solubility in common organic

solvents such as dichloromethane. As with the platinum(II) analogues, the ^{1}H and ^{19}F{^{1}H} NMR spectra of these types of complexes are generally uninformative as they remain essentially the same as those for the free ligands.

$$PR_3 = Ph_2P(OC_6H_4\text{-}4\text{-}C_6F_{13}) \quad (3.15)$$

$$PhP(OC_6H_4\text{-}4\text{-}C_6F_{13})_2 \quad (3.16)$$
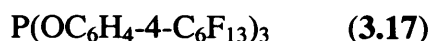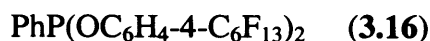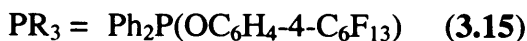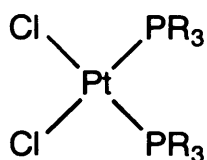
$$P(OC_6H_4\text{-}4\text{-}C_6F_{13})_3 \quad (3.17)$$

The ^{1}H NMR spectra of the product from the reaction of $Ph_2P(OC_6H_4\text{-}4\text{-}C_6F_{13})$ (2.2) with $trans$-[PdCl$_2$(MeCN)$_2$] was far more complex than expected, indicating a mixture of species. This was confirmed by the ^{31}P NMR spectrum of the crude product which exhibits two singlets, one at 113.1 δ and a second singlet at a significantly lower frequency at 78.2 δ. The palladium complexes are not as easy to characterise from their ^{31}P NMR spectra as their platinum analogues since palladium has no convenient spin active isotopes. Therefore, only singlets are observed in these spectra for symmetrical complexes of the type [PdCl$_2$L$_2$]. The resonance at 113.1 δ is assigned to (3.15) by comparison of the $\delta(^{31}$P) literature values for Pd(II)-phosphinite complexes.[17,25] The two components of the crude product were successfully separated by fractional recrystallisation from acetone. The compound which gives rise to the resonance at 78.2 δ was obtained as pale yellow crystals. Surprisingly, the ^{19}F NMR spectra of this complex exhibits *no* fluorine resonances, suggesting that no perfluoroalkyl tails were present in the complex. The ^{1}H NMR spectrum exhibits resonances assigned to a phenyl ring, but does not exhibit the AB pattern typical of the *para* substituted phenoxy group. Single crystals of the unknown complex suitable for X-ray crystallographic analysis were obtained from acetone solution. The complex was determined to be [Pd$_2$Cl$_2${(C$_6$H$_5$)$_2$PO$\cdots$H$\cdots$OP(C$_6$H$_5$)$_2$}$_2$] (3.18) which is consistent with the NMR data and elemental analysis.
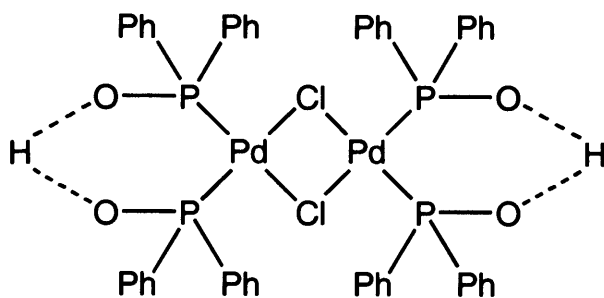
(3.18)

The crystal structure of the complex (Figure 3.7) shows that it consists of dinuclear chlorine bridged palladium units with two diphenylphosphinito groups coordinated to each palladium atom. Complex (3.18) has previously been prepared by Dixon and Rattray from diphenylphosphine oxide and sodium chloropalladate.[54] Ghaffar et al.[55] have also prepared, and structurally characterised, the same complex from the reaction of an orthometallated azobenzenepalladium chloride dimer with diphenylphosphine. It was initially thought that the complex formed as a result of the reaction of trans-[PdCl$_2$(MeCN)$_2$] with the hydrolysis product of Ph$_2$P(OC$_6$H$_4$-4-C$_6$F$_{13}$) which is diphenylphosphine oxide. The analogous reaction of ligand (2.2) with cis-[PtCl$_2$(MeCN)$_2$] yields cis-[PtCl$_2${PhP(OC$_6$H$_4$-4-C$_6$F$_{13}$)$_2$}] (3.1) in high yield, indicating that significant hydrolysis of the phosphinite ligand does not occur under similar reaction conditions. Comparison of the ^{31}P{^{1}H} NMR spectra of the crude product before and after refluxing in acetone showed an increase in the integration of the resonance attributed to (3.18) in comparison to the resonance for (3.15). This showed that complex (3.15) had been converted to complex (3.18) in solution, thereby demonstrating that the dimeric complex was not formed as a result of hydrolysis of the ligand prior to the reaction with trans-[PdCl$_2$(MeCN)$_2$]. The mode of formation of this unusual, but obviously thermodynamically favoured, product is unclear. The conversion of (3.15) to (3.18) could occur if the phosphinite ligand is highly labile and is able to dissociate from the metal centre. Hydrolysis of the free ligand in solution could then occur, thereby forming diphenylphosphine oxide that could then react with a dimeric palladium complex to give (3.18). However, no evidence to support this mechanism has been observed by ^{31}P{^{1}H} NMR spectroscopy, such as broadening/fluxionality of spectra normally associated with ligand lability.
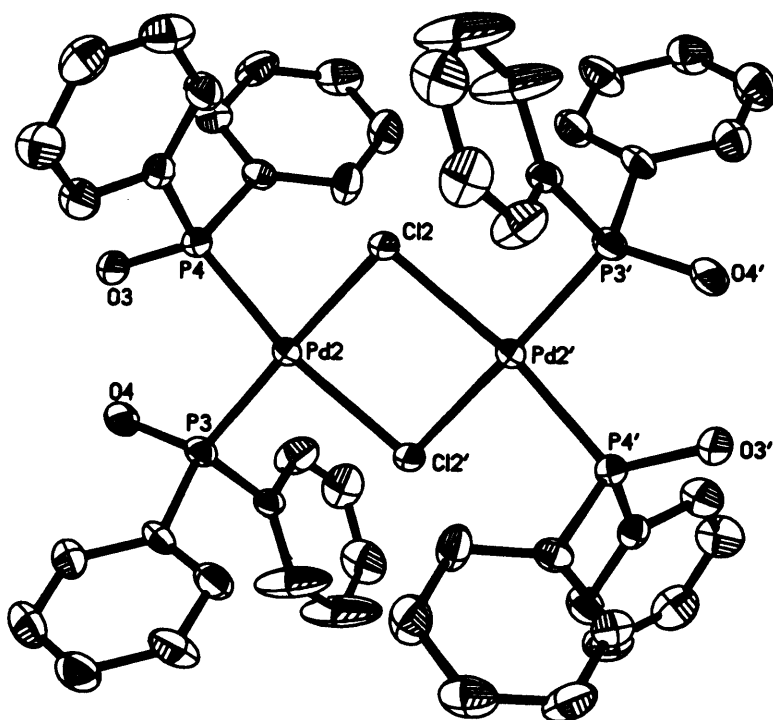
Figure 3.7 Crystal structure of [Pd₂Cl₂{(C₆H₅)₂PO···H···OP(C₆H₅)₂}₂] (**3.18**) showing 30% displacement ellipsoids. H atoms are omitted for clarity.

The reaction of the *meta* and *ortho* derivatised phosphites (**2.13**) and (**2.14**) with *trans*-[PdCl₂(MeCN)₂] in refluxing dichloromethane yields the complexes *cis*-[PdCl₂{P(OC₆H₄-3-C₆F₁₃)₃}₂] (**3.19**) and *trans*-[PdCl₂{P(OC₆H₄-2-C₆F₁₃)₃}₂] (**3.20**) which were found to be air- and moisture-stable. Both complexes exhibit characteristic peaks for the fragments [(M-Cl)⁺] and [(M-2Cl)⁺] in their FAB mass spectra. As with the analogous platinum(II) complex the *meta* phosphite complex (**3.19**) was isolated as a clear viscous oil. The far IR spectra obtained for both complexes are uninformative and, therefore, the geometries of the complexes have been tentatively assigned by comparison of $\delta(^{31}P)$ values with literature values for Pd(II)-phosphite complexes (Table 3.7).[56] As expected (**3.20**) was obtained as the *trans*-isomer due to the steric requirements of the bulky *ortho* derivatised phosphite.

PR₃ = P(OC₆H₄-3-C₆F₁₃)₃   (**3.19**)

R_3P, Cl, Pd, Cl, PR_3

$PR_3 = P(OC_6H_4\text{-}2\text{-}C_6F_{13})_3$ **(3.20)**
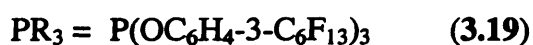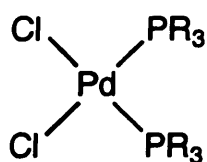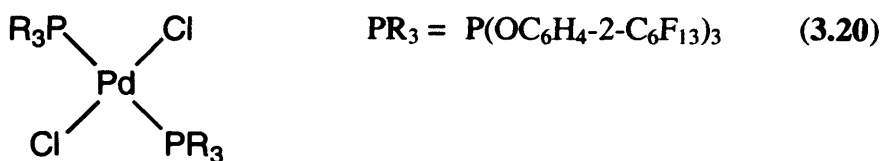
Table 3.7 $^{31}P\{^1H\}$ NMR data for **(3.18)** and $[PdCl_2L_2]$ complexes **(3.15-3.23)**.

Complex		$\delta(^{31}P)$
cis-[PdCl$_2${Ph$_2$P(OC$_6$H$_4$-4-C$_6$F$_{13}$)}$_2$][a]	**(3.15)**	113.1
cis-[PdCl$_2${PhP(OC$_6$H$_4$-4-C$_6$F$_{13}$)$_2$}$_2$][a]	**(3.16)**	122.2
cis-[PdCl$_2${P(OC$_6$H$_4$-4-C$_6$F$_{13}$)$_3$}$_2$][a]	**(3.17)**	83.6
[Pd$_2$Cl$_2${(C$_6$H$_5$)$_2$PO···H···OP(C$_6$H$_5$)$_2$}$_2$][a]	**(3.18)**	78.2
cis-[PdCl$_2${P(OC$_6$H$_4$-3-C$_6$F$_{13}$)$_3$}$_2$][a]	**(3.19)**	83.0
trans-[PdCl$_2${P(OC$_6$H$_4$-2-C$_6$F$_{13}$)$_3$}$_2$][b]	**(3.20)**	85.5
cis-[PdCl$_2${Ph$_2$P(OC$_2$H$_4$C$_6$F$_{13}$)}$_2$][a]	**(3.21)**	112.9
cis-[PdCl$_2${PhP(OC$_2$H$_4$C$_6$F$_{13}$)$_2$}$_2$][a]	**(3.22)**	126.4
[PdCl$_2${P(OC$_2$H$_4$C$_6$F$_{13}$)$_3$}$_2$][a,c]	**(3.23)**	94.4
cis-[PdCl$_2${P(OPh)$_3$}$_2$][a,d]		83.4
trans-[PdCl$_2${P(OC$_6$H$_4$-2-CH$_3$)$_3$}$_2$][a,d]		86.8

[a] Recorded in CDCl$_3$. [b] Recorded in (CD$_3$)$_2$CO. [c] Recorded in PP3 with D$_2$O insert.
[d] Ref. 28.

3.4.2 Reaction of the alkoxy ligands PPh$_x$(OR)$_{3-x}$ with trans-[PdCl$_2$(MeCN)$_2$].

The reaction of trans-[PdCl$_2$(MeCN)$_2$] with ligands **(2.16)** and **(2.17)** in refluxing dichloromethane yields the complexes cis-[PdCl$_2${Ph$_2$P(OC$_2$H$_4$C$_6$F$_{13}$)}$_2$] **(3.21)** and cis-[PdCl$_2${PhP(OC$_2$H$_4$C$_6$F$_{13}$)$_2$}$_2$] **(3.22)** as off-white air- and moisture-stable solids. Due to the air- and moisture-sensitivity of the alkyl phosphite **(2.18)** the reaction with trans-[PdCl$_2$(MeCN)$_2$] was carried out in a Schlenk flask under nitrogen using dry dichloromethane as solvent, affording [PdCl$_2${P(OC$_2$H$_4$C$_6$F$_{13}$)$_3$}$_2$] **(3.23)** as an air and moisture stable, pale yellow oil. The complexes have been characterised by elemental analysis and FAB mass spectrometry, with each of the complexes exhibiting peaks in their mass spectra for the fragments [(M-Cl)$^+$] and [(M-2Cl)$^+$].

$$Cl\diagdown{}_{Pd}\diagup{}^{PR_3} \qquad Cl\diagup{}^{}\diagdown{}_{PR_3}$$

PR$_3$ = Ph$_2$P(OC$_2$H$_4$C$_6$F$_{13}$) (3.21)

PhP(OC$_2$H$_4$C$_6$F$_{13}$)$_2$ (3.22)

P(OC$_2$H$_4$C$_6$F$_{13}$)$_3$ (3.23)
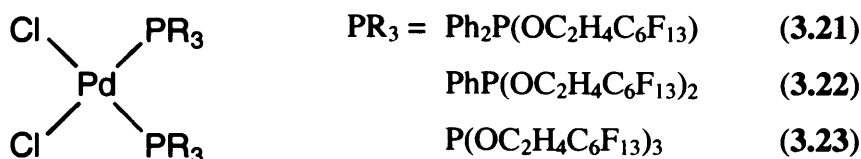
The geometry of complexes (3.21) and (3.22) have been assigned on the basis of their characteristic $\delta(^{31}P)$ values and from their far IR spectra which exhibit two bands assigned to *sym* and *asym* v(Pd-Cl) between 350-380 cm^{-1}. No assignment of geometry has been made for [PdCl$_2${P(OC$_2$H$_4$C$_6$F$_{13}$)$_3$}$_2$] (3.23) as an informative far IR spectra could not be obtained. Direct comparison of the NMR spectroscopic data with that for other Pd(II)-phosphite complexes cannot be made since complex (3.23) was found to be sparingly soluble in deuterated solvents. The ^{31}P NMR spectra was, therefore, obtained in PP3 with a D$_2$O insert, which may account for the significantly higher $\delta(^{31}P)$ value in comparison to the analogous aryl phosphite complex. Complex (3.23) was found to be soluble in perfluorinated solvents and preferentially soluble in the fluorous phase of a PP3/dichloromethane biphase. This result suggests that P(OC$_2$H$_4$C$_6$F$_{13}$)$_3$ is more efficient than P(OC$_6$H$_4$-4-C$_6$F$_{13}$)$_3$ at solubilising metal complexes in perfluorocarbon media as no solubility in PFC solvents was observed for *cis*-[PdCl$_2${P(OC$_6$H$_4$-4-C$_6$F$_{13}$)$_3$}$_2$]. The increased solubility of the alkyl phosphite can be attributed to the lower organic bulk of the non-polar, aliphatic C$_2$H$_4$ spacer in comparison to that for the larger C$_6$H$_4$ group.

3.5 Rhodium(III) complexes of the type [RhCl$_2$(η^5-C$_5$Me$_5$)L].

Rhodium complexes of general formula [RhCl$_2$(η^5-C$_5$Me$_5$)L] are easily prepared by the reaction of the chloro-bridged dimeric species [{RhCl(μ-Cl)(η^5-C$_5$Me$_5$)}$_2$][57,58] with a suitable donor ligand such as a tertiary phosphine (Scheme 3.4). The coordination chemistry of these complexes with triphenylphosphinite, phosphonite and phosphite ligands has been extensively investigated by Saunders and co-workers.[46] It is, therefore, of interest to make comparisons of the coordination chemistry of such complexes with the perfluoroalkyl chain derivatised ligands.
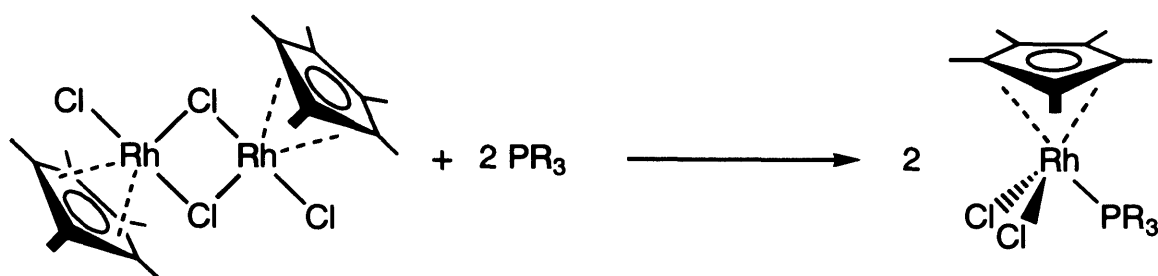
Scheme 3.4 Reaction of tertiary phosphorus ligands with [{RhCl(μ-Cl)(η^5-C$_5$Me$_5$)}$_2$].

The characterisation and structural assignment of [RhCl$_2$(η^5-C$_5$Me$_5$)L] complexes with phosphorus ligands is considerably aided by coupling between the rhodium atom and the phosphorus nucleus ($^1J_{Rh-P}$) which provides important information about the geometry of the complex beyond that derived from the symmetry of the spectra. The magnitude of the $^1J_{Rh-P}$ coupling constant also provides information regarding the nature of the M-P bond and the electronic properties of the ligand.

3.5.1 Reaction of the phenoxy PPh$_x$(OR)$_{3-x}$ ligands with [{RhCl(μ-Cl)(η^5-C$_5$Me$_5$)}$_2$].

The reaction of ligands (2.2-2.4) with [{RhCl(μ-Cl)(η^5-C$_5$Me$_5$)}$_2$] in refluxing dichloromethane yields the complexes [RhCl$_2$(η^5-C$_5$Me$_5$){Ph$_2$P(OC$_6$H$_4$-4-C$_6$F$_{13}$)}] (3.24), [RhCl$_2$(η^5-C$_5$Me$_5$){PhP(OC$_6$H$_4$-4-C$_6$F$_{13}$)$_2$}] (3.25), and [RhCl$_2$(η^5-C$_5$Me$_5$){P(OC$_6$H$_4$-4-C$_6$F$_{13}$)$_3$}] (3.26) which were isolated as air- and moisture-stable orange solids. The meta and ortho derivatised ligands (2.14) and (2.15) react similarly with [{RhCl(μ-Cl)(η^5-C$_5$Me$_5$)}$_2$] to give the complexes [RhCl$_2$(η^5-C$_5$Me$_5$){P(OC$_6$H$_4$-3-C$_6$F$_{13}$)$_3$}] (3.27) and [RhCl$_2$(η^5-C$_5$Me$_5$){P(OC$_6$H$_4$-2-C$_6$F$_{13}$)$_3$}] (3.28). The complexes were found to be highly soluble in most organic solvents and completely insoluble in perfluorinated solvents. The low fluorous affinity was expected due to the bulk of the C$_5$Me$_5$ group and the inclusion of only one modified ligand in each molecule. Despite the bulky nature of the ortho derivatised phosphite, complex (3.28) was formed in high yield, suggesting that the flexibility of the P-O-C linkage minimises steric interactions between the phosphite and the C$_5$Me$_5$ ring.
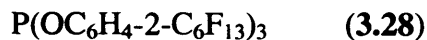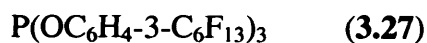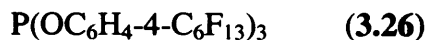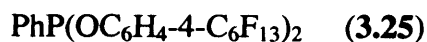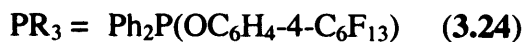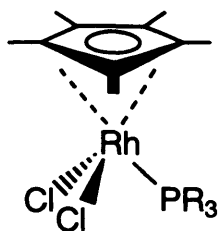
PR$_3$ =	Ph$_2$P(OC$_6$H$_4$-4-C$_6$F$_{13}$)	(3.24)
	PhP(OC$_6$H$_4$-4-C$_6$F$_{13}$)$_2$	(3.25)
	P(OC$_6$H$_4$-4-C$_6$F$_{13}$)$_3$	(3.26)
	P(OC$_6$H$_4$-3-C$_6$F$_{13}$)$_3$	(3.27)
	P(OC$_6$H$_4$-2-C$_6$F$_{13}$)$_3$	(3.28)

The complexes have been characterised by ^{1}H, ^{19}F{^{1}H} and ^{31}P{^{1}H} NMR spectroscopy and mass spectrometry and elemental analysis. Complexes (3.24-3.28) exhibit characteristic peaks in their FAB mass spectra for the fragments [(M-Cl)$^+$] and [(M-2Cl)$^+$]. The ^{1}H NMR spectra are similar to those for the free ligands with the addition of a doublet at ca. 1.5 δ assigned to the C$_5$Me$_5$ group with a J_{P-H} coupling constant of 4-6 Hz. Assignment of doublet coupling of the methyl protons of the pentamethylcyclopentadienyl ring with the phosphorus nucleus as opposed to with the rhodium atom arises from the analogy with the literature where the ^{1}H NMR spectrum of [IrCl$_2$(η^5-C$_5$Me$_5$){P(OC$_6$H$_3$-2,6-F$_2$)$_3$}] exhibits a doublet assigned to the C$_5$Me$_5$ ring with a coupling constant of similar magnitude.[59] The resonances in the ^{31}P{^{1}H} NMR spectra of complexes (3.24-3.28) are observed as doublets due to $^1J_{Rh-P}$ coupling. The values of δ(^{31}P) show the same variation with the number of phenoxy groups on the phosphorus ligand as the platinum and palladium complexes discussed previously (see Table 3.8). The magnitude of the $^1J_{Rh-P}$ coupling constant follows the trend (3.24) < (3.25) < (3.26) ≈ (3.27) ≈ (3.28) increasing in the order phosphinite < phosphonite < phosphite. This order is expected on the basis of increasing M-P π-bonding of the ligand with the increasing numbers of phenoxy groups on the ligand. The $^1J_{Rh-P}$ value of 245 Hz for [RhCl$_2$(η^5-C$_5$Me$_5$){P(OC$_6$H$_4$-4-C$_6$F$_{13}$)$_3$}] compares closely to the literature value of 240 Hz for [RhCl$_2$(η^5-C$_5$Me$_5$){P(OPh)$_3$}][47] suggesting that the electron-withdrawing effect of the perfluoroalkyl substituent has a negligible impact on the M-P bond.

Table 3.8 ^{31}P{^{1}H} NMR data for [RhCl$_2$(η^5-C$_5$Me$_5$)L] complexes (3.24-3.31).

Complex		$\delta(^{31}$P)	$^{1}J_{Rh-P}$ (Hz)
[RhCl$_2$(η^5-C$_5$Me$_5$){Ph$_2$P(OC$_6$H$_4$-4-C$_6$F$_{13}$)}]^a	(3.24)	116	171
[RhCl$_2$(η^5-C$_5$Me$_5$){PhP(OC$_6$H$_4$-4-C$_6$F$_{13}$)$_2$}]^a	(3.25)	146	203
[RhCl$_2$(η^5-C$_5$Me$_5$){P(OC$_6$H$_4$-4-C$_6$F$_{13}$)$_3$}]^a	(3.26)	106	245
[RhCl$_2$(η^5-C$_5$Me$_5$){P(OC$_6$H$_4$-3-C$_6$F$_{13}$)$_3$}]^a	(3.27)	107	244
[RhCl$_2$(η^5-C$_5$Me$_5$){P(OC$_6$H$_4$-2-C$_6$F$_{13}$)$_3$}]^a	(3.28)	110	251
[RhCl$_2$(η^5-C$_5$Me$_5$){Ph$_2$P(OC$_2$H$_4$C$_6$F$_{13}$)}]^a	(3.29)	117	157
[RhCl$_2$(η^5-C$_5$Me$_5$){PhP(OC$_2$H$_4$C$_6$F$_{13}$)$_2$}]^a	(3.30)	147	181
[RhCl$_2$(η^5-C$_5$Me$_5$){P(OC$_2$H$_4$C$_6$F$_{13}$)$_3$}]^a	(3.31)	120	224

^{a} Recorded in CDCl$_3$.

Single crystals of complexes (3.25) and (3.26) suitable for X-ray crystallographic analysis were obtained from acetone solutions. Selected bond distances and angles about the rhodium atom for both complexes are given in Table 3.9. Complexes (3.25) (Figure 3.8) and (3.26) (Figure 3.9) display the expected three-legged piano-stool geometry about the rhodium centre with P-Rh-Cl and Cl-Rh-Cl angles of approximately 90°. The two molecules contain one shorter and one longer Rh-Cl bond with the bonds for (3.26) being shorter than those of (3.25).
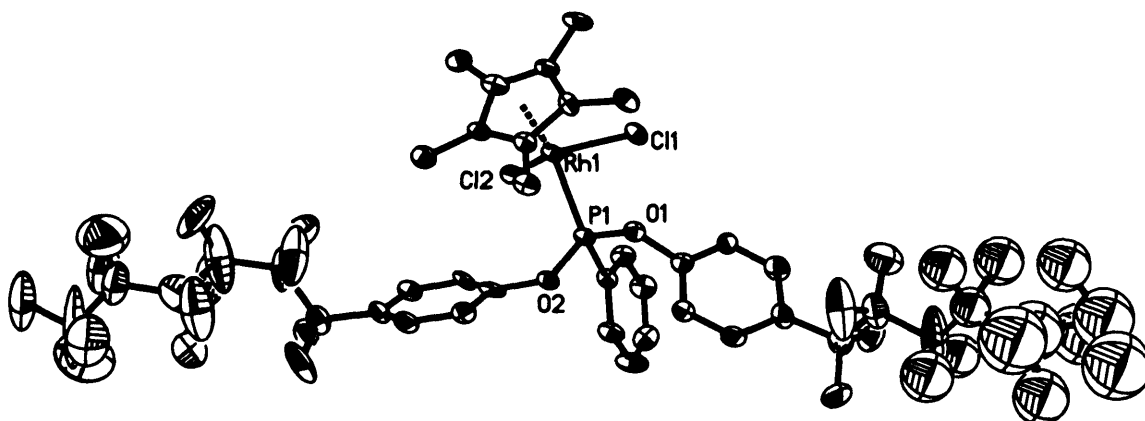
Figure 3.8 Crystal structure of [RhCl$_2$(η^5-C$_5$Me$_5$){PhP(OC$_6$H$_4$-4-C$_6$F$_{13}$)$_2$}] (3.25) showing 30% displacement ellipsoids. H atoms are omitted for clarity.

The Rh-P bond distance for the phosphite complex is *ca.* 0.02 Å shorter than that for the phosphonite complex as a result of greater π-bonding between the metal and the phosphite ligand. Comparison of the Rh-P bond distance in $[RhCl_2(\eta^5\text{-}C_5Me_5)\{PhP(OPh)_2\}]^{47}$ of 2.256(3) Å with that for complex (3.25) shows that they are the same within experimental error. This indicates that the electronic effect of the perfluoroalkyl substituent on the M-P bond length in this complex is negligible and is consistent with the $^{31}P\{^1H\}$ NMR data. Comparison of the bond angle data for the two complexes shows no significant variation, indicating that the geometries about the rhodium atoms in the two complexes are almost identical. The steric effect of the perfluoroalkyl substituents on the bond lengths and bond angles of $[RhCl_2(\eta^5\text{-}C_5Me_5)\{PhP(OC_6H_4\text{-}4\text{-}C_6F_{13})_2\}]$ is, therefore, negligible. As with other structures discussed previously in this section, the fluorine atoms towards the end of the perfluoroalkyl chains of complex (3.25) show high displacement parameters.
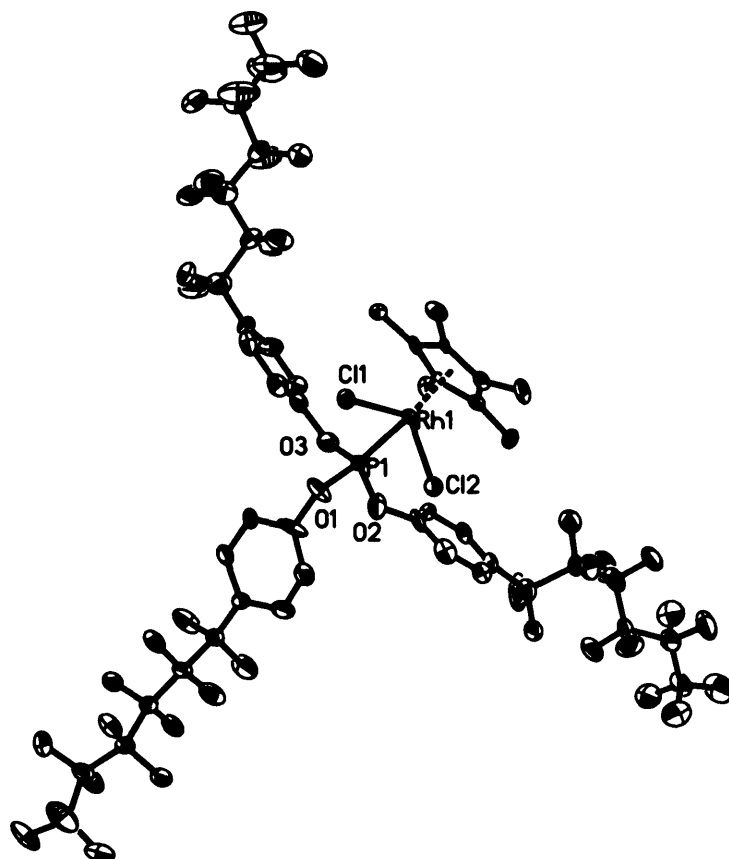
Figure 3.9 Crystal structure of $[RhCl_2(\eta^5\text{-}C_5Me_5)\{P(OC_6H_4\text{-}4\text{-}C_6F_{13})_3\}]$ (3.26) showing 30% displacement ellipsoids. H atoms are omitted for clarity.

92

The crystal structure of (3.26) gives a clear indication of the size of the derivatised phosphite ligand in comparison to the metal centre. The P-Rh-Cl and Cl-Rh-Cl bond angles are similar to those of the iridium(III) triphenylphosphite complex [IrCl$_2$(η^5-C$_5$Me$_5$){P(OC$_6$H$_3$-2,6-F$_2$)$_2$}][62] which range from 87.9(1) to 92.0(1)°. The three O-P-O angles which range from 95.5(7) to 102.9(6)° are also similar to those for [IrCl$_2$(η^5-C$_5$Me$_5$){P(OC$_6$H$_3$-2,6-F$_2$)$_2$}] which range from 98.4(3)-102.3(3)°. The average P-O bond distance for (3.26) is 1.583(6) Å, which is slightly smaller than the average for coordinated triphenylphosphite ligands of 1.600(11) Å.[60]

Table 3.9   Selected bond distances (Å) and bond angles (°) with e.s.d.s in parentheses for complexes [RhCl$_2$(η^5-C$_5$Me$_5$){PhP(OC$_6$H$_4$-4-C$_6$F$_{13}$)$_2$}] (3.25) and [RhCl$_2$(η^5-C$_5$Me$_5$){P(OC$_6$H$_4$-4-C$_6$F$_{13}$)$_3$}] (3.26).

	(3.25)	(3.26)
Rh (1) – P (1)	2.257(3)	2.238(3)
Rh (1) – Cl (1)	2.411(3)	2.404(3)
Rh (1) – Cl (2)	2.405(3)	2.386(3)
Rh (1) – C (1)	2.233(11)	2.201(11)
Rh (1) – C (2)	2.166(10)	2.230(12)
Rh (1) – C (3)	2.179(11)	2.231(12)
Rh (1) – C (4)	2.238(13)	2.173(12)
Rh (1) – C (5)	2.238(13)	2.194(12)
P (1) – O (1)	1.596(7)	1.580(11)
P (1) – O (2)	1.630(7)	1.572(11)
P (1) – O (3)	-	1.597(11)
Cl (1) – Rh (1) – Cl (2)	92.09(10)	89.71(12)
P (1) – Rh (1) – Cl (1)	86.80(11)	89.97(11)
P (1) – Rh (1) – Cl (2)	93.35(10)	87.81(12)
O (1) – P (1) – O (2)	96.7(4)	97.3(7)
O (1) – P (1) – O (3)	-	102.9(6)
O (2) – P (1) – O (3)	-	95.5(7)

3.5.2 Reaction of the alkoxy PPh$_x$(OR)$_{3-x}$ ligands with [{RhCl(μ-Cl)(η^5-C$_5$Me$_5$)}$_2$].

The reaction of [{RhCl(μ-Cl)(η^5-C$_5$Me$_5$)}$_2$] with ligands (2.5-2.7) in refluxing dichloromethane yields the complexes [RhCl$_2$(η^5-C$_5$Me$_5$){Ph$_2$P(OC$_2$H$_4$C$_6$F$_{13}$)}] (3.29), [RhCl$_2$(η^5-C$_5$Me$_5$){PhP(OC$_2$H$_4$C$_6$F$_{13}$)$_2$}] (3.30) and [RhCl$_2$(η^5-C$_5$Me$_5$){P(OC$_2$H$_4$C$_6$F$_{13}$)$_3$}] (3.31) which were isolated as air- and moisture-stable orange/red solids. In common with their aryl analogues no solubility in perfluorinated solvents was observed for complexes (3.29-3.31). Evidence for the formation of the complexes is provided by elemental analysis and their FAB mass spectra which exhibit peaks assigned to the fragments [(M-Cl)$^+$] and [(M-2Cl)$^+$].

PR$_3$ =	Ph$_2$P(OC$_2$H$_4$C$_6$F$_{13}$)	(3.29)
	PhP(OC$_2$H$_4$C$_6$F$_{13}$)$_2$	(3.30)
	P(OC$_2$H$_4$C$_6$F$_{13}$)$_3$	(3.31)
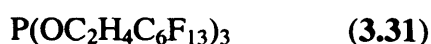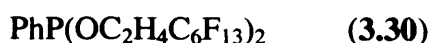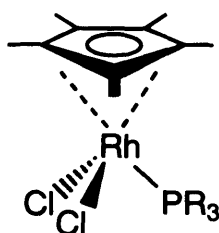
The ^{31}P{^{1}H} NMR data for the alkyl phosphinite, phosphonite and phosphite complexes show the same trends as for their aryl analogues (Table 3.8). The $^1J_{\text{Rh-P}}$ coupling constants for complexes (3.29-3.31) are ca. 20 Hz smaller than those of their aryl counterparts. A similar variation has been observed in the coupling constants of the alkyl and aryl platinum complexes, which can be ascribed to the smaller σ-component of the Rh-P bond due to weaker π-bonding between the rhodium atom and the alkyl ligands in comparison to their aryl analogues.

3.6 Iridium(III) complexes of the type [IrCl$_2$(η^5-C$_5$Me$_5$)L].

Iridium complexes of general formula [IrCl$_2$(η^5-C$_5$Me$_5$)L] are prepared in a similar manner to the analogous [RhCl$_2$(η^5-C$_5$Me$_5$)L] complexes (discussed in Section 3.5) by the reaction of the chloro-bridged dimeric species [{IrCl(μ-Cl)(η^5-C$_5$Me$_5$)}$_2$] with a suitable donor ligand such as a tertiary phosphine (Scheme 3.5). Unlike rhodium, iridium has no naturally occurring spin active isotopes, therefore characterisation of the complexes by ^{31}P NMR spectroscopy is not as convenient as for the analogous rhodium complexes.
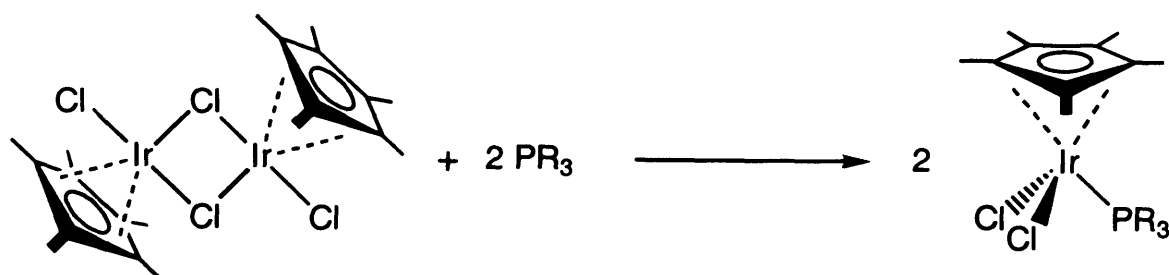
Scheme 3.5 Reaction of tertiary phosphorus ligands with [{IrCl(μ-Cl)(η^5-C$_5$Me$_5$)}$_2$].

3.6.1 Reaction of phenoxy PPh$_x$(OR)$_{3-x}$ ligands with [{IrCl(μ-Cl)(η^5-C$_5$Me$_5$)}$_2$].

The reaction of the aryl phosphinite, phosphonite and phosphite ligands (2.2-2.4) with [{IrCl(μ-Cl)(η^5-C$_5$Me$_5$)}$_2$] in refluxing dichloromethane yields the complexes [IrCl$_2$(η^5-C$_5$Me$_5$){Ph$_2$P(OC$_6$H$_4$-4-C$_6$F$_{13}$)}] (3.32), [IrCl$_2$(η^5-C$_5$Me$_5$){PhP(OC$_6$H$_4$-4-C$_6$F$_{13}$)$_2$}] (3.33), and [IrCl$_2$(η^5-C$_5$Me$_5$){P(OC$_6$H$_4$-4-C$_6$F$_{13}$)$_3$}] (3.34) which were isolated as air- and moisture-stable orange/yellow solids. In common with the rhodium analogues, complexes (3.32-3.34) were found to be highly soluble in most organic solvents and completely insoluble in perfluorinated solvents.

PR$_3$ =	Ph$_2$P(OC$_6$H$_4$-4-C$_6$F$_{13}$)	(3.32)
	PhP(OC$_6$H$_4$-4-C$_6$F$_{13}$)$_2$	(3.33)
	P(OC$_6$H$_4$-4-C$_6$F$_{13}$)$_3$	(3.34)
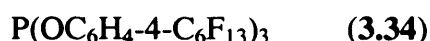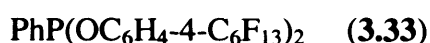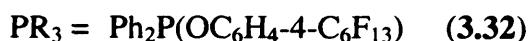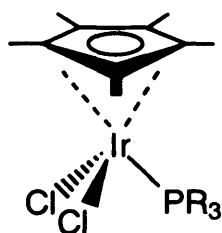
Complexes (3.32-3.34) were characterised by ^{1}H, ^{19}F{^{1}H} and ^{31}P{^{1}H} NMR spectroscopy and mass spectrometry and elemental analysis. The ^{1}H NMR spectra in common with those for the analogous rhodium species exhibit the characteristic doublet resonance at ca. 1.5 δ assigned to the C$_5$Me$_5$ ring. The J_{P-H} coupling constants are in the range 3-4 Hz, which increase with the number of phenoxy groups attached to the phosphorus atom and which are lower in magnitude than for the rhodium analogues. The ^{31}P{^{1}H} NMR spectra of the complexes exhibit singlet resonances due to iridium having no spin active isotopes. The spectra, therefore, yield little information about the nature of the M-P bond. The values of $\delta(^{31}$P) for complexes

(3.32-3.34) are *ca.* 40 Hz to lower frequency than the rhodium complexes and show the same variation with the number of phenoxy groups (Table 3.10).

Table 3.10 $^{31}P\{^1H\}$ NMR data for [IrCl$_2$(η^5-C$_5$Me$_5$)L] complexes (3.32-3.34).

Complex		$\delta(^{31}P)$
[IrCl$_2$(η^5-C$_5$Me$_5$){Ph$_2$P(OC$_6$H$_4$-4-C$_6$F$_{13}$)}]^a	(3.32)	75
[IrCl$_2$(η^5-C$_5$Me$_5$){PhP(OC$_6$H$_4$-4-C$_6$F$_{13}$)$_2$}]^a	(3.33)	102
[IrCl$_2$(η^5-C$_5$Me$_5$){P(OC$_6$H$_4$-4-C$_6$F$_{13}$)$_3$}]^a	(3.34)	67
[IrCl$_2$(η^5-C$_5$Me$_5$){Ph$_2$P(OC$_2$H$_4$C$_6$F$_{13}$)}]^a	(3.35)	77
[IrCl$_2$(η^5-C$_5$Me$_5$){PhP(OC$_2$H$_4$C$_6$F$_{13}$)$_2$}]^a	(3.36)	105
[IrCl$_2$(η^5-C$_5$Me$_5$){P(OC$_2$H$_4$C$_6$F$_{13}$)$_3$}]^a	(3.37)	83

^{a} Recorded in CDCl$_3$.

Single crystals of complex (3.33) were obtained from an acetone solution and analysed by X-ray crystallography. Selected bond distances and angles about the iridium atom are given in Table 3.11. Complex (3.33) exhibits the same three-legged piano-stool geometry as [RhCl$_2$(η^5-C$_5$Me$_5$){PhP(OC$_6$H$_4$-4-C$_6$F$_{13}$)$_2$}] (3.25) with P-Ir-Cl and Cl-Ir-Cl bond angles of *ca.* 90° (Figure 3.10). The M-P bond distance is *ca.* 0.03 Å shorter than in the analogous rhodium complex (3.25) suggesting that the Ir-P bond is slightly stronger than the Rh-P bond. The Ir-P bond distance of [IrCl$_2$(η^5-C$_5$Me$_5$){PMe$_3$}][61] of 2.281 Å is significantly longer than that of complex (3.25) demonstrating the greater π-bonding ability of the derivatised phosphonite in comparison to that for trimethylphosphine.

Table 3.11   Selected bond distances and angles with e.s.d.s in parentheses for [IrCl$_2$(η^5-C$_5$Me$_5$){PhP(OC$_6$H$_4$-4-C$_6$F$_{13}$)$_2$}] (3.33).

Bond Length (Å)		Bond Angle (°)	
Ir (1) – P (1)	2.231(2)	Cl (1) – Ir (1) – Cl (2)	86.78(8)
Ir (1) – Cl (1)	2.405(2)	P (1) – Ir (1) – Cl (1)	89.76(8)
Ir (1) – Cl (2)	2.397(2)	P (1) – Ir (1) – Cl (2)	93.65(9)
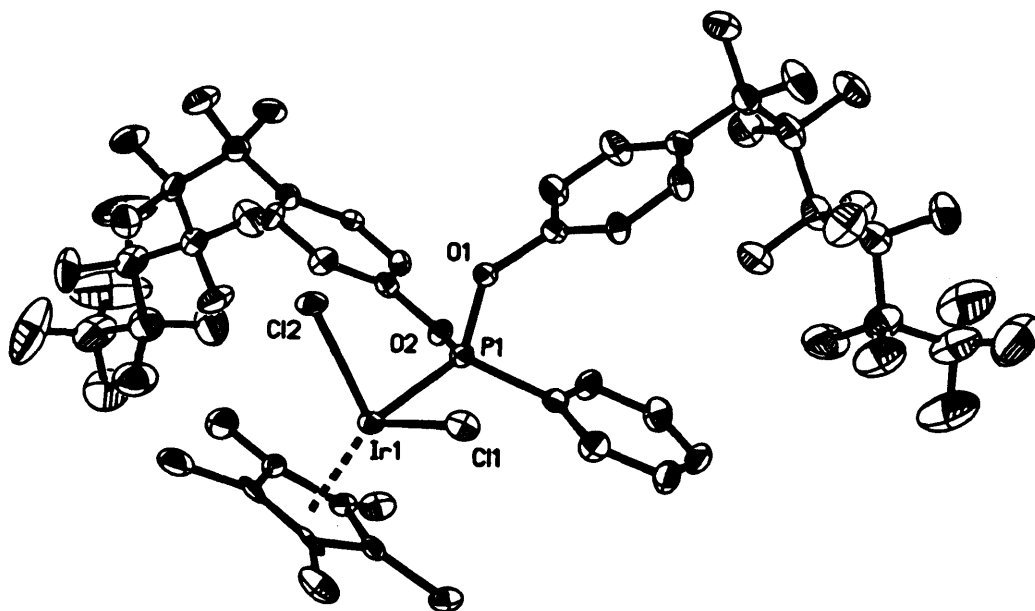
Figure 3.10 Crystal structure of [IrCl$_2$(η^5-C$_5$Me$_5$){PhP(OC$_6$H$_4$-4-C$_6$F$_{13}$)$_2$}] (**3.33**).

3.6.2 Reaction of alkoxy PPh$_x$(OR)$_{3-x}$ ligands with [{IrCl(μ-Cl)(η^5-C$_5$Me$_5$)}$_2$].

Ligands (**2.5-2.7**) were each allowed to react with [{IrCl(μ-Cl)(η^5-C$_5$Me$_5$)}$_2$] in refluxing dichloromethane over several hours. The volume of dichloromethane was reduced *in vacuo* and hexane added to precipitate the complexes [IrCl$_2$(η^5-C$_5$Me$_5$){Ph$_2$P(OC$_2$H$_4$C$_6$F$_{13}$)}] (**3.35**), [IrCl$_2$(η^5-C$_5$Me$_5$){PhP(OC$_2$H$_4$C$_6$F$_{13}$)$_2$}] (**3.36**), and [IrCl$_2$(η^5-C$_5$Me$_5$){P(OC$_2$H$_4$C$_6$F$_{13}$)$_3$}] (**3.37**) which were isolated as air- and moisture-stable yellow solids. In common with their aryl analogues, the alkyl complexes were found to be completely insoluble in perfluorinated solvents. Evidence for the formation of (**3.35-3.37**) is provided by their FAB mass spectra which exhibit peaks for the fragments of the parent ion [(M-Cl)$^+$] and [(M-2Cl)$^+$] and by elemental analysis.

	PR$_3$ =	Ph$_2$P(OC$_2$H$_4$C$_6$F$_{13}$)	(**3.35**)
		PhP(OC$_2$H$_4$C$_6$F$_{13}$)$_2$	(**3.36**)
		P(OC$_2$H$_4$C$_6$F$_{13}$)$_3$	(**3.37**)
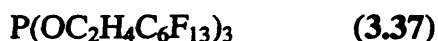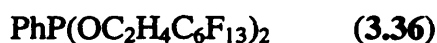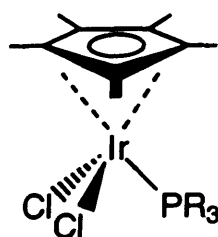
The ^{31}P{^{1}H} NMR spectra of the complexes bearing alkoxy ligands exhibit the same trends as the aryloxy complexes (Table 3.10). The difference in $\delta(^{31}$P) values between the phosphinite and phosphonite complexes and their aryl analogues are small being 2-3 ppm to higher frequency. The difference in $\delta(^{31}$P) between the phosphite complexes is significantly greater with the resonance of the alkyl complex (3.37) being 16 ppm to higher frequency than that for (3.34).

Single crystals of complex (3.35) were obtained from acetone solution and the structure determined by X-ray crystallography (Figure 3.11). Selected bond lengths and bond angles are given in Table 3.12. The geometry about the iridium atom is the same as that for the aryl phosphonite complex (3.33) with P-Ir-Cl and Cl-Ir-Cl angles of ca. 90°. The Ir-Cl bond lengths for the two complexes are also the same within experimental error. The Ir-P bond distance for the alkyl phosphinite complex (3.35) of 2.255(6) Å is significantly longer than that for the phosphonite complex (3.33) of 2.231(2) Å, as a result of greater π-bonding between the metal centre and the phosphonite ligand.
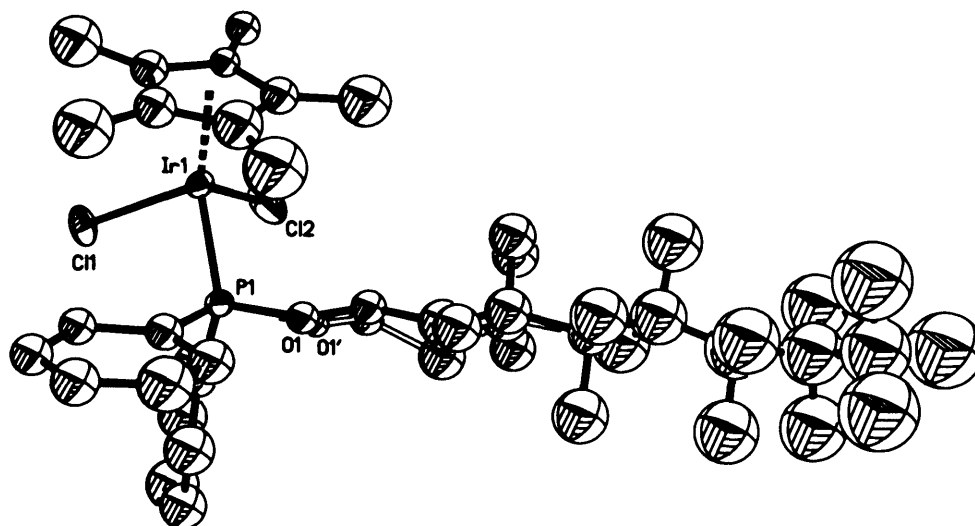
Figure 3.11   Crystal   structure   of   [IrCl$_2$(η^5-C$_5$Me$_5$){Ph$_2$P(OC$_2$H$_4$C$_6$F$_{13}$)}]   (3.35) showing 30% displacement ellipsoids. H atoms are omitted for clarity. Disordered atoms shown with prime and open bonds.

As indicated in Figure 3.11, the crystal structure of (3.35) exhibits significant disorder at the P-O bond, depicted by open and prime bonds. This disorder has consequences for the rest of the perfluoroalkyl chain, which shows increasing displacement parameters for atoms with increasing distance from the metal centre.

Table 3.12 Selected bond distances and angles with e.s.d.s in parentheses for $[IrCl_2(\eta^5-C_5Me_5)\{Ph_2P(OC_2H_4C_6F_{13})\}]$ (3.35).

Bond Length (Å)		Bond Angle (°)	
Ir (1) – P (1)	2.255(6)	Cl (1) – Ir – Cl (2)	92.2(3)
Ir (1) – Cl (1)	2.398(5)	P (1) – Ir (1) – Cl (1)	88.4(2)
Ir (1) – Cl (2)	2.393(7)	P (1) – Ir (1) – Cl (2)	94.2(4)

3.7 Rhodium(I) complexes of the type [RhCl(CO)L₂].

Rhodium complexes of the type [RhCl(CO)L₂] in which L represents the derivatised phosphinite, phosphonite or phosphite ligands are of interest in examining the electronic nature of the perfluoroalkyl derivatised ligands as the stretching frequency of the carbonyl group (v_{CO}) is sensitive to the electronic influence of the ligands (see Section 3.7.3).[62,63] Further impetus for the synthesis of such complexes was provided by the initial research of Horváth and Rábai which demonstrated the fluorous solubility of the rhodium complex $[HRh(CO)\{P(C_2H_4C_6F_{13})_3\}_3]$ and its application as a hydroformylation catalyst under fluorous biphase conditions.[64] On this basis it was believed that [RhCl(CO)L₂] complexes bearing the perfluoroalkyl derivatised phosphite ligands would be preferentially soluble in perfluorocarbon solvents. Rhodium carbonyl complexes are readily prepared by the reaction of the chloro-bridged dimeric species $[\{Rh(\mu-Cl)(CO)_2\}_2]$[65] under mild conditions with a stoichiometric amount of a tertiary phosphorus ligand (Scheme 3.6). The reaction generally proceeds with cleavage of the chlorine bridge accompanied by the liberation of CO gas to yield the complex trans-[RhCl(CO)L₂]. The trans-isomer is normally formed as CO is a strong π-acid and, therefore, exerts a large trans-influence.

The structure scheme at the top (dirhodium complex reacting with 2 PR₃):

$$OC, Cl, CO \text{ dirhodium bridged structure} + 2\ PR_3 \longrightarrow 2 \begin{array}{c} OC \diagdown \diagup PR_3 \\ Rh \\ R_3P \diagup \diagdown Cl \end{array}$$
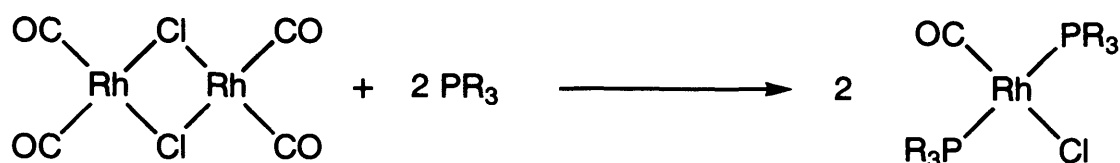
Scheme 3.6 Reaction of tertiary phosphorus ligands with [{Rh(μ-Cl)(CO)$_2$}$_2$].

3.7.1 Reaction of phenoxy PPh$_x$(OR)$_{3-x}$ ligands with [{RhCl(CO)$_2$}$_2$].

The reaction of the aryl phosphinite ligand (2.2) with [{Rh(μ-Cl)(CO)$_2$}$_2$] was performed using Schlenk techniques to ensure anaerobic conditions were maintained throughout. The reaction was carried out at room temperature by the addition of a solution of the ligand in dried and degassed dichloromethane via canular to a stirred solution of [{Rh(μ-Cl)(CO)$_2$}$_2$] in dried and degassed dichloromethane. The observed effervescence of the reaction mixture provided evidence for the liberation of CO during the reaction. The solvent was removed in vacuo and the crude product recrystallized from dichloromethane/hexane to yield trans-[RhCl(CO){Ph$_2$P(OC$_6$H$_4$-4-C$_6$F$_{13}$)}$_2$] (3.38) as a yellow solid. The reaction of the aryl phosphonite ligand (2.3) with [{Rh(μ-Cl)(CO)$_2$}$_2$] was carried out similarly to yield the complex trans-[RhCl(CO){PhP(OC$_6$H$_4$-4-C$_6$F$_{13}$)$_2$}$_2$] (3.39).

$$\begin{array}{c} OC \diagdown \diagup PR_3 \\ Rh \\ R_3P \diagup \diagdown Cl \end{array}$$

PR$_3$ = Ph$_2$P(OC$_6$H$_4$-4-C$_6$F$_{13}$)   (3.38)

PhP(OC$_6$H$_4$-4-C$_6$F$_{13}$)$_2$ (3.39)
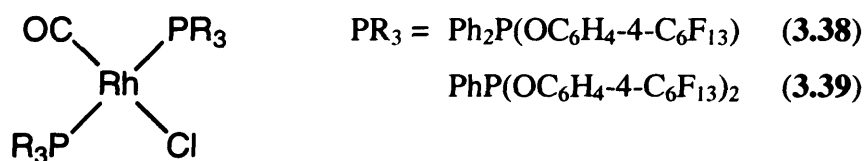
The FAB mass spectra of the complexes (3.38) and (3.39) exhibit characteristic peaks assigned to the fragment [(M-Cl-CO)$^+$]. The geometries assigned to the complexes were confirmed by their ^{31}P{^{1}H} NMR spectra which each exhibit a single doublet resonance due to the coupling of equivalent phosphorus nuclei with the rhodium atom. The magnitudes of the $^1J_{Rh-P}$ coupling constants for complexes (3.38) and (3.39) (see Table 3.13) are indicative of phosphinite and phosphonite complexes of the type trans-[RhCl(CO)L$_2$].[66] Complexes (3.38) and (3.39) were found to be highly air- and moisture-sensitive, decomposing over several hours to brown oils on exposure to the atmosphere. The ^{31}P{^{1}H} NMR spectra of the brown oils exhibit a

multitude of peaks at low frequency associated with the products of ligand decomposition.

Table 3.13 $^{31}P\{^1H\}$ NMR data for [RhCl(CO)L$_2$]^a and [{Rh(μ-Cl)L$_2$}$_2$]^b complexes (3.40-3.47).

Complex		$\delta(^{31}P)$	$^1J_{Rh-P}$ (Hz)
trans-[RhCl(CO){Ph$_2$P(OC$_6$H$_4$-4-C$_6$F$_{13}$)}$_2$]^a (3.38)		125	141
trans-[RhCl(CO){PhP(OC$_6$H$_4$-4-C$_6$F$_{13}$)$_2$}$_2$]^a (3.39)		149	176
[Rh(μ-Cl){P(OC$_6$H$_4$-4-C$_6$F$_{13}$)$_3$}$_2$]$_2$^{b}	(3.40)	113	313
[Rh(μ-Cl){P(OC$_6$H$_4$-4-C$_8$F$_{17}$)$_3$}$_2$]$_2$^{b}	(3.41)	113	314
[Rh(μ-Cl){P(OC$_6$H$_4$-4-C$_{10}$F$_{21}$)$_3$}$_2$]$_2$^{b}	(3.42)	114	313
[Rh(μ-Cl){P(OC$_6$H$_4$-3-C$_6$F$_{13}$)$_3$}$_2$]$_2$^{b}	(3.43)	114	309
trans-[RhCl(CO){P(OC$_6$H$_4$-2-C$_6$F$_{13}$)$_3$}$_2$]^a	(3.44)	115	223
trans-[RhCl(CO){Ph$_2$P(OC$_2$H$_4$C$_6$F$_{13}$)}$_2$]^a	(3.45)	121	136
trans-[RhCl(CO){PhP(OC$_2$H$_4$C$_6$F$_{13}$)$_2$}$_2$]^a	(3.46)	154	167
trans-[RhCl(CO){P(OC$_2$H$_4$C$_6$F$_{13}$)$_3$}$_2$]^a	(3.47)	130	199

^{a} Recorded in CDCl$_3$. ^{b} Recorded in PP3 with C$_6$D$_6$ insert.

The reaction of a stoichiometric quantity of aryl phosphite (2.4) with [{Rh(μ-Cl)(CO)$_2$}$_2$] was performed under anaerobic conditions. A colourless solution of ligand (2.4) in dried and degassed PP3 was added via canular to a stirred, orange solution of [{Rh(μ-Cl)(CO)$_2$}$_2$] in dried and degassed dichloromethane. Effervescence of the reaction mixture was observed along with the formation of a biphasic system. The upper organic phase decolourised over several minutes, as the lower fluorous phase became yellow, indicating that the product of the reaction was preferentially soluble in perfluorocarbon solvents. The fluorous phase was transferred to a Schlenk flask and the PP3 removed in vacuo to yield the crude product which was recrystallized from ethanol, affording complex (3.40) as an air- and moisture-stable yellow solid.

No peaks assignable to the expected rhodium carbonyl species were evident in the FAB mass spectra of (3.40). The $^{31}P\{^1H\}$ NMR spectra of the complex exhibits the expected doublet resonance, however, the $^1J_{Rh-P}$ coupling constant of 313 Hz is

significantly larger than the literature value of 230 Hz for [RhCl(CO){P(OPh)$_3$}$_2$].[67] Surprisingly, the IR spectrum of (3.40) exhibits no absorptions in the region 1800-2100 cm^{-1} associated with the symmetric (A$_1$) stretch of a carbonyl group, indicating the absence of CO in the complex. On the basis of the IR and ^{31}P{^{1}H} NMR spectra and elemental analysis the complex (3.40) has been assigned as the chloro bridged dimeric species [Rh(μ-Cl){P(OC$_6$H$_4$-4-C$_6$F$_{13}$)$_3$}$_2$]$_2$.

$$R_3P \diagdown \diagup Cl \diagdown \diagup PR_3$$
$$Rh \qquad Rh$$
$$R_3P \diagup \diagdown Cl \diagup \diagdown PR_3$$

PR$_3$ = P(OC$_6$H$_4$-4-C$_6$F$_{13}$)$_3$ (3.40)
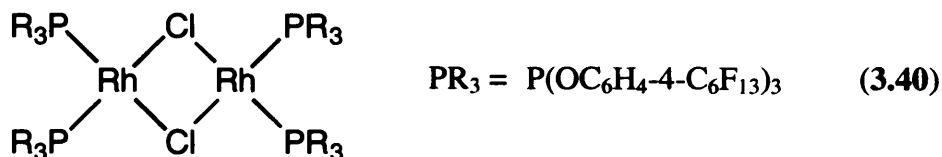
Further attempts to synthesise the rhodium carbonyl complex with ligand (2.4) were undertaken using different solvent systems resulted in the formation of the same dimeric product. A different synthetic route was also employed, similar to that used in the preparation of the analogous iridium Vaska's complexes.[68,69] A solution of ligand (2.4) in PP3 was added via canular to a solution of the chloro-bridged dimeric species [{Rh(η^2-C$_8$H$_{12}$)(μ-Cl)}$_2$] in dichloromethane. A stream of CO gas was then passed through the stirred reaction mixture in an attempt to cleave the chloride bridge with CO to give the desired carbonyl complex. The solvents were removed in vacuo to yield the reaction product as a yellow solid which was identified by IR and NMR spectroscopies as [Rh(μ-Cl){P(OC$_6$H$_4$-4-C$_6$F$_{13}$)$_3$}$_2$]$_2$. This is the only instance in which the chemistry of the para derivatised phosphite differs significantly from that of P(OPh)$_3$. The exclusive formation of the dimeric complex (3.40) rather than trans-[RhCl(CO){P(OC$_6$H$_4$-4-C$_6$F$_{13}$)$_3$}$_2$] demonstrates that the introduction of C$_6$F$_{13}$ substituents in the para positions of the phenyl rings of triphenylphosphite has an impact on the chemistry of the ligand. The observed difference between ligand (2.4) and triphenylphosphite is believed to be due to the electronic rather than steric effects of the perfluoroalkyl groups. If significant steric constraints were imposed on complex formation by the derivatised ligand it is implausible that the ligands would adopt the more sterically demanding cis-configuration as in complex (3.40) as opposed to the trans-configuration expected for [RhCl(CO){P(OC$_6$H$_4$-4-C$_6$F$_{13}$)$_3$}$_2$]. Saunders and co-workers have prepared the analogous complex trans-[RhCl(CO){P(OC$_6$H$_3$-2,6-F$_2$)$_3$}$_2$] in which the triphenylphosphite ligand contains

fluorine atoms in the *ortho* positions.[46] Structural studies have revealed that $P(OC_6H_3\text{-}2,6\text{-}F_2)_3$ is considerably more bulky than $P(OPh)_3$, which can be ascribed solely to the presence of the *ortho*-fluorine atoms. The value of ν_{CO} for *trans*-$[RhCl(CO)\{P(OC_6H_3\text{-}2,6\text{-}F_2)_3\}_2]$ of 2020 cm^{-1} obtained as a nujol mull was found to be similar to that of 2018 cm^{-1} for *trans*-$[RhCl(CO)\{P(OPh)_3\}_2]$,[70] which suggests that the σ-donor and π-acceptor properties of $P(OPh)_3$ and $P(OC_6H_3\text{-}2,6\text{-}F_2)_3$ are similar in such systems. It is, therefore, likely that the formation of *trans*-$[RhCl(CO)\{P(OC_6H_4\text{-}4\text{-}C_6F_{13})_3\}_2]$ is prevented solely by the electronic effect of the perfluoroalkyl substituents in the *para* positions of the triphenylphosphite ligand.

Previous investigations of the reaction of the chloro-bridged rhodium(I) dimers $[Rh(COD)Cl]_2$ and $[Rh(CO)_2Cl]_2$ with tertiary phosphite ligands have noted their contrasting behaviour compared to other monodentate ligands containing second-row group 5 or group 6 donor atoms.[70,71] The reactions of stoichiometric amounts of the latter ligands give rise to cleavage of the chloride bridges, whereas displacement of CO and COD occurred with phosphite ligands. In order to establish the species and equilibria that exist in solution reactions of d^8 systems, Drago and co-workers quantitatively investigated the spectroscopic titration of trimethylphosphite with $[Rh(COD)Cl]_2$ and $[Rh(CO)_2Cl]_2$.[72] The infrared spectroscopic study of the titration of $[Rh(CO)_2Cl]_2$ with 1 mol equivalent additions of trimethylphosphite indicates that more than just simple substitution of a carbonyl ligand by phosphite occurs in solution when 1 mol of trimethylphosphite is added. The bands observed in the IR spectrum have been tentatively assigned to a range of species including $[Rh_2Cl_2(CO)_3\{P(OCH_3)_3\}]$, *cis*-$[RhCl(CO)_2\{P(OCH_3)_3\}]$, $[Rh_2Cl_2(CO)_2\{P(OCH_3)_3\}_2]$ and *trans*-$[Rh(CO)Cl\{P(OCH_3)_3\}_2]$. The addition of a second equivalent of phosphite gives rise solely to the complex *trans*-$[Rh(CO)Cl\{P(OCH_3)_3\}_2]$. A similarly broad range of species were observed from the *in situ* $^{31}P\{^1H\}$ NMR study of the addition of trimethylphosphite to $[Rh(COD)Cl]_2$. The results of the reactions with $[Rh(CO)_2Cl]_2$ indicate that trimethylphosphite will preferentially displace CO and then cleave the dimer rather than displace a second CO to afford *trans*-$[Rh(CO)Cl\{P(OCH_3)_3\}_2]$. However, in the reaction with $[Rh(COD)Cl]_2$ it is apparent that trimethylphosphite possesses the necessary steric and electronic properties to cause simultaneous bridge cleavage and olefin displacement.

The formation of $[Rh(\mu\text{-}Cl)\{P(OC_6H_4\text{-}4\text{-}C_6F_{13})_3\}_2]_2$ (3.40) by the reaction of $P(OC_6H_4\text{-}4\text{-}C_6F_{13})_3$ with $[Rh(CO)_2Cl]_2$ indicates that the electronic properties of the derivatised phosphite favour substitution to give dimers as opposed to triphenylphosphite which favours bridge cleavage to give monomers. It can be concluded that the electron-withdrawing effect of the perfluoroalkyl substituents on the electronic properties of the phosphorus atom in $P(OC_6H_4\text{-}4\text{-}C_6F_{13})_3$ is responsible for the alteration in the reactivity of the phosphite ligand.

The reactions of the aryl phosphite ligands (2.7) bearing perfluorooctyl substituents and (2.8) bearing perfluorodecyl substituents with $[\{RhCl(CO)_2\}_2]$ were performed under the same conditions as those for preparation of (3.40). The reaction products were found to be the complexes $[Rh(\mu\text{-}Cl)\{P(OC_6H_4\text{-}4\text{-}C_8F_{17})_3\}_2]_2$ (3.41) and $[Rh(\mu\text{-}Cl)\{P(OC_6H_4\text{-}4\text{-}C_{10}F_{21})_3\}_2]_2$ (3.42) which were isolated as air- and moisture-stable yellow solids. The complexes have been characterised by elemental analysis and by their IR and $^{31}P\{^1H\}$ NMR spectra which were essentially the same as those for (3.40). Both complexes were found to be highly soluble in perfluorinated solvents, however, unlike (3.40) virtually no solubility in organic solvents was observed.

	$PR_3 =$		
	$P(OC_6H_4\text{-}4\text{-}C_8F_{17})_3$	(3.41)
	$P(OC_6H_4\text{-}4\text{-}C_{10}F_{21})_3$	(3.42)
	$P(OC_6H_4\text{-}3\text{-}C_6F_{13})_3$	(3.43)
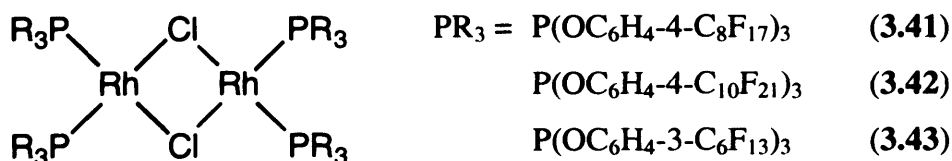
To investigate the effect of changing the steric requirements of the derivatised phosphite ligand, similar reactions with the *meta*- and *ortho*-substituted aryl phosphites were undertaken. The reaction of the *meta*-derivatised ligand, $P(OC_6H_4\text{-}3\text{-}C_6F_{13})_3$ (2.14), with $[\{RhCl(CO)_2\}_2]$ yields the complex $[Rh(\mu\text{-}Cl)\{P(OC_6H_4\text{-}3\text{-}C_6F_{13})_3\}_2]_2$ (3.43) which was isolated as an air- and moisture-sensitive yellow oil. As with the complexes of the *para*-derivatised phosphites, complex (3.43) contains no CO ligands as evidenced by IR spectroscopy. The $^{31}P\{^1H\}$ NMR spectra of complex (3.43) is almost identical to that of (3.40) exhibiting a doublet resonance at 113 δ with a $^1J_{Rh\text{-}P}$ coupling constant of 309 Hz. Complex (3.43) was found to be preferentially soluble in the fluorous phase of a dichloromethane/PP3 biphasic system.

$$OC\diagdown\diagup PR_3$$
$$\diagup Rh \diagdown$$
$$R_3P\diagup \diagdown Cl$$

$PR_3 = P(OC_6H_4\text{-}2\text{-}C_6F_{13})_3$ (3.44)
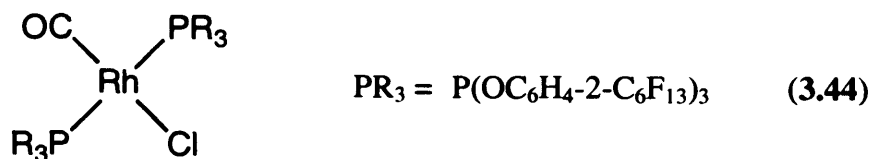
A colourless solution of the *ortho*-derivatised aryl phosphite (2.15) in PP3 was added to a stirred, orange solution of [{RhCl(CO)$_2$}$_2$] in dichloromethane. After approximately one hour the stirring was stopped and a biphasic system was generated, consisting of a clear, colourless upper organic phase and a clear, yellow lower fluorous phase. The colouration of the fluorous phase indicated that a preferentially fluorous-phase soluble rhodium phosphite complex had been formed. The fluorous phase was transferred to a Schlenk flask and the solvent removed *in vacuo* to yield *trans*-[RhCl(CO){P(OC$_6$H$_4$-2-C$_6$F$_{13}$)$_3$}$_2$] (3.44) which was recrystallized from dichloromethane/hexane and isolated as yellow crystals. Evidence for the formation of (3.44) was provided by its FAB mass spectrum which exhibits peaks for the parent ion [(M)$^+$] and the fragment [(M-Cl)$^+$] at m/z = 2694 and 2660 respectively. The IR spectrum of the compound exhibits a strong band at 2046 cm^{-1} indicating the presence of a carbonyl ligand in complex (3.44). The structural assignment of the complex is consistent with the ^{31}P{^{1}H} NMR spectrum, which exhibits a doublet resonance at 115 δ with $^1J_{Rh-P}$ coupling of 223 Hz. The formation of the rhodium carbonyl complex as opposed to a chloro-bridged dimeric species like those formed with the *meta* and *para* derivatised ligands, indicates that significant steric demands are imposed by the perfluoroalkyl substituents in the *ortho* positions. The bulky nature of the ligand makes the sterically demanding *cis*-configuration unfavourable and is also evident in the exclusive formation of the *trans*-isomers of the [PtCl$_2$L$_2$] and [PdCl$_2$L$_2$] complexes (see sections 3.2.1 and 3.4.1).

3.7.2 Reaction of alkoxy PPh$_x$(OR)$_{3-x}$ ligands with [{RhCl(CO)$_2$}$_2$].

The complexes *trans*-[RhCl(CO){Ph$_2$P(OC$_2$H$_4$C$_6$F$_{13}$)}$_2$] (3.45) and *trans*-[RhCl(CO){PhP(OC$_2$H$_4$C$_6$F$_{13}$)$_2$}$_2$] (3.46) were prepared by the addition of a solution of the alkyl phosphinite and phosphonite ligands (2.5) and (2.6) to [{RhCl(CO)$_2$}$_2$] in dichloromethane. Complex (3.45) was isolated as an air- and moisture-stable yellow solid which was recrystallized from ethanol, whereas complex (3.46) was obtained as

an air- and moisture-sensitive yellow oil. Evidence for the formation of (3.45-3.46) was provided by their FAB mass spectra which exhibit characteristic peaks for the fragments [(M-Cl)$^+$] and [(M-Cl-CO)$^+$]. Complexes (3.45) and (3.46) exhibit a strong band in their IR spectra at 1990 and 2012 cm^{-1} respectively, assigned to the carbonyl stretch. The ^{31}P{^{1}H} NMR spectra of complexes (3.45) and (3.46) exhibit the expected doublet resonances with $^1J_{Rh-P}$ coupling constants of 136 and 167 Hz respectively. In common with the phenoxy phosphinite and phosphonite analogues, complexes (3.24-3.46) were found to be insoluble in perfluorinated solvents. The reaction of the alkyl phosphite (2.7) with [{RhCl(CO)$_2$}$_2$] was performed in a biphasic system of PP3 and dichloromethane to yield the preferentially fluorous phase soluble complex trans-[RhCl(CO){P(OC$_2$H$_4$C$_6$F$_{13}$)$_3$}$_2$] (3.47) which was isolated as an air- and moisture-sensitive, yellow oil. The ^{31}P{^{1}H} NMR spectrum of (3.47) exhibits a characteristic doublet resonance with $^1J_{Rh-P}$ coupling of 199 Hz. The assignment of the complex was confirmed by IR spectroscopy which exhibits a distinctive band corresponding to v_{CO} at 2026 cm^{-1}. The $^1J_{Rh-P}$ coupling constants for complexes (3.45) and (3.46) are of lower magnitude than for the analogous phenoxy complexes, demonstrating the greater π-bonding ability of the phenoxy ligands in comparison to their alkoxy analogues. The difference in $^1J_{Rh-P}$ values between the alkoxy and phenoxy complexes increases in the order phosphinite < phosphonite.

	PR$_3$ =	Ph$_2$P(OC$_2$H$_4$C$_6$F$_{13}$)$_3$	(3.45)
		PhP(OC$_2$H$_4$C$_6$F$_{13}$)$_2$	(3.46)
		P(OC$_2$H$_4$C$_6$F$_{13}$)$_3$	(3.47)
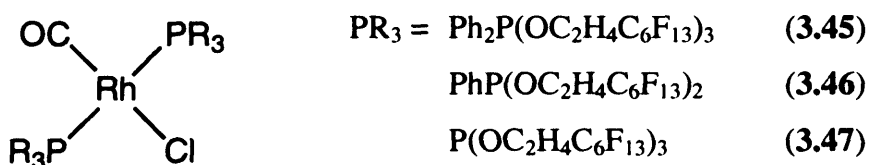
The synthesis of trans-[RhCl(CO){Ph$_2$P(OC$_2$H$_4$C$_6$F$_{13}$)}$_2$] and trans-[RhCl(CO){P(OC$_2$H$_4$C$_6$F$_{13}$)$_3$}$_2$] have recently been reported by Haar et al.[73] Solution calorimetric investigations of ligand substitution in the formation of [RhCl(CO)L$_2$] complexes were undertaken to determine the effect of the perfluoroalkyl substituents on the electronic properties of the ligands.[74,75] As the phosphorus ligands in these complexes adopt a mutually trans arrangement, the predominant factor which determines the magnitude of the enthalpy of substitution is the donor ability of the ligand. The enthalpy of substitution with the ligand P(OC$_2$H$_4$C$_6$F$_{13}$)$_3$ in the formation of trans-[RhCl(CO){P(OC$_2$H$_4$C$_6$F$_{13}$)$_3$}$_2$] was found to be -56.6 kcal mol^{-1}. The value

of -63.7 kcal mol^{-1} obtained for P(OMe)$_3$ in the formation of *trans*-[RhCl(CO){P(OMe)$_3$}$_2$] demonstrates that the fluorous ligand is a significantly poorer σ-donor than trimethylphosphite. Similar observations have recently been made by Horváth *et al.* for the same rhodium system with tertiary phosphine ligands.[76] The perfluoroalkyl chain derivatised phosphine P(C$_2$H$_4$C$_6$F$_{13}$)$_3$ was found to exhibit electronic parameters closer to PPhMe$_2$ than PEt$_3$.

3.7.3 Discussion of carbonyl stretching frequency for complexes of the type [RhCl(CO)L$_2$].

The use of carbonyl stretching frequency (ν_{CO}) as a tool to investigate the bonding characteristics of tertiary phosphorus ligands in metal carbonyl complexes has been extensively investigated by Tolman using nickel complexes of the type [Ni(CO)$_3$PR$_3$].[77] The interaction of the molecular orbitals of the carbon monoxide ligand with metal *d*-orbitals is such that the carbonyl stretching frequency is sensitive to variations in electron density at the metal centre and, consequently, the electronic properties of other metal-bound ligands. The molecular orbital description of CO shows the HOMO to be an s_σ* orbital corresponding to the carbon-centred lone pair with degenerate π* LUMOs. The carbon lone pair donates electron density into an empty metal orbital with the π* orbital being of the correct symmetry to accept electron density from an occupied metal *d*-orbital (Figure 3.12). The delocalization of electron density over the ligand π* system through synergic back-bonding stabilises the M-CO bond. Since the acceptor orbitals are anti-bonding, extensive back-bonding in electron-rich complexes lowers the C-O bond order and hence the CO stretching frequency. Conversely, if the complex contains strongly electron-withdrawing ligands a reduction in back-bonding to the carbonyl group occurs and ν_{CO} increases. Occupancy of the energetically high lying π* orbitals, which are comparable in energy to metal 3*d*, 4*d* or 5*d* orbitals, through back-bonding leads to a substantial overall energy gain. Since back-bonding is dependent on the electron density at the metal, it not only strengthens the M-CO bond but also gives an indication of the electronic characteristics of the metal centre.
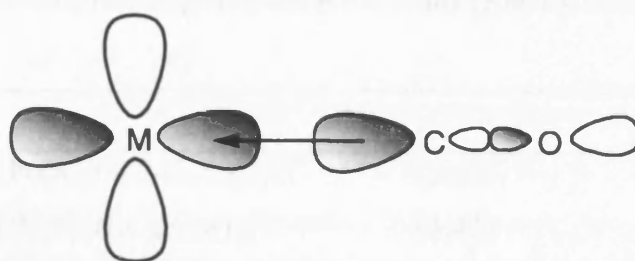
Carbon to metal σ-bonding
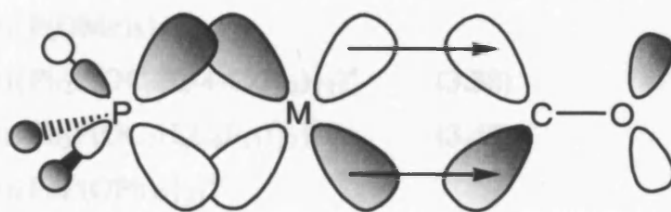
Metal to CO(π*) π-bonding

Figure 3.12   Metal-carbonyl bonding in transition metal complexes.

The investigation of the carbonyl stretching frequencies of the [RhCl(CO)L$_2$] complexes bearing the perfluoroalkyl chain derivatised ligands was undertaken to provide information on the influence of the perfluoroalkyl substituents on the electronic properties of the rhodium centre. Due to the air- and moisture-sensitivity of several of the complexes, the IR spectra were recorded in solutions of either dichloromethane or PP3. Values of v_{CO} for the rhodium carbonyl complexes with the perfluoroalkyl-substituted ligands are given in Table 3.14. The magnitude of v_{CO} for the rhodium carbonyl complexes increases with the number of alkoxy or phenoxy groups, following the accepted order of ligand π-acidity R$_2$POR < RP(OR)$_2$ < P(OR)$_3$. The values of v_{CO} obtained for complex (3.38) is 6 cm^{-1} higher than that for *trans*-[RhCl(CO){Ph$_2$P(OPh)}$_2$] as a result of decreased carbonyl back-bonding. The reduction in back-bonding to the carbonyl group indicates lower electron density at the metal centre in (3.38) as a result of the electron-withdrawing effect of the perfluoroalkyl group.

Table 3.14   Carbonyl stretching frequencies of *trans*-[RhCl(CO)L$_2$] complexes.

Complex		v_{CO} (cm^{-1})
trans-[RhCl(CO){P(OC$_6$H$_4$-2-C$_6$F$_{13}$)$_3$}$_2$][b]	(3.44)	2045
trans-[RhCl(CO){P(OC$_2$H$_4$C$_6$F$_{13}$)$_3$}$_2$][b]	(3.47)	2036
trans-[RhCl(CO){P(OPh)$_3$}$_2$][a,c]		2016
trans-[RhCl(CO){PhP(OC$_6$H$_4$-4-C$_6$F$_{13}$)$_2$}$_2$][a]	(3.39)	2013
trans-[RhCl(CO){PhP(OC$_2$H$_4$C$_6$F$_{13}$)$_2$}$_2$][a]	(3.46)	2008
trans-[RhCl(CO){P(OMe)$_3$}$_2$][a]		2006
trans-[RhCl(CO){Ph$_2$P(OC$_6$H$_4$-4-C$_6$F$_{13}$)}$_2$][a]	(3.38)	1996
trans-[RhCl(CO){Ph$_2$P(OC$_2$H$_4$C$_6$F$_{13}$)}$_2$][a]	(3.45)	1993
trans-[RhCl(CO){PhP(OPh)$_2$}$_2$][a,c]		2004
trans-[RhCl(CO){Ph$_2$P(OPh)}$_2$][a]		1900
trans-[RhCl(CO){PPh$_3$}$_2$][a]		1978

[a] Recorded in CH$_2$Cl$_2$.   [b] Recorded in PP3.   [c] Ref. 74.

The increase in the magnitude of v_{CO} for the phosphonite complex (3.39) in comparison to that for *trans*-[RhCl(CO){PhP(OPh)$_2$}$_2$] of 9 cm^{-1} is greater than the difference in v_{CO} of 6 cm^{-1} between the derivatised and non-derivatised phenyl phosphinite complexes, suggesting that the electron-withdrawing effects of the perfluoroalkyl groups are magnified by the number of phenoxy substituents. It also demonstrates that the phenoxy group does not fully insulate the phosphorus atom from the electronic effects of the perfluoroalkyl substituent. The carbonyl stretching frequency for complex (3.44) containing the *ortho* derivatised phosphite is 29 cm^{-1} higher than that for *trans*-[RhCl(CO){P(OPh)$_3$}$_2$] indicating a significant reduction in carbonyl back-bonding as a result of the perfluoroalkyl substituents. This variation may not be solely due to the electron-withdrawing effect of the perfluoroalkyl group, as substitution in the *ortho* position of the phenoxy groups results in a ligand with dramatically different steric parameters in comparison to triphenylphosphite. However, the literature value of 2012 cm^{-1} for the v_{CO} of *trans*-[RhCl(CO){P(OC$_6$H$_4$-2-CH$_3$)$_3$}$_2$][78] is only slightly lower than the value of 2014 cm^{-1} for the v_{CO} of *trans*-[RhCl(CO){P(OC$_6$H$_4$-3-CH$_3$)$_3$}$_2$],[78] indicating that the steric effect of the methyl substituents on the magnitude of v_{CO} is small. It is, therefore, assumed that the

electronic properties of the phosphite ligand in complex (**3.44**) are the dominant influence on the magnitude of v_{CO}.

The carbonyl stretching frequencies for the complexes bearing the derivatised alkoxy groups are between 3-10 cm^{-1} lower in comparison with their analogues containing the derivatised phenoxy groups. This indicates that electron-density is removed from the metal centre to a greater extent by ligands containing phenoxy groups with C_6F_{13} substituents than ligands containing the derivatised alkoxy groups. Interestingly, the value of v_{CO} for *trans*-[RhCl(CO){Ph$_2$P(OC$_2$H$_4$C$_6$F$_{13}$)}$_2$] (**3.45**) is greater than that for *trans*-[RhCl(CO){Ph$_2$P(OPh)}$_2$], demonstrating that the derivatised alkoxy group has a greater electron withdrawing effect than a phenoxy group. Correspondingly, a similar difference in the value of v_{CO} is observed between the phosphonite complexes *trans*-[RhCl(CO){PhP(OC$_2$H$_4$C$_6$F$_{13}$)$_2$}$_2$] (**3.46**) and *trans*-[RhCl(CO){PhP(OPh)$_2$}$_2$]. In common with the increases in v_{CO} observed for complexes with the derivatised phenoxy ligands in comparison to their protio analogues, the carbonyl stretching frequency for the alkyl phosphite complex (**3.47**) is 30 cm^{-1} higher than that for *trans*-[RhCl(CO){P(OMe)$_3$}$_2$]. This indicates that the electron-density at the metal centre available for back-bonding with the carbonyl group is substantially lower in (**3.47**) than in the complex with trimethylphosphite due to the electron-withdrawing effect of the perfluoroalkyl groups. Notably, the value of v_{CO} for the alkyl phosphonite complex (**3.46**) is greater than that for the *trans*-[RhCl(CO){P(OMe)$_3$}$_2$]. This demonstrates that the electron-withdrawing effect of the perfluoroalkyl substituents on the electronic properties of the phosphorus atom is great enough to cause the phosphonite ligand to act as a stronger π-acid than trimethylphosphite, contrary to the usual order of π-acidity. In contrast, the value of v_{CO} for the phenyl phosphonite complex (**3.39**) is lower than that for *trans*-[RhCl(CO){P(OPh)$_3$}$_2$], thereby indicating that the electron withdrawing effect of the perfluoroalkyl substituents on the aryl phosphonite ligand is not sufficient to make it a stronger π-acceptor ligand than triphenylphosphite. This indicates that the OC$_2$H$_4$ group is not as effective as the OC$_6$H$_4$ group in shielding the phosphorus atom of the respective ligands, and hence the rhodium atom of the resulting complexes, from the electronic influence of the perfluoroalkyl groups.

3.8 Rhodium(I) complexes of the type [RhClL₃].

Complexes of the type [RhClL₃] in which L is a tertiary phosphorus ligand are some of the most extensively studied compounds in organometallic chemistry. Interest in these compounds was sparked by the synthesis and catalytic application of the complex [RhCl(PPh₃)₃] which was first reported by Wilkinson and co-workers in 1966.[79] The complex was found to be an active catalyst for the homogeneous hydrogenation of olefins under relatively mild conditions. The catalytic properties of the complex can be tuned by variation of the phosphorus ligands, which has led to the investigation of a number of catalytic systems based on 'Wilkinson's complex'.[80,81,82] The phosphite analogue [RhCl{P(OPh)₃}₃] was first prepared by Vallarino by the reaction of an excess of triphenylphosphite with [{RhCl(CO)₂}₂] in benzene.[83] Vallarino reported that the reaction of triaryl phosphines with [{RhCl(CO)₂}₂] do not give [RhClL₃] compounds even under forcing conditions. As the character of phosphinite and phosphonite ligands lies between those of phosphines and phosphites, it was feared that mixtures of products may be formed by this reaction. The complex [{Rh(η^2-C₂H₄)₂(μ-Cl)}₂] in which the ethylene ligands are more easily displaced than the carbonyl groups was, therefore, chosen as a convenient starting material (see Scheme 3.7).
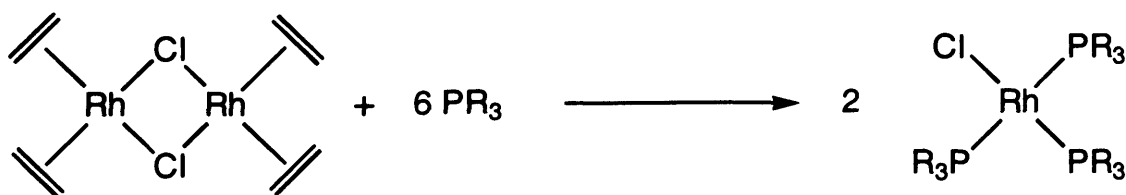
Scheme 3.7 Reaction of tertiary phosphorus ligands with [{Rh(η^2-C₂H₄)₂(μ-Cl)}₂].

Tertiary phosphorus ligands react rapidly with [{Rh(η^2-C₂H₄)₂(μ-Cl)}₂] under mild conditions. The displaced ligands bubble out of the solution as free ethylene gas, therefore the desired [RhClL₃] is easily isolated by removal of the reaction solvent *in vacuo*.

3.8.1 Reaction of phenoxy $PPh_x(OR)_{3-x}$ ligands with $[\{Rh(\eta^2\text{-}C_2H_4)_2(\mu\text{-}Cl)\}_2]$.

The phosphinite, phosphonite and phosphite ligands (2.2-2.4) were allowed to react with $[\{Rh(\eta^2\text{-}C_2H_4)_2(\mu\text{-}Cl)\}_2]$ to yield the complexes $[RhCl\{Ph_2P(OC_6H_4\text{-}4\text{-}C_6F_{13})\}_3]$ (3.48), $[RhCl\{PhP(OC_6H_4\text{-}4\text{-}C_6F_{13})_2\}_3]$ (3.49) and $[RhCl\{P(OC_6H_4\text{-}4\text{-}C_6F_{13})_3\}_3]$ (3.50) which were isolated as orange/yellow solids. The reactions were carried out under anaerobic conditions using Schlenk techniques. Complexes (3.48-3.49) with the derivatised phosphinite and phosphonite ligands were found to be air- and moisture-sensitive while the phosphite complex (3.50) was found to be air- and moisture-stable. As expected complex (3.50) was found to be preferentially soluble in perfluorinated solvents.

$$
\begin{array}{ccc}
\text{Cl} & & \text{PR}_3 \\
& \diagdown \quad \diagup & \\
& \text{Rh} & \\
& \diagup \quad \diagdown & \\
\text{R}_3\text{P} & & \text{PR}_3
\end{array}
$$

$PR_3 = Ph_2P(OC_6H_4\text{-}4\text{-}C_6F_{13})$ (3.48)

$PhP(OC_6H_4\text{-}4\text{-}C_6F_{13})_2$ (3.49)

$P(OC_6H_4\text{-}4\text{-}C_6F_{13})_3$ (3.50)
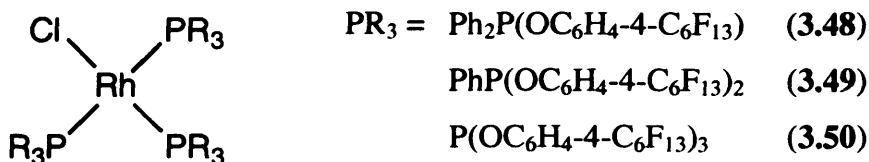
The complexes have been characterised by NMR spectroscopy, mass spectrometry and elemental analysis. The FAB mass spectra of the compounds exhibit characteristic peaks for the fragment of the parent ion $[(M\text{-}Cl)^+]$. The $^{31}P\{^1H\}$ NMR spectra of (3.48-3.50) are distinctive, exhibiting a doublet of doublets and at higher frequency a doublet of triplets, consistent with the square planar geometry assigned to the complexes. The doublet of doublets resonance at low frequency is assigned to the two equivalent phosphorus atoms cis to chlorine, arising from $^1J_{Rh\text{-}P}$ coupling and $^2J_{P\text{-}P}$ coupling with the cis phosphorus nucleus. The high frequency resonance can be assigned to the phosphorus $trans$ to chlorine and appears as a doublet of triplets as a result of $^1J_{Rh\text{-}P}$ coupling and $^2J_{P\text{-}P}$ coupling to the two equivalent cis phosphorus atoms. The $^{31}P\{^1H\}$ NMR data for complexes (3.48-3.57) is given in Table 3.15.

Table 3.15 $^{31}P\{^1H\}$ NMR data for complexes (3.48-3.57).

Complex	$\delta_1{}^a$	$^1J_{Rh\text{-}P}$ (Hz)	$\delta_2{}^b$	$^1J_{Rh\text{-}P}$ (Hz)	$^2J_{P\text{-}P}$ (Hz)
(3.48)^c	143	216	130	162	37
(3.49)^c	152	245	147	187	44
(3.50)^d	121	286	114	225	54
(3.51)^d	120	283	113	225	53
(3.52)^d	123	287	113	225	53
(3.53)^d	119	276	111	227	45
(3.54)^d	108	318	-	-	-
(3.55)^c	131	207	125	160	41
(3.56)^c	159	236	157	181	41
(3.57)^d	140	268	132	209	53

^{a} P *trans* to Cl. ^{b} P *trans* to P. ^{c} Recorded in CDCl$_3$. ^{d} Recorded in PP3 with a D$_2$O insert.

As observed previously for the [RhCl(CO)L$_2$] complexes the $^1J_{Rh\text{-}P}$ coupling constants for (3.48-3.50) increase with the number of phenoxy groups present. The $^2J_{P\text{-}P}$ coupling constants also increase with increasing π-acceptor ability of the ligand in the order phosphinite < phosphonite < phosphite. In each complex the magnitude of the $^1J_{Rh\text{-}P}$ coupling constant for the ligand *trans* to chlorine is substantially greater than for the mutually *trans* ligands as a direct result of the *trans*-effect. The phosphorus ligands exert a greater *trans*-influence than chloride, therefore, the M-Cl bond *trans* to phosphorus is weakened with concomitant strengthening of the M-P bond. The $^{31}P\{^1H\}$ NMR spectrum of (3.50) is almost identical to that of [RhCl{P(OPh)$_3$}$_3$][84] which exhibits a doublet of triplets at 118.9 δ and a doublet of doublets at 111.9 δ with $^1J_{Rh\text{-}P}$ coupling constants of 285 and 224 Hz respectively and $^2J_{P\text{-}P}$ coupling of 53 Hz. The similarity of the values obtained for the two complexes indicates that $^1J_{Rh\text{-}P}$ coupling constants are not particularly sensitive to changes in the electronic character of the phosphorus ligand.

The complexes [RhCl{P(OC$_6$H$_4$-4-C$_8$F$_{17}$)$_3$}$_3$] (3.51) and [RhCl{P(OC$_6$H$_4$-4-C$_{10}$F$_{21}$)$_3$}$_3$] (3.52) were prepared by the reaction of [{Rh(η^2-C$_2$H$_4$)$_2$(μ-Cl)}$_2$] with the derivatised phosphites (2.7-2.8). The compounds were isolated as air- and moisture-

stable yellow solids and were found to be exceptionally soluble in perfluorinated solvents. The $^{31}P\{^1H\}$ NMR spectral data obtained for complexes (3.51-3.52) are virtually identical to that for complex (3.50). The reaction of the *meta*-derivatised phosphite (2.14) with [{Rh(η^2-C$_2$H$_4$)$_2$(μ-Cl)}$_2$] yields the complex [RhCl{P(OC$_6$H$_4$-3-C$_6$F$_{13}$)$_3$}$_3$] (3.53) which was obtained as an air- and moisture-sensitive, yellow oil. In common with the *para* phosphite derivative (3.53), this was found to be preferentially soluble in the fluorous phase of a dichloromethane/PP3 biphasic system. The similarity of the spectral data obtained for the complexes of the *meta* and *para* derivatised phosphites indicates that substitution of the phenoxy groups in the *meta* position with perfluoroalkyl groups has no significant impact on the stereoelectronic properties of the ligand.

PR$_3$ = P(OC$_6$H$_4$-4-C$_8$F$_{17}$)$_3$	(3.51)
P(OC$_6$H$_4$-4-C$_{10}$F$_{21}$)$_3$	(3.52)
P(OC$_6$H$_4$-3-C$_6$F$_{13}$)$_3$	(3.53)
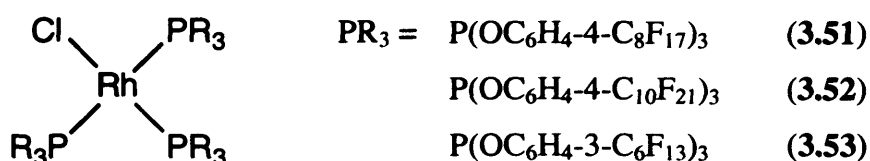
The reaction of the *ortho*-derivatised phosphite (2.15) with [{Rh(η^2-C$_2$H$_4$)$_2$(μ-Cl)}$_2$] was performed under the same conditions as for the *meta*- and *para*-derivatised phosphites. The reaction solvent was removed *in vacuo* to yield the crude product as a sticky yellow solid. The $^{31}P\{^1H\}$ NMR of the crude product was found to exhibit a doublet resonance at 108 δ with $^1J_{Rh-P}$ coupling of 318 Hz and a singlet at 124 δ corresponding to the free phosphite. The presence of a large quantity of free ligand in the crude product suggested that the desired [RhClL$_3$] compound had not been formed. The species giving rise to the doublet was isolated as a yellow solid by recrystallization of the crude product from hexane and assigned as [Rh(μ-Cl){P(OC$_6$H$_4$-2-C$_6$F$_{13}$)$_3$}$_2$]$_2$ (3.54) on the basis of its characteristic $^{31}P\{^1H\}$ NMR spectra.

PR$_3$ = P(OC$_6$H$_4$-2-C$_6$F$_{13}$)$_3$ (3.54)
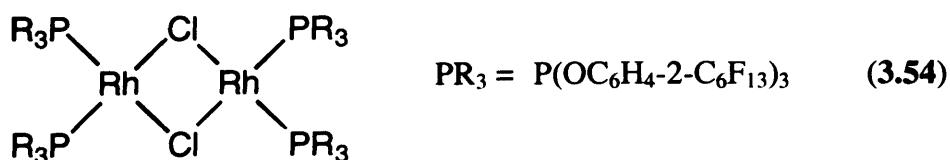
3.8.2 Reaction of alkoxy $PPh_x(OR)_{3-x}$ ligands with $[\{Rh(\eta^2\text{-}C_2H_4)_2(\mu\text{-}Cl)\}_2]$.

The reactions of the alkyl phosphinite, phosphonite and phosphite ligands **(2.16-2.18)** with $[\{Rh(\eta^2\text{-}C_2H_4)_2(\mu\text{-}Cl)\}_2]$ were performed under anaerobic conditions using Schlenk techniques to yield the complexes $[RhCl\{Ph_2P(OC_2H_4C_6F_{13})\}_3]$ **(3.55)**, $[RhCl\{PhP(OC_2H_4C_6F_{13})_2\}_3]$ **(3.56)** and $[RhCl\{P(OC_2H_4C_6F_{13})_3\}_3]$ **(3.57)**. Complexes **(3.56-3.57)** were isolated as air- and moisture-sensitive, yellow oils and **(3.55)** as an air- and moisture-sensitive orange solid. As expected, complexes **(3.55-3.57)** exhibit similar solubility in perfluorinated solvents to their phenoxy analogues with only the phosphite complex having preferential solubility in the fluorous phase of a dichloromethane/PP3 biphasic system. The $^{31}P\{^1H\}$ NMR spectra for complexes **(3.55-3.57)** exhibit the same resonances as their aryl analogues (see Table 3.15) and the same trends in $^1J_{Rh\text{-}P}$ and $^2J_{P\text{-}P}$ coupling constants. The $^1J_{Rh\text{-}P}$ coupling constants for the complexes with the ligands containing alkoxy groups are of lower magnitude than those for the analogous complexes containing the derivatised phenoxy groups. These results are consistent with the greater π-acceptor ability of phenoxy phosphinite, phosphonite and phosphite ligands in comparison to their aryloxy analogues.

$$
\begin{array}{ll}
\text{Cl} \diagdown \quad \diagup \text{PR}_3 \\
\qquad \text{Rh} \\
\text{R}_3\text{P} \diagup \quad \diagdown \text{PR}_3
\end{array}
\qquad
\begin{array}{lll}
PR_3 = & Ph_2P(OC_2H_4C_6F_{13}) & \textbf{(3.55)} \\
& PhP(OC_2H_4C_6F_{13})_2 & \textbf{(3.56)} \\
& P(OC_2H_4C_6F_{13})_3 & \textbf{(3.57)}
\end{array}
$$
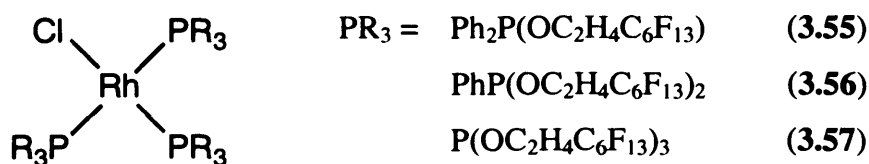
The alkyl phosphinite ligand **(2.16)** and the 'RhClL$_3$' catalyst derived therefrom has been applied by Haar *et al.* to the homogeneous hydrogenation of hex-1-ene.[73] The catalyst was prepared *in situ* from $[Rh(COD)Cl]_2$ and 6 equivalents of ligand, however, no attempt was made to characterise the resulting complex. The catalytic reaction was carried out in neat hex-1-ene under 1 atmosphere of H_2. Under these conditions the phosphinite-derived catalyst was found to convert 395 equivalents of olefin per Rh atom to hexane in 24 hours. The activity of the catalyst is far lower than that for Wilkinson's complex $[RhCl(PPh_3)_3]$ which is capable of 650 turnovers per hour. The low activity of the phosphinite catalyst is unsurprising as the electronic properties of phosphinite and phosphine ligands are significantly different. The electron density at phosphorus is lower for phosphinite ligands as a result of the

greater electron-withdrawing effect of oxygen in comparison to carbon. This would lead to a corresponding reduction in the electron density at the metal which results in a reduction in the rate of formation of the alkyl rhodium hydride, by the migratory insertion of the olefin into a rhodium hydrogen bond, which is the rate determining step (see Section 1.1). Similar observations regarding the rate of hydrogenation have been made using triphenylphosphine ligands bearing electron-withdrawing substituents.[85,86]

3.9 Coordination Chemistry Conclusions

The coordination chemistry discussed in this chapter demonstrates that, in general, the perfluoroalkyl chain derivatised ligands exhibit similar chemical behaviour and reactivity to their protio analogues. The notable exceptions to this are the derivatised aryl phosphite ligands, which exhibit dramatically different reactivity towards the dimeric species $[Rh(CO)_2(\mu-Cl)]_2$ in comparison to triphenylphosphite. The formation of chlorine bridged dimeric species of the type $[Rh(\mu-Cl)L_2]_2$ rather than the expected $[Rh(CO)ClL_2]$ complexes is believed to be due to the difference in the electronic properties of the derivatised phosphite ligands as a result of the electron-withdrawing effect of the perfluoroalkyl substituents. The mutually *trans* configuration of the ligands in $[Rh(CO)ClL_2]$ is less favourable for the derivatised phosphites than for triphenylphosphite due to the increased π-acceptor ability of the ligands and hence their greater *trans*-influence. The formation of the complex *trans*-$[Rh(CO)Cl\{P(OC_6H_4-2-C_6F_{13})_3\}_2]$ using the sterically demanding *ortho* derivatised phosphite suggests that, in this case, the *trans* configuration of the ligands is energetically more favourable than the sterically strained *cis*-configuration demanded by the formation of the $[Rh(\mu-Cl)L_2]_2$ species.

The incorporation of the perfluoroalkyl substituents in the periphery of the alkoxy and *para*-derivatised phenoxy ligands has a negligible steric effect on the resulting coordination complexes. Comparison of molecular structures obtained for complexes with the derivatised ligands with those for the protio analogues suggests that the geometry about the metal centre is almost unaffected by the perfluoroalkyl groups. The potential steric demands of a large substituent such as C_6F_{13} can be alleviated by the flexibility of the P-O-C linkage, therefore, the steric effect of the

perfluoroalkyl group is greatly reduced in the phosphinite, phosphonite and phosphite complexes in comparison to the analogous phosphines modified with perfluoroalkyl groups.[87] Derivatisation of triphenylphosphite in the *ortho* positions of the phenyl rings has a significant steric impact as evidenced by the formation of the *trans*-isomers of the [PtCl$_2$L$_2$] and [PdCl$_2$L$_2$] complexes. The steric demands are so great that the Wilkinson's analogue could not be prepared as is was not physically possible to coordinate three of the *ortho*-phosphite ligands to rhodium.

The perfluoroalkyl substituents have a dramatic effect on the physical properties of the coordination complexes. All the complexes of the *meta*-derivatised aryl phosphite were isolated as viscous oils as were many of the complexes of the alkyl phosphonite and phosphite ligands. The air- and moisture-stability of the complexes were also affected, particularly the [Rh(CO)ClL$_2$] and [RhClL$_3$] species which were found to be exceptionally moisture sensitive. Most importantly, the solubilities of the complexes were substantially altered. It was found that as the number of perfluoroalkyl groups was increased the solubility of the complexes in organic solvents decreased and their solubility in perfluorinated solvents increased. The only metal species found to be soluble in perfluorocarbon solvents were complexes of the phosphite ligands, which contain three perfluoroalkyl groups, with a minimum of two phosphite ligands coordinated to the metal. Increasing the length of the fluorous chain from perfluorohexyl to perfluorooctyl and perfluorodecyl significantly reduces the solubility of complexes of the aryl phosphite ligands in organic solvents. This could have a considerable influence on the efficiency of segregation of the metal complexes into the fluorous phase of a biphasic catalytic system.

The NMR and IR spectroscopic data obtained for the coordination complexes indicates that the electron-withdrawing effect of the perfluoroalkyl chains reduces the electron density at phosphorus for the derivatised ligands in comparison to their protio analogues. This reduces the σ-donor ability of the ligands and hence leads to a reduction in electron-density at the metal centres of the complexes. The energy of the P-O σ* hybrid π-acceptor orbitals is also affected, resulting in increased π-acceptor ability of the ligands as evidenced by the IR spectroscopic studies of the *trans*-[Rh(CO)ClL$_2$] species. The degree to which the electronic properties of the ligand are effected increases with the number of perfluoroalkyl substituents, therefore,

complexes which are fluorous soluble generally experience the greatest change in electronic character due to the incorporation of a greater number of perfluoroalkyl moieties. For example, the electronic properties of the *para*-derivatised aryl phosphite ligand differ from those of triphenylphosphite to a greater extent than the derivatised aryl phosphinite ligand in comparison to triphenylphosphinite. The IR studies of the rhodium carbonyl complexes of the derivatised ligands suggest that the ethoxy spacer in ligands (**2.16-2.18**) is not as effective as the phenoxy spacer in ligands (**2.2-2.3**) and (**2.15**) at shielding the phosphorus atom from the electron-withdrawing effect of the perfluoroalkyl substituents.

Having established the parameters necessary to prepare fluorous soluble complexes an investigation into the catalytic application of such complexes under fluorous biphase conditions was undertaken. The catalytic experiments are described and discussed in Chapter 4.

References for Chapter Three

[1]   M. J. S. Dewar, *Bull. Soc. Chem. Fr.*, 1951, **18**, C71.

[2]   J. Chatt and L. A. Duncanson, *J. Chem. Soc.*, 1953, 2939.

[3]   Z. Berkovitch-Yellin, D. E. Ellis, W. C. Trogler and S. -X. Xiao, *J. Am. Chem. Soc.*, 1983, **105**, 7033.

[4]   D. S. Marynick, *J. Am. Chem. Soc.*, 1984, **106**, 4064.

[5]   M. Braga, *Inorg. Chem.*, 1985, **24**, 2702.

[6]   N. G. Connelly and A. G. Orpen, *J. Chem. Soc., Chem. Commun.*, 1985, 1310.

[7]   P. S. Bagus and G. Pacchioni, *Inorg. Chem.*, 1992, **31**, 4391.

[8]   P. D. Lyne and D. M. P. Mingos, *J. Org. Chem.*, 1994, **478**, 141.

[9]   S. P. Bagus, C. W. Bauschlicher and K. Hermann, *J. Chem. Phys.*, 1984, **80**, 4378.

[10]   S. P. Bagus, C. W. Bauschlicher and K. Hermann, *J. Chem. Phys.*, 1984, **81**, 1966.

[11]   *'Catalytic Aspects of Metal Phosphine Compplexes'*, Eds. E. C. Alyea and D. W. Meek, ACS publications, US, 1982, pp. 1-22.

[12]   F. R. Hartley, C. A. McAuliffe and S. G. Murray, *Inorg. Chem.*, 1979, **18**, 1394.

[13]   D. A. Couch, S. D. Robinson and J. N. Wingfield, *J. Chem. Soc. Dalton Trans.*, 1974, 1309.

[14]   D. G. Gilheany, *Chem. Rev.*, 1994, 94, 1339.

[15]   A. Crispini, K. N. Harrison, A. G. Orpen, P. G. Pringle and J. R. Wheatcroft, *J. Chem. Soc., Dalton Trans.*, 1996, 1069.

[16]   *'Dictionary of Inorganic Compounds'*, Vol.2, Chapman and Hall London, 1992.

[17]   K. Hirabayashi and I. Yasumori, *Trans. Faraday Soc.*, 1971, 67, 3283.

[18]   L. I. Flowers, Y. Kawabata and C. U. Pittman, *J. Chem. Soc., Chem. Commun.*, 1982, 473.

[19]   J. F. Knifton, *J. Organomet. Chem.*, 1980, **188**, 223.

[20]   F. H. Allen, A. Pidcock and C. R. Waterhouse, *J. Chem. Soc. (A)*, 1970, 2087.

[21]   P. Berdagué, J. Courtieu, H. Adams, N. A. Bailey and P. M. Maitlis, *J. Chem. Soc. Chem. Commun.*, 1994, 1589.

[22]   W. R. Meyer and L. M. Venanzi, *Angew. Chem.*, 1984, **96**, 505.

[23]   '*Phosphorus-31 NMR Spectroscopy in Stereochemical Analysis*' Eds. J. G. Verkade and L. D. Quin, VCH Publishers, Florida, 1987.

[24]   A. Albinati, P. S. Pregosin and H. Rüegger, *Inorg. Chem.*, 1984, **23**, 3223.

[25]   J. C. Bailar and H. Itatani, *J. Am. Chem. Soc.*, 1967, **89**, 1592.

[26]   D. W. Bruce, B. Donnio, A. A. Maggs and J. R. Marsden, *Inorg. Chim. Acta*, 1991, **188**, 41.

[27]   D. E. Berry, K. A. Beveridge, G. W. Bushnell and K. R. Dixon, *Can. J. Chem.*, 1985, **63**, 2949.

[28]   R. C. Weast, '*Handbook of Chemistry and Physics*', 1st Ed., CRC Press, 1988.

[29]   N. Ahmad, E. W. Ainscough, T. A. James and S. D. Robinson, *J. Chem. Soc., Dalton*, 1973, 1148.

[30]   D. R. Paige, *The Synthesis, Coordination Chemistry and Catalytic Applications of Phosphine Ligands Containing Long-Chain Perfluoroalkyl Groups*, Ph.D. Thesis, University of Leicester, 1997, p. 70.

[31]   S. O. Grim and R. L. Keiter, *Inorg. Chim. Acta.*, 1970, **4**, 56.

[32]   F. R. Hartley, *Chem. Soc. Rev.*, 1973, **2**, 163.

[33]   G. G. Mather, A. Pidcock and G. J. N. Rapsey, *J. Chem. Soc. Dalton Trans.*, 1973, 2095.

[34]   N. F. Ramsey, *Phys. Rev.*, 1953, **91**. 203.

[35]   J. A. Pople, *Mol. Phys.*, 1958, **1**, 216.

[36]   J. A. Pople and D. P. Santry, *Mol. Phys.*, 1964, **8**, 1.

[37]   D. P. Craig, A. Maccoll, R. S. Nyholm, L. E. Orgel and L. E. Sutton, *J. Chem. Soc.*, 1954, 332.

[38]   J. K. Burdett and T. A. Albright, *Inorg. Chem.*, 1979, **18**, 2112.

[39]   A. Pidcock, R. E. Richards and L. M. Venanzi, *J. Chem. Soc. A*, 1966, 1707.

[40]   C. J. Cobley and P. G. Pringle, *Inorg. Chim. Acta*, 1997, **265**, 107.

[41]   C. A. Tolman, *Chem. Rev.*, 1977, 313.

[42]   M. J. Atherton, K. S. Coleman, J. H. Holloway, E. G. Hope, D. R. Russell and G. C. Saunders, *Polyhedron*, 1995, **14**, 2107.

[43]   R. F. Gould, 'Platinum Group Metals and Compounds', A.C.S. Publications, Washington D. C., 1971.

[44]   M. A. Mazid and D. R. Russell, J. Chem. Soc. Dalton, 1980, 1737.

[45]   M. A. Cairns, K. R. Dixon and G. A. Rivett, J. Organomet. Chem., 1979, 171, 373.

[46]   M. J. Atherton, J. Fawcett, A. P. Hill, J. H. Holloway, E. G. Hope, D. R. Russell, G. C. Saunders and R. M. J. Stead, J. Chem. Soc., Dalton Trans., 1997, 1137.

[47]   P. B. Hitchcock, B. Jacobson, and A. Pidcock, J. Chem. Soc., Dalton Trans., 1977, 2043.

[48]   F. H. Allen and S. N. Sze, J. Chem. Soc. (A), 1971, 2054.

[49]   A. D. U. Hardy and G. A. Sim, J. Chem. Soc., Dalton Trans., 1972, 1900.

[50]   A. N. Caldwell, L. M-. Muir and K. W. Muir, J. Chem. Soc. Dalton Trans., 1977, 2265.

[51]   J. M. Jenkins and J. G. Verkade, Inorg. Synth., 1968, 11, 108.

[52]   T. Ikariya, S. Iwasa, Y. Kayaki, Y. Noguchi and R. Noyori, Chem. Comm., 1999, 1235.

[53]   E. Chiarparin, F. Garbassi, G. Mestroni, B. Milani, A. Sommazzi, L. Vicentini and E. Zangrando, J. Chem. Soc., Dalton Trans., 1996, 3139.

[54]   K. R. Dixon and A. D. Rattray, Can. J. Chem., 1971, 49, 3997.

[55]   T. Ghaffar, A. Kieszkiewicz, S. C. Nyburg and A. W. Parkins, Acta Cryst., 1994, C50, 697.

[56]   S. Affolter, A. Albinati and P. S. Pregosin, Organometallics, 1990, 9, 379.

[57]   J. W. Kang, K. Moseley and P. M. Maitlis, J. Am. Chem. Soc., 1969, 91, 5970.

[58]   B. L. Booth, R. N. Haszeldine and M. Hill, J. Chem. Soc (A), 1969, 1299.

[59]   J. H. Holloway, E. G. Hope, K. Jones, G. C. Saunders, J. Fawcett, N. Reeves, D. R. Russell and M. J. Atherton, Polyhedron, 1993, 12, 2681.

[60]   A. G. Orpen, L. Brammer, F. H. Allen, O. Kennard, D. G. Watson and R. Taylor, J. Chem. Soc., Dalton Trans., 1989, S1.

[61]   F. W. B. Einstein, D. C. Sutton and X. Yan, Acta Cryst., 1991, C47, 1975.

[62]   L. M. Haines, Inorg. Chem., 1971, 10, 1693.

[63]   K. G. Moloy and J. L. Petersen, J. Am. Chem. Soc., 1995, 117, 7696.

[64]   I. T. Horváth and J. Rábai, Science, 1994, 266, 72.

[65]   R. Colton, R. H. Farthing and J. E. Knapp, *Aust. J. Chem.,* 1970, 1351.

[66]   L. M. Venanzi, *Pure Appl. Chem.,* 1980, **52**, 1117.

[67]   E. F. Hoy and W. Partenheimer, *Inorg. Chem.,* 1973, **12**, 2805.

[68]   L. Vaska, *J. Am. Chem. Soc.,* 1961, **83**, 756.

[69]   R. H. Crabtree, M. B. Hall, X. L. Luo and D. Michos, *Inorg. Chim. Acta,* 1992, **198**, 429.

[70]   R. S. Drago and M. P. Li, *J. Am. Chem. Soc.,* 1976, **98**, 5129.

[71]   R. S. Drago and A. J. Pribula, *J. Am. Chem. Soc.,* 1976, **98**, 2784.

[72]   M. J. Desmond, R. S. Drago and M. L. Wu, *Inorg. Chem.,* 1979, **18**, 679.

[73]   C. M. Haar, J. Huang, S. P. Nolan and J. L. Petersen, *Organometallics,* 1998, **17**, 5018.

[74]   K. G. Moloy, S. P. Nolan and S. A. Serron, *Organometallics,* 1996, **15**, 4301.

[75]   A. Huang, J. E. Marcone, W. J. Marshall, K. L. Mason, K. G. Moloy, S. P. Nolan and S. A. Serron, *Organometallics,* 1997, **16**, 3377.

[76]   I. T. Horváth, C. Li and S. P. Nolan, *Organometallics,* 1998, **17**, 452.

[77]   C. A. Tolman, *J. Am. Chem. Soc.,* 1970, **92**, 2953.

[78]   T. Lis, A. M. Trzeciak and J. J. Ziólkowski, *J. Organomet. Chem.,* 1991, **419**, 391.

[79]   F. H. Jardine, J. A. Osborn, G. Wilkinson and J. F. Young, *J. Chem. Soc. (A),* 1966, 1711.

[80]   D. J. Cole-Hamilton and M. C. Simpson, *Coord. Chem. Rev.,* 1996, **155**, 163.

[81]   *'Comprehensive Coordination Chemistry'* Vol. 4, Eds. G. Wilkinson, R. D. Gillard and J. A. McCleverty, Pergamon Press, New York, 1987, pp. 913-918 and references therein.

[82]   R. M. Pike, M. M. Singh and Z. Szafran, *Abs. Am. Chem. Soc.,* 1990, **199**, 244.

[83]   L. Vallarino, *J. Chem. Soc.,* 1957, 2473.

[84]   A. M. Trzeciak and J. J. Ziólkowski, *Transition Met. Chem.,* **1989**, 14, 135.

[85]   D. R. Paige, *The Synthesis, Coordination Chemistry and Catalytic Applications of Phosphine Ligands Containing Long-Chain Perfluoroalkyl Groups,* Ph.D. Thesis, University of Leicester, 1997, pp. 135-138.

[86]   C. O'Connor and G. Wilkinson, *Tetrahedron Lett.,* 1969, 1375.

[87]   D. J. Cole-Hamilton, J. Fawcett, E. G. Hope, R. D. W. Kemmitt, D. R. Paige, M. J. Payne and A. M. Stuart, *Chem. Commun.*, 1997, 1127.

Chapter Four

4.1 Fluorous Biphase Catalysis

The application of fluorous biphase systems to homogeneous catalysis confers the benefits of heterogeneous facile catalyst/product separation while maintaining the advantages of homogeneous reactions (see Section 1.6). From the extensive coordination chemistry undertaken using the perfluoroalkyl chain derivatised ligands (see Chapter 3) it has been concluded that only the phosphite ligands bearing three perfluoro-*n*-hexyl substituents confer preferential fluorous phase solubility to metal complexes. The derivatised phosphite ligands are therefore the most compatible with the FBS approach and it was, therefore, of interest to investigate their application as modifying ligands in homogeneous catalysis under fluorous biphase conditions. In this section the application of the derivatised phosphite ligands as auxiliary ligands in the rhodium-catalysed hydroformylation of olefins is discussed.

4.2 Hydroformylation

Since its discovery by Roelen in 1938,[1] the hydroformylation of olefins has developed into an industrially important process. It is also one of the most versatile methods for the functionalisation of carbon-carbon double bonds and is therefore a useful synthetic reaction for the preparation of fine chemicals. The hydroformylation reaction is the addition of a hydrogen atom and a formyl group to a carbon-carbon double bond as shown in Scheme 4.1.
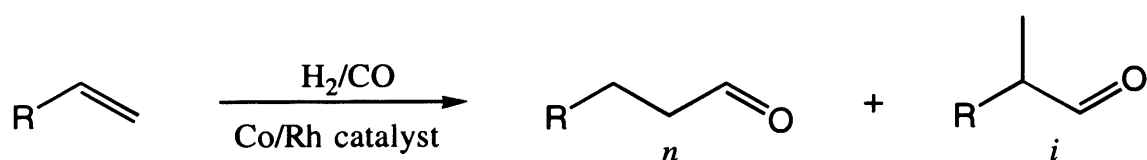
Scheme 4.1 The hydroformylation of a linear olefin.

The hydroformylation reaction gives rise to linear (*n*) and branched (*i*) aldehydes. The relative proportions of linear and branched isomers produced, known as the *n/i* ratio, depends on both the catalyst used and the reaction conditions. In the

hydroformylation of non-functionalised linear olefins high n/i ratios are generally desired due to the widespread commercial application of linear aldehydes in the production of plasticizers and detergents. Conversely, high i/n ratios are preferred in the enantioselective hydroformylation of functionalised olefins for the production of fine chemicals and pharmaceuticals. The rhodium-catalysed hydroformylation of alkenes has been widely studied with recent fundamental studies directed towards improving the rate and selectivity of the reaction through variation of the modifying ligands. The use of phosphites as modifying ligands has received much attention, particularly in the patent literature.[2,3] Phosphite containing metal complexes have been shown to be highly active and selective catalysts for hydroformylation, with monophosphites having replaced triphenylphosphine as the modifying ligands in some commercial catalyst systems.[4] The steric effects of phosphorus ligands in the hydroformylation of alkenes have a significant impact on the reaction rate and product distribution.[5] The rate of hydroformylation decreases with increasing steric hindrance in the ligand and the substrate. Conversely, the linear to branched (n/i) ratio of aldehyde products increases with increasing steric hindrance, the linear isomers being the products of highest commercial value.[6]

Van Leeuwen and Roobeek demonstrated that normally unreactive substituted terminal and internal alkenes were hydroformylated under mild conditions using rhodium catalysts incorporating the bulky phosphite ligand, tris(2-tert-butyl-4-methylphenyl)phosphite (4.1).[7] Significant increases in the rate of hydroformylation of 1,2- and 2,2'-dialkylalkenes were observed using the bulky phosphite-modified catalyst in comparison to triphenylphosphine. The increased reactivity was attributed to the impact of the large cone angle of the phosphite ($\theta = 172°$) on the nature of the active species. Van Leeuwen and co-workers found the tricarbonyl species [RhH(CO)$_3$L], prepared *in situ* from [Rh(CO)$_2$(pentane-2,4-dionate)] and the bulky phosphite (4.1), to be a highly active catalyst for the hydroformylation of 1-octene giving turnover frequencies in excess of 160 000 mol (mol Rh^{-1}) h^{-1}.[8] The observed rates were found to be over 10 times higher than those observed when triphenylphosphine was employed as the modifying ligand, while the selectivity and low rate of isomerisation were retained.[9]

$$P \left(O - \begin{array}{c} {}^tBu \\ \end{array} - R \right)_3$$

R = Me (4.1)

    = H (4.2)
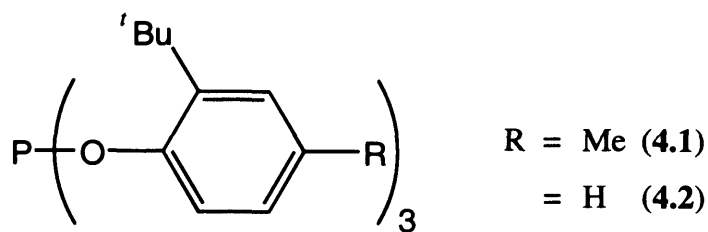
Van Leeuwen and co-workers[10] have also employed the bulky phosphite ligand (4.2) in the hydroformylation of a range of substrates. Bayón et al.[11] have used the phosphite ligand (4.2) in the rhodium catalysed hydroformylation of 2,3-dihydrofuran. Complete conversion to tetrahydrofuran-2-carbaldehyde and tetrahydrofuran-3-carbaldehyde in a 77/23 ratio was observed using the bulky phosphite. When triphenylphosphine was used as the auxiliary ligand similar conversions were observed, but the reaction was found to be less selective with the two products obtained in almost equal quantities. Furthermore, in the case of triphenylphosphine the conversion decreased markedly when the ligand/Rh ratio was increased.

Bulky bisphosphites such as (4.3), reported by Union Carbide, give rise to very selective hydroformylation catalysts. High n/i ratios were obtained for the rhodium-catalysed hydroformylation of 1-propene under mild conditions when (4.3) was used as the modifying ligand. Following this disclosure by Union Carbide, Buchwald et al. used the same catalytic system for the hydroformylation of a series of functionalised α-olefins.[12] Conversions of substrates containing functional groups such as ketones, esters, acids, and amides to aldehydes were high while excellent regioselectivity was achieved with n/i ratios typically $\geq$ 40/1. Olefinic alcohols, nitriles and halides were also efficiently hydroformylated, although a decrease in regioselectivity was observed for substrates containing allylic functional groups. Similar bisphosphites derived from 2,2'-biphenols have been used by Van Leeuwen and co-workers[13,14] and Gladfelter et al.[15] for the selective hydroformylation of 1-octene and styrene.

MeO   OMe

^{t}Bu ^{t}Bu
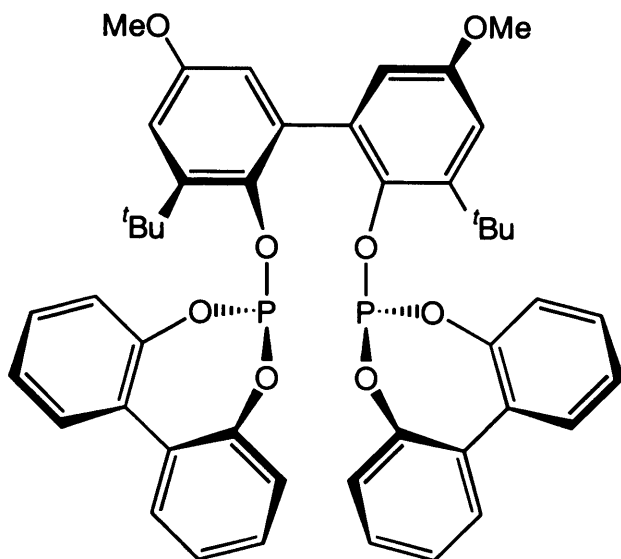
(4.3)

Recently, bisphosphite ligands have been applied to the asymmetric hydroformylation of alkenes. Wink and co-workers reported the first example using bis(dioxaphospholane) ligands as the modifying ligand in the rhodium-catalysed hydroformylation of styrene. The resulting aldehyde was obtained as a racemic mixture with a branched to normal ratio of 75/25. The bulky bisphosphite (4.4), prepared by Babin and Whiteker, was found to give rise to a far more selective catalyst for the hydroformylation of styrene, affording hydrotropaldehyde with a branched to normal ratio of 94/6 and 67% ee.[16] A range of bisphosphite ligands closely related to (4.4) have since been prepared in which the chiral backbone of the ligand is based on butane-2,3-diol, pentane-2,4-diol, hexane-2,5-diol and diphenylpropane-1,3-diol.[17]

Phosphite ligands similar to (4.4) are readily synthesised by the reaction of a stoichiometric amount of the 2,2'-biphenol derivative with PCl$_3$ followed by the addition of a second diol to provide the bisphosphite back-bone. This methodology allows for the synthesis of a variety of asymmetric bisphosphites through the use of commercially available chiral diols. The synthesis of fluorous soluble bisphosphites based on diols bearing perfluorohexyl substituents is discussed in chapter 5.

(4.4)
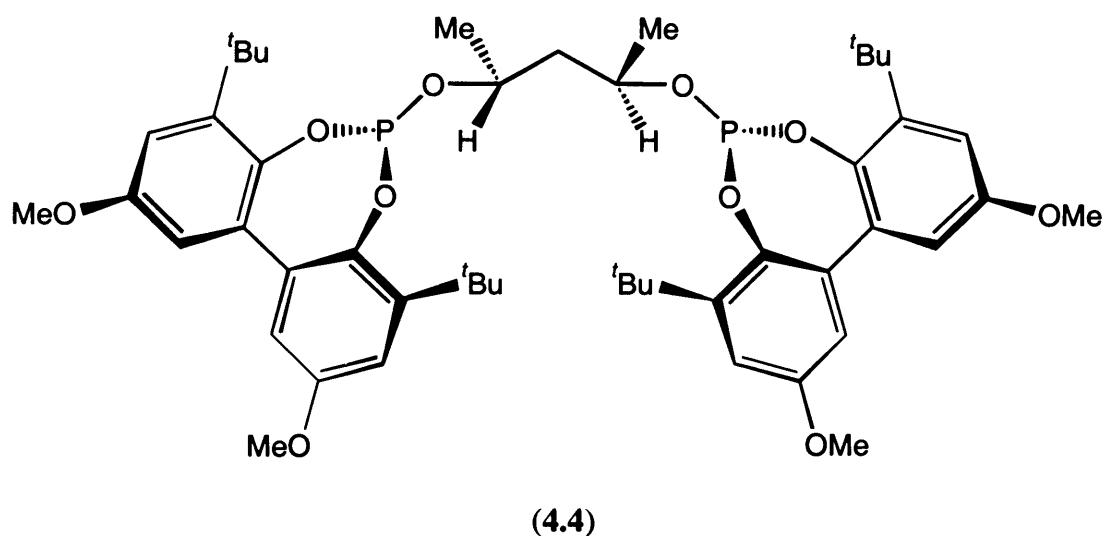
The chiral bisphosphite ligands (4.5-4.6) derived from binaphthol bearing a variety of substituents at phosphorus have been synthesised by Takaya and co-workers.[18] The ligands have been applied to the rhodium-catalysed hydroformylation of vinyl acetate to give chiral 2-acetoxypropanal (Scheme 4.1), an important precursor in the Strecker synthesis of the amino acid threonine.[19] High regio- and stereo-selectivities were observed with branched to normal ratios ≥ 15/1 in 47% ee. Ligands (4.5-4.6) are readily prepared by the reaction of 2 equivalents of phenol with PCl_3 to form a diphenylphosphorochlorodite, which is then further reacted with 2,2'-binaphthol.

Ar = Ph   (4.5)

   = p-tolyl   (4.6)

$$\frac{H_2/CO \ (1:1)}{[Rh(CO)_2(acac)]/(4.5)}$$
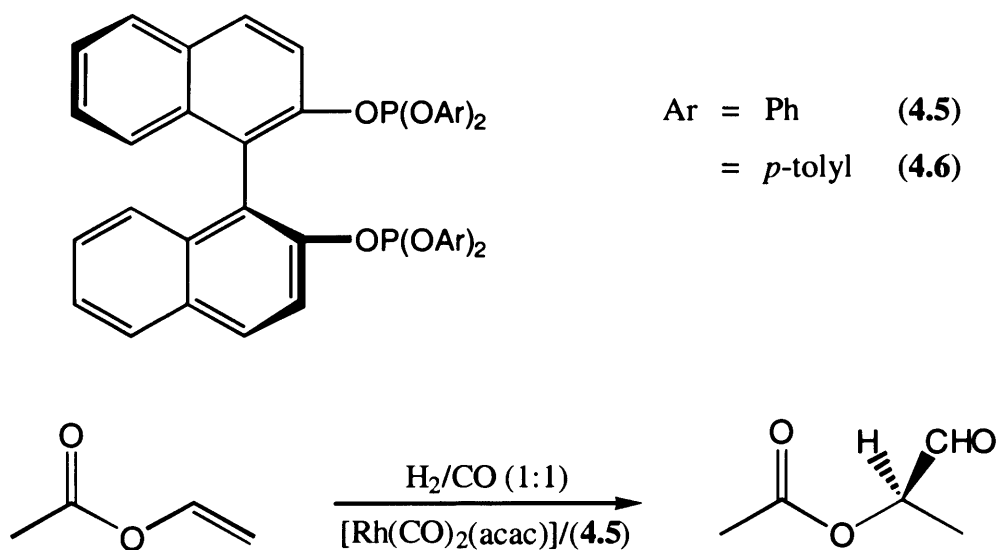
Scheme 4.1 Asymmetric hydroformylation of vinyl acetate.

128

Union Carbide have developed an asymmetric route to the anti-inflammatory drug (S)-(+)-ibuprofen by the enantioselective hydroformylation of isobutylstyrene.[20] High branched to normal ratios of aldehyde products are obtained by using a chiral bisphosphite ligand instead of phosphine ligands. The product aldehyde is obtained in 82% ee, which after stereospecific oxidation gives (S)-(+)-ibuprofen (Scheme 4.2).
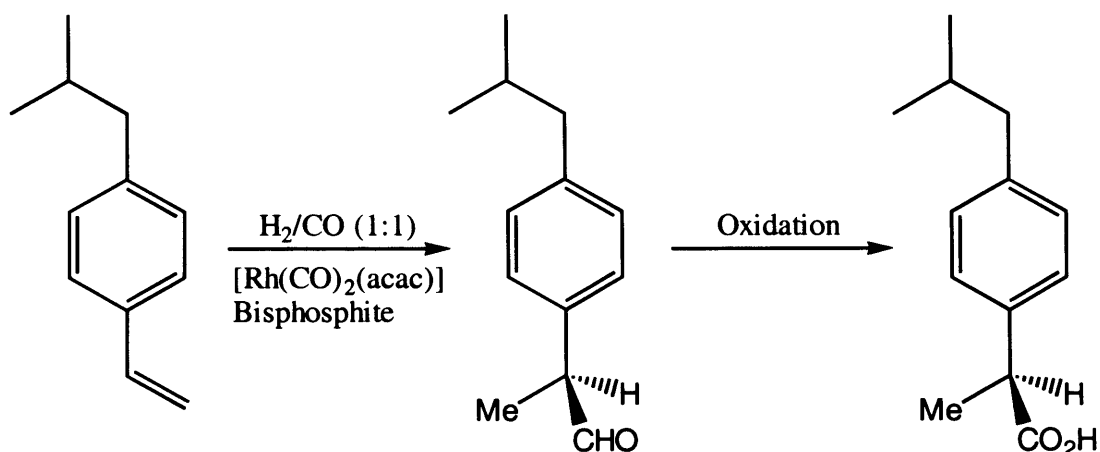
Scheme 4.2 Synthesis of (S)-(+)-ibuprofen via enantioselective hydroformylation.

Takaya and co-workers recently introduced the use of mixed phosphine-phosphite ligands such as (4.7) containing a binaphthyl core for the asymmetric hydroformylation of alkenes.[21,22]
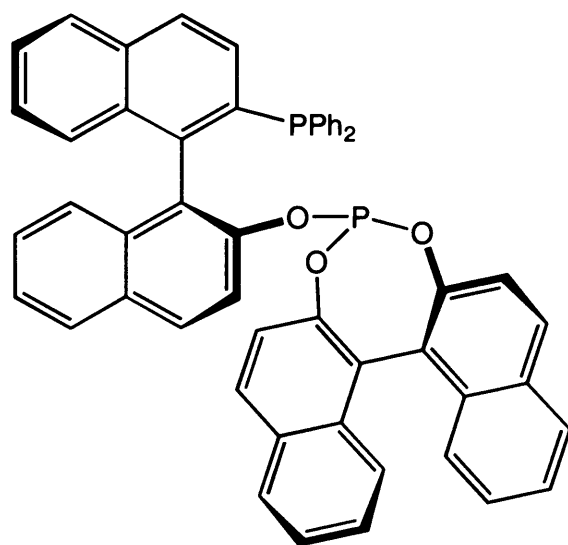
(4.7)

The so-called BINAPHOS ligands are amongst the most selective ever reported for rhodium-based catalysts giving a conversion > 99% and 92% ee for the hydroformylation of vinyl acetate.[23] The enantioselectivities were found to have a marked dependence on the structure of the phosphite moiety relative to the 2-(diphenylphosphino)1,1'-binaphthyl back-bone. The (R,S) ligand and its enantiomer (S,R) were found to provide the highest ee's, whereas the (R,R) equivalents gave lower values. The unsymmetrical mixed phosphine-phosphite ligands based on the binaphthyl architecture are systematically superior to any other rhodium system for the enantioselective hydroformylation of a wide range of alkenes.

4.3 Hydroformylation of 1-Hexene

The hydroformylation of 1-hexene (Scheme 4.3) results in the formation of two major aldehyde products. Addition of the formyl group to the terminal carbon of the double bond results in the formation of the linear product heptanal (**4.8**), whereas addition to the internal carbon of the double bond results in the formation of the branched product 2-methylhexanal (**4.9**). The linear aldehyde is desired as it is of greater commercial value than the branched product. Linear aldehydes can be reduced to the corresponding alcohols which are used in the synthesis of plasticizers and detergents.[24] Minor reaction products which can also be formed include hexene isomers formed by the migration of the double bond, 2-ethylpentanal and hexane. The branched aldehyde 2-ethylpentanal is formed by the hydroformylation of the isomerisation product 2-hexene, and hexane arises through the hydrogenation of the substrate.
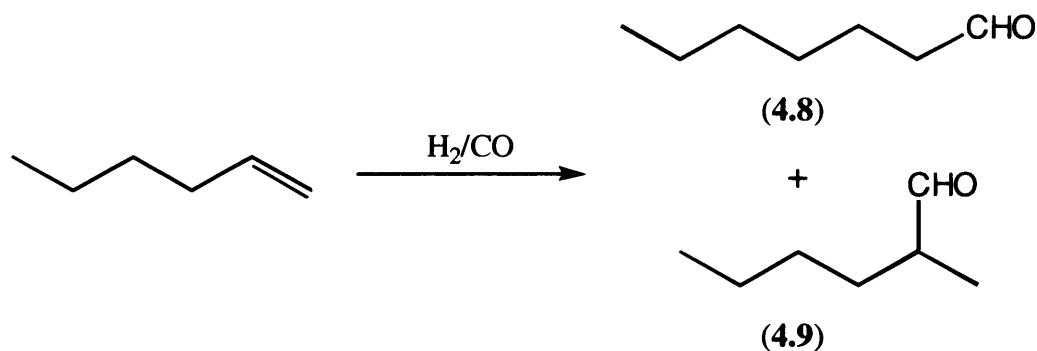
Scheme 4.3 Hydroformylation of 1-hexene.

The hydroformylation of 1-hexene under fluorous biphase conditions was investigated using a rhodium catalyst rendered preferentially soluble in perfluorinated solvents by the incorporation of perfluoroalkyl chain derivatised phosphite ligands. Only catalytic systems incorporating the aryl phosphite $P(OC_6H_4-4-C_6F_{13})_3$ (**2.4**) as modifying ligand were examined as the extreme air- and moisture-sensitivity of the alkyl phosphite $P(OC_2H_4C_6F_{13})_3$ (**2.17**) made handling extremely difficult. The catalyst precursor was prepared *in situ* under hydroformylation conditions from [Rh(CO)$_2$(acac)] and phosphite (**2.4**) in a biphasic system consisting of toluene and PP3. The system was stirred rapidly and brought to equilibrium at 70 °C at which point the substrate, 1-hexene, was injected into the autoclave and the pressure of H_2/CO (1:1) increased to 20 bar and maintained throughout the reaction using a ballast tank connected to the autoclave (see Section 6.4.3). The reactions were run for 1 hour after which time the autoclave was allowed to cool to room temperature and the reaction mixture transferred to a sample tube. Complete separation of the lower fluorous and upper organic phases was observed after each catalytic run. The toluene phase was clear and colourless, while the PP3 phase was coloured orange due to the rhodium catalyst, indicating efficient catalyst/product separation. The reaction products were then analysed by gas chromatography and the results are collected in Table 4.1.

Table 4.1   Results of the hydroformylation of 1-hexene.[a]

Run	Ligand	Conversion %	Selectivity %	n/i
1[b]	PPh$_3$	99.6	96.1	2.5
2	PPh$_3$	99.0	98.2	3.1
3	P(OPh)$_3$	99.6	92.0	2.9
4	(**2.4**)	99.7	82.3	6.4
5	(**2.4**)	99.2	85.3	8.4
6[c]	(**2.4**)	98.6	90.6	3.1
7[d]	(**2.4**)	99.7	89.3	6.6

[a] [Rh(CO)$_2$(acac)] = 0.01 mol dm^{-3}, ligand = 0.03 mol dm^{-3}, 70 °C, 20 bar, 1 hr. [b] In toluene. [c] [Rh(CO)$_2$(acac)] = 0.001 mol dm^{-3}, ligand = 0.003 mol dm^{-3}. [d] 8 bar.

Catalysis with the phosphite (2.4) as with triphenylphosphine and triphenylphosphite gave almost quantitative conversions of 1-hexene. The selectivity towards aldehyde is slightly lower for the derivatised phosphite in comparison to both triphenylphosphine and triphenylphosphite as a result of greater isomerisation of the substrate to 2-hexene. Significant improvements in selectivity towards the linear aldehyde were found using ligand (2.4) with n/i ratios almost three times greater than those obtained with triphenylphosphite. According to the dissociative hydroformylation mechanism proposed by Wilkinson (Scheme 4.3), aldehyde selectivity is determined during the hydride addition step that converts the five-coordinate [H(alkene)Rh(CO)L$_2$] species into either a primary or secondary four-coordinate [(alkyl)Rh(CO)L$_2$] species. In the case of monodentate phosphines and phosphites the rhodium hydride species can have the phosphorus ligands coordinated in an apical-equatorial or diequatorial geometry (Figure 4.1).

diequatorial (ee)　　　　apical-equatorial (ae)
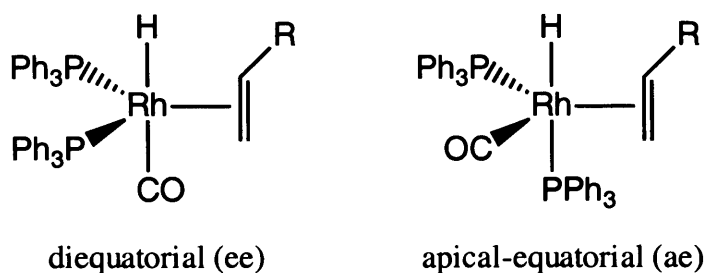
Figure 4.1 Diequatorial and apical-equatorial coordination of [H(alkene)Rh(CO)L$_2$].
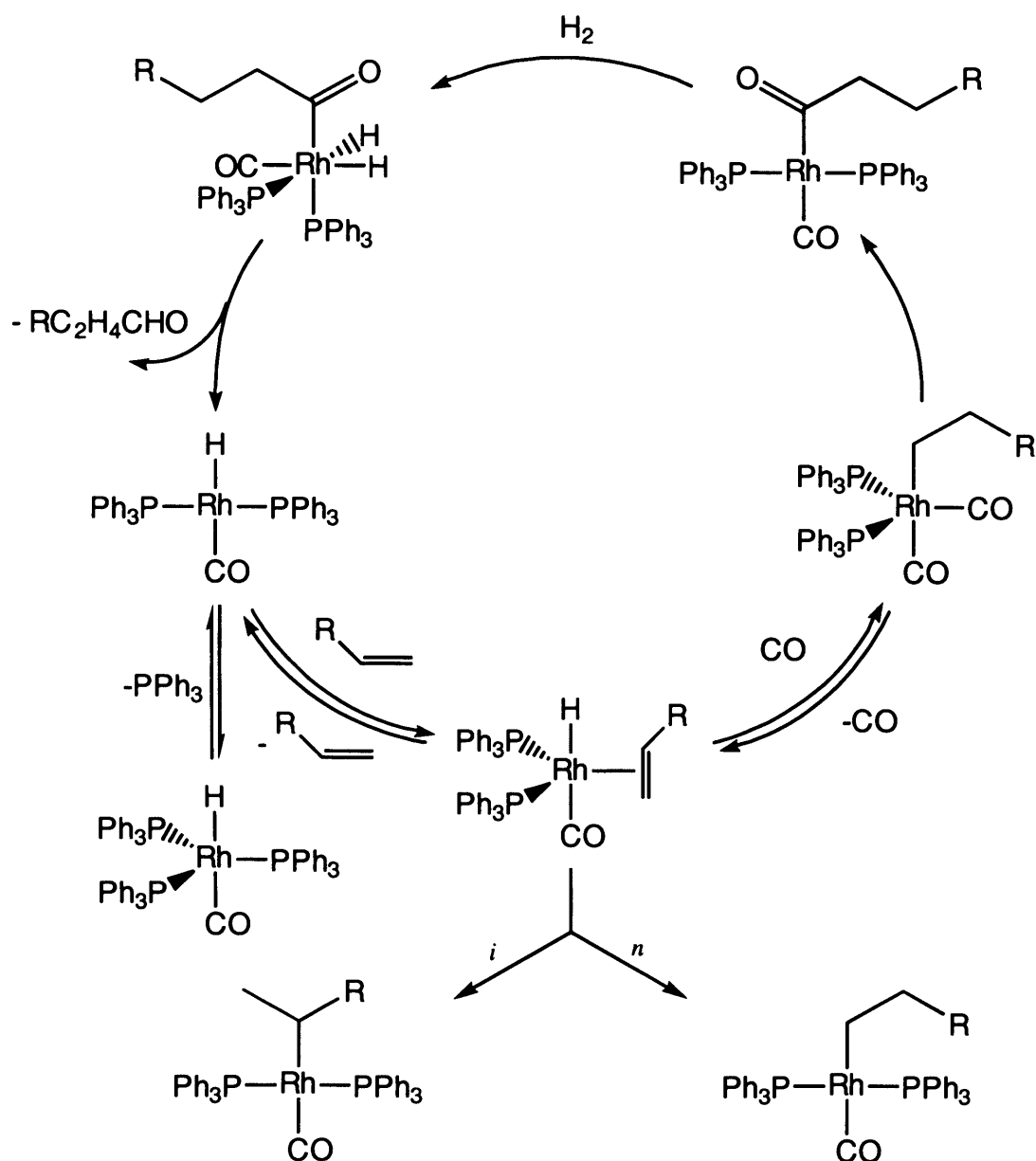
Scheme 4.3 Mechanism of [HRh(CO)(PPh₃)₃] catalysed olefin hydroformylation.

³¹P NMR spectroscopy studies by Brown *et al.* have shown that in the case of PPh₃ the diequatorial/apical-equatorial isomers exist in an 85/15 mixture which is in rapid equilibrium at room temperature.[25] Phosphines bearing electron withdrawing groups are expected to increase the proportion of diequatorial isomer, which should in turn result in increased selectivity towards the linear aldehyde. The investigation by Brannon *et al.* into the rhodium-catalysed hydroformylation of alkenes found increased reaction rates and regioselectivity were obtained using triarylphosphines bearing electron withdrawing groups in the *para* positions of the phenyl substituents

in comparison to PPh_3.[26] Casey *et al.* have shown that in the case of bidentate phosphines, those which chelate diequatorially display much higher n/i ratios than those which chelate with apical-equatorial coordination.[27] Furthermore, the inclusion of electron withdrawing groups into diequatorially chelating bisphosphines increased the regioselectivity to the linear aldehyde two-fold. These studies indicate that the increase in the n/i ratio observed for (2.4) in comparison to triphenylphosphite is due in part to the electron withdrawing effect of the perfluoroalkyl substituents. However, the improvement in selectivity cannot be solely due to electron-withdrawing effects since the increase in the n/i ratio for the derivatised phosphite (2.4) is much larger than the difference observed between triphenylphosphine and the derivatised phosphine, $P(C_6H_4\text{-}4\text{-}C_6F_{13})_3$.[28]

Steric effects associated with the perfluoroalkyl chains are also likely to have an impact on the regioselectivity of the reaction. When a bulky phosphite is used the alkene binds preferentially *via* the terminal carbon of the double bond, which gives rise to the linear aldehyde. This minimises unfavourable steric interactions with the ligand which are more likely to occur when bound *via* the internal carbon of the double bond which gives rise to the branched aldehyde (Scheme 4.3). Maitlis *et al.* have compared the caged phosphites (4.10-4.13) with bulkier aryl phosphine and phosphite ligands in the hydroformylation of 1-hexene.[29] Higher n/i ratios were obtained for phosphites (4.10-4.13) despite having smaller cone angles ($\theta = 109°$) than triphenylphosphite ($\theta = 128°$). Interestingly, the n/i ratios for the slim phosphites were found to increase with increasing length of the substituent R, indicating that the tails are responsible for the enhanced regioselectivity. The good regioselectivity observed for the derivatised phosphite (2.4) is, therefore, likely to be a combination of both the steric and electronic effects of the perfluoroalkyl substituents.

R = C_2H_5	(4.10)
= C_8H_{17}	(4.11)
= $CH_2O_2CC_6H_{13}$	(4.12)
= $CH_2O_2CC_{11}H_{23}$	(4.13)

During the course of the catalytic runs the change in pressure of the ballast tank was recorded at five second intervals. Initial rate values and turnover frequencies (TOFs) were obtained by analysis of the data for the rate of gas consumption and are collected in Table 4.2. The derivatised phosphite (2.4) gave rise to a highly active hydroformylation catalyst with turnover frequencies up to four times greater than that obtained using PPh_3, although lower activity was found in comparison to $P(OPh)_3$. The lower turnover frequencies obtained for (2.4) in comparison to $P(OPh)_3$ may be a result of greater steric hindrance in the phosphite due to the long perfluoroalkyl substituents. Activity with the derivatised phosphite remained high even with a low catalyst loading and at reduced pressure. Catalysis with PPh_3 shows some solvent dependency as an increase in reaction rate was observed when the experiments were performed under fluorous biphase conditions in comparison to those undertaken in only toluene.

Table 4.2   Results of the hydroformylation of 1-hexene.[a]

Run	Ligand	Initial Rate/mol dm^{-3} s^{-1}	TOF/mol [mol Rh^{-1}] h^{-1}
1[b]	PPh_3	2.3×10^{-3}	828
2	PPh_3	3.2×10^{-3}	1152
3	$P(OPh)_3$	4.8×10^{-2}	17280
4	(2.4)	1.2×10^{-2}	4320
5	(2.4)	9.2×10^{-3}	3312
6[c]	(2.4)	3.6×10^{-3}	1296
7[d]	(2.4)	6.4×10^{-3}	2304

[a] $[Rh(CO)_2(acac)]$ = 0.01 mol dm^{-3}, ligand = 0.03 mol dm^{-3}, 70 °C, 20 bar, 1 hr. [b] In toluene. [c] $[Rh(CO)_2(acac)]$ = 0.001 mol dm^{-3}, ligand = 0.003 mol dm^{-3}. [d] 8 bar.

The extremely high hydroformylation rates observed by Van Leeuwen and co-workers[30] with bulky ligands such as tris(2-tert-butyl-4-methyl)phosphite have been attributed to the formation of the complex $[HRh(CO)_3L]$ instead of $[HRh(CO)L_3]$ which is formed with phosphine ligands. The tricarbonyl complex has a strong tendency to lose CO due to the high electron accepting ability of the phosphite ligand forming the more electronegative and less sterically hindered complex $[HRh(CO)_2L]$.

The coordination of alkene, which is the rate determining step, occurs more readily resulting in higher reaction rates. The rate determining step is now the last step in the mechanism, the reductive elimination of aldehyde product. The formation of the catalyst precursor is dependent on the cone angle and the π-acidity of the phosphorus ligand. Ligands such as triphenylphosphine ($\theta = 145°$) were found to give complexes of the type [HRh(CO)L$_3$], while ligands with large cone angles such as tris(2-tert-butyl-4-methyl)phosphite($\theta = 172°$) only give complexes of the type [HRh(CO)$_3$L]. Electron rich ligands which form a strong metal-phosphorus bond tend to readily form complexes analogous to [HRh(CO)L$_3$]. In contrast, strongly electron withdrawing ligands such as P{OCH(CF$_3$)$_2$}$_3$ do not give stable complexes containing three ligands, therefore [HRh(CO)$_3$L] complexes are formed.[7] Substitution of the phenyl groups of triphenylphosphite in the *para* position with long perfluoroalkyl chains does not significantly change the steric parameters of the ligand as evidenced by the coordination chemistry of (2.4) (see Chapter 3). On this basis the hydroformylation mechanism is likely to involve a precursor of the type [HRh(CO)L$_3$] which is in agreement with the turnover frequencies obtained for (2.4). If a species of the type [HRh(CO)$_3$L] was formed as is the case for bulky phosphites the reaction rates and turnover frequencies would be greater than those for triphenylphosphite. On the contrary, the reaction rate and turnover frequency obtained with triphenylphosphite are four times greater than those for the perfluoroalkylated phosphite.

4.4 Hydroformylation of 1- and 2-Nonene

The fluorous soluble aryl phosphite (2.4) was also tested as a modifying ligand in the rhodium-catalysed hydroformylation of nonenes. The two major products of the hydroformylation of 1-nonene are decanal (4.14) and 2-methylnonanal (4.15) (Scheme 4.4). Other branched aldehydes such as 2-ethyloctanal and 2-propylheptanal can be formed by the hydroformylation of 2- and 3-nonene respectively, which arise due to isomerisation of the substrate. Catalytic reactions were performed similarly to the hydroformylation of 1-hexene and the products analysed by gas chromatography, the results of which are collected in Tables 4.3 and 4.5.
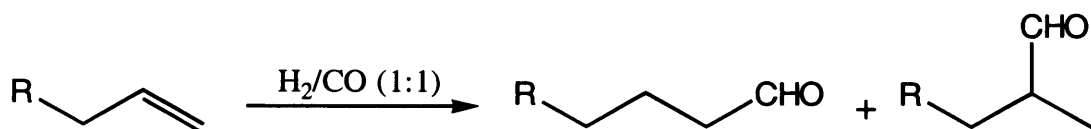
Scheme 4.4 Hydroformylation of 1-nonene. R = C_6H_{13}.

Similarly high conversion of the substrate and selectivity to aldehyde were observed for the hydroformylation of 1-nonene in comparison to 1-hexene under identical conditions. The regioselectivity of the reaction was also similar with a linear to branched aldehyde ratio of 6.9. The rhodium-catalysed hydroformylation of the internal alkene 2-nonene with phosphite (2.4) was also investigated. High substrate conversion was found with the two major products being the branched aldehydes 2-methylnonanal and 2-ethyloctanol. Surprisingly, a significant quantity of decanal was obtained as a result of the isomerisation of 2-nonene to 1-nonene and subsequent hydroformylation. Reduction in the pressure of H_2/CO resulted in an increased proportion of decanal formation, while the high substrate conversion was maintained. This reaction is of interest as feed-stocks for the commercial hydroformylation of alkenes often contain mixtures of isomers. A catalytic system which isomerised internal alkenes to terminal alkenes and gave good conversions to the desired linear aldehydes would be economically beneficial as increased yields of the commercially valuable products would be obtained. As with the hydroformylation of 1-hexene, excellent separation of the fluorous and organic phases was found with no colouration of the upper organic phase observed, suggesting that the catalyst was completely retained in the fluorous phase.

Table 4.3 Results for the hydroformylation of 1- and 2-nonene.[a]

Run	Substrate	Conversion %	Selectivity %	n/i
1	1-nonene	99.0	85.9	6.90
2	2-nonene	86.1	87.0	0.16
3[b]	2-nonene	88.2	76.8	0.29
4[b,c]	2-nonene	79.0	50.5	0.55

[a] $[Rh(CO)_2(acac)]$ = 0.01 mol dm^{-3}, ligand = 0.03 mol dm^{-3}, 70 °C, 20 bar, 1 hr. [b] 8 bar. [c] 90 °C.

Table 4.4 Aldehyde distribution in the hydroformylation of 1- and 2-nonene.[a]

Run	2-propylheptanal %	2-ethyloctanol %	2-methylnonanal %	Decanal %
1	0.0	1.0	9.8	74.2
2	7.2	17.8	39.5	10.4
3[b]	7.3	12.0	33.0	15.4
4[b,c]	4.2	5.2	16.3	14.2

[a] $[Rh(CO)_2(acac)]$ = 0.01 mol dm^{-3}, ligand = 0.03 mol dm^{-3}, 70 °C, 20 bar, 1 hr. [b] 8 bar. [c] 90 °C.

4.5 Hydroformylation Conclusions

The results of the catalytic experiments show that the derivatised aryl phosphite ligand (2.4) gives rise to highly active rhodium(I) complexes for the catalytic hydroformylation of both terminal and internal alkenes. The regioselectivity of the catalyst is significantly different to that observed for the triphenylphosphine and triphenylphosphite modified catalysts with greater selectivity to the linear aldehyde in the hydroformylation of 1-hexene and 1-nonene. The rhodium complex derived from (2.4) was also found to be an active alkene isomerisation catalyst as evidenced during the hydroformylation of 2-nonene. A combination of the steric influence of the perfluoroalkyl substituents and the increased π-acceptor ability of the

ligands is responsible for the improved *n/i* ratios observed in comparison to triphenylphosphite. The perfluoroalkyl substituents give rise to increased steric hindrance of the ligand which lowers the activity in comparison to $P(OPh)_3$, although the activity is substantially greater than for PPh_3.

Most importantly, phosphite (**2.4**) gives rise to rhodium(I) complexes which are preferentially soluble in perfluorinated solvents. The complete retention of the catalyst in the fluorous phase of a toluene/PP3 biphasic system after the hydroformylation of 1-hexene and 1- and 2-nonene demonstrates the efficient catalyst/product separation possible with FBS catalysis.

References for Chapter Four

[1]   O. Roelen, *Angew. Chem.*, 1948, **62**, 60.

[2]   A. G. Abatjoglou, E. Billig and D. R. Bryant, U.S. Patent 4 668 651, (1987) to Union Carbide.

[3]   A. G. Abatjoglou, E. Billig and D. R. Bryant, U.S. Patent 4 769 498, (1988) to Union Carbide.

[4]   N. Yoshinura and Y. Tokito, Eur. Patent 223 103, (1987) to Kuraray.

[5]   C. A. Tolman, *Chem. Rev.*, 1977, **77**, 313.

[6]   J. P. Collman, L. S. Hegedus, J. R. Norton and R. G. Finke, *Principles and Applications of Organotransition Metal Chemistry*, University Science Books, Mill Valley, CA, 1987, pp. 625-630.

[7]   P. W. N. M. van Leeuwen and C. F. Roobeek, *J. Organomet. Chem.*, 1983, **258**, 343.

[8]   F. van den Aardweg, P. C. J. Kamer, P. W. N. M. van Leeuwen, E. N. Orij and A. van Rooy, *J. Chem. Soc., Chem. Commun.*, 1991, 1096.

[9]   D. Neibecker and R. Reau, *J. Mol. Catal.*, 1989, **57**, 153.

[10]   G. Challa, T. Jongsma and P. W. N. M. van Leeuwen, *J. Organomet. Chem.*, 1991, **421**, 121.

[11]   J. C. Bayon, S. Castillon, C. Claver, A. Polo and J. Real, *J. Chem. Soc., Chem. Commun.*, 1990, 600.

[12]   S. L. Buchwald and G. D. Cuny, *J. Am. Chem. Soc.*, 1993, **115**, 2066.

[13]   P. C. J. Kamer, P. W. N. M. van Leeuwen, A. van Rooy, A. L. Spek and N. Veldman, *J. Organomet. Chem.*, 1995, **494**, C15.

[14]   J. Fraanje, K. Goubitz, P. C. J. Kamer, P. W. N. M. van Leeuwen, A. van Rooy, A. L. Spek and N. Veldman, *Organometallics.*, 1996, **15**, 835.

[15]   W. L. Gladfelter and B. Moasser, *Organometallics*, 1995, **14**, 3832.

[16]   J. E. Babin and G. T. Whiteker, *Chem. Abstr.*, 1993, **119**, 159872h.

[17]   G. J. H. Buisman, P. C. J. Kamer, P. W. N. M. van Leeuwen and E. J. Vos, *J. Chem. Soc., Dalton Trans.*, 1995, 409.

[18]   K. Mashima, K. Nozaki, N. Sakai and H. Takaya, *Tetrahedron: Asymmetry*, 1992, **3**, 583.

[19]   I. Chibata, *Synthetic Production and Utilization of Amino Acids*, Eds. I. Chibata, T. Kaneoko, T. Itoh and Y. Izumi, Wiley, New York, 1974, 201.

[20]   J. E. Babin and G. T. Whiteker, Int. Patent WO 93/03839, (1993) to Union Carbide.

[21]   S. Mano, K. Nozaki, N. Sakai and H. Takaya, *J. Am. Chem. Soc.*, 1993, **115**, 7033.

[22]   T. Higashizima, K. Nozaki, N. Sakai and H. Takaya, *Tetrahedron Lett.*, 1994, **35**, 2023.

[23]   T. Higashizima, T. Horiuchi, S. Mano, T. Nanno, K. Nozaki, N. Sakai and H. Takaya, *J. Am. Chem. Soc.*, 1997, **119**, 4413.

[24]   B. Cornils, W. A. Herrmann and M. Rasch, *Angew. Chem., Int. Ed. Engl.*, 1994, **33**, 2144.

[25]   J. W. Brown and A. G. Kent, *J. Chem. Soc., Perkin Trans. II*, 1987, 1597.

[26]   D. A. Brannon, R. A. Duwell, W. R. Moser, C. J. Papile and S. J. Weininger, *J. Mol. Catal.*, 1987, **41**, 271.

[27]   E. W. Beuttenmueller, C. P. Casey, B. A. Matter, E. L. Paulsen, L. M. Petrovich, D. R. Powell and B. R. Proft, *J. Am. Chem. Soc.*, 1997, **119**, 11817.

[28]   D. R. Paige, *The Synthesis, Coordination Chemistry and Catalytic Applications of Phosphine Ligands Containing Long-Chain Perfluoroalkyl Groups*, Ph.D. Thesis, University of Leicester, 1997.

[29]   P. M. Maitlis and S. N. Poelsma, *J. Organomet. Chem.*, 1993, **451**, C15.

[30]   J. N. H. de Bruijn, P. C. J. Kamer, P. W. N. M. van Leeuwen, K. F. Roobeek and A. van Rooy, *J. Organomet. Chem.*, 1996, **507**, 69.

Chapter Five

5.1 Bidentate Ligands

The coordination chemistry and catalytic application of the perfluoroalkyl chain derivatised ligands has identified the air- and moisture-sensitivity of the ligands and their Rh(I) complexes to be a major impediment to their application in fluorous biphase catalysis. To overcome this problem investigations were undertaken to find ways of increasing the stability of the phosphite ligands. Phosphites can be made more robust towards hydrolysis by incorporating the phosphorus atom into a cyclic system, increasing the stability due to the chelate effect, resulting in the formation of bidentate phosphite ligands. Chelating bisphosphine ligands are well established and widely used in homogeneous catalysis,[1,2] although by comparison the bisphosphites are a relatively new class of ligand which has only recently been exploited.[3,4] Biphenol derived bisphosphite ligands, developed at Union Carbide, have been employed commercially in the rhodium-catalysed hydroformylation of α-olefins.[5,6] The enhanced stability of these ligands towards hydrolysis is attributed to the incorporation of phosphorus in a seven membered ring within the ligand.

Chelating bidentate phosphines of general formula $R_2P(CH_2)_nPR_2$ have been extensively studied,[1,7] and have been applied to a variety of catalytic transformations.[8] Similar bidentate ligands could be easily prepared by the reaction of the derivatised phenol with bidentate chlorophosphines. The size of the carbon backbone would be a crucial factor in determining the solubility of the resulting ligand in perfluorocarbon solvents, and so 1,2-bis(dichlorophosphino)ethane which contains a small C_2H_4 bridging unit was used. The bidentate phosphonite (5.1) was prepared by the reaction of 1,2-bis(dichlorophosphino)ethane with 4-perfluoro-n-hexyl phenol in the presence of base, according to a modified literature procedure.[9] Ligand (5.1) was found to be air- and moisture-sensitive, although this was expected as the hydrolytically sensitive P-O bonds are not contained within a ring system.

$$R = C_6H_4\text{-}4\text{-}C_6F_{13} \quad (5.1)$$
$$R = C_6H_4\text{-}4\text{-}C_6F_{13} \quad (5.1)$$
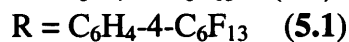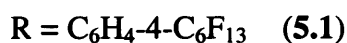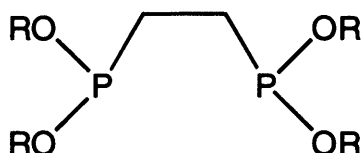
The ^{1}H NMR spectrum of the ligand exhibits resonances in the aryl region displaying the characteristic AA'BB' pattern typical of *para* disubstituted phenyl rings and a virtual triplet resonance at *ca.* 2.1 δ with J_{P-H} coupling of 8.2 Hz, assigned to the protons of the C_2H_4 backbone. The $^{31}P\{^1H\}$ NMR spectrum exhibits a singlet resonance at 181 δ which, on proton coupling is observed as a virtual quintet with J_{P-H} coupling of 8.2 Hz. The chemical shift of (5.1) is shifted to significantly higher frequency than the value of 138 δ obtained for the analogous species 1,2-bis(diphenoxyphosphino)ethane (dpope).[10] A direct quantitative comparison of the NMR spectroscopic data cannot be made as (5.1) is virtually insoluble in deuterobenzene, the solvent used to record the ^{31}P NMR spectrum of dpope. However, it is reasonable to assume that a difference of *ca.* 40 Hz between the chemical shifts for the two species is not merely due to solvent effects. Surprisingly, the chemical shift for (5.1) is closer to that for the methyl bridged species $(PhO)_2PCH_2P(OPh)_2$ which exhibits a singlet at 174 δ in its $^{31}P\{^1H\}$ NMR spectrum.[11] Ligand (5.1) was found to be substantially less soluble in PP3 than $P(OC_6H_4-4-C_6F_{13})_3$ and did not partition selectively into the fluorous phase of a biphasic system consisting of dichloromethane and PP3 as evidenced by the ^{31}P NMR spectrum of the organic phase.

5.2 Coordination chemistry

An initial study into the coordination chemistry of the derivatised diphosphonite ligand was carried out to determine what effect, if any, the perfluoroalkyl chains would have on the ligands ability to chelate to a metal centre. Ligand (5.1) was allowed to react with $[PtCl_2(MeCN)_2]$ in refluxing dichloromethane, under nitrogen to afford the complex *cis*-$[PtCl_2(C_6F_{13}-4-C_6H_4O)_2PC_2H_4P(OC_6H_4-4-C_6F_{13})_2]$ (5.2). The reaction product was isolated as an air- and moisture-stable, white solid which was found to have a low solubility in organic solvents and was completely insoluble in perfluorinated solvents. The $^{31}P\{^1H\}$ NMR spectrum exhibits a singlet at 136 δ with platinum satellites indicating a single product with a chemical shift to lower frequency of that for the free ligand, providing evidence for coordination of the

ligand to platinum. The $^1J_{Pt-P}$ coupling constant of 4673 Hz is similar in magnitude to that observed for the monodentate phosphonite complex cis-[PtCl$_2$\{PhP(OC$_6$H$_4$-4-C$_6$F$_{13}$)$_2$\}$_2$] which exhibits $^1J_{Pt-P}$ coupling of 4859 Hz. Further evidence for the formation of (5.2) is provided by its FAB mass spectrum which exhibits characteristic peaks for [(M - Cl + H)$^+$] and [(M - 2Cl)$^+$] at m/z = 1965 and 1929 respectively.

$$R = C_6H_4\text{-}4\text{-}C_6F_{13} \quad (5.2)$$
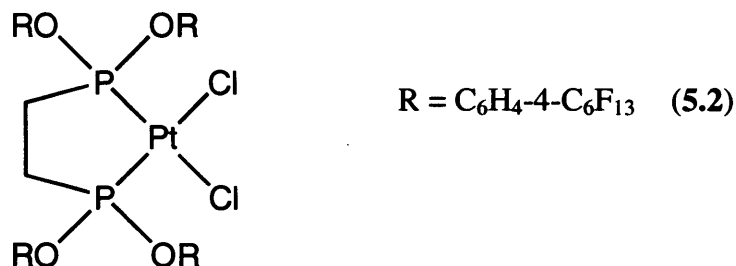
The reaction of (5.1) with [\{Rh(η^2-C$_2$H$_4$)$_2$(μ-Cl)\}$_2$] was undertaken to investigate whether the diphosphonite was sufficiently fluorophilic to render a rhodium complex soluble in perfluorinated solvents. A clear solution of (5.1) in dichloromethane was added, via canular, to an orange solution of [Rh(η^2-C$_2$H$_4$)$_2$Cl]$_2$ in dichloromethane. A rapid colour change from orange to yellow was observed, accompanied by mild effervescence, indicating the release of ethene gas. The reaction product immediately crashed out of solution as a yellow oil which stuck to the walls of the reaction vessel. The solvent was decanted and the crude product recrystallized from diethyl ether to afford the binuclear complex [Rh$_2$(μ-Cl)$_2$\{(C$_6$F$_{13}$-4-C$_6$H$_4$O)$_2$PC$_2$H$_4$P(OC$_6$H$_4$-4-C$_6$F$_{13}$)$_2$\}$_2$] (5.3) as a yellow, crystalline solid. The ^{1}H and ^{19}F\{^{1}H\} NMR spectra are uninformative as they are essentially the same as those for the free ligand. The ^{31}P\{^{1}H\} NMR spectrum exhibits a doublet at 190 δ with $^1J_{Rh-P}$ coupling of 265 Hz which is comparable to the $^1J_{Rh-P}$ coupling of 256 Hz for the binuclear rhodium hydride complex [Rh$_2$(μ-H)$_2$\{(Pr^{i}O)$_2$PC$_2$H$_4$P(OPr^i)$_2$\}$_2$].[12] The complex was found to have low solubility in organic solvents such as dichloromethane as well as PP3. In common with binuclear rhodium chloride complexes of the aryl phosphites, good solubility in diethyl ether was observed for (5.3).

$$R = C_6H_4\text{-}4\text{-}C_6F_{13} \quad (5.3)$$
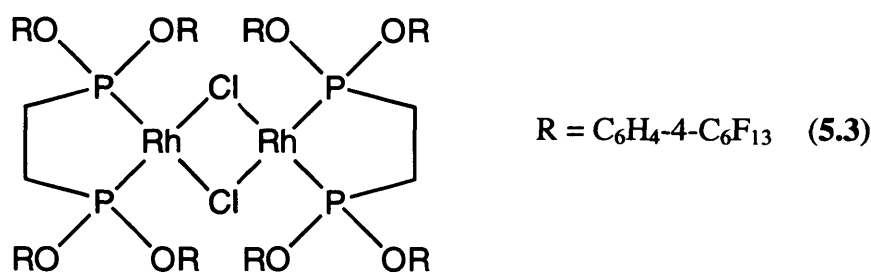
The poor solubility of complex (5.3) in PP3 can be attributed to their being only two perfluoroalkyl groups per phosphorus atom in the diphosphinite ligand, and the presence of a carbon backbone. The fluorous character of the diphosphonite is, therefore, lower than that for the alkyl and aryl phosphites, and is not sufficient to render complexes preferentially soluble in perfluorinated solvents. To overcome the problems of low fluorous solubility associated with the diphosphonite (5.3) and potentially increase the stability of the ligand towards hydrolysis, an investigation into ligands with bisphosphite architecture was undertaken.

5.3 Synthesis of a Catechol Derived Bisphosphite Ligand

Bisphosphites are readily prepared by the reaction of diols with phosphorus trichloride using similar experimental procedures to those employed in the synthesis of monodentate phosphites.[13] In order to render the bisphosphite fluorous soluble it would need to be derivatised with perfluoroalkyl substituents which would be introduced into the diol using the same copper-mediated cross-coupling reaction used in the synthesis of the perfluoroalkyl derivatised phenols. It was, therefore, necessary to obtain a diol bearing iodine substituents which could be substituted for perfluorohexyl chains. The organic bulk of the diol and the number of perfluoroalkyl groups with which it should be functionalised was an obvious consideration. In order to ensure fluorous solubility, the bisphosphite ligand would be required to have similar fluorous character to the monodentate phosphites. The diol would, therefore, need to be functionalised with a minimum of two perfluorohexyl substituents.

1,2-Dihydroxybenzene was chosen as the starting diol as it was believed that functionalisation in the 4,5 positions with perfluoroalkyl chains would render the compound fluorous soluble. It was also believed that functionalisation in the 4,5 positions of the ring would minimise the steric impact of the perfluoroalkyl substituents in the resulting bisphosphite. Due to the lack of commercially available 1,2-dihydroxy-4,5-diiodobenzene, it was necessary to selectively iodinate 1,2-dihydroxybenzene in the 4,5 positions. Iodine is usually the least reactive halogen in aromatic substitution with reversibility between iodine and the hydrogen iodide liberated during the reaction being of such significance that it necessitates the presence of a suitable species to remove the hydrogen iodide as soon as it forms. A variety of oxidising agents such as HgO, HNO_3, HIO_3 and H_2O_2 have been used for this purpose. Other reagents applied to aromatic iodination include iodine-copper(II) chloride,[14] iodine monochloride,[15] and benzyltrimethylammonium dichloroiodate.[16] The mercury(II) oxide-iodine system has been found to selectively iodinate alkyl aryl ethers, although the reaction is dependent on the presence of electron donating groups to activate the ring.[17] This system was found to selectively iodinate 1,2-methylenedioxybenzene in the 4,5 positions and was, therefore, chosen as the synthetic route to the proposed perfluoroalkylated diol as the methylene bridge could be cleaved to yield the dihydroxy species.

The iodination of 1,2-methylenedioxy-4,5-diiodobenzene with mercury(II) oxide and iodine in dichloromethane was carried out according to a modified literature procedure (Scheme 5.1).[17] The crude reaction product was found to be a mixture of 1,2-methylenedioxy-4-iodobenzene (5.4) and 1,2-methylenedioxy-4,5-diiodobenzene (5.5) as evidenced by the ^{1}H NMR spectrum. The monoiodinated species was separated as a red liquid by heating in a Kugelröhr apparatus at 60 °C under dynamic vacuum (0.01 mmHg) to leave the impure diiodinated compound as a red crystalline solid. The remaining solid was recrystallised from methanol to afford 1,2-methylenedioxy-4,5-diiodobenzene in low yield as a cream coloured solid. The ^{1}H NMR spectrum of (5.5) exhibits a singlet at 7.2 δ assigned to the aryl protons and a second singlet at 5.9 δ of the same integration, assigned to the protons of the methylene bridge. This is supported by the EI mass spectrum of (5.5) which exhibits a characteristic peak for the parent ion at m/z = 374.
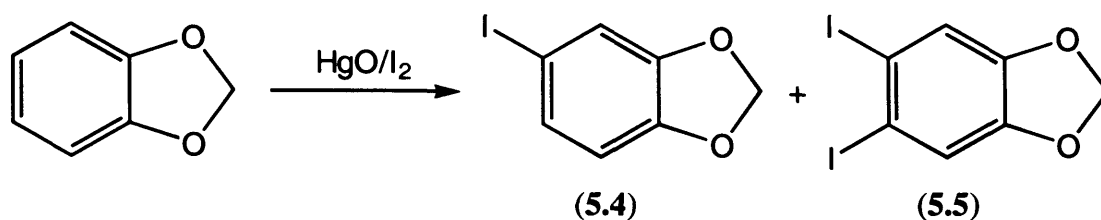
Scheme 5.1   Reaction of 1,2-methylenedioxybenzene with mercury(II) oxide-iodine.

The reaction of (5.5) with perfluoro-n-hexyl iodide was carried out under the same conditions used for the preparation of the perfluoroalkylated phenols (Scheme 5.2). The ^{1}H NMR spectrum of the crude product showed it to be a mixture of 1,2-methylenedioxy-4-perfluoro-n-hexylbenzene (5.6) and 1,2-methylenedioxy-4,5-bis(perfluoro-n-hexyl)benzene (5.7). The formation of the mono-substituted species (5.6), in which an iodine has been replaced by a proton, suggests that the introduction of a second perfluoroalkyl group is sterically hindered. The copper intermediate which is formed during the reaction (see Chapter 2) is therefore hydrolysed during the aqueous work-up and results in the substitution of the iodine with a proton. The mono- and di-substituted products were separated by distillation on Kugelröhr apparatus and isolated as clear, colourless oils.
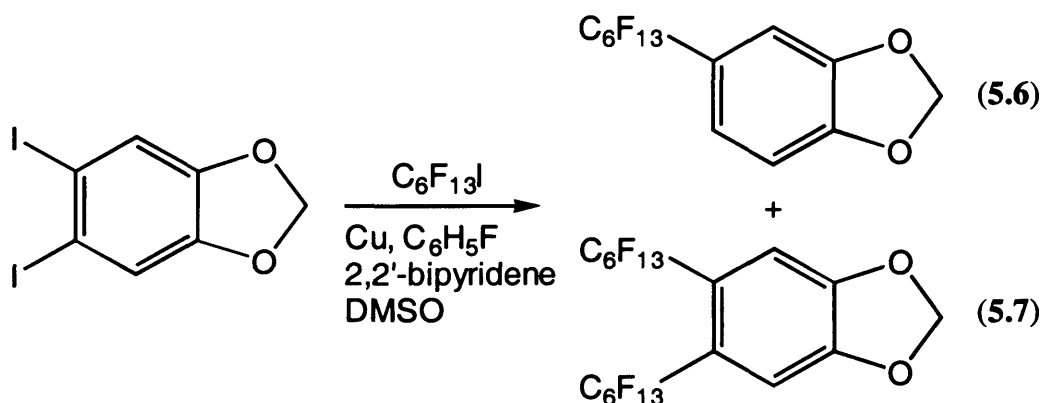
Scheme 5.2   Copper-coupling reaction of 1,2-methylenedioxy-4,5-diiodobenzene with perfluoro-n-hexyl iodide.

The ^{1}H NMR spectrum of (5.7) is essentially the same as that for 1,2-methylenedioxy-4,5-diiodobenzene exhibiting singlet resonances at 7.1 δ assigned to the aryl protons and at 6.1 δ assigned to the methylene bridge. The ^{19}F{^{1}H} NMR spectrum exhibits the six multiplet resonances typical of the perfluoro-n-hexyl groups, however, the

resonance associated with the $^{\alpha}CF_2$ groups of the perfluoroalkyl chains occurs at -103 δ as compared to -113 δ for the $^{\alpha}CF_2$ group of the derivatised phenol.

In order to obtain the dihydroxy derivative, it was necessary to cleave the methylene bridge of 1,2-methylenedioxy-4,5-bis(perfluoro-n-hexyl)benzene. The reagent used initially for this reaction was boron trichloride, which has been used extensively as a reagent for the cleavage of ethers, acetals and esters.[18,19] The reaction of (5.7) with BCl_3 in dichloromethane was found to give a low conversion to the dihydroxy species, which was not significantly improved by refluxing the reaction mixture. Subsequent use of the stronger Lewis acid, boron triiodide[20] gave almost quantitative conversion to 1,2-dihydroxy-4,5-bis(perfluoro-n-hexyl)benzene (5.8) as evidenced by the ^1H NMR spectrum which exhibits a singlet at 7.2 δ assigned to the aryl protons, and a broad singlet at 6.2 δ corresponding to the hydroxy protons.

C_6F_{13} \ OH

C_6F_{13} / OH

(5.8)
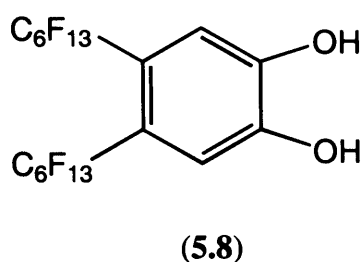
In an attempt to synthesise the bisphosphite ligand (5.9), 1,2-dihydroxy-4,5-bis(perfluoro-n-hexyl)benzene was allowed to react with PCl_3 in the presence of triethylamine. As for the preparation of the monodentate phosphites, scrupulously anhydrous conditions were maintained throughout. A white precipitate of $Et_3NH^+Cl^-$ was obtained immediately on addition of the diol to the solution of PCl_3 and Et_3N, providing an indication that a reaction with PCl_3 was occurring, and P-O bonds were being formed. The reaction mixture was filtered and the solvent removed *in vacuo* to yield the crude product as a colourless, viscous oil. The reaction product was found to be virtually insoluble in toluene, unlike the alkyl and aryl phosphites, which would be expected for the bisphosphite as a result of the high number of perfluoroalkyl groups. The solubility in deuterated dichloromethane was sufficient to obtain the $^{31}P\{^1H\}$ NMR spectrum which exhibits a singlet at 151 δ and several minor singlets below 12 δ. The chemical shift of the high frequency singlet is typical of bisphosphites, and

close to the literature value of 140 δ for the analogous catechol derived bisphosphite.[21] The smaller singlet resonances below 12 δ are likely to be due to hydrolysis products, having similar chemical shifts to the hydrolysis products of the monodentate phosphites. The ^{1}H NMR spectrum of the crude product exhibits multiple resonances in the aryl region, indicating a mixture of products, consistent with the ^{31}P{^{1}H} NMR spectrum. The FAB mass spectrum of the mixture, however, provides no evidence for the formation of the bisphosphite ligand.
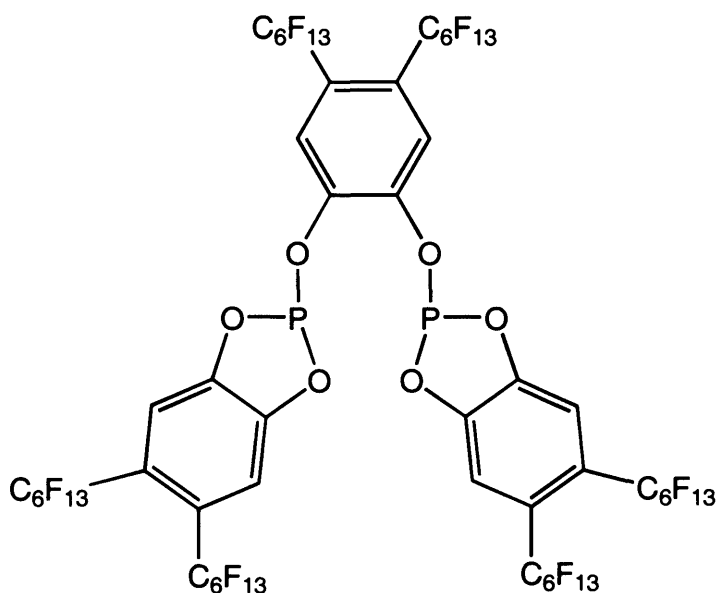
(5.9)

An attempt to isolate the species giving rise to the singlet at 151 δ in the ^{31}P{^{1}H} NMR spectrum by Kugelröhr distillation was ineffective and resulted in complete decomposition of the product. The reaction was repeated, although again it was not possible to isolate and fully characterise the main reaction product. A major problem with synthesising the bisphosphite based on the 1,2-dihydroxy-4,5-bis(perfluoro-n-hexyl)benzene derivative was the difficulty associated with the purification of the diol and its precursors, and the subsequently low yields. It is unclear whether the bisphosphite (5.9) had indeed been prepared. In view of the electronic influence of one perfluoroalkyl tail per ring on the derivatised phosphite ligand (2.4), it is possible that the introduction of two tails per ring had too large an electronic influence for (5.9) to be prepared and isolated. It was, therefore, decided

that another approach to preparing a fluorous soluble bisphosphite would be made, using a fluorous soluble 2,2'-biphenol derivative.

5.4 Synthesis of a Biphenol Derived Bisphosphite Ligand

In order to prepare the fluorous soluble phosphite it was first necessary to synthesise a derivative of 2,2'-biphenol with perfluoroalkyl substituents. The oxidative coupling of phenolic compounds using a variety of reagents has been widely studied owing to its utility as a synthetic reaction.[22] An attempt was therefore made to prepare 5,5'-bis(perfluoro-n-hexyl)-2,2'-biphenol by the oxidative coupling of 4-perfluoro-n-hexylphenol using vanadium oxytrifluoride[23] (Scheme 5.3). Analysis of the crude product by ^{1}H NMR and EI mass spectroscopy indicated that selective phenolic coupling in the *ortho* position had occurred, although a low yield was obtained (<10%). It was, therefore, decided to attempt to incorporate the perfluoroalkyl groups into 2,2'-biphenol using the same copper-coupling methodology used in the synthesis of the perfluoroalkylated phenols.
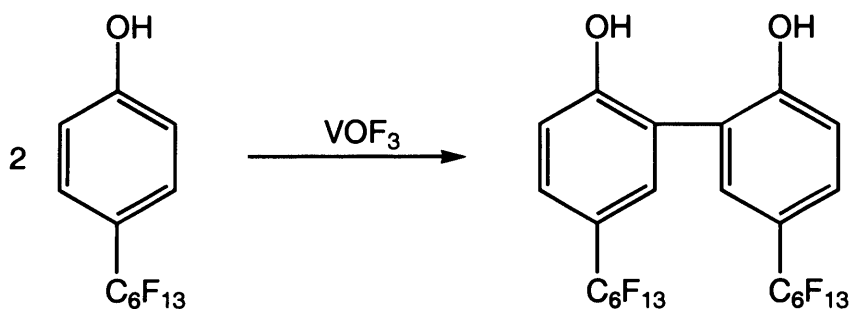
Scheme 5.3 Oxidative coupling of 4-perfluoro-n-hexylphenol using VOF$_3$.

2,2'-biphenol was brominated selectively in the 5,5' positions by the addition of neat bromine to a solution of 2,2'-biphenol in chloroform to yield 5,5'-dibromo-2,2'-biphenol. The initial copper-coupling reaction of perfluoro-n-hexyliodide with 5,5'-dibromo-2,2'-biphenol gave an unexpectedly complex, intractable mixture of products. It was thought that the majority of products were associated with oxidation of the biphenol to give quinones, which would be exacerbated by the inclusion of

perfluoroalkyl substituents. To prevent these undesired reactions occurring the hydroxyl groups of the biphenol were protected by conversion to acetoxy groups to give 5,5'-dibromo-2,2'-diacetoxybiphenyl (5.10). The copper-mediated cross-coupling reaction of perfluoro-*n*-hexyliodide with the protected biphenol gave 5,5'-bis(perfluoro-*n*-hexyl)-2,2'-diacetoxybiphenyl (5.11) with no trace of the previous oxidation products (Scheme 5.4). The ^{1}H NMR spectrum of the coupled product exhibits a doublet of doublets at 7.6 δ assigned to aryl protons *meta* to the acetoxy groups, a doublet at 7.5 δ assigned to the aryl protons adjacent to the C-C bond between the two phenyl rings, and a doublet of doublets at 7.3 δ assigned to the aryl protons *ortho* to the acetoxy groups. The spectrum also exhibits a singlet at 2.0 δ assigned to the methyl protons of the acetoxy protecting groups. As expected, the ^{19}F{^{1}H} NMR spectrum is almost identical to that obtained for 4-perfluoro-*n*-hexyl phenol.
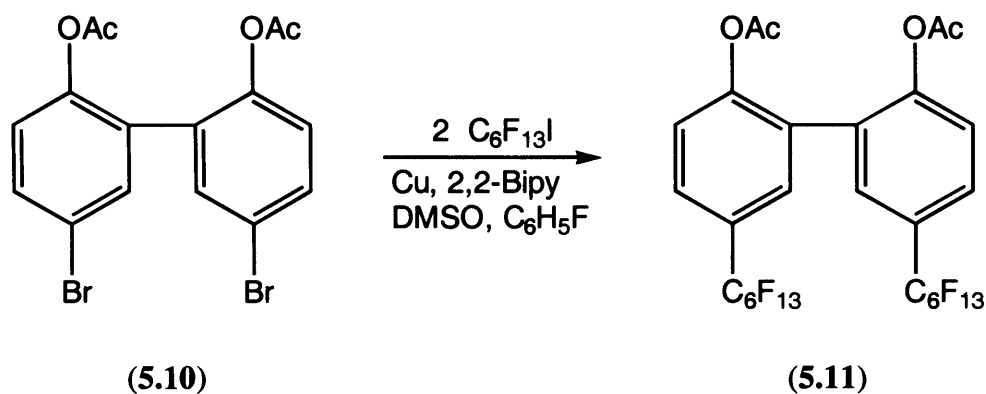
Scheme 5.4 Copper-coupling of 5,5'-dibromo-2,2'-diacetoxybiphenyl and $C_6F_{13}I$.

The initial attempt at cleaving the acetoxy protecting groups using sodium methoxide in methanol resulted in a complex mixture of products which could not be separated. The protecting groups were subsequently cleaved by sodium methoxide generated *in situ* by the addition of sodium hydride to a solution of (5.11) in methanol. The reaction mixture was quenched by the addition of HCl and extracted with PP3 to afford 5,5'-bis(perfluoro-*n*-hexyl)-2,2'-biphenol (5.12) which was recrystallized from dichloromethane. Evidence for the formation of the biphenol is provided by the ^{1}H NMR spectrum which exhibits a broad singlet at 4.8 δ assigned to the deprotected

hydroxyl groups. The NMR data is consistent with the EI mass spectrum of (5.12) which exhibits characteristic peaks for the parent ion at m/z = 822.

The synthesis of the bisphosphite ligand (5.13) was attempted by the addition of a solution of 5,5'-bis(perfluoro-n-hexyl)-2,2'-biphenol to a solution of PCl_3 and triethylamine in Et_2O. The reaction mixture was filtered and the solvent removed *in vacuo* to yield the crude product as an air- and moisture-sensitive, off-white solid. The crude product was found to have a low solubility in organic solvents such as dichloromethane and toluene, although good solubility in Et_2O was observed.

(5.13)
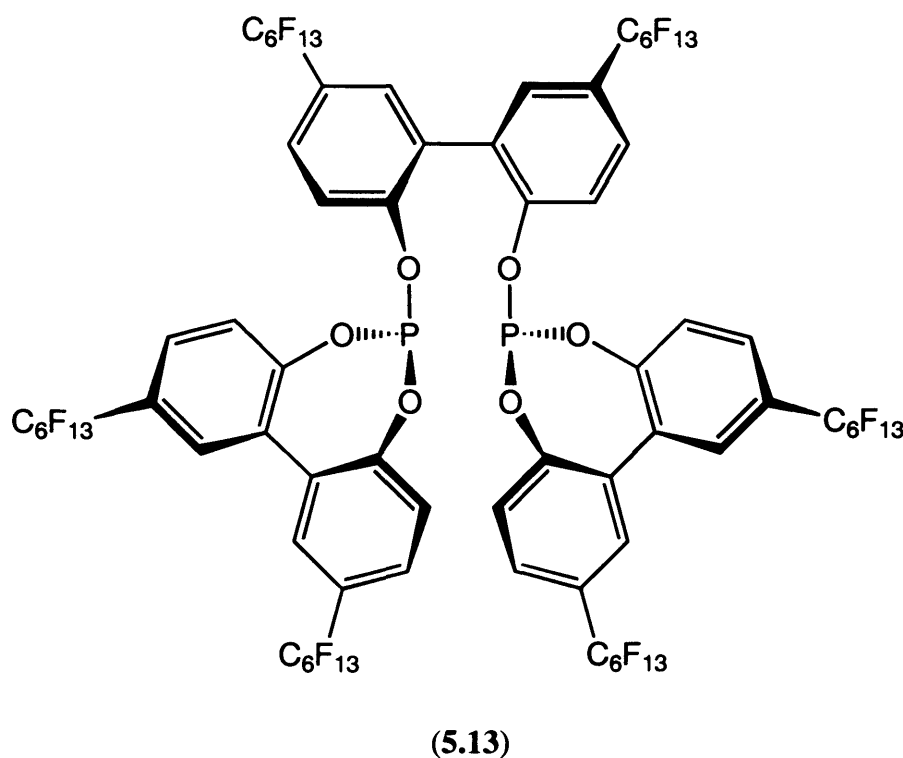
The $^{31}P\{^1H\}$ NMR spectrum of the crude product shown in Figure 5.1 exhibits a broad resonance with shoulders at *ca.* 146.0 δ in the region expected for a bisphosphite.[24] The ^1H NMR spectrum is highly complex, exhibiting a highly complex multiplet at 7.7-6.9 δ assigned to the protons of the biphenyl rings. The $^{19}F\{^1H\}$ NMR spectrum is similar to that for 5,5'-bis(perfluoro-n-hexyl)-2,2'-biphenol with additional multiplet resonances at *ca.* 109 δ and 122 δ assigned to the $^\alpha CF_2$ and $^\beta CF_2$ groups of the perfluoroalkyl chains. The broadness of the resonance observed in the $^{31}P\{^1H\}$ NMR spectrum and the evidence of shoulder peaks suggests that the crude product is composed of several species. The mass spectrum obtained for the

crude product is uninformative with no sign of peaks characteristic of the parent ion of (5.13), only showing peaks associated with the derivatised biphenol.
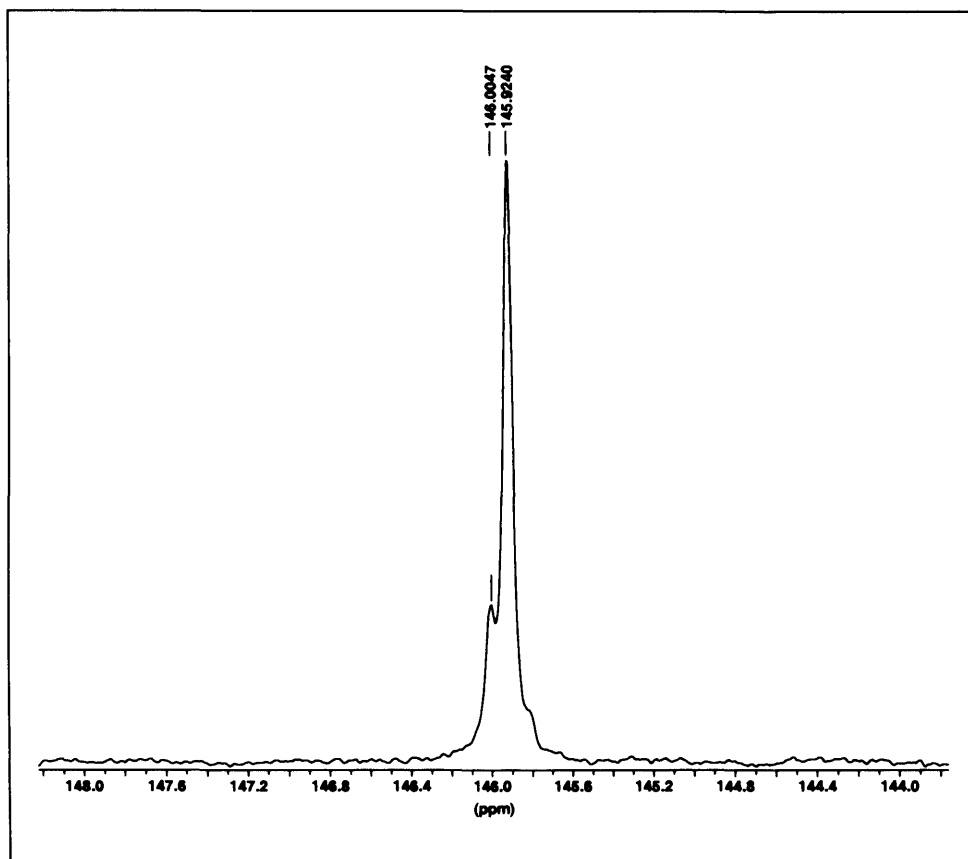
Figure 5.1 ^{31}P{^{1}H} NMR spectrum of tris(5,5'-perfluoro-n-hexyl-2,2'-biphenyl) bisphosphite (5.13).

The non-perfluoroalkylated analogue of (5.13), reported by Baker and Pringle, has been prepared by the reaction of 2,2-biphenol with PCl_3.[25] The crystal structure of the bisphosphite indicates that the dibenzo[d,f][1,3,2]dioxaphosphepin moieties (Figure 5.2) are stereogenic as a consequence of torsion about the C-C bond connecting the two aryl groups. The bisphosphite, therefore, has three possible diastereoisomeric forms, which differ in the absolute configuration of the biphenyl groups. Baker and Pringle observed a single resonance at 144.6 δ in the ^{31}P NMR of the bisphosphite, obtained at room temperature, which was attributed to the existence of a single diastereoisomer.[27] Whiteker and co-workers have investigated the interconversion of diastereoisomeric bisphosphite ligands similar to (5.13) by the

atropisomerisation of dibenzo[d,f][1,3,2]dioxaphosphepin moieties (Figure 5.2).[26] This group studied a bisphosphite ligand containing two dibenzo[d,f][1,3,2]dioxaphosphepin groups bridged by a *neo*-pentyl group by variable temperature NMR. The ^{1}H NMR spectrum of the ligand at 25 °C exhibits a single resonance for the methyl groups of the *neo*-pentyl bridge at 0.8 δ. Upon cooling to -90 °C, the spectrum exhibits three broadened methyl resonances at *ca.* 0.7 δ due to the interconversion of diastereoisomeric forms of the bisphosphite by biphenyl epimerisation. The ^{31}P{^{1}H} NMR spectra, however, was found to be insensitive to atropisomerism, exhibiting a single resonance between -100 and 25 °C.
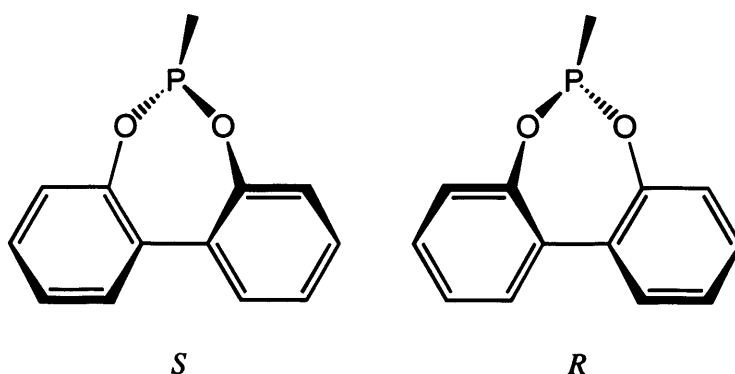
Figure 5.2 Atropisomerism in dibenzo[d,f][1,3,2]dioxaphosphepins.

The NMR spectral data obtained for the crude product from the reaction of 5,5'-bis(perfluoro-*n*-hexyl)-2,2'-biphenol with PCl$_3$ is consistent with the formation of diastereoisomers of bisphosphite (5.13). The bulky perfluoroalkyl groups in the 5,5'-positions of the biphenyl rings may hinder rotation about the C-C bonds connecting the phenyl rings making rotation slow on the NMR timescale. Despite storing the crude product in a dry-box under nitrogen atmosphere it decomposed over several days to give a viscous, pale orange oil. The ^{31}P{^{1}H} NMR spectrum of the oil showed multiple resonances below 2 δ assigned to decomposition products with no resonances at *ca.* 146 δ. The reason for decomposition of the product is unclear, although it was believed that the biphenol may not have been completely dry, as phenols are known to be highly hygroscopic. The synthesis of the bisphosphite ligand was, therefore, repeated using 5,5'-bis(perfluoro-*n*-hexyl)-2,2'-biphenol which had been

azeotropically distilled with dry toluene. The $^{31}P\{^1H\}$ NMR of the crude product was found to be identical to that obtained for the product of the first reaction (Figure 5.1), consistent with the formation of diastereoisomers of (5.13). Surprisingly, despite the scrupulously anhydrous conditions, decomposition of the crude product was again observed, thereby preventing the low temperature $^{31}P\{^1H\}$ NMR spectra of the product from being obtained. To determine whether there was an intrinsic problem with the derivatised biphenol the reaction with 1,2-bis(dichlorophosphino)ethane was investigated.

5.5 Synthesis of a Biphenol Derived Bisphosphonite

The reaction of 5,5'-bis(perfluoro-*n*-hexyl)-2,2'-biphenol with 1,2-bis(dichlorophosphino)ethane afforded the bisphosphonite ligand (5.14) as a white crystalline solid. The ^1H NMR spectrum of the ligand is almost identical to that of the biphenol with the exception of a triplet at 1.65 δ assigned to the protons of the ethyl bridge which exhibits J_{P-H} coupling of 6.8 Hz. The $^{31}P\{^1H\}$ NMR spectrum exhibits a singlet at 216 δ which on proton coupling is observed as a quintet due to coupling of the phosphorus nuclei with the protons of the ethyl bridge. Unlike the bisphosphite (5.13) the bisphosphonite (5.14) showed no sign of decomposition when stored in a dry-box under nitrogen.

(5.14)
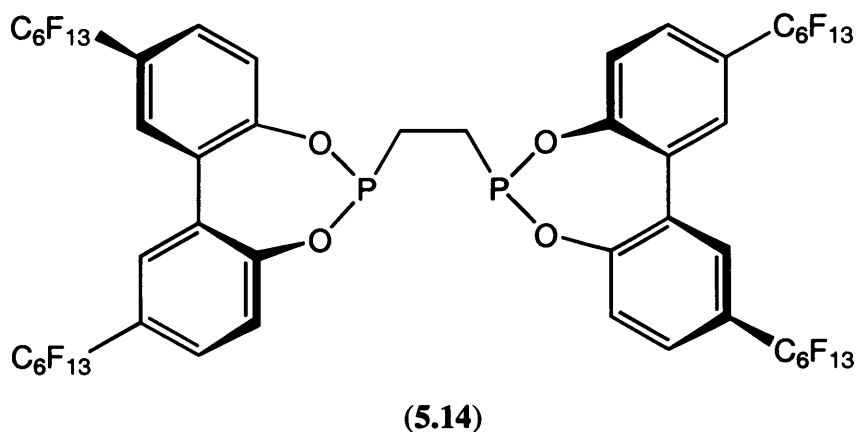
Ligand (5.14) was allowed to react with [{Rh(η^2-C$_2$H$_4$)$_2$(μ-Cl)}$_2$] in dichloromethane to determine if the coordination chemistry of the bisphosphonite prepared from 5,5'-bis(perfluoro-n-hexyl)-2,2'-biphenol was similar to that observed for the bisphosphonite (5.1) prepared from 4-perfluoro-n-hexyl phenol. The yellow reaction mixture was filtered and the solvent removed *in vacuo* to afford the dinuclear rhodium species (5.15). The rhodium complex exhibits similarly low solubility to complex (5.3) in organic solvents with the exception of Et$_2$O and increased solubility in PP3. The improved solubility of (5.15) is attributed to the fewer protons of the biphenol derived bisphosphonite. The ^{31}P{^{1}H} NMR spectrum of the complex exhibits a doublet at 212 δ with a $^1J_{Rh-P}$ coupling constant of 276 Hz. The chemical shift of the doublet resonance for complex (5.15) is 21 δ to higher frequency than that for complex (5.3), indicating that the phosphorus nuclei are deshielded due to their incorporation into a seven membered ring present in the dibenzo[d,f][1,3,2]dioxaphosphepin moiety.

PR =

(5.15)
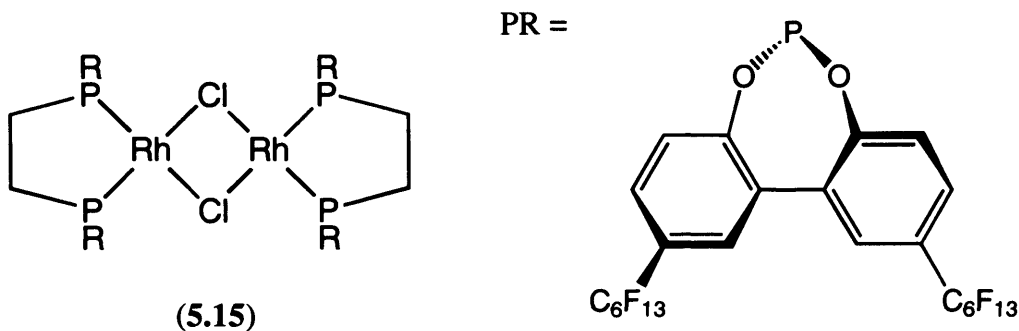
5.6 Conclusion

It can be concluded from the work described in this chapter that the chemical behaviour and reactivity of the chelating bisphosphonite (5.1) is similar to that of the protio analogue dpope. The inclusion of the alkyl bridging unit results in the ligand having lower fluorous character in comparison to the phosphite ligand (2.4) and subsequently lower solubility in perfluorinated solvents. The partitioning between the fluorous and organic phases is accentuated by the coordination of the ligand with the rhodium complex [Rh(η^2-C$_2$H$_4$)$_2$Cl]$_2$. The resulting rhodium complex (5.3) was found

to have poor solubility in fluorous media due to an insufficient number of perfluoro-*n*-hexyl substituents. However, the fluorous character of the complex is sufficient to afford only limited solubility in organic solvents such as dichloromethane. In comparison, the analogous rhodium complex (3.40) containing the derivatised-phosphite exhibits preferential fluorous solubility.

The attempted preparation of bisphosphite ligands bearing perfluoro-*n*-hexyl substituents has revealed that the chemical behaviour and reactivity of 1,2-dihydroxy-4,5-bis(perfluoro-*n*-hexyl)benzene (5.8) and 5,5'-bis(perfluoro-*n*-hexyl)-2,2'-biphenol (5.12) differs significantly from that of their protio analogues. The physical properties of the diols are also significantly modified by the introduction of the perfluoroalkyl substituents. Diol (5.8) was found to be a sticky, viscous oil, thereby making it more difficult to handle than its protio analogue 1,2-dihydroxybenzene which is a crystalline solid. As expected, the solubilities of the diols are greatly changed by the incorporation of the perfluoroalkyl substituents, giving rise to preferential solubility in perfluorinated solvents.

The difficulty in preparing/isolating the bisphosphite ligands (5.9) and (5.13) may be a result of the electronic effects of the perfluorinated chains. As discussed in chapter 2, the introduction of the fluorous chains into phosphite ligands results in a dramatic increase in the hydrolytic sensitivity. The introduction of two tails per aryl ring in the case of bisphosphite (5.9) may, therefore, have resulted in too large an electronic influence to allow for the preparation and/or isolation of the ligand. In the case of diol (5.12) there is only one fluorous chain per aryl ring, therefore, the electronic effect of the perfluoroalkyl groups should be similar to that observed for the monodentate ligands. The $^{31}P\{^{1}H\}$ NMR of the crude product from the reaction of 5,5'-bis(perfluoro-*n*-hexyl)-2,2'-biphenol with PCl₃ is consistent with the formation of diastereomers of bisphosphite (5.13). It is unclear why decomposition of the products of this reaction occurred, considering the ease with which the bisphosphonite (5.14) was prepared, although it is likely that both steric and electronic effects arising from the introduction of the perfluoroalkyl chains into the biphenyl groups are responsible. Unfortunately, time limitations prevented a more in-depth analysis of this ligand system, which could prove to be a useful modifying ligand for the rhodium catalysed fluorous biphase hydroformylation of alkenes. It can be concluded from the work discussed in this chapter that potentially fluorous soluble bidentate phosphonite

ligands can be readily prepared by the reaction of bidentate chlorophosphines with phenols or diols bearing perfluoroalkyl substituents. The difficulty in preparing and handling fluorous soluble bisphosphite ligands reiterates the dramatic steric and electronic influence the introduction of perfluoroalkyl substituents can have on ligands and their metal complexes.

References for Chapter Five

[1]   L. H. Pignolet, *Homogeneous Catalysis with Metal Phosphine Complexes*, Plenum, New York, 1983.

[2]   A. Castellanos, S. Castillón, C. Claver, A. M. Masdeu-Bultó and A. Orejon, *Tetrahedron: Asymmetry*, 1996, **7**, 1834.

[3]   B. M. Trost, B. A. Vos, C. M. Brzezowski and D. P. Martina, *Tetrahedron Lett.*, 1992, **33**, 717.

[4]   D. J. Wink, T. J. Kwok and A. Yee, *Inorg Chem.*, 1990, **29**, 5006.

[5]   E. Billig, A. G. Abatjoglou and D. R. Bryant, *U.S. Pat.*, 4, 769, 498, 1988.

[6]   J. E. Babin and G. T. Whiteker, *U.S. Pat.*, 5, 360, 938, 1994.

[7]   R. J. Puddephatt, *Chem. Soc. Rev.*, 1983, 99.

[8]   *Applied Homogeneous Catalysis with Organometallic Compounds*, Vol. 1, Eds. B. Cornils and W. A. Herrmann, VCH Publishers, New York, 1996.

[9]   E. H. Mottus and M. R. Ort, *J. Organomet. Chem.*, 1973, **50**, 47.

[10]   J. Chatt, W. Hussain, G. J. Leigh, H. Mohd-Ali, C. J. Pickett and D. A. Rankin, *J. Chem. Soc. Dalton Trans.*, 1985, 1131.

[11]   I. R. Jobe, L. Manojlovic-Muir, B. J. Maya and R. J. Puddephatt, *J. Chem. Soc. Dalton Trans.*, 1987, 2117.

[12]   M. D. Fryzuk, *Can. J. Chem.*, 1983, **61**, 1347.

[13]   G. Märkl and W. Burger, *Tetrahedron Lett.*, 1983, **24**, 2545.

[14]   W. C. Baird. Jr. and J. H. Surridge, *J. Org. Chem.*, 1970, **35**, 3436.

[15]   D. A. Whiting, *Comprehensive Organic Chemistry*, Ed. by J. F. Stoddart, Pergamon Press, Oxford, 1979.

[16]   S. Kajigaeshi, T. Kakinami, H. Yamasaki, S. Fujisaki, M. Kondo and T. Okamoto, *Chem. Lett.*, 1987, 2109.

[17]   T. Hatakeyama, K. Orito, H. Suginome and M. Takeo, *Synthesis*, 1995, 1277.

[18]   A. Brossi, J. O'Brien and S. Teitel, *J. Org. Chem.*, 1972, **37**, 3368.

[19]   M. V. Bhatt and S. U. Kulkarni, *Synthesis*, 1983, 249.

[20]   J. M. Lansinger and R. C. Ronald, *Synth. Commun.*, 1979, **9**, 341.

[21]   H. M. Buck, R. J. M. Hermans and J. J. C. Van Lier, *Phosphorus and Sulfur*, 1984, **19**, 173.

[22]   W. L. Carrick, G. L. Karapinka and G. T. Kwiatkowski, *J. Org. Chem.*, 1969, **34**, 2388.

[23]   A. G. Brown and P. D. Edwards, *Tetrahedron Lett.*, 1990, **31**, 6581.

[24]   F. H. Clarke, A. D. Debellis, S. D. Pastor, R. K. Rodebaugh and S. P. Shum, *Helv. Chim. Acta,* 1993, **76**, 900.

[25]   M. J. Baker and P. G. Pringle, *J. Chem. Soc., Chem. Commun.,* 1991, 1292.

[26]   A. G. Abatjoglou, A. M. Harrison and G. T. Whiteker, *J. Chem. Soc., Chem. Commun.,* 1995, 1805.

Chapter Six

6.1 General Experimental Details

6.1.1 NMR Spectroscopy

^{1}H, ^{19}F{^{1}H}, ^{31}P{^{1}H}, and ^{13}C{^{1}H} NMR spectra were recorded at the ambient temperature of the probe unless otherwise stated using deuterated solvents to provide the field/frequency lock. ^{1}H NMR spectra were referenced internally using the residual protio solvent resonance relative to TMS (δ = 0 ppm). ^{19}F{^{1}H} NMR spectra were referenced externally to $CFCl_3$ (δ = 0 ppm). ^{31}P NMR were referenced externally to 85% H_3PO_4 (δ = 0 ppm). All chemical shifts are quoted in δ (ppm) and coupling constants in Hz using the high-frequency positive convention. NMR spectra were recorded on the following spectrometers:

^{1}H NMR spectra; Bruker ARX 250 spectrometer at 250.13 MHz, Bruker AM 300 at 301.37 MHz and Bruker DRX 400 at 400.13 Hz.

^{19}F{^{1}H} NMR spectra; Bruker ARX 250 spectrometer at 235.36 MHz, Bruker AM300 at 283.54 MHz and Bruker DRX 400 at 376.50 MHz.

^{31}P{^{1}H} NMR spectra; Bruker ARX 250 spectrometer at 250.13 MHz, Bruker AM300 at 301.37 MHz and Bruker DRX 400 at 161.98 MHz.

^{13}C{^{1}H} NMR spectra; Bruker AM 300 spectrometer at 301.37 MHz.

NMR samples of air sensitive species were prepared under inert atmosphere in a dry-box and the spectra run using a 5 mm NMR tube fitted with a Youngs' tap. Samples which were insoluble in deuterated solvents were run in a 4 mm tube inserted into a 5 mm tube containing D_2O as the lock solvent or in a 5 mm tube containing a sealed capillary tube containing C_6D_6 as the lock solvent.

6.1.2 Mass Spectrometry

Electron impact (EI) and fast atom bombardment (FAB) mass spectra were recorded on a Kratos Concept 1H mass spectrometer. Mass spectra were obtained in positive-ion mode with 3-nitrobenzyl alcohol used as the matrix for the FAB spectra.

6.1.3 IR spectroscopy

IR spectra were recorded as Nujol mulls between KBr plates on a Digilab FTS40 Fourier transform spectrometer. Far IR spectra recorded below 500 cm^{-1} were recorded as Nujol mulls between polythene plates. Solution spectra were recorded in degassed dichloromethane or PP3 solutions held in an IR solution cell with a volume of 0.2 cm^3 with KBr windows. All spectra were obtained using 64 scans at a resolution of 2 cm^{-1}.

6.1.4 Elemental Analysis

Elemental analyses were performed by Butterworth Laboratories Ltd. using the following instruments: Carbon, Hydrogen and Nitrogen – PE 2400; Phosphorus – Leeman 440; Chlorine – Leco 932. Analysis for fluorine was found, in many cases, to be inaccurate and has therefore not been included. Satisfactory elemental analyses for several compounds could not be obtained due to incomplete combustion of the sample as a result of their high fluorine content. Where applicable, accurate mass spectroscopy has been used as a replacement to elemental analysis.

6.1.5 X-Ray Crystallography

Crystal structure determinations were performed by Dr. J. Fawcett and Dr. D. R. Russell. X-Ray crystallographic data was collected on a Siemens P4 four circle diffractometer using a Mo Kα radiation source (λ = 0.71073 Å). The crystallographic data and numerical results for the structural determinations reported in this thesis are given in the appendix.

6.2 Anhydrous Solvents

Where dried and degassed solvents were required they were prepared and stored as follows. Dichloromethane, chloroform, and PP3 were dried by refluxing over calcium hydride, under nitrogen for 3 days and transferred under nitrogen to a closed ampoule,

stored over 4Å molecular sieves and freeze/pump/thaw degassed prior to use. Toluene and diethyl ether were dried by refluxing over sodium metal, under nitrogen for 3 days and transferred to a sealed ampoule under nitrogen, stored over 4Å molecular sieves and freeze/pump/thaw degassed prior to use. Hexane and THF were dried by refluxing over potassium metal, under nitrogen for 3 days and transferred to a sealed ampoule under nitrogen, stored over 4Å molecular sieves and freeze/pump/thaw degassed prior to use.

6.3 Experimental Materials

All chemicals, unless otherwise stated, were purchased from Aldrich Chemical Co. and used as supplied. Triethylamine was purified by distillation and stored over CaH_2. PCl_3, $PhPCl_2$, and Ph_2PCl were refluxed under nitrogen to remove traces of HCl, distilled and stored under nitrogen. Perfluoro-n-hexyl iodide, perfluoro-n-octyl iodide and perfluoro-n-decyl iodide were purchased from Fluorochem Ltd. and distilled prior to use. 1H,1H,2H,2H-Perfluoro-n-octanol was distilled and degassed prior to use.

cis-$[PtCl_2(MeCN)_2]$ was synthesised according to a literature procedure.[1]

cis-$[Pt(PEt_3)Cl]_2$ was synthesised according to a literature procedure.[2]

trans-$[PdCl_2(MeCN)_2]$ was synthesised according to a literature procedure.[1]

$[Rh(COD)Cl]_2$ was synthesised according to a literature procedure.[3]

$Ph_2P(OPh)$ was synthesised according to a literature procedure.[4]

$PhP(OPh)_2$ was synthesised according to a literature procedure.[5]

$[Rh(CO)Cl\{Ph_2P(OPh)\}_2]$ was synthesised according to a literature procedure.[6]

$[Rh(CO)Cl\{PhP(OPh)_2\}_2]$ was synthesised according to a literature procedure.[6]

6.4 Experimental Procedures

6.4.1 Schlenk Line Procedures

Due to the air and moisture sensitive nature of reagents and products involved in the synthesis of the ligands and several metal complexes, scrupulously anhydrous

conditions and equipment were maintained throughout. Synthetic procedures with these materials were carried out on a Schlenk line consisting of a glass, dual-manifold line connected at either end to a vacuum outlet and to a nitrogen source. The vacuum was provided by an NGN PSR/2 rotary pump, protected by a liquid nitrogen trap. Vacuum and nitrogen outlets and all other outlets were isolable by ground Interkey or Youngs' greaseless taps. Apparatus was connected to the Schlenk line *via* Neoprene vacuum tubing connected to the outlets.

6.4.2 Inert Atmosphere Dry-box

Air and moisture sensitive materials were manipulated under a nitrogen atmosphere with an oxygen content of less than 5 ppm using a Faircrest auto-recirculating, positive pressure dry-box. The atmosphere was maintained by circulation through columns of molecular sieves and manganese dioxide to remove water and oxygen respectively.

6.5 Synthesis of Monodentate Ligands.

6.5.1 *Preparation of 4-perfluoro-n-hexylphenol* (2.1)

$C_6F_{13}I$ (48.204 g, 110 mmol) in hexafluorobenzene (150 cm^3) was added dropwise to a stirred solution of 4-iodophenol (24.029 g, 110 mmol), copper (30.825 g, 490 mmol), 2,2-bipyridine (1.327 g, 8.5 mmol) in dimethylsulphoxide (150 cm^3) over 3 hrs. The reaction mixture was then heated at 80°C under nitrogen for 6 days. After cooling to room temperature the mixture was hydrolysed with water, filtered and the filtrate washed with dichloromethane (2 x 100 cm^3). The deep red/brown organic layer was separated, dried over MgSO$_4$ and concentrated to *ca.* 100 cm^3 *in vacuo*. The product was extracted by shaking with perfluoro-1,3-dimethylcyclohexane (8 x 20 cm^3), the washings combined and the solvent removed *in vacuo* to leave an off-white solid. The product was purified by distillation on a Kugelröhr distillation apparatus at 55 °C (0.01 mmHg) to afford pure product as a white crystalline solid. Yield 27.977 g, 63%. δ ^{1}H NMR (CDCl$_3$) 7.31 [2 H, d, *meta* OC$_6$H$_4$C$_6$F$_{13}$ ^3J(HH) 7.1 Hz], 6.92 [2 H,

d, *ortho* $OC_6H_4C_6F_{13}$ ^3J(HH) 7.1 Hz] and 5.23 [1 H, s, OH]. δ $^{19}F\{^1H\}$ NMR ($CDCl_3$) -81.26 [3 F, tt, CF_3 ^3J(FF) 2.5 Hz, ^4J(FF) 10.1 Hz], -110.15 [2 F, tm, $^\alpha CF_2$ ^4J(FF) 14.6 Hz], -121.92 [2 F, m, $^\beta CF_2$], -122.42 [2 F, m, $^\delta CF_2$], -123.24 [2 F, m, $^\epsilon CF_2$], -126.55 [2 F, m, $^\gamma CF_2$]. Electron impact (EI) mass spectrum: m/z 412 ($[M]^+$), 393 ($[M - F]^+$. (Found: M^+, 412.01327. $C_{12}H_5F_{13}O$ requires M^+, 412.01328).

6.5.2 *Preparation of 4-perfluoro-n-hexylphenyl diphenyl phosphinite* (2.2)

4-Perfluoro-*n*-hexyl phenol (2.236 g, 5.4 mmol) in dry ether (50 cm^3) was added dropwise *via* cannular to a solution of Ph_2PCl (1.082 g, 4.9 mmol) and triethylamine (0.553 g, 5.5 mmol) in dry ether (50 cm^3) over a period of 1 hr. The reaction mixture was stirred for a further 3 hrs, after which it was filtered through celite under nitrogen to remove the triethylammonium hydrochloride formed in the reaction. The solvent was removed *in vacuo* to yield the impure product as a white solid. Unreacted triethylamine and 4-perfluoro-*n*-hexyl phenol were removed on a Kugelröhr distillation apparatus at 60 °C (0.01 mmHg) to afford pure product. Yield: 1.954 g, 67%. δ ^1H NMR (d^8 toluene) 7.60 [4 H, m, *ortho* PPh], 7.26 [2 H, d, *meta* $OC_6H_4C_6F_{13}$ ^3J(HH) 8.8 Hz], 7.15 [6 H, m, *meta/para* PPh] and 7.06 [2 H, d, *ortho* $OC_6H_4C_6F_{13}$ ^3J(HH) 8.8 Hz]. δ $^{19}F\{^1H\}$ NMR (d^8 toluene) -81.43 [3 F, tt, CF_3 ^3J(FF) 2.0 Hz, ^4J(FF) 10.0 Hz], -109.93 [2 F, t, $^\alpha CF_2$ ^4J(FF) 14.5 Hz], -121.69 [2 F, m, $^\beta CF_2$], -122.00 [2 F, m, $^\delta CF_2$], -123.08 [2 F, m, $^\epsilon CF_2$], -126.50 [2 F, m, $^\gamma CF_2$]. δ $^{31}P\{^1H\}$ NMR (d^8 toluene) 112.59 [s]. Electron impact (EI) mass spectrum: m/z 596 ($[M]^+$), 519 ($[M - C_6H_5]^+$), 277 ($[M - C_6F_{13}]^+$), 185 ($[M - OC_6H_4C_6F_{13}]^+$). Found: C, 48.7; H, 2.2; P, 5.2. Calc. for $Ph_2P(OC_6H_4C_6F_{13})$: C, 48.3; H, 2.4; P, 5.2%.

6.5.3 *Preparation of Bis(4-perfluoro-n-hexylphenyl)phenyl phosphonite* (2.3)

4-Perfluoro-*n*-hexyl phenol (2.704 g, 6.6 mmol) in dry ether (50 cm^3) was added dropwise via cannular to a solution of $PhPCl_2$ (0.541 g, 3.0 mmol) and triethylamine (0.664 g, 6.6 mmol) in dry ether (50 cm^3) over a period of 1 hr. The reaction mixture was stirred for a further 2 hrs, after which it was filtered through celite under nitrogen to remove the triethylammonium hydrochloride formed in the reaction. The solvent in

the filtrate was then removed under reduced pressure to yield impure product as an off white solid. The crude product was purified by distillation on a Kugelröhr distillation apparatus at 160 °C (0.01 mmHg) to afford pure product as a white solid. Yield: 2.220 g, 79%. δ ^{1}H NMR (d^8 toluene) 7.77 [2 H, m, ortho PPh], 7.30 [4 H, d, meta $OC_6H_4C_6F_{13}$ ^3J(HH) 8.6 Hz], 7.27 [3 H, m, meta/para PPh] and 6.97 [4 H, d, ortho $OC_6H_4C_6F_{13}$ ^3J(HH) 8.6 Hz]. δ ^{19}F{^{1}H} NMR (d^8 toluene) -81.47 [3 F, tt, CF_3 ^3J(FF) 2.2 Hz, ^4J(FF) 10.1 Hz], -110.35 [2 F, t, $^\alpha CF_2$ ^4J(FF) 14.6 Hz], -121.74 [2 F, m, $^\beta CF_2$], -122.21 [2 F, m, $^\delta CF_2$], -123.14 [2 F, m, $^\epsilon CF_2$], -126.54 [2 F, m, $^\gamma CF_2$]. δ ^{31}P{^{1}H} NMR (d^8 toluene) 159.12 [s]. Electron impact (EI) mass spectrum: m/z 946 ([M + O]$^+$), 853 ([M - C_6H_5]$^+$), 535 ([M - $C_6H_4C_6F_{13}$]$^+$). Found: C, 39.7; H, 1.3; P, 3.4. Calc. for $PhP(OC_6H_4C_6F_{13})_2$: C, 38.7; H, 1.4; P, 3.3%.

6.5.4 *Preparation of Tris(4-perfluoro-n-hexylphenyl) phosphite* (2.4)

4-Perfluoro-n-hexylphenol (9.585 g, 23.3 mmol) in dry ether (50 cm^3) was added dropwise via cannular to a solution of PCl$_3$ (1.023 g, 7.4 mmol) and triethylamine (2.351 g, 23.2 mmol) in dry ether (50 cm^3) over a period of 1 hr. The reaction mixture was stirred for a further 2 hrs, after which it was filtered through celite under nitrogen to remove the triethylammonium hydrochloride formed in the reaction. The solvent in the filtrate was then removed under reduced pressure to yield impure product as a clear yellow oil. The crude product was purified by distillation on Kugelröhr distillation apparatus at 220 °C (0.01 mmHg) to afford pure product as a clear colourless oil. Yield 8.280 g, 88%. δ ^{1}H NMR (d^8 toluene) 7.24 [6 H, d, meta $OC_6H_4C_6F_{13}$ ^3J(HH) 8.5 Hz] and 6.88 [6 H, d, ortho $OC_6H_4C_6F_{13}$ ^3J(HH) 8.5 Hz]. δ ^{19}F{^{1}H} NMR (d^8 toluene) -81.45 [3 F, tt, CF$_3$ ^3J(FF) 2.5 Hz, ^4J(FF) 10.1 Hz], -110.50 [2 F, t, $^\alpha CF_2$ ^4J(FF) 14.6 Hz], -121.68 [2 F, m, $^\beta CF_2$], -122.05 [2 F, m, $^\delta CF_2$], -123.09 [2 F, m, $^\epsilon CF_2$], -126.51 [2 F, m, $^\gamma CF_2$]. δ ^{31}P{^{1}H} NMR (d^8 toluene) 125.05 [s]. Electron impact (EI) mass spectrum: m/z 1264 ([M]$^+$), 995 ([M - C_5F_{11}]$^+$), 853 ([M - $OC_6H_4C_6F_{13}$]$^+$). Found: C, 34.0; H, 1.2. Calc. for $P(OC_6H_4C_6F_{13})_3$: C, 34.2; H, 1.0%.

6.5.5 Preparation of 4-perfluoro-n-octylphenol (2.5)

4-Perfluoro-n-octylphenol was prepared as for (2.1) using $C_8F_{17}I$ (35.292 g, 64.6 mmol), hexafluorobenzene (100 cm^3), 4-iodophenol (12.920 g, 58.7 mmol), copper (16.426 g, 259 mmol), 2,2'-bipyridine (0.712 g, 4.6 mmol) and dimethylsulphoxide (100 cm^3). The crude product was purified by distillation on a Kugelröhr distillation apparatus at 75 °C (0.01 mmHg) to afford (2.5) as a white solid. Yield 21.643 g, 72%. δ ^{1}H NMR (CDCl$_3$) 7.56 [2 H, d, meta $OC_6H_4C_6F_{13}$ ^3J(HH) 7.1 Hz], 7.04 [2 H, d, ortho $OC_6H_4C_6F_{13}$ ^3J(HH) 7.1 Hz] and 5.28 [1 H, s, OH]. δ $^{19}F\{^1H\}$ NMR (CDCl$_3$) - 81.29 [3 F, tt, CF$_3$ ^3J(FF) 2.5 Hz, ^4J(FF) 10.1 Hz], -110.19 [2 F, tm, $^\alpha$CF$_2$ ^4J(FF) 14.6 Hz], -121.72 [2 F, m, $^\beta$CF$_2$], -122.36 [6 F, m, $^\delta$CF$_2$], -123.16 [2 F, m, $^\epsilon$CF$_2$], -126.57 [2 F, m, $^\gamma$CF$_2$]. Electron impact (EI) mass spectrum: m/z 512 ([M]$^+$), 493 ([M - F]$^+$). (Found: M$^+$, 512.00711. $C_{14}H_5F_{17}O$ requires M$^+$, 512.00690).

6.5.6 Preparation of 4-perfluoro-n-decylphenol (2.6)

4-Perfluoro-n-decylphenol was prepared as for (2.1) using $C_{10}F_{21}I$ (22.020 g, 34.1 mmol), hexafluorobenzene (50 cm^3), 4-iodophenol (7.500 g, 34.1 mmol), copper (8.658 g, 136 mol), 2,2-bipyridine (0.372 g, 2.4 mmol) and dimethylsulphoxide (100 cm^3). The crude product was purified by distillation on a Kugelröhr distillation apparatus at 125 °C (0.01 mmHg) to afford (2.6) as a white solid. Yield 11.789 g, 57%. δ ^{1}H NMR (CDCl$_3$) 7.43 [2 H, d, meta $OC_6H_4C_6F_{13}$ ^3J(HH) 7.1 Hz], 6.96 [2 H, d, ortho $OC_6H_4C_6F_{13}$ ^3J(HH) 7.1 Hz] and 5.44 [1 H, s, OH]. δ $^{19}F\{^1H\}$ NMR (CDCl$_3$) -81.25 [3 F, bt, CF$_3$ ^4J(FF) 10.0 Hz], -110.04 [2 F, tm, $^\alpha$CF$_2$ ^4J(FF) 14.3 Hz], -121.71 [2 F, m, $^\beta$CF$_2$], -122.24 [10 F, m, $^\delta$CF$_2$], -123.14 [2 F, m, $^\epsilon$CF$_2$], -126.56 [2 F, m, $^\gamma$CF$_2$]. Electron impact (EI) mass spectrum: m/z 612 ([M]$^+$), 593 ([M - F]$^+$). (Found: M$^+$, 612.00059. $C_{16}H_5F_{21}O$ requires M$^+$, 612.00051).

6.5.7 Preparation of Tris(4-perfluoro-n-octylphenyl) phosphite (2.7)

4-Perfluoro-n-octyl phenol (14.003 g, 27.3 mmol) in dry ether (50 cm^3) was added dropwise via cannular to a solution of PCl$_3$ (1.191 g, 8.7 mmol) and triethylamine

(2.767 g, 27.3 mmol) in dry ether (50 cm^3) over a period of 1 hr. The reaction mixture was stirred for a further 2 hrs, after which it was filtered through celite under nitrogen to remove the triethylammonium hydrochloride formed in the reaction. The solvent was removed *in vacuo* to yield the impure product as an off white solid. The crude product was purified by distillation on Kugelröhr distillation apparatus at 235 °C (0.01 mmHg) to afford pure product as a white solid. Yield: 7.856 g, 55%. δ ^{1}H NMR (d^8 toluene) 7.30 [6 H, d, *meta* OC$_6$H$_4$C$_6$F$_{13}$ ^3J(HH) 8.6 Hz] and 6.97 [6 H, d, *ortho* OC$_6$H$_4$C$_6$F$_{13}$ ^3J(HH) 8.6 Hz]. δ ^{19}F{^{1}H} NMR (d^8 toluene) -81.47 [3 F, tt, CF$_3$ ^3J(FF) 2.2 Hz, ^4J(FF) 10.1 Hz], -110.35 [2 F, t, $^\alpha$CF$_2$ ^4J(FF) 14.6 Hz], -121.74 [2 F, m, $^\beta$CF$_2$], -122.21 [6 F, m, $^\delta$CF$_2$], -123.14 [2 F, m, $^\epsilon$CF$_2$], -126.54 [2 F, m, $^\gamma$CF$_2$]. δ ^{31}P{^{1}H} NMR (d^8 toluene) 125.08 [s]. Electron impact (EI) mass spectrum: *m/z* 1565 ([*M* + H]$^+$), 1053 ([*M* - OC$_6$H$_4$C$_6$F$_{13}$]$^+$).

6.5.8 *Preparation of Tris(4-perfluoro-n-decylphenyl) phosphite* (2.8)

4-Perfluoro-*n*-decyl phenol (7.500 g, 12.3 mmol) in dry ether (50 cm^3) was added dropwise *via* cannular to a solution of PCl$_3$ (0.535 g, 3.9 mmol) and triethylamine (1.245 g, 12.3 mmol) in dry ether (50 cm^3) over a period of 1 hr. The reaction mixture was stirred for a further 2 hrs, after which it was filtered through celite under nitrogen to remove the triethylammonium hydrochloride formed in the reaction. The solvent was removed *in vacuo* to yield the impure product as a white solid. Unreacted triethylamine and 4-perfluoro-*n*-decyl phenol were removed by heating on a Kugelröhr distillation apparatus at 130 °C (0.01 mmHg). Yield: 5.274 g, 73%. δ ^{1}H NMR (d^8 toluene) 7.28 [6 H, d, *meta* OC$_6$H$_4$C$_6$F$_{13}$ ^3J(HH) 8.6 Hz] and 6.94 [6 H, d, *ortho* OC$_6$H$_4$C$_6$F$_{13}$ ^3J(HH) 8.6 Hz]. δ ^{19}F{^{1}H} NMR (d^8 toluene) -82.16 [3 F, tm, CF$_3$ ^4J(FF) 10.0 Hz], -111.08 [2 F, t, $^\alpha$CF$_2$ ^4J(FF) 14.3 Hz], -122.07 [2 F, m, $^\beta$CF$_2$], -122.66 [10 F, m, $^\delta$CF$_2$], -123.63 [2 F, m, $^\epsilon$CF$_2$], -127.18 [2 F, m, $^\gamma$CF$_2$]. δ ^{31}P{^{1}H} NMR (d^8 toluene) 125.25 [s]. Electron impact (EI) mass spectrum: *m/z* 1864 ([*M* $^+$]), 1253 ([*M* - OC$_6$H$_4$C$_{10}$F$_{21}$]$^+$).

6.5.9 *Preparation of 3-perfluoro-n-hexylphenol* **(2.9)**

3-Perfluoro-*n*-hexylphenol was prepared as for **(2.1)** using $C_6F_{13}I$ (24.969 g, 56 mmol), hexafluorobenzene (100 cm^3), 3-iodophenol (11.197 g, 51 mmol), copper (12.945 g, 204 mmol), 2,2'-bipyridine (0.565 g, 3.6 mmol) and dimethylsulphoxide (100 cm^3). The crude product was purified by distillation on a Kugelröhr distillation apparatus at 60 °C (0.01 mmHg) to afford **(2.9)** as a clear oil. Yield 18.755 g, 89%. δ ^{1}H NMR (CDCl$_3$) 7.30 [1 H, t, *meta* OC$_6$H$_4$ ^3J(HH) 7.9 Hz], 7.09 [1 H, d, *ortho* OC$_6$H$_4$ ^3J(HH) 7.6 Hz], 6.96 [2 H, m, *ortho, para* OC$_6$H$_4$], 5.21 [1 H, s, OH]. δ ^{19}F{^{1}H} NMR (CDCl$_3$) -81.34 [3 F, tm, CF$_3$ ^4J(FF) 11.3 Hz], -111.03 [2 F, tm, $^\alpha$CF$_2$ ^4J(FF) 14.2 Hz], -122.05 [2 F, m, $^\beta$CF$_2$], -122.46 [2 F, m, $^\delta$CF$_2$], -123.34 [2 F, m, $^\varepsilon$CF$_2$], -126.67 [2 F, m, $^\gamma$CF$_2$]. Electron impact (EI) mass spectrum: *m/z* 412 ([M]$^+$), 393 ([M - F]$^+$). (Found: M^+, 412.01328. C$_{14}$H$_5$F$_{17}$O requires M^+, 412.01328).

6.5.10 *Preparation of 2-perfluoro-n-hexylphenol* **(2.10)**

2-Perfluoro-*n*-hexylphenol was prepared as for **(2.1)** using $C_6F_{13}I$ (29.736 g, 67 mmol), hexafluorobenzene (100 cm^3), 2-iodophenol (13.353 g, 61 mmol), copper (15.420 g, 243 mmol), 2,2'-bipyridine (0.673 g, 4.3 mmol) and dimethylsulphoxide (100 cm^3). The crude product was purified by distillation on a Kugelröhr distillation apparatus at 96 °C (20 mmHg) to afford **(2.5)** as a pale yellow oil. Yield 17.171 g, 69%. δ ^{1}H NMR (CDCl$_3$) 7.31 [2 H, m, *meta, ortho* OC$_6$H$_4$], 6.89 [2 H, m, *meta, para* OC$_6$H$_4$] and 6.32 [1 H, t, OH J(HF) 8.3 Hz]. δ ^{19}F{^{1}H} NMR (CDCl$_3$) -81.30 [3 F, tm, CF$_3$ ^4J(FF) 10.1 Hz], -108.66 [2 F, tm, $^\alpha$CF$_2$ ^4J(FF) 14.8 Hz], -122.09 [2 F, m, $^\beta$CF$_2$], -123.24 [6 F, m, $^\delta$CF$_2$], -126.65 [2 F, m, $^\varepsilon$CF$_2$], -126.57 [2 F, m, $^\gamma$CF$_2$]. Electron impact (EI) mass spectrum: *m/z* 412 ([M]$^+$), 393 ([M - F]$^+$). (Found: M^+, 412.01328. C$_{14}$H$_5$F$_{17}$O requires M^+, 412.01328).

6.5.13 *Preparation of Tris(3-perfluoro-n-hexylphenyl) phosphite* **(2.14)**

The synthesis of **(2.14)** was performed similarly to **(2.4)** by the reaction of 3-perfluoro-*n*-hexylphenol (7.844 g, 19.0 mmol) with PCl$_3$ (0.834 g, 6.1 mmol) in the

presence of triethylamine (1.965 g, 19.4 mmol). The crude product was purified by distillation on a Kugelröhr distillation apparatus at 185 °C (0.01 mmHg) to afford pure product as a clear colourless oil. Yield 3.555 g, 45%. δ ^{1}H NMR (d^8 toluene) 7.31 [3 H, s, *ortho* OC$_6$H$_4$], 7.14 [3 H, d, *ortho* OC$_6$H$_4$ ^{3}J(HH) 7.6 Hz], 6.99 [3 H, d, *para* OC$_6$H$_4$ ^{3}J(HH) 8.0 Hz], 6.75 [3 H, d, *meta* OC$_6$H$_4$ ^{3}J(HH) 8.0 Hz]. δ ^{19}F{^{1}H} NMR (d^8 toluene) -81.86 [3 F, tt, CF$_3$ ^{3}J(FF) 2.5 Hz, ^{4}J(FF) 9.3 Hz], -111.38 [2 F, t, $^\alpha$CF$_2$ ^{4}J(FF) 15.9 Hz], -121.99 [2 F, m, $^\beta$CF$_2$], -122.27 [2 F, m, $^\delta$CF$_2$], -123.40 [2 F, m, $^\epsilon$CF$_2$], -126.85 [2 F, m, $^\gamma$CF$_2$]. δ ^{31}P{^{1}H} NMR (d^8 toluene) 126.13 [s]. Electron impact (EI) mass spectrum: *m/z* 1264 ([M]$^+$), 995 ([M - C$_5$F$_{11}$]$^+$), 853 ([M - OC$_6$H$_4$C$_6$F$_{13}$]$^+$). Found: C, 34.2; H, 1.04; P, 2.25. Calc. for P(OC$_6$H$_4$C$_6$F$_{13}$)$_3$: C, 34.2; H, 1.0; P, 2.45%.

6.5.14 *Preparation of Tris(2-perfluoro-n-hexylphenyl) phosphite* (2.15)

The synthesis of (2.15) was performed similarly to (2.4) by the reaction of 2-perfluoro-*n*-hexylphenol (9.477 g, 23.0 mmol) with PCl$_3$ (1.054 g, 7.7 mmol) in the presence of triethylamine (2.451 g, 24.2 mmol). The crude product was purified by distillation on a Kugelröhr distillation apparatus at 180 °C (0.01 mmHg) to afford pure product as a clear colourless oil. Yield 5.051 g, 52%. δ ^{1}H NMR (d^8 toluene) 7.50 [3 H, d, *ortho* OC$_6$H$_4$ ^{3}J(HH) 8.1 Hz], 7.41 [3 H, d, *meta* OC$_6$H$_4$ ^{3}J(HH) 8.1 Hz], 7.10 [3 H, t, *meta* OC$_6$H$_4$ ^{3}J(HH) 8.1 Hz], 6.79 [3 H, t, *para* OC$_6$H$_4$ ^{3}J(HH) 8.1 Hz]. δ ^{19}F{^{1}H} NMR (d^8 toluene) -81.86 [3 F, tt, CF$_3$ ^{3}J(FF) 2.5 Hz, ^{4}J(FF) 9.3 Hz], -111.38 [2 F, t, $^\alpha$CF$_2$ ^{4}J(FF) 15.9 Hz], -121.99 [2 F, m, $^\beta$CF$_2$], -122.27 [2 F, m, $^\delta$CF$_2$], -123.40 [2 F, m, $^\epsilon$CF$_2$], -126.85 [2 F, m, $^\gamma$CF$_2$]. δ ^{31}P{^{1}H} NMR (d^8 toluene) 126.13 [s]. Electron impact (EI) mass spectrum: *m/z* 1264 ([M]$^+$), 995 ([M - C$_5$F$_{11}$]$^+$), 853 ([M - OC$_6$H$_4$C$_6$F$_{13}$]$^+$). Found: C, 34.0; H, 1.02; P, 2.46. Calc. for P(OC$_6$H$_4$C$_6$F$_{13}$)$_3$: C, 34.2; H, 1.0; P, 2.45%.

6.5.15 *Preparation of 1H,1H,2H,2H-perfluoro-n-octyl(diphenyl) phosphinite* (2.16)

1H,1H,2H,2H-Perfluoro-*n*-octan-1-ol (8.224 g, 22.6 mmol) in dry ether (50 cm^3) was added dropwise *via* cannular to a solution of Ph$_2$PCl (4.793 g, 21.7 mmol) and

triethylamine (2.293 g, 22.7 mmol) in dry ether (50 cm^3) over a period of 1 hr. The reaction mixture was stirred for a further 2 hrs, after which it was filtered through celite under nitrogen to remove the triethylammonium hydrochloride formed in the reaction. The solvent in the filtrate was then removed under reduced pressure to yield the impure product as a clear colourless oil. Unreacted triethylamine and 1H,1H,2H,2H perfluoro-n-octan-1-ol were removed by heating on a Kugelröhr distillation apparatus at 60 °C (0.01 mmHg). Yield: 10.168 g, 85%. δ ^{1}H NMR (d^8 toluene) 7.70 [4 H, m, *ortho* PPh], 7.27 [6 H, m, *meta/para* PPh], 4.05 [2 H, cq, OCH$_2$, ^3J(HH) ≈ ^3J(PH) 5.9 Hz], 2.31 [2 H, tt, CH$_2$CF$_2$ ^3J(HH) 6.6 Hz, ^4J(HF) 18.7 Hz]. δ ^{19}F{^{1}H} NMR (d^8 toluene) -81.49 [3 F, tt, CF$_3$ ^3J(FF) 2.5 Hz, ^4J(FF) 10.1 Hz], -113.46 [2 F, tm, $^\alpha$CF$_2$ ^4J(FF) 14.5 Hz], -122.21 [2 F, m, $^\beta$CF$_2$], -123.24 [2 F, m, $^\delta$CF$_2$], -123.92 [2 F, m, $^\epsilon$CF$_2$], -126.57 [2 F, m, $^\gamma$CF$_2$]. δ ^{31}P{^{1}H} NMR (d^8 toluene) 116.10 [s]. Electron impact (EI) mass spectrum: m/z 548 ([M]$^+$), 529 ([M - F]$^+$), 201 ([M - C$_2$H$_4$C$_6$F$_{13}$]$^+$) (Found: M$^+$, 548.05731. C$_{20}$H$_{14}$F$_{13}$OP requires M$^+$, 548.05747).

6.5.16 *Preparation of Bis(1H,1H,2H,2H-perfluoro-n-octyl)phenyl phosphonite* (2.17)

1H,1H,2H,2H-Perfluoro-n-octan-1-ol (15.334 g, 42.1 mmol) in dry ether (50 cm^3) was added dropwise *via* cannular to a solution of PhPCl$_2$ (3.560 g, 19.9 mmol) and triethylamine (4.048 g, 44.0 mmol) in dry ether (50 cm^3) over a period of 1 hr. The reaction mixture was stirred for a further 2 hrs, after which it was filtered through celite under nitrogen to remove the triethylammonium hydrochloride formed in the reaction. The solvent was removed *in vacuo* to yield the impure product as a clear, colourless oil. Unreacted triethylamine and 1H,1H,2H,2H perfluoro-n-octan-1-ol were removed by heating on a Kugelröhr distillation apparatus at 60 °C (0.01 mmHg). Yield: 8.998 g, 54%. δ ^{1}H NMR (d^8 toluene) 7.34 [2 H, m, *ortho* PPh], 6.95 [3 H, m, *meta/para* PPh], 4.52 [2 H, m, OCH], 4.30 [2 H, m, OCH] and 1.80 [4 H, m, CH$_2$CF$_2$]. δ ^{19}F{^{1}H} NMR (d^8 toluene) -81.65 [3 F, tt, CF$_3$ ^3J(FF) 2.6 Hz, ^4J(FF) 10.1 Hz], -113.91 [2 F, tt, $^\alpha$CF$_2$ ^3J(FF) 2.5 Hz, ^4J(FF) 13.9 Hz], -122.30 [2 F, m, $^\beta$CF$_2$], -123.34 [2 F, m, $^\delta$CF$_2$], -124.08 [2 F, m, $^\epsilon$CF$_2$], -126.70 [2 F, m, $^\gamma$CF$_2$]. δ ^{31}P{^{1}H} NMR (d^8 toluene) 156.70 [s]. Electron impact (EI) mass spectrum: m/z 834 ([M]$^+$), 565 ([M

- $C_5F_{11}]^+$), 471 ([M - $OC_2H_4C_6F_{13}]^+$). Found: C, 31.7; H, 1.5. Calc. for $PhP(OC_2H_4C_6F_{13})_2$: C, 31.7; H, 1.6%.

6.5.17 *Preparation of Tris(1H,1H,2H,2H-perfluoro-n-octyl) phosphite* (2.18)

1H,1H,2H,2H-Perfluoro-n-octan-1-ol (9.746 g, 26.8 mmol) in dry ether (50 cm^3) was added dropwise *via* cannular to a solution of PCl_3 (1.196 g, 8.7 mmol) and triethylamine (2.708 g, 26.8 mmol) in dry ether (50 cm^3) over a period of 1 hr. The reaction mixture was stirred for a further 2 hrs, after which it was filtered through celite under nitrogen to remove the triethylammonium hydrochloride formed in the reaction. The solvent in the filtrate was then removed under reduced pressure to yield the impure product as a clear, colourless oil. The crude product was purified by distillation on a Kugelrohr distillation apparatus at 125 °C (0.01 mmHg). Yield 5.292 g, 54%. δ ^{1}H NMR (d^8 toluene) 3.16 [6 H, cq, OCH_2, ^3J(HH) ≈ ^3J(PH) 6.0 Hz], 2.00 [6 H, tt, CH_2CF_2 ^3J(HH) 6.3 Hz, ^4J(HF) 18.6 Hz]. δ ^{19}F{^{1}H} NMR (d^8 toluene) -81.40 [3 F, tt, CF_3 ^3J(FF) 2.7 Hz, ^4J(FF) 10.1 Hz], -114.54 [2 F, tm, $^\alpha CF_2$ ^4J(FF) 14.5 Hz], -122.92 [2 F, m, $^\beta CF_2$], -123.96 [2 F, m, $^\delta CF_2$], -124.67 [2 F, m, $^\epsilon CF_2$], -127.38 [2 F, m, $^\gamma CF_2$]. δ ^{31}P{^{1}H} NMR (d^8 toluene) 138.70 [s]. Electron impact (EI) mass spectrum: m/z 548 ([M]$^+$), 529 ([M - F]$^+$), 201 ([M - $C_2H_4C_6F_{13}]^+$) (Found: M^+, 548.05731. Found: C, 25.0; H, 0.9. Calc. for $P(OC_2H_4C_6F_{13})_3$: C, 25.7; H, 1.1%.

6.6 Synthesis of Metal Complexes of Monodentate Ligands.

6.6.1 Synthesis of Platinum(II) complexes of the type [PtCl$_2$L$_2$].

6.6.1.1 *Preparation of cis-PtCl$_2$[Ph$_2$P(OC$_6$H$_4$-4-C$_6$F$_{13}$)]$_2$* (3.1)

A slurry of $PtCl_2(MeCN)_2$ (0.101 g, 0.29 mmol) and $Ph_2P(OC_6H_4-4-C_6F_{13})$ (0.477 g, 0.80 mmol) in dichloromethane (30 cm^3) was heated under reflux under nitrogen for 2 hrs to give a clear colourless solution. The solution was allowed to cool and concentrated by rotary evaporation. Addition of petroleum ether precipitated the product as a fine white solid, which was filtered, washed with petroleum ether and dried *in vacuo*. Yield 0.304 g, 72%. δ ^{1}H NMR (CDCl$_3$) 7.54 [4 H, m, *ortho* PPh],

7.32 [2 H, d, *meta* $OC_6H_4C_6F_{13}$, $^3J(HH)$ 8.7 Hz], 7.22 [6 H, m, *meta/para* PPh] and 6.63 [2 H, d, *ortho* $OC_6H_4C_6F_{13}$, $^3J(HH)$ 8.7 Hz]. δ $^{19}F\{^1H\}$ NMR ($CDCl_3$) -81.21 [3 F, t, CF_3 $^4J(FF)$ 10.6 Hz], -110.55 [2 F, tm, $^\alpha CF_2$ $^4J(FF)$ 14.1 Hz], -121.84 [2 F, m, $^\beta CF_2$], -122.27 [2 F, m, $^\delta CF_2$], -123.22 [2 F, m, $^\epsilon CF_2$] and -126.55 [2 F, m, $^\gamma CF_2$]. δ $^{31}P\{^1H\}$ NMR ($CDCl_3$) 87.60 [1 P, s, $^1J(PtP)$ 4189 Hz]. FAB mass spectrum: m/z 1423 ($[M - Cl]^+$), 1386 ($[M - 2Cl]^+$). Found: C, 39.8; H, 1.7; P, 5.0. Calc. for $PtCl_2\{Ph_2P(OC_6H_4C_6F_{13})\}_2$: C, 39.5; H, 1.9; P, 5.0%. IR (Nujol) v (Pt-Cl) 290, 315 cm^{-1}.

6.6.1.2 Preparation of cis-PtCl₂{PhP(OC₆H₄-4-C₆F₁₃)₂}₂ (3.2)

Cis-$PtCl_2\{PhP(OC_6H_4-4-C_6F_{13})_2\}_2$ was prepared similarly to (3.1) using $PtCl_2(MeCN)_2$ (0.057 g, 0.16 mmol) and $PhP(OC_6H_4-4-C_6F_{13})_2$ (0.431 g, 0.46 mmol) to afford the product as a fine, white solid. Yield 0.213 g, 61%. δ ^1H NMR ($CDCl_3$) 7.49 [2 H, m, *ortho* PPh], 7.41 [4 H, d, *meta* $OC_6H_4C_6F_{13}$, $^3J(HH)$ 8.8 Hz], 7.26 [3 H, m, *meta/para* PPh] and 7.05 [4 H, d, *ortho* $OC_6H_4C_6F_{13}$, $^3J(HH)$ 8.8 Hz]. δ $^{19}F\{^1H\}$ NMR ($CDCl_3$) -81.33 [3 F, tt, CF_3 $^3J(FF)$ 2.2 Hz, $^4J(FF)$ 10.1 Hz], -110.78 [2 F, tm, $^\alpha CF_2$ $^4J(FF)$ 14.1 Hz], -121.90 [2 F, m, $^\beta CF_2$], -122.23 [2 F, m, $^\delta CF_2$], -123.27 [2 F, m, $^\epsilon CF_2$] and -126.60 [2 F, m, $^\gamma CF_2$]. δ $^{31}P\{^1H\}$ NMR ($CDCl_3$) 94.99 [1 P, s, $^1J(PtP)$ 4859 Hz]. FAB mass spectrum: m/z 2090 ($[M - Cl]^+$), 2054 ($[M - 2Cl]^+$). Found: C, 33.9; H, 1.1; P, 2.6. Calc. for $PtCl_2\{PhP(OC_6H_4C_6F_{13})_2\}_2$: C, 33.9; H, 1.2; P, 2.9%. IR (Nujol) v (Pt-Cl) 305, 327 cm^{-1}.

6.6.1.3 Preparation of cis-PtCl₂{P(OC₆H₄-4-C₆F₁₃)₃}₂ (3.3)

Cis-$PtCl_2\{P(OC_6H_4-4-C_6F_{13})_3\}_2$ was prepared similarly to (3.1) using $PtCl_2(MeCN)_2$ (0.041 g, 0.16 mmol) and $P(OC_6H_4-4-C_6F_{13})_3$ (0.473 g, 0.37 mmol) to afford the product as a fine, white solid. Yield 0.261 g, 59%. Yield 0.261 g, 59%. δ ^1H NMR (($CD_3)_2CO$) 7.80 [12 H, d, *ortho* OC_6H_4, $^3J(HH)$ 8.8 Hz] and 7.64 [12 H, d, *meta* OC_6H_4, $^3J(HH)$ 8.8 Hz]. δ $^{19}F\{^1H\}$ NMR (D_2O) -82.17 [3 F, t, CF_3, $^4J(FF)$ 10.0 Hz], -111.20 [2 F, t, $^\alpha CF_2$, $^4J(FF)$ 13.9 Hz], -122.36 [4 F, m, $^\beta CF_2$ and $^\delta CF_2$], -123.78 [2 F, m, $^\epsilon CF_2$], -127.24 [2 F, m, $^\gamma CF_2$]. δ $^{31}P\{^1H\}$ NMR (D_2O) 65.36 [s, $^1J(PtP)$ 5660 Hz].

Electron impact (FAB) mass spectrum: m/z 2759 [(M-Cl+H)$^+$], 2722 [(M-2Cl-H)$^+$]. Found: C, 29.18; H, 0.82; Cl, 3.68. Calc. for PtCl$_2$\{P(OC$_6$H$_4$C$_6$F$_{13}$)$_2$\}$_2$ C, 30.94; H, 0.87; Cl, 2.54 %. IR (Nujol) v (Pt-Cl) 308, 330 cm^{-1}.

6.6.1.4   Preparation of cis-PtCl$_2$\{P(OC$_6$H$_4$-3-C$_6$F$_{13}$)$_3$\}$_2$ (3.4)

Cis-PtCl$_2$\{P(OC$_6$H$_4$-3-C$_6$F$_{13}$)$_3$\}$_2$ was prepared similarly to (3.1) using PtCl$_2$(MeCN)$_2$ (0.041 g, 0.16 mmol) and P(OC$_6$H$_4$-3-C$_6$F$_{13}$)$_3$ (0.307 g, 0.24 mmol) to afford the product as a fine, white solid. Yield 0.201 g, 60%. δ ^{1}H NMR (d^6 acetone) 7.45 [3 H, m, ortho, meta, para OC$_6$H$_4$], 7.08 [1 H, s, ortho OC$_6$H$_4$]. δ ^{19}F\{^{1}H\} NMR (d^6 acetone) -81.85 [3 F, m, CF$_3$], -111.79 [2 F, tm, $^\alpha$CF$_2$ ^{4}J(FF) 14.2 Hz], -122.41 [2 F, m, $^\beta$CF$_2$], -122.65 [2 F, m, $^\delta$CF$_2$], -123.68 [2 F, m, $^\epsilon$CF$_2$], -127.01 [2 F, m, $^\gamma$CF$_2$]. δ ^{31}P\{^{1}H\} NMR (d^6 acetone) 60.85 [s, ^{1}J(PtP) 5777 Hz]. FAB mass spectrum: m/z 2759 ([M - Cl]$^+$), 2723 ([M - 2Cl]$^+$). Found: C, 30.96; H, 0.84; P 2.3. Calc. for PtCl$_2$\{P(OC$_6$H$_4$C$_6$F$_{13}$)$_3$\}$_2$: C, 30.94; H, 0.87; P, 2.22%.

6.6.1.5   Preparation of trans-PtCl$_2$\{P(OC$_6$H$_4$-2-C$_6$F$_{13}$)$_3$\}$_2$ (3.5)

Trans-PtCl$_2$\{P(OC$_6$H$_4$-2-C$_6$F$_{13}$)$_3$\}$_2$ was prepared similarly to (3.1) using PtCl$_2$(MeCN)$_2$ (0.039 g, 0.11 mmol) and P(OC$_6$H$_4$-2-C$_6$F$_{13}$)$_3$ (0.291 g, 0.23 mmol) to afford the product as a fine, white solid. Yield 0.077 g, 25%. δ ^{1}H NMR (d^6 acetone) 7.76 [1 H, d, ortho OC$_6$H$_4$ ^{3}J(HH) 8.5 Hz], 7.69 [1 H, d, meta OC$_6$H$_4$ ^{3}J(HH) 8.5 Hz], 7.58 [1 H, t, meta OC$_6$H$_4$ ^{3}J(HH) 7.3 Hz], 7.48 [1 H, t, para OC$_6$H$_4$ ^{3}J(HH) 7.6 Hz]. δ ^{19}F\{^{1}H\} NMR (d^6 acetone) -82.29 [3 F, tm, CF$_3$ ^{4}J(FF) 8.5 Hz], -108.87 [2 F, tm, $^\alpha$CF$_2$ ^{4}J(FF) 14.2 Hz], -121.84 [2 F, m, $^\beta$CF$_2$], -122.65 [2 F, m, $^\delta$CF$_2$], -123.90 [2 F, m, $^\epsilon$CF$_2$], -127.39 [2 F, m, $^\gamma$CF$_2$]. δ ^{31}P\{^{1}H\} NMR (d^6 acetone) 77.23 [s, ^{1}J(PtP) 4589 Hz]. FAB mass spectrum: m/z 2759 ([M - Cl]$^+$), 2723 ([M - 2Cl]$^+$). Found: C, 30.84; H, 0.85; P 2.1. Calc. for PtCl$_2$\{P(OC$_6$H$_4$C$_6$F$_{13}$)$_3$\}$_2$: C, 30.94; H, 0.87; P, 2.22%.

6.6.1.6 Preparation of cis-PtCl₂{Ph₂P(OC₂H₄C₆F₁₃)}₂ (3.6)

Cis-PtCl₂{Ph₂P(OC₂H₄C₆F₁₃)}₂ was prepared similarly to (3.1) using PtCl₂(MeCN)₂ (0.110 g, 0.32 mmol) and Ph₂P(OC₂H₄C₆F₁₃) (0.403 g, 0.74 mmol) to afford the product as a fine, pale yellow solid. Yield 0.332 g, 77%. δ ¹H NMR (CDCl₃) 7.84 [4 H, m, *ortho* PPh], 7.53 [6 H, m, *meta/para* PPh], 3.99 [2 H, cq, OCH₂, ³*J*(HH) ≈ ³*J*(PH) 6.3 Hz], 2.07 [2 H, tt, ᵝCH₂ ³*J*(HH) 6.3 Hz, ³*J*(FH) 18.4 Hz]. δ ¹⁹F{¹H} NMR (CDCl₃) -81.39 [3 F, tt, CF₃ ⁴*J*(FF) 10.0 Hz, ³*J*(FF) 2.0 Hz], -113.99 [2 F, tm, ᵅCF₂ ⁴*J*(FF) 12.6 Hz], -122.44 [2 F, m, ᵝCF₂], -123.44 [2 F, m, ᵟCF₂], -124.21 [2 F, m, ᵋCF₂] and -126.71 [2 F, m, ᵞCF₃]. δ ³¹P{¹H} NMR (CDCl₃) 86.23 [1 P, s, ¹*J*(PtP) 4141 Hz]. FAB mass spectrum: m/z 1327 ([*M* - Cl]⁺), 1290 ([*M* - 2Cl]⁺). Found: C, 34.7; H, 1.90; Cl, 5.1. Calc. for PtCl₂{Ph₂P(OC₂H₄C₆F₁₃)}₂: C, 35.3; H, 2.07; Cl, 5.2%. IR (Nujol) v (Pt-Cl) 292, 317 cm⁻¹.

6.6.1.7 Preparation of cis-PtCl₂{PhP(OC₂H₄C₆F₁₃)₂}₂ (3.7)

Cis-PtCl₂{PhP(OC₂H₄C₆F₁₃)₂}₂ was prepared similarly to (3.1) using PtCl₂(MeCN)₂ (0.052 g, 0.15 mmol) and PhP(OC₂H₄C₆F₁₃)₂ (0.347 g, 0.42 mmol) to afford the product as a fine, white solid. Yield 0.183 g, 63%. δ ¹H NMR (CDCl₃) 7.71 [2 H, m, *ortho* PPh], 7.49 [3 H, m, *meta/para* PPh], 4.41 [2 H, m, OCH], 4.17 [2 H, m, OCH], 2.37 [4 H, m, CH₂CF₂]. δ ¹⁹F{¹H} NMR (CDCl₃) -81.44 [3 F, m, CF₃], -114.11 [2 F, m, ᵅCF₂], -122.48 [2 F, m, ᵝCF₂], -123.49 [2 F, m, ᵟCF₂], -124.12 [2 F, m, ᵋCF₂] and -126.76 [2 F, m, ᵞCF₂]. δ ³¹P{¹H} NMR (CDCl₃) 100.03 [1 P, s, ¹*J*(PtP) 4754 Hz]. FAB mass spectrum: m/z 1899 ([*M* - Cl]⁺), 1864 ([*M* - 2Cl]⁺). Found: C, 27.4; H, 1.27; Cl, 3.0. Calc. for PtCl₂{PhP(OC₂H₄C₆F₁₃)₂}₂: C, 27.3; H, 1.35; Cl, 3.67%. IR (Nujol) v (Pt-Cl) 301, 322 cm⁻¹.

6.6.1.8 Preparation of PtCl₂{P(OC₂H₄C₆F₁₃)₃}₂ (3.8)

PtCl₂{P(OC₂H₄C₆F₁₃)₃}₂ was prepared by the reaction of PtCl₂(MeCN)₂ (0.038 g, 0.011 mmol) and P(OC₂H₄C₆F₁₃)₃ (0.253 g, 0.23 mmol) in refluxing dichloromethane (30 cm⁻³). The solvent was removed *in vacuo* to afford the product as a clear,

colourless oil. Yield 0.246 g, 90%. δ ^{1}H NMR (d^6 acetone) 4.63 [6 H, m, OCH$_2$], 2.25 [6 H, tt, CH$_2$CF$_2$ ^{3}J(HH) 6.1 Hz, ^{3}J(FH) 18.6 Hz]. δ ^{19}F{^{1}H} NMR (d^6 acetone) -74.78 [3 F, m, CF$_3$], -106.85 [2 F, m, $^\alpha$CF$_2$], -115.23 [2 F, m, $^\beta$CF$_2$], -126.29 [2 F, m, $^\delta$CF$_2$], -116.87 [2 F, m, $^\epsilon$CF$_2$] and -119.77 [2 F, m, $^\gamma$CF$_2$]. FAB mass spectrum: m/z 2407 ([M - Cl]$^+$), 2435 ([M - 2Cl]$^+$).

6.6.2 Synthesis of Platinum (II) complexes of the type [PtCl$_2$(PEt$_3$)L].

6.6.2.1   *Preparation of cis-PtCl$_2$(PEt$_3$){Ph$_2$P(OC$_6$H$_4$-4-C$_6$F$_{13}$)}* (3.9)

A slurry of [{PtCl(μ-Cl)(PEt$_3$)}$_2$] (0.153 g, 0.20 mmol) and Ph$_2$P(OC$_6$H$_4$-4-C$_6$F$_{13}$) (0.358 g, 0.60 mmol) in dichloromethane (30 cm^3) was heated under reflux under nitrogen for 10 min to give a clear colourless solution. The solution was allowed to cool and concentrated by rotary evaporation. Addition of petroleum ether precipitated the product as a fine white solid, which was filtered, washed with petroleum ether and dried *in vacuo*. Yield 0.322 g, 83%. δ ^{1}H NMR (CDCl$_3$) 7.62 [4 H, m, *ortho* PPh], 7.22 [8 H, d, *meta/para* PPh, *meta* OC$_6$H$_4$C$_6$F$_{13}$], 6.96 [2 H, d, *ortho* OC$_6$H$_4$C$_6$F$_{13}$ ^{3}J(HH) 8.2 Hz], 1.79 [6 H, dq, CH$_2$, ^{2}J(PH) 10.2 Hz, ^{3}J(HH) 7.6 Hz] and 0.80 [9 H, dt, CH$_3$, ^{3}J(HH) 7.6 Hz, ^{3}J(PH) 17.6 Hz]. δ ^{19}F{^{1}H} NMR (CDCl$_3$) -81.28 [3 F, tt, CF$_3$ ^{3}J(FF) 2.1 Hz, ^{4}J(FF) 10.0 Hz], -110.93 [2 F, t, $^\alpha$CF$_2$ ^{4}J(FF) 14.6 Hz], -121.84 [2 F, m, $^\beta$CF$_2$], -122.44 [2 F, m, $^\delta$CF$_2$], -123.25 [2 F, m, $^\epsilon$CF$_2$] and -126.58 [2 F, m, $^\gamma$CF$_2$]. δ ^{31}P{^{1}H} NMR (CDCl$_3$) 88.68 [1 P, d, ^{1}J(PtP) 4362 Hz, ^{2}J(PP) 15.9 Hz] and 12.56 [1 P, d, ^{1}J(PtP) 3356 Hz, ^{2}J(PP) 15.9 Hz]. FAB mass spectrum: m/z 945 ([M - Cl]$^+$), 908 ([M - 2Cl]$^+$). Found: C, 37.2; H, 2.7; P, 5.7. Calc. for PtCl$_2$(PEt$_3$){Ph$_2$P(OC$_6$H$_4$C$_6$F$_{13}$)}: C, 36.7; H, 3.0; P, 6.3%.

6.6.2.2   *Preparation of cis-PtCl$_2$(PEt$_3$){PhP(OC$_6$H$_4$-4-C$_6$F$_{13}$)$_2$}* (3.10)

Cis-PtCl$_2$(PEt$_3$){PhP(OC$_6$H$_4$-4-C$_6$F$_{13}$)$_2$} was prepared similarly to (3.9) using [{PtCl(μ-Cl)(PEt$_3$)}$_2$] (0.122 g, 0.16 mmol) and PhP(OC$_6$H$_4$-4-C$_6$F$_{13}$)$_2$ (0.324 g, 0.35 mmol) to afford the product as a fine, white solid. Yield 0.233 g, 56%. δ ^{1}H NMR (CDCl$_3$) 7.77 [2 H, m, *ortho* PPh], 7.49 [4 H, d, *meta* OC$_6$H$_4$C$_6$F$_{13}$, ^{3}J(HH) 8.8 Hz],

7.40 [3 H, m, *meta/para* PPh], 7.31 [4 H, d, *ortho* $OC_6H_4C_6F_{13}$, $^3J(HH)$ 8.8 Hz], 2.02 [6 H, q, CH_2, $^3J(HH)$ 7.5 Hz], 0.93 [9 H, t, CH_3, $^3J(HH)$ 7.5 Hz]. δ $^{19}F\{^1H\}$ NMR ($CDCl_3$) -81.25 [3 F, tt, CF_3 $^3J(FF)$ 2.2 Hz, $^4J(FF)$ 10.0 Hz], -110.96 [2 F, t, $^\alpha CF_2$ $^4J(FF)$ 14.6 Hz], -121.85 [2 F, m, $^\beta CF_2$], -122.35 [2 F, m, $^\delta CF_2$], -123.24 [2 F, m, $^\epsilon CF_2$] and -126.58 [2 F, m, $^\gamma CF_2$]. δ $^{31}P\{^1H\}$ NMR ($CDCl_3$) 97.92 [1 P, d, $^1J(PtP)$ 5195 Hz, $^2J(PP)$ 15.8 Hz] and 16.10 [1 P, d, $^1J(PtP)$ 3276 Hz, $^2J(PP)$ 15.8 Hz]. Electron impact (EI) mass spectrum: *m/z* 1280 ($[M - Cl]^+$), 1242 ($[M - 2Cl]^+$). Found: C, 33.2; H, 2.1; P, 4.7. Calc. for $PtCl_2(PEt_3)\{PhP(OC_6H_4C_6F_{13})_2\}$: C, 32.9; H, 2.1; P, 4.7%.

6.6.2.3   *Preparation of cis-PtCl₂(PEt₃){P(OC₆H₄-4-C₆F₁₃)₃} (3.11)*

Cis-$PtCl_2(PEt_3)\{P(OC_6H_4-4-C_6F_{13})_3$ was prepared similarly to (**3.9**) using [{$PtCl(\mu$-Cl)(PEt_3)\}_2$] (0.067 g, 0.09 mmol) and $P(OC_6H_4-4-C_6F_{13})_3$ (0.272 g, 0.22 mmol) to afford the product as a fine white solid. Yield 0.209 g, 73%. δ ^1H NMR ($CDCl_3$) 7.73 [6 H, m, *meta* $OC_6H_4C_6F_{13}$, $^3J(HH)$ 8.7 Hz], 7.62 [6 H, m, *ortho* $OC_6H_4C_6F_{13}$, $^3J(HH)$ 8.7 Hz], 2.21 [6 H, dq, CH_2, $^2J(PH)$ 10.2 Hz, $^3J(HH)$ 7.6 Hz] and 1.04 [9 H, m, CH_3, $^3J(PH)$ 18.2 Hz, $^3J(HH)$ 7.6 Hz]. δ $^{19}F\{^1H\}$ NMR ($CDCl_3$) -81.33 [3 F, tt, CF_3 $^4J(FF)$ 10.1 Hz, $^3J(FF)$ 2.3 Hz], -111.03 [2 F, t, $^\alpha CF_2$ $^4J(FF)$ 14.3 Hz], -121.90 [2 F, m, $^\beta CF_2$], -122.23 [2 F, m, $^\delta CF_2$], -123.28 [2 F, m, $^\epsilon CF_2$] and -126.62 [2 F, m, $^\gamma CF_2$]. δ $^{31}P\{^1H\}$ NMR ($CDCl_3$) 66.32 [1 P, d, $^1J(PtP)$ 6300 Hz, $^2J(PP)$ 19.9 Hz] and 17.59 [1 P, d, $^1J(PtP)$ 3105 Hz, $^2J(PP)$ 19.9 Hz]. FAB mass spectrum: *m/z* 1613 ($[M - Cl]^+$), 1576 ($[M - 2Cl]^+$). Found: C, 30.6; H, 1.38; Cl, 4.14. Calc. for $PtCl_2(PEt_3)\{P(OC_6H_4C_6F_{13})_3\}$: C, 30.6; H, 1.65; Cl, 4.30%.

6.6.2.4   *Preparation of cis-PtCl₂(PEt₃){Ph₂P(OC₂H₄C₆F₁₃)} (3.12)*

Cis-$PtCl_2(PEt_3)\{Ph_2P(OC_2H_4C_6F_{13})\}$ was prepared similarly to (**3.9**) using [{$PtCl(\mu$-Cl)(PEt_3)\}_2$] (0.150 g, 0.2 mmol) and $Ph_2P(OC_2H_4C_6F_{13})$ (0.274 g, 0.5 mmol) to afford the product as a fine, white solid. Yield 0.261 g, 72%. δ ^1H NMR ($CDCl_3$) 8.07 [4 H, m, *ortho* PPh], 7.75 [6 H, m, *meta/para* PPh], 4.27 [4 H, cq, OCH_2, $^3J(HH) \approx$ $^3J(PH)$ 6.0 Hz], 2.48 [2 H, tt, CH_2CF_2 $^3J(HH)$ 6.0 Hz, $^3J(FH)$ 18.4 Hz], 2.27 [6 H, dq,

CH$_2$ ^2J(PH) 10.5 Hz, ^3J(HH) 7.6 Hz] and 1.35 [9 H, dt, CH$_3$ ^3J(PH) 17.6 Hz, ^3J(HH) 7.6 Hz]. δ ^{19}F{^{1}H} NMR (CDCl$_3$) -81.21 [3 F, tt, CF$_3$ ^4J(FF) 10.0 Hz, ^3J(FF) 2.3 Hz], -113.58 [2 F, tm, $^\alpha$CF$_2$ ^4J(FF) 13.9 Hz], -122.25 [2 F, m, $^\beta$CF$_2$], -123.27 [2 F, m, $^\delta$CF$_2$], -124.06 [2 F, m, $^\epsilon$CF$_2$] and -126.58 [2 F, m, $^\gamma$CF$_2$]. δ ^{31}P{^{1}H} NMR (CDCl$_3$) 86.61 [1 P, d, ^1J(PtP) 4342 Hz, ^2J(PP) 16.2 Hz] and 12.89 [1 P, d, ^1J(PtP) 3423 Hz, ^2J(PP) 16.2 Hz]. FAB mass spectrum: m/z 897 ([M - Cl]$^+$), 862 ([M - 2 Cl]$^+$). Found: C, 33.5; H, 2.79; Cl, 6.9. Calc. for PtCl$_2$(PEt$_3$){Ph$_2$P(OC$_6$H$_4$C$_6$F$_{13}$)}: C, 33.5; H, 3.13; Cl, 7.6%.

6.6.2.5   Preparation of cis-PtCl$_2$(PEt$_3$){PhP(OC$_2$H$_4$C$_6$F$_{13}$)$_2$} (3.13)

Cis-PtCl$_2$(PEt$_3$){PhP(OC$_2$H$_4$C$_6$F$_{13}$)$_2$} was prepared similarly to (3.9) using [{PtCl(μ-Cl)(PEt$_3$)}$_2$] (0.100 g, 0.13 mmol) and PhP(OC$_2$H$_4$C$_6$F$_{13}$)$_2$ (0.318 g, 0.38 mmol) to afford the product as a fine, white solid. Yield 0.081 g, 26%. δ ^{1}H NMR (CDCl$_3$) 7.80 [2 H, m, *ortho* PPh], 7.59 [3 H, m, *meta/para* PPh], 4.67 [2 H, m, OCH], 4.36 [2 H, m, OCH], 2.57 [4 H, m, CH$_2$CF$_2$], 2.25 [6 H, dq, CH$_2$, ^2J(PH) 10.5 Hz, ^3J(HH) 7.7 Hz] and 1.29 [9 H, dt, CH$_3$, ^3J(PH) 17.6 Hz, ^3J(HH) 7.7 Hz]. δ ^{19}F{^{1}H} NMR (CDCl$_3$) -81.31 [3 F, tm, CF$_3$ ^4J(FF) 10.0 Hz], -113.84 [2 F, m, $^\alpha$CF$_2$ ^4J(FF) 13.9 Hz], -122.33 [2 F, m, $^\beta$CF$_2$], -123.34 [2 F, m, $^\delta$CF$_2$], -124.06 [2 F, m, $^\epsilon$CF$_2$] and -126.61 [2 F, m, $^\gamma$CF$_2$]. δ ^{31}P{^{1}H} NMR (CDCl$_3$) 100.67 [1 P, d, ^1J(PtP) 4912 Hz, ^2J(PP) 16.6 Hz] and 15.60 [1 P, d, ^1J(PtP) 3383 Hz, ^2J(PP) 16.6 Hz]. Electron impact (EI) mass spectrum: m/z 1183 ([M - Cl]$^+$), 1147 ([M - 2Cl]$^+$). Found: C, 28.0; H, 2.1; P, 4.7. Calc. for PtCl$_2$(PEt$_3$){PhP(OC$_6$H$_4$C$_6$F$_{13}$)$_2$}: C, 27.6; H, 2.3; P, 5.1%.

6.6.2.6   Preparation of cis-PtCl$_2$(PEt$_3$){P(OC$_2$H$_4$C$_6$F$_{13}$)$_3$} (3.14)

A slurry of [{PtCl(μ-Cl)(PEt$_3$)}$_2$] (0.081 g, 0.10 mmol) and P(OC$_2$H$_4$C$_6$F$_{13}$)$_3$ (0.239 g, 0.21 mmol) in dichloromethane (30 cm^3) was heated under reflux under nitrogen to give a clear solution. The solution was cooled, extracted with PP3 (3 x 10 cm^3) to remove excess phosphite, and the solvent removed *in vacuo* to afford product as a sticky white solid. Yield 0.187 g, 62%. δ ^{1}H NMR (CDCl$_3$) 4.53 [6 H, m, OCH$_2$], 2.49 [6 H, tt, CH$_2$CF$_2$, ^3J(HH) 5.4 Hz, ^3J(HF) 18.3 Hz], 2.03 [6 H, dq, PCH$_2$, ^3J(HH) 7.6

Hz, ^2J(PH) 10.7 Hz] and 1.10 [9 H, dt, CH$_3$, ^3J(HH) 7.6 Hz, ^3J(PH) 17.9 Hz]. δ ^{19}F{^{1}H} NMR (CDCl$_3$) -81.48 [3 F, tt, CF$_3$ ^3J(FF) 2.3 Hz, ^4J(FF) 10.0 Hz], -113.93 [2 F, bt, $^\alpha$CF$_2$, ^4J(FF) 14.0 Hz], -122.46 [2 F, m, $^\beta$CF$_2$], -123.48 [2 F, m, $^\delta$CF$_2$], -124.14 [2 F, m, $^\epsilon$CF$_2$], -126.78 [2 F, m, $^\gamma$CF$_2$]. δ ^{31}P{^{1}H} NMR (CDCl$_3$) 75.28 [1 P, d, P(O)$_3$, ^1J(PtP) 5875 Hz, ^2J(PP) 21.2 Hz], and 16.72 [1 P, d, P(CH$_2$)$_3$, ^1J(PtP) 3288 Hz, ^2J(PP) 21.2 Hz]. FAB mass spectrum: m/z 1468 [$(M)^+$]. Found: C, 23.9; H, 1.81; P, 4.1. Calc. for PtCl$_2$(PEt$_3$){P(OC$_2$H$_4$C$_6$F$_{13}$)$_3$}: C, 23.9; H, 1.70; P, 4.0%.

6.6.3 Synthesis of Palladium (II) complexes of the type [PdCl$_2$L$_2$].

6.6.3.1 *Preparation of cis-PdCl$_2${Ph$_2$P(OC$_6$H$_4$-4-C$_6$F$_{13}$)}$_2$ (3.15)*

A slurry of PdCl$_2$(MeCN)$_2$ (0.075 g, 0.29 mmol) and Ph$_2$P(OC$_6$H$_4$-4-C$_6$F$_{13}$) (0.400 g, 0.67 mmol) in dichloromethane (30 cm^3) was heated under reflux under nitrogen for 2 hrs to give a clear colourless solution. The solution was allowed to cool and concentrated by rotary evaporation. Addition of petroleum ether precipitated the product as a fine pale yellow solid, which was filtered, washed with petroleum ether and dried *in vacuo*. Yield 0.192 g, 57%. δ ^{1}H NMR (CDCl$_3$) 7.49 [4 H, m, *ortho* PPh], 7.29 [2 H, d, *meta* OC$_6$H$_4$C$_6$F$_{13}$ ^3J(HH) 8.8 Hz], 7.19 [6 H, m, *meta/para* PPh] and 7.16 [2 H, d, *ortho* OC$_6$H$_4$C$_6$F$_{13}$ ^3J(HH) 8.8 Hz]. δ ^{19}F{^{1}H} NMR (CDCl$_3$) -81.24 [3 F, tt, CF$_3$ ^3J(FF) 2.2 Hz, ^4J(FF) 10.0 Hz], -110.69 [2 F, tm, $^\alpha$CF$_2$ ^4J(FF) 14.5 Hz], -121.86 [2 F, m, $^\beta$CF$_2$], -122.29 [2 F, m, $^\delta$CF$_2$], -123.24 [2 F, m, $^\epsilon$CF$_2$] and -126.57 [2 F, m, $^\gamma$CF$_2$]. δ ^{31}P{^{1}H} NMR (CDCl$_3$) 113.1 [s]. IR (Nujol) ν (Pd-Cl) 290, 316 cm^{-1}.

6.6.3.2 *Preparation of cis-PdCl$_2${PhP(OC$_6$H$_4$-4-C$_6$F$_{13}$)$_2$}$_2$ (3.16)*

Cis-PdCl$_2${PhP(OC$_6$H$_4$-4-C$_6$F$_{13}$)$_2$}$_2$ was prepared similarly to (3.15) using PdCl$_2$(MeCN)$_2$ (0.035 g, 0.14 mmol) and PhP(OC$_6$H$_4$-4-C$_6$F$_{13}$)$_2$ (0.300 g, 0.32 mmol) to afford the product as a fine, pale yellow solid. Yield 0.093 g, 34%. δ ^{1}H NMR (CDCl$_3$) 7.59 [2 H, m, *ortho* PPh], 7.54 [4 H, d, *meta* OC$_6$H$_4$C$_6$F$_{13}$ ^3J(HH) 8.7 Hz], 7.38 [3 H, m, *meta/para* PPh] and 7.19 [4 H, d, *ortho* OC$_6$H$_4$C$_6$F$_{13}$ ^3J(HH) 8.7 Hz]. δ ^{19}F{^{1}H} NMR (CDCl$_3$) -81.27 [3 F, tm, CF$_3$ ^4J(FF) 9.8 Hz], -111.01 [2 F, tm, $^\alpha$CF$_2$

^4J(FF) 13.8 Hz], -121.88 [2 F, m, $^\beta$CF$_2$], -122.22 [2 F, m, $^\delta$CF$_2$], -123.27 [2 F, m, $^\epsilon$CF$_2$], -126.59 [2 F, m, $^\gamma$CF$_2$]. δ ^{31}P{^{1}H} NMR (CDCl$_3$) 122.23 [1 P, s]. Electron impact (EI) mass spectrum: m/z 2001 ([M - Cl]$^+$), 1966 ([M - 2Cl]$^+$). Found: C, 35.3; H, 1.20; Cl, 3.42. Calc. for PdCl$_2${PhP(OC$_6$H$_4$-4-C$_6$F$_{13}$)$_2$}$_2$: C, 35.4; H, 1.29; Cl, 3.48%. IR (Nujol) v (Pd-Cl) 294, 326 cm^{-1}.

6.6.3.3 Preparation of cis-PdCl$_2${P(OC$_6$H$_4$-4-C$_6$F$_{13}$)$_3$}$_2$ (3.17)

Cis-PdCl$_2${P(OC$_6$H$_4$-4-C$_6$F$_{13}$)$_3$}$_2$ was prepared similarly to (3.15) using PdCl$_2$(MeCN)$_2$ (0.036 g, 0.14 mmol) and P(OC$_6$H$_4$-4-C$_6$F$_{13}$)$_3$ (0.400 g, 0.32 mmol) to afford the product as a fine pale, yellow solid. Yield 0.233 g, 62%. δ ^{1}H NMR (CDCl$_3$) 7.82 [2 H, d, meta OC$_6$H$_4$C$_6$F$_{13}$ ^3J(HH) 8.7 Hz] and 8.10 [2 H, d, ortho OC$_6$H$_4$C$_6$F$_{13}$ ^3J(HH) 8.7 Hz]. δ ^{19}F{^{1}H} NMR (CDCl$_3$) -80.86 [3 F, tt, CF$_3$ ^3J(FF) 2.2 Hz, ^4J(FF) 10.0 Hz], -109.75 [2 F, tm, $^\alpha$CF$_2$ ^4J(FF) 14.6 Hz], -121.17 [2 F, m, $^\beta$CF$_2$], -121.63 [2 F, m, $^\delta$CF$_2$], -122.57 [2 F, m, $^\epsilon$CF$_2$] and -125.98 [2 F, m, $^\gamma$CF$_2$]. δ ^{31}P{^{1}H} NMR (CDCl$_3$) 83.59 [1 P, s]. Electron impact (EI) mass spectrum: m/z 2671 ([M - Cl]$^+$), 2636 ([M - 2Cl]$^+$). Found: C, 30.6; H, 0.77; Cl, 2.20. Calc. for PdCl$_2${P(OC$_6$H$_4$-4-C$_6$F$_{13}$)$_3$}$_2$: C, 31.9; H, 0.89; Cl, 2.62%. IR (Nujol) v (Pd-Cl) 308, 332 cm^{-1}.

6.6.3.4 Preparation of Pd$_2$Cl$_2${(C$_6$H$_5$)$_2$PO$\cdots$H$\cdots$OP(C$_6$H$_5$)$_2$}$_2$ (3.18)

Pd$_2$Cl$_2${(C$_6$H$_5$)$_2$PO$\cdots$H$\cdots$OP(C$_6$H$_5$)$_2$}$_2$ was isolated from (3.15) from the reaction of PdCl$_2$(MeCN)$_2$ and Ph$_2$P(OC$_6$H$_4$-4-C$_6$F$_{13}$) by recrystallisation from acetone to afford the product yellow crystals. δ ^{1}H NMR (CDCl$_3$) 7.53 [2 H, m, ortho OC$_6$H$_5$], 7.31 [1 H, m, para OC$_6$H$_5$] and 7.19 [2 H, m, meta OC$_6$H$_5$]. δ ^{31}P{^{1}H} NMR (CDCl$_3$) 78.16 [s]. FAB mass spectrum: m/z 509 ([M - PdCl$_2${(C$_6$H$_5$)$_2$PO$\cdots$H$\cdots$OP(C$_6$H$_5$)$_2$}]$^+$). Found: C, 53.0; H, 3.61; Cl, 7.50. Calc. for Pd$_2$Cl$_2${(C$_6$H$_5$)$_2$PO$\cdots$H$\cdots$OP(C$_6$H$_5$)$_2$}$_2$: C, 53.0; H, 3.70; Cl, 6.51%.

6.6.3.5 *Preparation of cis-PdCl$_2${P(OC$_6$H$_4$-3-C$_6$F$_{13}$)$_3$}$_2$* **(3.19)**

Cis-PdCl$_2${P(OC$_6$H$_4$-3-C$_6$F$_{13}$)$_3$}$_2$ was prepared similarly to **(3.15)** using PdCl$_2$(MeCN)$_2$ (0.041 g, 0.16 mmol) and P(OC$_6$H$_4$-3-C$_6$F$_{13}$)$_3$ (0.402 g, 0.32 mmol) to afford the product as a pale, orange oil. Yield 0.276 g, 62%. δ ^{1}H NMR (CDCl$_3$) 7.42 [3 H, m, *ortho, meta, para* OC$_6$H$_4$] and 7.11 [1 H, s, *ortho* OC$_6$H$_4$]. δ ^{19}F{^{1}H} NMR (CDCl$_3$) -81.54 [3 F, tm, CF$_3$ ^4J(FF) 11.3 Hz], -111.72 [2 F, tm, $^\alpha$CF$_2$ ^4J(FF) 14.2 Hz], -122.25 [2 F, m, $^\beta$CF$_2$], -122.39 [2 F, m, $^\delta$CF$_2$], -123.62 [2 F, m, $^\epsilon$CF$_2$] and -126.89 [2 F, m, $^\gamma$CF$_2$]. δ ^{31}P{^{1}H} NMR (CDCl$_3$) 82.97 [s]. Electron impact (EI) mass spectrum: *m/z* 2669 ([*M* - Cl]$^+$), 2633 ([*M* - 2Cl-H]$^+$). Found: C, 31.7; H, 0.98; P, 2.2. Calc. for PdCl$_2${P(OC$_6$H$_4$C$_6$F$_{13}$)$_3$}$_2$: C, 31.9; H, 0.89; P, 2.3%.

6.6.3.6 *Preparation of trans-PdCl$_2${P(OC$_6$H$_4$-2-C$_6$F$_{13}$)$_3$}$_2$* **(3.20)**

Trans-PdCl$_2${P(OC$_6$H$_4$-2-C$_6$F$_{13}$)$_3$}$_2$ was prepared similarly to **(3.15)** using PdCl$_2$(MeCN)$_2$ (0.031 g, 0.12 mmol) and P(OC$_6$H$_4$-2-C$_6$F$_{13}$)$_3$ (0.301 g, 0.24 mmol) to afford the product as a pale, yellow solid. Yield 0.142 g, 43%. δ ^{1}H NMR (d^6 acetone) 7.50 [4 H, m, *ortho, meta, para* OC$_6$H$_4$]. δ ^{19}F{^{1}H} NMR (d^6 acetone) -82.31 [3 F, tm, CF$_3$ ^4J(FF) 11.0 Hz], -108.91 [2 F, m, $^\alpha$CF$_2$], -121.90 [2 F, m, $^\beta$CF$_2$], -122.67 [2 F, m, $^\delta$CF$_2$], -123.91 [2 F, m, $^\epsilon$CF$_2$] and -127.41 [2 F, m, $^\gamma$CF$_2$]. δ ^{31}P{^{1}H} NMR (d^6 acetone) 85.52 [s]. FAB mass spectrum: *m/z* 2636 ([*M* - 2Cl]$^+$). Found: C, 31.9; H, 0.91; P, 2.1. Calc. for PdCl$_2${P(OC$_6$H$_4$-2-C$_6$F$_{13}$)$_3$}$_2$: C, 31.9; H, 0.89; P, 2.3%.

6.6.3.7 *Preparation of cis-PdCl$_2${Ph$_2$P(OC$_2$H$_4$C$_6$F$_{13}$)}$_2$* **(3.21)**

Cis-PdCl$_2${Ph$_2$P(OC$_2$H$_4$C$_6$F$_{13}$)}$_2$ was prepared similarly to **(3.15)** using PdCl$_2$(MeCN)$_2$ (0.090 g, 0.35 mmol) and Ph$_2$P(OC$_2$H$_4$C$_6$F$_{13}$) (0.436 g, 0.83 mmol) to afford the product as a pale, yellow solid. Yield 0.350 g, 79%. δ ^{1}H NMR (CDCl$_3$) 7.73 [4 H, m, *ortho* PPh], 7.41 [6 H, m, *meta/para* PPh], 3.84 [2 H, cq, OCH$_2$ ^3J(HH) ≈ ^3J(PH) 6.3 Hz] and 1.92 [2 H, tt, CH$_2$CF$_2$ ^3J(HH) 6.3 Hz, ^3J(FH) 18.4 Hz]. δ ^{19}F{^{1}H} NMR (CDCl$_3$) -81.36 [3 F, tm, CF$_3$ ^4J(FF) 10.0 Hz], -113.97 [2 F, tm, $^\alpha$CF$_2$ ^4J(FF) 13.6 Hz], -122.42 [2 F, m, $^\beta$CF$_2$], -123.42 [2 F, m, $^\delta$CF$_2$], -124.18 [2 F, m, $^\epsilon$CF$_2$]

and -126.69 [2 F, m, $^\gamma$CF$_2$]. δ ^{31}P{^{1}H} NMR (CDCl$_3$) 112.92 [1 P, s]. Electron impact (EI) mass spectrum: m/z 1237 ([M - Cl]$^+$), 1202 ([M - 2Cl]$^+$). Found: C, 37.7; H, 2.04; P5.02, 6.9. Calc. for PdCl$_2${Ph$_2$P(OC$_2$H$_4$C$_6$F$_{13}$)}$_2$: C, 37.7; H, 2.22; P, 4.86%. IR (Nujol) v (Pd-Cl) 290, 315 cm^{-1}.

6.6.3.8   *Preparation of cis-PdCl$_2${PhP(OC$_2$H$_4$C$_6$F$_{13}$)$_2$}$_2$* (3.22)

Cis-PdCl$_2${PhP(OC$_2$H$_4$C$_6$F$_{13}$)$_2$}$_2$ was prepared similarly to (**3.15**) using PdCl$_2$(MeCN)$_2$ (0.102 g, 0.39 mmol) and PhP(OC$_2$H$_4$C$_6$F$_{13}$)$_2$ (0.634 g, 0.82 mmol) to afford the product as a pale, yellow solid. Yield 0.608 g, 84%. δ ^{1}H NMR (CDCl$_3$) 7.77 [2 H, m, *ortho* PPh], 7.56 [3 H, m, *meta/para* PPh], 4.58 [2 H, m, OCH$_2$], 4.36 [2 H, m, OCH$_2$] and 2.48 [4 H, m, CH$_2$CF$_2$]. δ ^{19}F{^{1}H} NMR (CDCl$_3$) -81.67 [3 F, tm, CF$_3$ ^4J(FF) 10.0 Hz], -114.17 [2 F, dt, $^\alpha$CF$_2$ ^4J(FF) 14.3 Hz], -122.59 [2 F, m, $^\beta$CF$_2$], -123.61 [2 F, m, $^\delta$CF$_2$], -124.21 [2 F, m, $^\varepsilon$CF$_2$] and -126.98 [2 F, m, $^\gamma$CF$_2$]. δ ^{31}P{^{1}H} NMR (CDCl$_3$) 126.38 [1 P, s]. Electron impact (EI) mass spectrum: 1809 ([M - Cl]$^+$), 1774 ([M - 2Cl]$^+$). IR (Nujol) v (Pd-Cl) 304, 325 cm^{-1}.

6.6.3.9   *Preparation of cis-PdCl$_2${P(OC$_2$H$_4$C$_6$F$_{13}$)$_3$}$_2$* (3.23)

Cis-PdCl$_2${P(OC$_2$H$_4$C$_6$F$_{13}$)$_3$}$_2$ was prepared similarly to (**3.15**) using [PdCl$_2$(MeCN)$_2$] (0.029 g, 0.12 mmol) and P(OC$_2$H$_4$C$_6$F$_{13}$)$_3$ (0.300 g, 0.27 mmol). The reaction solution was cooled to precipitate the product as a viscous, orange oil which was washed with dichloromethane. Yield 0.173 g, 64%. δ ^{1}H NMR (D$_2$O) 4.65 [6 H, m, OCH$_2$], and 2.60 [6 H, m, CH$_2$CF$_2$]. δ ^{19}F{^{1}H} NMR (d^6 acetone) -81.58 [3 F, m, CF$_3$], -113.97 [2 F, m, $^\alpha$CF$_2$], -122.45 [2 F, m, $^\beta$CF$_2$], -123.58 [2 F, m, $^\delta$CF$_2$], -124.22 [2 F, m, $^\varepsilon$CF$_2$] and -126.91 [2 F, m, $^\gamma$CF$_2$]. δ ^{31}P{^{1}H} NMR (D$_2$O) 94.40 [s]. FAB mass spectrum: m/z 2381 ([M - Cl]$^+$), 2346 ([M - 2Cl]$^+$). IR (Nujol) v (Pd-Cl) 303, 335 cm^{-1}.

6.6.4 Synthesis of Rhodium (III) complexes of the type [Rh(η^5-C$_5$Me$_5$)Cl$_2$L].

6.6.4.1 *Preparation of Cp*RhCl$_2${Ph$_2$P(OC$_6$H$_4$-4-C$_6$F$_{13}$)} (3.24)*

A slurry of [Cp*RhCl$_2$]$_2$ (0.150 g, 0.24 mmol) and Ph$_2$P(OC$_6$H$_4$-4-C$_6$F$_{13}$) (0.350 g, 0.58 mmol) were refluxed in dichloromethane (50 cm^3) under nitrogen for 1 hr to give a clear red solution. The solution was allowed to cool and concentrated by rotary evaporation. Addition of petroleum ether precipitated the product as a fine orange solid, which was filtered, washed with petroleum ether and dried *in vacuo*. Yield 0.346 g, 79%. δ ^{1}H NMR (CDCl$_3$) 8.13 [4 H, m, *ortho* PPh], 7.55 [2 H, d, *meta* OC$_6$H$_4$C$_6$F$_{13}$ ^{3}J(HH) 8.8 Hz], 7.39 [2 H, d, *ortho* OC$_6$H$_4$C$_6$F$_{13}$ ^{3}J(HH) 8.8 Hz], 7.31 [6 H, m, *meta/para* PPh] and 1.26 [15 H, d, J(PH) 4.1 Hz]. δ ^{19}F{^{1}H} NMR (CDCl$_3$) -81.28 [3 F, tt, CF$_3$ ^{3}J(FF) 2.3 Hz, ^{4}J(FF) 10.0 Hz], -110.62 [2 F, tt, $^\alpha$CF$_2$ ^{4}J(FF) 14.1 Hz, ^{3}J(FF) 3.3 Hz], -121.89 [2 F, m, $^\beta$CF$_2$], -122.51 [2 F, m, $^\delta$CF$_2$], -123.25 [2 F, m, $^\epsilon$CF$_2$], -126.58 [2 F, m, $^\gamma$CF$_2$]. δ ^{31}P{^{1}H} NMR (CDCl$_3$) 116.65 [d, ^{1}J(RhP) 171 Hz]. FAB mass spectrum: m/z 869 ([M + O]$^+$), 833 ([M - C$_6$H$_5$]$^+$). Found: C, 45.63; H, 3.25; Cl, 7.60. Calc. for Cp*RhCl$_2${Ph$_2$P(OC$_6$H$_4$C$_6$F$_{13}$)}: C, 45.11; H, 3.23; Cl, 7.83%.

6.6.4.2 *Preparation of Cp*RhCl$_2${PhP(OC$_6$H$_4$-4-C$_6$F$_{13}$)$_2$} (3.25)*

Cp*RhCl$_2${PhP(OC$_6$H$_4$C$_6$F$_{13}$)$_2$} was prepared similarly to (3.24) using [Cp*RhCl$_2$]$_2$ (0.119 g, 0.15 mmol) and PhP(OC$_6$H$_4$-4-C$_6$F$_{13}$)$_2$ (0.300 g, 0.32 mmol) to afford the product as a pale, orange solid. Yield 0.264 g, 67 %. δ ^{1}H NMR (CDCl$_3$) 8.03 [2 H, m, *ortho* C$_6$H$_5$] 7.32 [8 H, m, *ortho/meta* OC$_6$H$_4$C$_6$F$_{13}$], 7.22 [3 H, m, *meta/para* C$_6$H$_5$] and 1.33 [15 H, d, J(PH) 4.7 Hz]. δ ^{19}F{^{1}H} NMR (CDCl$_3$) -81.25 [3 F, tm, CF$_3$, ^{4}J(FF) 10.0 Hz], -110.85 [2 F, tm, $^\alpha$CF$_2$, ^{4}J(FF) 14.0 Hz], -121.85 [2 F, m, $^\beta$CF$_2$], -122.60 [2 F, m, $^\delta$CF$_2$], -123.26 [2 F, m, $^\epsilon$CF$_2$], -126.60 [2 F, m, $^\gamma$CF$_2$]. ^{31}P{^{1}H} NMR (CDCl$_3$) 145.83 [d, ^{1}J(RhP) 203 Hz]. FAB mass spectrum: m/z 1203 [(M - Cl)$^+$], 1167 [(M - 2Cl - H)$^+$]. Found: C, 39.16; H, 2.12; Cl, 5.60. Calc. for Cp*RhCl$_2${PhP(OC$_6$H$_4$C$_6$F$_{13}$)$_2$}: C, 38.76; H, 2.28; Cl, 5.72 %.

6.6.4.3 Preparation of Cp*RhCl₂{P(OC₆H₄-4-C₆F₁₃)₃} (3.26)

Cp*RhCl₂{P(OC₆H₄-4-C₆F₁₃)₃} was prepared similarly to (3.24) using [Cp*RhCl₂]₂ (0.100 g, 0.16 mmol) and P(OC₆H₄-4-C₆F₁₃)₃ (0.446 g, 0.35 mmol) to afford the product as a pale, orange solid. Yield 0.337 g, 66%. δ ^{1}H NMR (CDCl₃) 7.32 [6 H, d, *meta* OC₆H₄C₆F₁₃ ^{3}J(HH) 8.8 Hz], 7.22 [6 H, d, *ortho* OC₆H₄C₆F₁₃ ^{3}J(HH) 8.8 Hz] and 1.41 [15 H, d, J(PH) 6.3 Hz]. δ ^{19}F{^{1}H} NMR (CDCl₃) -81.41 [3 F, tt, CF₃ ^{4}J(FF) 10.0 Hz, ^{3}J(FF) 2.2 Hz], -110.99 [2 F, tm, ^{α}CF₂ ^{4}J(FF) 14.4 Hz], -121.95 [2 F, m, ^{β}CF₂], -122.43 [2 F, m, ^{δ}CF₂], -123.38 [2 F, m, ^{ε}CF₂], -126.71 [2 F, m, ^{γ}CF₂]. δ ^{31}P{^{1}H} NMR (CDCl₃) 106.45 [d, ^{1}J(RhP) 245 Hz]. FAB mass spectrum: m/z 1537 ([M - Cl]⁺), 1502 ([M - 2 Cl]⁺). Found: C, 35.9; H, 1.4; Cl, 4.1. Calc. for Cp*RhCl₂{P(OC₆H₄C₆F₁₃)₃}: C, 35.2; H, 1.73; Cl, 4.5%.

6.6.4.4 Preparation of Cp*RhCl₂{P(OC₆H₄-3-C₆F₁₃)₃} (3.27)

Cp*RhCl₂{P(OC₆H₄-3-C₆F₁₃)₃} was prepared similarly to (3.24) using [Cp*RhCl₂]₂ (0.053 g, 0.09 mmol) and P(OC₆H₄-3-C₆F₁₃)₃ (0.216 g, 0.17 mmol) to afford the product as a pale, orange solid. Yield 0.216 g, 76%. δ ^{1}H NMR (CDCl₃) 7.71 [1 H, d, *ortho* OC₆H₄ ^{3}J(HH) 7.6 Hz], 7.45 [1 H, t, *meta* OC₆H₄ ^{3}J(HH) 7.9 Hz], 7.38 [1 H, d, *para* OC₆H₄ ^{3}J(HH) 7.9 Hz], 7.21 [1 H, s, *ortho* OC₆H₄] and 1.41 [15 H, d, J(PH) 6.3 Hz]. δ ^{19}F{^{1}H} NMR (CDCl₃) -81.42 [3 F, tm, CF₃ ^{4}J(FF) 8.5 Hz], -111.34 [2 F, tm, ^{α}CF₂ ^{4}J(FF) 14.2 Hz], -122.11 [2 F, m, ^{β}CF₂], -122.34 [2 F, m, ^{δ}CF₂], -123.51 [2 F, m, ^{ε}CF₂], -126.78 [2 F, m, ^{γ}CF₂]. δ ^{31}P{^{1}H} NMR (CDCl₃) 107.07 [d, ^{1}J(RhP) 244 Hz]. FAB mass spectrum: m/z 1537 ([M - Cl]⁺). Found: C, 35.3; H, 1.7; P, 1.2. Calc. for Cp*RhCl₂{P(OC₆H₄C₆F₁₃)₃}: C, 35.2; H, 1.73; P, 1.9%.

6.6.4.5 Preparation of Cp*RhCl₂{P(OC₆H₄-2-C₆F₁₃)₃} (3.28)

Cp*RhCl₂{P(OC₆H₄-2-C₆F₁₃)₃} was prepared similarly to (3.24) using [Cp*RhCl₂]₂ (0.068 g, 0.11 mmol) and P(OC₆H₄-2-C₆F₁₃)₃ (0.280 g, 0.22 mmol) to afford the product as a pale, orange solid. Yield 0.143 g, 41%. δ ^{1}H NMR (CDCl₃) 8.05 [1 H, d, *ortho* OC₆H₄ ^{3}J(HH) 8.0 Hz], 7.39 [2 H, m, OC₆H₄]], 7.21 [1 H, m, OC₆H₄] and 1.36 [15 H, d, J(PH) 6.2 Hz]. δ ^{19}F{^{1}H} NMR (CDCl₃) -81.52 [3 F, tm, CF₃ ^{4}J(FF) 11.3

Hz], -107.52 [2 F, m, $^\alpha$CF$_2$], -121.55 [2 F, m, $^\beta$CF$_2$], -122.35 [2 F, m, $^\delta$CF$_2$], -123.53 [2 F, m, $^\epsilon$CF$_2$], -126.90 [2 F, m, $^\gamma$CF$_2$]. δ ^{31}P{^{1}H} NMR (CDCl$_3$) 109.83 [d, ^{1}J(RhP) 251 Hz]. FAB mass spectrum: m/z 1572 ([M - Cl]$^+$), 1537 ([M - Cl]$^+$). Found: C, 35.09; H, 1.68; P, 1.8. Calc. for Cp*RhCl$_2$\{P(OC$_6$H$_4$C$_6$F$_{13}$)$_3$\}: C, 35.2; H, 1.73; P, 1.97%.

6.6.4.6   Preparation of Cp*RhCl$_2$\{Ph$_2$P(OC$_2$H$_4$C$_6$F$_{13}$)\} (3.29)

Cp*RhCl$_2$\{Ph$_2$P(OC$_2$H$_4$C$_6$F$_{13}$)\} was prepared similarly to (3.24) using [Cp*RhCl$_2$]$_2$ (0.200 g, 0.32 mmol) and Ph$_2$P(OC$_2$H$_4$C$_6$F$_{13}$) (0.417 g, 0.76 mmol) to afford the product as a pale, orange solid. Yield 0.400 g, 72%. δ ^{1}H NMR (CDCl$_3$) 7.93 [4 H, m, ortho PPh], 7.32 [6 H, m, meta/para PPh], 4.09 [2 H, cq, OCH$_2$, ^{3}J(HH) $\approx$ ^{3}J(PH) 6.1 Hz], 2.24 [2 H, tt, CH$_2$CF$_2$ ^{3}J(HH) 5.4 Hz, ^{3}J(FH) 18.9 Hz] and 1.36 [15 H, d, J(PH) 3.8 Hz]. δ ^{19}F{^{1}H} NMR (CDCl$_3$) -81.22 [3 F, tm, CF$_3$ ^{4}J(FF) 10.0 Hz], -113.57 [2 F, tm, $^\alpha$CF$_2$ ^{4}J(FF) 14.1 Hz], -122.18 [2 F, m, $^\beta$CF$_2$], -123.28 [2 F, m, $^\delta$CF$_2$], -124.01 [2 F, m, $^\epsilon$CF$_2$], -126.54 [2 F, m, $^\gamma$CF$_2$]. δ ^{31}P{^{1}H} NMR (CDCl$_3$) 117.12 [1P, d, ^{1}J(RhP) 157 Hz]. FAB mass spectrum: m/z 821 ([M - Cl]$^+$), 786 ([M - 2 Cl]$^+$). Found: C, 42.08; H, 3.26; P, 3.05. Calc. for Cp*RhCl$_2$\{Ph$_2$(OC$_2$H$_4$C$_6$F$_{13}$)\}: C, 42.03; H, 3.41; P, 3.61%.

6.6.4.7   Preparation of Cp*RhCl$_2$\{PhP(OC$_2$H$_4$C$_6$F$_{13}$)$_2$\} (3.30)

Cp*RhCl$_2$\{PhP(OC$_2$H$_4$C$_6$F$_{13}$)$_2$\} was prepared similarly to (3.24) using [Cp*RhCl$_2$]$_2$ (0.207 g, 0.33 mmol) and PhP(OC$_2$H$_4$C$_6$F$_{13}$)$_2$ (0.600 g, 0.72 mmol) to afford the product as a red solid. Yield 0.261 g, 34%. δ ^{1}H NMR (CDCl$_3$) 7.95 [2 H, m, ortho PPh], 7.44 [3 H, m, meta/para PPh], 4.68 [2 H, m, OCH$_2$], 4.41 [2 H, m, OCH$_2$] 2.45 [4 H, m, CH$_2$ CF$_2$], 1.39 [15 H, d, J(PH) 4.1 Hz]. δ ^{19}F{^{1}H} NMR (CDCl$_3$) -81.34 [3 F, t, CF$_3$ ^{4}J(FF) 9.8 Hz], -113.79 [2 F, m, $^\alpha$CF$_2$], -122.35 [2 F, m, $^\beta$CF$_2$], -123.38 [2 F, m, $^\delta$CF$_2$], -124.13 [2 F, m, $^\epsilon$CF$_2$], -126.66 [2 F, m, $^\gamma$CF$_2$]. δ ^{31}P{^{1}H} NMR (CDCl$_3$) 147.40 [1 P, d, ^{1}J(RhP) 181 Hz]. FAB mass spectrum: m/z 1143 ([M]$^+$), 1107 ([M - Cl]$^+$). Found: C, 34.0; H, 2.35; Cl, 5.8. Calc. for Cp*RhCl$_2$\{PhP(OC$_2$H$_4$C$_6$F$_{13}$)$_2$\}: C, 33.6; H, 2.47; Cl, 6.2%.

6.6.4.8 Preparation of Cp*RhCl₂{P(OC₂H₄C₆F₁₃)₃} (3.31)

Cp*RhCl₂{P(OC₂H₄C₆F₁₃)₃} was prepared similarly to (3.24) using [Cp*RhCl₂]₂ (0.105 g, 0.17 mmol) and P(OC₂H₄C₆F₁₃)₃ (0.446 g, 0.40 mmol). The reaction solvent was removed by rotary evaporation to afford impure product as a red oil which was purified by solvent extraction with PP3 from chloroform. Yield 0.204 g, 42%. δ ^{1}H NMR (CDCl₃) 4.48 [6 H, cq, OCH₂, ^3J(HH) ≈ ^3J(PH) 6.0 Hz], 2.42 [6 H, tt, CH₂CF₂ ^3J(HH) 6.0 Hz, ^3J(FH) 18.4 Hz] and 1.62 [15 H, d, J(PH) 5.7 Hz]. δ ^{19}F{^{1}H} NMR (CDCl₃) -81.47 [3 F, tt, CF₃ ^4J(FF) 10.0 Hz, ^3J(FF) 2.3 Hz], -113.85 [2 F, tm, $^\alpha$CF₂ ^4J(FF) 13.9 Hz], -122.46 [2 F, m, $^\beta$CF₂], -123.49 [2 F, m, $^\delta$CF₂], -124.18 [2 F, m, $^\epsilon$CF₂], -126.78 [2 F, m, $^\gamma$CF₂]. δ ^{31}P{^{1}H} NMR (CDCl₃) 120.25 [1P, d, ^1J(RhP) 224 Hz]. FAB mass spectrum: m/z 1393 ([M + O]$^+$), 1357 ([M - C₆H₅]$^+$). Found: C, 28.54; H, 2.00; P, 1.99. Calc. for Cp*RhCl₂{P(OC₂H₄C₆F₁₃)₃}: C, 28.57; H, 1.90; P, 2.17%.

6.6.5 Synthesis of Iridium (III) complexes of the type [Ir(η⁵-C₅Me₅)Cl₂L].

6.6.5.1 Preparation of Cp*IrCl₂{Ph₂P(OC₆H₄-4-C₆F₁₃)} (3.32)

A slurry of [Cp*IrCl₂]₂ (0.100 g, 0.13 mmol) and Ph₂P(OC₆H₄-4-C₆F₁₃) (0.200 g, 0.34 mmol) were refluxed in benzene (50 cm³) under nitrogen for 6 hrs to give a clear orange solution. The solution was allowed to cool and concentrated by rotary evaporation. Addition of petroleum ether precipitated the product as a fine light orange solid, which was filtered, washed with petroleum ether and dried *in vacuo*. Yield 0.119 g, 48%. δ ^{1}H NMR (CDCl₃) 8.35 [4 H, m, *ortho* PPh], 7.72 [2 H, d, *meta* OC₆H₄C₆F₁₃ ^3J(HH) 8.8 Hz], 7.61 [2 H, d, *ortho* OC₆H₄C₆F₁₃ ^3J(HH) 8.8 Hz], 7.51 [6 H, m, *meta/para* PPh] and 1.46 [15 H, d, J(PH) 2.2 Hz]. δ ^{19}F{^{1}H} NMR (CDCl₃) -81.23 [3 F, tm, CF₃ ^4J(FF) 10.0 Hz], -110.60 [2 F, tm, $^\alpha$CF₂ ^4J(FF) 14.1 Hz], -121.85 [2 F, m, $^\beta$CF₂], -122.45 [2 F, m, $^\delta$CF₂], -123.23 [2 F, m, $^\epsilon$CF₂], -126.55 [2 F, m, $^\gamma$CF₂]. δ ^{31}P{^{1}H} NMR (CDCl₃) 75.17 [s]. FAB mass spectrum: m/z 994 ([M]$^+$), 923 ([M - 2 Cl]$^+$). Found: C, 41.05; H, 2.85; Cl, 6.22. Calc. for Cp*RhCl₂{Ph₂P(OC₂H₄C₆F₁₃)}: C, 41.06; H, 2.94; Cl, 7.13%.

6.6.5.2 *Preparation of Cp*IrCl₂{PhP(OC₆H₄-4-C₆F₁₃)₂}* (3.33)

Cp*IrCl₂{PhP(OC₆H₄-4-C₆F₁₃)₂} was prepared similarly to (3.32) using [Cp*IrCl₂]₂ (0.119 g, 0.15 mmol) and PhP(OC₆H₄-4-C₆F₁₃)₂ (0.300 g, 0.32 mmol) to afford the product as a pale, orange solid. Yield 0.264 g, 67%. δ ^{1}H NMR (CDCl₃) 8.35 [2 H, m, *ortho* C₆H₅], 7.63 [11 H, m, *meta/para* C₆H₅, *ortho/meta* OC₆H₄C₆F₁₃] and 1.62 [15 H, d, Cp*, J(PH) 3.1 Hz]. δ ^{19}F{^{1}H} NMR (CDCl₃) -81.25 [3 F, tt, CF₃, ^{3}J(FF) 2.3 Hz, ^{4}J(FF) 10.0 Hz], -110.85 [2 F, tm, $^\alpha$CF₂, ^{4}J(FF) 14.0 Hz], -121.85 [2 F, m, $^\beta$CF₂], -122.58 [2 F, m, $^\delta$CF₂], -123.27 [2 F, m, $^\epsilon$CF₂], -126.59 [2 F, m, $^\gamma$CF₂]. δ ^{31}P{^{1}H} NMR (CDCl₃) 102.39 [s]. Electron impact (FAB) mass spectrum: m/z 1328 [(M)⁺], 1293 [(M - Cl)⁺]. Found: C, 36.30; H, 1.97; Cl, 4.95. Calc. for Cp*IrCl₂{PhP(OC₆H₄C₆F₁₃)₂}: C, 36.16; H, 2.12; Cl, 5.34%.

6.6.5.3 *Preparation of Cp*IrCl₂{P(OC₆H₄-4-C₆F₁₃)₃}* (3.34)

Cp*IrCl₂{P(OC₆H₄-4-C₆F₁₃)₃} was prepared similarly to (3.32) using [Cp*IrCl₂]₂ (0.090 g, 0.12 mmol) and P(OC₆H₄-4-C₆F₁₃)₃ (0.310 g, 0.25 mmol) to afford the product as a pale orange solid. Yield 0.196 g, 52%. δ ^{1}H NMR (CDCl₃) 7.47 [6 H, d, *meta* OC₆H₄C₆F₁₃ ^{3}J(HH) 8.7 Hz], 7.38 [6 H, d, *ortho* OC₆H₄C₆F₁₃ ^{3}J(HH) 8.7 Hz] and 1.49 [15 H, d, J(PH) 3.8 Hz]. δ ^{19}F{^{1}H} NMR (CDCl₃) -81.30 [3 F, tt, CF₃ ^{4}J(FF) 10.0 Hz, ^{3}J(FF) 2.3 Hz], -110.93 [2 F, tm, $^\alpha$CF₂ ^{4}J(FF) 14.4 Hz], -121.88 [2 F, m, $^\beta$CF₂], -122.33 [2 F, m, $^\delta$CF₂], -123.29 [2 F, m, $^\epsilon$CF₂], -126.62 [2 F, m, $^\gamma$CF₂]. δ ^{31}P{^{1}H} NMR (CDCl₃) 67.69 [s]. Found: C, 33.19; H, 1.45; Cl, 3.41. Calc. for Cp*IrCl₂{P(OC₆H₄C₆F₁₃)₃}: C, 33.23; H, 1.64; Cl, 4.26%.

6.6.5.4 *Preparation of Cp*IrCl₂{Ph₂P(OC₂H₄C₆F₁₃)}* (3.35)

Cp*IrCl₂{Ph₂P(OC₂H₄C₆F₁₃)} was prepared similarly to (3.32) using [Cp*IrCl₂]₂ (0.140 g, 0.18 mmol) and Ph₂P(OC₂H₄C₆F₁₃) (0.220 g, 0.40 mmol) to afford the product as an orange solid. Yield 0.278 g, 84%. δ ^{1}H NMR (CDCl₃) 8.04 [4 H, m, *ortho* C₆H₅], 7.47 [6 H, m, *meta/para* C₆H₅], 4.20 [2 H, cq, OCH₂, ^{3}J(HH) ≈ ^{3}J(PH) 5.9 Hz], 2.39 [2 H, tt, CH₂CF₂, ^{3}J(HH) 5.9 Hz, ^{3}J(FH) 18.7 Hz] and 1.51 [15 H, d, Cp* J(PH) 2.2 Hz]. δ ^{19}F{^{1}H} NMR (CDCl₃) -81.20 [3 F, tt, CF₃, ^{3}J(FF) 2.5 Hz,

^4J(FF) 9.8 Hz], -113.59 [2 F, tm, $^{\alpha}$CF$_2$, ^4J(FF) 14.1 Hz], -122.19 [2 F, m, $^{\beta}$CF$_2$], -123.27 [2 F, m, $^{\delta}$CF$_2$], -124.01 [2 F, m, $^{\epsilon}$CF$_2$], -126.52 [2 F, m, $^{\gamma}$CF$_2$]. δ ^{31}P{^{1}H} NMR (CDCl$_3$) 77.32 [s]. FAB mass spectrum: m/z 946 [(M)$^+$], 911 [(M-Cl)$^+$]. Found: C, 38.04; H, 2.92; P, 3.45. Calc. for Cp*IrCl$_2$\{Ph$_2$P(OC$_6$H$_4$C$_6$F$_{13}$)\}: C, 38.06; H, 3.09; P, 3.27%.

6.6.5.5   Preparation of Cp*IrCl$_2$\{PhP(OC$_2$H$_4$C$_6$F$_{13}$)$_2$\} (3.36)

Cp*IrCl$_2$\{PhP(OC$_2$H$_4$C$_6$F$_{13}$)$_2$\} was prepared as for (3.32) using [Cp*IrCl$_2$]$_2$ (0.105 g, 0.13 mmol) and PhP(OC$_2$H$_4$C$_6$F$_{13}$)$_2$ (0.243 g, 0.29 mmol) to afford the product as an orange powder. Yield 0.289 g, 89 %. δ ^{1}H NMR (CDCl$_3$) 8.16 [2 H, m, *ortho* C$_6$H$_5$], 7.72 [2 H, m, *meta/para* C$_6$H$_5$], 4.82 [2 H, m, OCH], 4.62 [2 H, m, OCH], 2.72 [4 H, m, CH$_2$CF$_2$] and 1.69 [15 H, d, Cp*, J(PH) 2.8 Hz]. δ ^{19}F{^{1}H} NMR (CDCl$_3$) -81.34 [3 F, tt, CF$_3$, ^3J(FF) 2.3 Hz, ^4J(FF) 10.0 Hz], -113.85 [2 F, m, $^{\alpha}$CF$_2$], -122.36 [2 F, m, $^{\beta}$CF$_2$], -123.38 [2 F, m, $^{\delta}$CF$_2$], -124.14 [2 F, m, $^{\epsilon}$CF$_2$], -126.65 [2 F, m, $^{\gamma}$CF$_2$]. δ ^{31}P{^{1}H} NMR (CDCl$_3$) 105.48 [s]. FAB mass spectrum: m/z 1232 [(M)$^+$], 1197 [(M-Cl)$^+$]. Found: C, 31.15; H, 2.07; P, 2.69. Calc. for Cp*IrCl$_2$\{PhP(OC$_6$H$_4$C$_6$F$_{13}$)$_2$\}: C, 31.18; H, 2.29; P, 2.51%.

6.6.5.6   Preparation of Cp*IrCl$_2$\{P(OC$_2$H$_4$C$_6$F$_{13}$)$_3$\} (3.37)

Cp*IrCl$_2$\{P(OC$_2$H$_4$C$_6$F$_{13}$)$_3$\} was prepared as for (3.32) using [Cp*IrCl$_2$]$_2$ (0.056 g, 0.07 mmol) and P(OC$_2$H$_4$C$_6$F$_{13}$)$_3$ (0.190 g, 0.17 mmol) to yield the product as an orange solid. Yield 0.135 g, 63 %. δ ^{1}H NMR (CDCl$_3$) 4.44 [6 H, dt, $^{\alpha}$CH$_2$, ^3J(HH) 6.0 Hz, ^2J(PH) 7.6 Hz], 2.43 [6 H, tt, $^{\beta}$CH$_2$, ^3J(HH) 6.0 Hz, ^3J(FH) 18.4 Hz] and 1.63 [15 H, d, Cp*, J(PH) 3.5 Hz]. δ ^{19}F{^{1}H} NMR (CDCl$_3$) -81.45 [3 F, tt, CF$_3$, ^3J(FF) 2.3 Hz, ^4J(FF) 10.0 Hz], -113.86 [2 F, tm, $^{\alpha}$CF$_2$, ^4J(FF) 13.9 Hz], -122.45 [2 F, m, $^{\beta}$CF$_2$], -123.47 [2 F, m, $^{\delta}$CF$_2$], -124.16 [2 F, m, $^{\epsilon}$CF$_2$], -126.79 [2 F, m, $^{\gamma}$CF$_2$]. δ ^{31}P{^{1}H} NMR (CDCl$_3$) 83.36 [s]. FAB mass spectrum: m/z 1518 [(M)$^+$], 1483 [(M-Cl)$^+$]. Found: C, 27.14; H, 1.72; P, 2.59. Calc. for Cp*IrCl$_2$\{P(OC$_2$H$_4$C$_6$F$_{13}$)$_3$\}: C, 26.89; H, 1.79; P, 2.04 %.

6.6.6 Synthesis of Rhodium (I) complexes of the type [Rh(CO)ClL₂].

6.6.6.1 Preparation of trans-Rh(CO)Cl{Ph₂P(OC₆H₄C₆F₁₃)}₂ (3.38)

Trans-Rh(CO)Cl{Ph₂P(OC₆H₄C₆F₁₃)}₂ was prepared by the addition of a solution of Ph₂P(OC₆H₄C₆F₁₃) (0.314 g, 0.53 mmol) in dichloromethane (30 cm³) via cannular to a solution of [Rh(CO)₂Cl]₂ (0.050 g, 0.13 mmol) in dichloromethane (30 cm³). The solvent was removed under reduced pressure to yield product as a yellow solid, which was recrystallised from dichloromethane/hexane and dried in vacuo. Yield 0.274 g, 77%. δ ¹H NMR (CDCl₃) 7.92 [8 H, m, ortho C₆H₅], 7.78 [20 H, m, meta, para C₆H₅, ortho, meta OC₆H₄]. δ ¹⁹F{¹H} NMR (CDCl₃) -81.26 [3 F, tm, CF₃, ⁴J(FF) 10.0 Hz], -110.63 [2 F, tm, ᵅCF₂, ⁴J(FF) 14.4 Hz], -121.91 [2 F, m, ᵝCF₂], -122.25 [2 F, m, ᵟCF₂], -123.25 [2 F, m, ᵋCF₂], -126.59 [2 F, m, ᵞCF₂]. ³¹P{¹H} NMR (CDCl₃) 136.03 [d, ¹J(RhP) 141 Hz]. FAB mass spectrum: m/z 1295 [(M - Cl - CO)⁺]. Found: C, 43.27; H, 1.91; P, 4.88. Calc. for Rh(CO)Cl{Ph₂P(OC₆H₄C₆F₁₃)}: C, 43.31; H, 2.08; P, 4.56%. IR (dichloromethane) ν(C≡O) 1996 cm⁻¹.

6.6.6.2 Preparation of trans-Rh(CO)Cl{PhP(OC₆H₄C₆F₁₃)₂}₂ (3.39)

Trans-Rh(CO)Cl{PhP(OC₆H₄C₆F₁₃)₂}₂ was prepared similarly to (3.38) using [Rh(CO)₂Cl]₂ (0.042 g, 0.11 mmol) and PhP(OC₆H₄C₆F₁₃)₂ (0.405 g, 0.44 mmol) to yield product as a cream solid. Yield 0.230 g, 53%. δ ¹H NMR (CDCl₃) 7.60 [4 H, m, ortho C₆H₅], 7.32 [8 H, d, ortho OC₆H₄, ³J(HH) 8.8 Hz], 7.21 [6 H, m, meta/para C₆H₅], 7.11 [8 H, d, meta OC₆H₄, ³J(HH) 8.8 Hz]. δ ¹⁹F{¹H} NMR (CDCl₃) -81.25 [3 F, tt, CF₃, ³J(FF) 2.2 Hz, ⁴J(FF) 10.0 Hz], -110.76 [2 F, tm, ᵅCF₂, ⁴J(FF) 14.5 Hz], -121.91 [2 F, m, ᵝCF₂], -122.38 [2 F, m, ᵟCF₂], -123.29 [2 F, m, ᵋCF₂], -126.61 [2 F, m, ᵞCF₂]. ³¹P{¹H} NMR (CDCl₃) 149.33 [d, ¹J(RhP) 176 Hz]. FAB mass spectrum: m/z 1963 [(M - Cl - CO)⁺]. Found: C, 36.26; H, 1.24; P, 3.60. Calc. for Rh(CO)Cl{PhP(OC₆H₄C₆F₁₃)₂}: C, 36.14; H, 1.29; P, 3.06 %. IR (dichloromethane) ν(C≡O) 2013 cm⁻¹.

6.6.6.3 *Preparation of [Rh(μ-Cl){P(OC₆H₄-4-C₆F₁₃)₃}₂]₂ (3.40)*

$[Rh(\mu\text{-Cl})\{P(OC_6H_4\text{-}4\text{-}C_6F_{13})_3\}_2]_2$ was prepared by the addition of a solution of $P(OC_6H_4\text{-}4\text{-}C_6F_{13})_3$ (0.420 g, 0.77 mmol) in dry PP3 (40 cm^3) to a solution of $[Rh(CO)_2Cl]_2$ (0.031 g, 0.08 mmol) in dry dichloromethane (40 cm^3). The fluorous phase was transferred to a Schlenk flask and the solvent removed under reduced pressure to yield product as a yellow solid, which was recrystallised from ethanol and dried *in vacuo*. Yield 0.204 g, 48%. δ ^{1}H NMR (D$_2$O) 7.21 [6 H, d, *meta* OC₆H₄ ^3J(HH) 8.3 Hz] and 6.88 [6 H, d, *para* OC₆H₄ ^3J(HH) 8.3 Hz]. δ ^{19}F{^{1}H} NMR (D$_2$O) -82.08 [3 F, tm, CF$_3$ ^4J(FF) 10.0 Hz], -110.72 [2 F, tm, $^\alpha$CF$_2$, ^4J(FF) 14.2 Hz], -122.05 [2 F, m, $^\beta$CF$_2$], -122.66 [2 F, m, $^\delta$CF$_2$], -123.56 [2 F, m, $^\epsilon$CF$_2$], -127.12 [2 F, m, $^\gamma$CF$_2$]. δ ^{31}P{^{1}H} NMR (CDCl$_3$) 113.17 [d, ^1J(RhP) 313 Hz]. Found: C, 32.81; H, 0.88; Cl, 1.26. Calc. for $[RhCl\{P(OC_6H_4C_6F_{13})_3\}_2]_2$: C, 32.42; H, 0.91; Cl, 1.33%.

6.6.6.4 *Preparation of [Rh(μ-Cl){P(OC₆H₄-4-C₈F₁₇)₃}₂]₂ (3.41)*

$[Rh(\mu\text{-Cl})\{P(OC_6H_4\text{-}4\text{-}C_8F_{17})_3\}_2]_2$ was prepared similarly to (3.40) using $P(OC_6H_4\text{-}4\text{-}C_8F_{17})_3$ (0.428 g, 0.27 mmol) and $[Rh(CO)_2Cl]_2$ (0.027 g, 0.07 mmol) to yield product as a yellow solid. Yield 0.364 g, 81%. δ ^{1}H NMR (D$_2$O) 7.10 [6 H, d, *meta* OC₆H₄ ^3J(HH) 8.2 Hz] and 6.89 [6 H, d, *para* OC₆H₄ ^3J(HH) 8.2 Hz]. δ ^{19}F{^{1}H} NMR (D$_2$O) -82.19 [3 F, m, CF$_3$], -110.34 [2 F, m, $^\alpha$CF$_2$], -122.35 [2 F, m, $^\beta$CF$_2$], -122.78 [2 F, m, $^\delta$CF$_2$], -123.38 [2 F, m, $^\epsilon$CF$_2$], -127.16 [2 F, m, $^\gamma$CF$_2$]. δ ^{31}P{^{1}H} NMR (CDCl$_3$) 112.77 [d, ^1J(RhP) 314 Hz].

6.6.6.5 *Preparation of [Rh(μ-Cl){P(OC₆H₄-4-C₁₀F₂₁)₃}₂]₂ (3.42)*

$[Rh(\mu\text{-Cl})\{P(OC_6H_4\text{-}4\text{-}C_{10}F_{21})_3\}_2]_2$ was prepared similarly to (3.40) using $P(OC_6H_4\text{-}4\text{-}C_{10}F_{21})_3$ (0.416 g, 0.22 mmol) and $[Rh(CO)_2Cl]_2$ (0.021 g, 0.05 mmol) to yield product as a yellow solid. Yield 0.295 g, 70%. δ ^{1}H NMR (D$_2$O) 7.53 [6 H, d, *meta* OC₆H₄ ^3J(HH) 8.6 Hz] and 6.98 [6 H, d, *para* OC₆H₄ ^3J(HH) 8.2 Hz]. δ ^{19}F{^{1}H} NMR (D$_2$O) -82.35 [3 F, tm, CF$_3$ ^4J(FF) 9.9 Hz], -110.72 [2 F, tm, $^\alpha$CF$_2$, ^4J(FF) 14.0

Hz], -122.05 [2 F, m, $^\beta$CF$_2$], -122.66 [2 F, m, $^\delta$CF$_2$], -123.98 [2 F, m, $^\epsilon$CF$_2$], -127.12 [2 F, m, $^\gamma$CF$_2$]. δ ^{31}P{^{1}H} NMR (CDCl$_3$) 114.38 [d, ^1J(RhP) 313 Hz].

6.6.6.6 Preparation of [Rh(µ-Cl){P(OC$_6$H$_4$-3-C$_6$F$_{13}$)$_3$}$_2$]$_2$ (3.43)

[Rh(µ-Cl){P(OC$_6$H$_4$-3-C$_6$F$_{13}$)$_3$}$_2$]$_2$ was prepared similarly to (3.40) using P(OC$_6$H$_4$-3-C$_6$F$_{13}$)$_3$ (0.362 g, 0.29 mmol) and [Rh(CO)$_2$Cl]$_2$ (0.028 g, 0.07 mmol) to afford the product as a yellow oil. Yield 0.141 g, 39%. δ ^{1}H NMR (D$_2$O) 6.91 [4 H, m, ortho, meta, para OC$_6$H$_4$]. δ ^{31}P{^{1}H} NMR (CDCl$_3$) 113.63 [d, ^1J(RhP) 309 Hz]. Found: C, 32.45; H, 0.89; P, 2.64. Calc. for [RhCl{P(OC$_6$H$_4$-3-C$_6$F$_{13}$)$_3$}$_2$]$_2$: C, 32.42; H, 0.91; P, 2.32%.

6.6.6.7 Preparation of trans-Rh(CO)Cl{P(OC$_6$H$_4$-2-C$_6$F$_{13}$)$_3$}$_2$ (3.44)

Trans-Rh(CO)Cl{P(OC$_6$H$_4$-2-C$_6$F$_{13}$)$_3$}$_2$ was prepared similarly to (3.40) using P(OC$_6$H$_4$-2-C$_6$F$_{13}$)$_3$ (0.373 g, 0.30 mmol) and [Rh(CO)$_2$Cl]$_2$ (0.030 g, 0.08 mmol) to yield product as a yellow solid. Yield 0.215 g, 50%. δ ^{1}H NMR (C$_6$D$_6$) 7.55 [1 H, d, ortho OC$_6$H$_4$ ^3J(HH) 8.2 Hz], 7.22 [1 H, d, meta OC$_6$H$_4$ ^3J(HH) 7.6 Hz], 6.98 [1 H, t, meta OC$_6$H$_4$ ^3J(HH) 7.6 Hz], 6.84 [1 H, t, para OC$_6$H$_4$ ^3J(HH) 7.6 Hz]. δ ^{19}F{^{1}H} NMR (C$_6$D$_6$) -82.25 [3 F, tm, CF$_3$ ^4J(FF) 9.9 Hz], -108.64 [2 F, tm, $^\alpha$CF$_2$, ^4J(FF) 14.2 Hz], -121.449 [2 F, m, $^\beta$CF$_2$], -122.44 [2 F, m, $^\delta$CF$_2$], -123.65 [2 F, m, $^\epsilon$CF$_2$], -127.29 [2 F, m, $^\gamma$CF$_2$]. δ ^{31}P{^{1}H} NMR (C$_6$D$_6$) 115.22 [d, ^1J(RhP) 223 Hz]. Found: C, 31.98; H, 0.84; P, 3.0. Calc. for Rh(CO)Cl{P(OC$_6$H$_4$-2-C$_6$F$_{13}$)$_3$}$_2$: C, 32.53; H, 0.90; P, 2.3%. IR (PP3) v(C≡O) 2045 cm^{-1}.

6.6.6.8 Preparation of trans-Rh(CO)Cl{Ph$_2$P(OC$_2$H$_4$C$_6$F$_{13}$)}$_2$ (3.45)

Trans-Rh(CO)Cl{Ph$_2$P(OC$_2$H$_4$C$_6$F$_{13}$)}$_2$ was prepared similarly to (3.38) using [Rh(CO)$_2$Cl]$_2$ (0.074 g, 0.18 mmol) and Ph$_2$P(OC$_2$H$_4$C$_6$F$_{13}$) (0.420 g, 0.77 mmol) to yield a yellow solid which was recrystallised from ethanol and dried in vacuo. Yield 0.284 g, 49%. δ ^{1}H NMR (CDCl$_3$) 7.77 [4 H, m, ortho PPh], 7.43 [6 H, m, meta/para PPh], 4.47 [2 H, m, OCH$_2$], 2.58 [2 H, tm, CH$_2$CF$_2$ ^3J(FH) 18.6 Hz]. δ ^{19}F{^{1}H} NMR

(CDCl$_3$) -81.30 [3 F, tm, CF$_3$ ^4J(FF) 9.6 Hz], -113.58 [2 F, tm, $^\alpha$CF$_2$ ^4J(FF) 12.3 Hz], -122.30 [2 F, m, $^\beta$CF$_2$], -123.34 [2 F, m, $^\delta$CF$_2$], -124.04 [2 F, m, $^\epsilon$CF$_2$] and -126.59 [2 F, m, $^\gamma$CF$_2$]. δ ^{31}P{^{1}H} NMR (CDCl$_3$) 121.12 [d, ^1J(RhP) 136 Hz]. FAB mass spectrum: m/z 1234 ([M - CO]$^+$), 1227 ([M - Cl]$^+$). Found: C, 38.93; H, 1.77; Cl, 2.98. Calc. for Rh(CO)Cl{Ph$_2$P(OC$_2$H$_4$C$_6$F$_{13}$)}$_2$: C, 38.97; H, 2.22; Cl, 2.81%. IR (dichloromethane) v(C≡O) 1990 cm^{-1}.

6.6.6.9 Preparation of trans-Rh(CO)Cl{PhP(OC$_2$H$_4$C$_6$F$_{13}$)$_2$}$_2$ (3.46)

Trans-Rh(CO)Cl{PhP(OC$_2$H$_4$C$_6$F$_{13}$)$_2$}$_2$ was prepared as for (3.38) using [Rh(CO)$_2$Cl]$_2$ (0.027 g, 0.07 mmol) and PhP(OC$_6$H$_4$C$_6$F$_{13}$)$_2$ (0.258 g, 0.31 mmol) to afford the product as a yellow oil. δ ^{1}H NMR (d^8-toluene) 8.05 [2 H, m, ortho C$_6$H$_5$], 7.40-7.18 [3 H, m, meta/para C$_6$H$_5$], 4.54 [2 H, m, OCH], 4.18 [2 H, m, OCH], 2.30 [4 H, m, CH$_2$CF$_2$]. δ ^{19}F{^{1}H} NMR (d^8-toluene) -81.48 [3 F, tt, CF$_3$, ^3J(FF) 2.3 Hz, ^4J(FF) 10.0 Hz], -113.64 [2 F, m, $^\alpha$CF$_2$], -122.19 [2 F, m, $^\beta$CF$_2$], -123.23 [2 F, m, $^\delta$CF$_2$], -123.93 [2 F, m, $^\epsilon$CF$_2$], -126.60 [2 F, m, $^\gamma$CF$_2$]. ^{31}P{^{1}H} NMR (d^8-toluene) 153.71 [2 P, d, ^1J(RhP) 167 Hz]. FAB mass spectrum: m/z 1805 [(M - CO - H)$^+$]. IR (dichloromethane) v(C≡O) 2008 cm^{-1}.

6.6.6.10 Preparation of trans-Rh(CO)Cl{P(OC$_2$H$_4$C$_6$F$_{13}$)$_3$}$_2$ (3.47)

Trans-Rh(CO)Cl{P(OC$_2$H$_4$C$_6$F$_{13}$)$_3$}$_2$ was prepared as for (3.38) using [Rh(CO)$_2$Cl]$_2$ (0.048 g, 0.12 mmol) and P(OC$_2$H$_4$C$_6$F$_{13}$)$_3$ (0.549 g, 0.49 mmol) to yield product as a yellow oil. Yield 0.534 g, 90%. δ ^{1}H NMR (D$_2$O) 4.41 [6 H, m, OCH$_2$], 2.47 [6 H, m, CH$_2$CF$_2$]. ^{31}P{^{1}H} NMR (D$_2$O) 128.69 [d, ^1J(RhP) 199 Hz]. FAB mass spectrum: m/z 2378 [(M - CO)$^+$]. Found: C, 24.13; H, 1.08; P, 2.49. Calc. for Rh(CO)Cl{P(OC$_2$H$_4$C$_6$F$_{13}$)$_3$}$_2$: C, 24.45; H, 1.01; P, 2.57%. IR (PP3) v(C≡O) 2036 cm^{-1}.

6.6.7 Synthesis of Rhodium (I) complexes of the type [RhClL₃].

6.6.7.1 *Preparation of RhCl{Ph₂P(OC₆H₄-4-C₆F₁₃)}₃ (3.48)*

RhCl{Ph₂P(OC₆H₄-4-C₆F₁₃)}₃ was prepared by the addition of a solution of Ph₂P(OC₆H₄-4-C₆F₁₃) (0.321 g, 0.54 mmol) in dry dichloromethane (40 cm³) to a solution of [Rh(η^2-C₂H₄)₂Cl]₂ (0.035 g, 0.09 mmol) in dry dichloromethane (40 cm³). Yield 0.311 g, 54 %. δ ¹H NMR (CDCl₃) 7.6 - 7.0 [42 H, m, C₆H₅, OC₆H₄]. δ ¹⁹F{¹H} NMR (CDCl₃) -81.26 [9 F, tt, CF₃, ^3J(FF) 2.3 Hz, ^4J(FF) 10.0 Hz], -110.22 [4 F, tm, $^\alpha$CF₂, ^4J(FF) 14.6 Hz], -110.41 [2 F, tm, $^\alpha$CF₂, ^4J(FF) 14.4 Hz] -121.91 [6 F, m, $^\beta$CF₂], -122.40 [6 F, m, $^\delta$CF₂], -123.26 [6 F, m, $^\epsilon$CF₂], -126.57 [6 F, m, $^\gamma$CF₂]. δ ³¹P{¹H} NMR (CDCl₃) 142.68 [dt, P *trans* Cl ^1J(RhP) 216 Hz, ^2J(PP) 37 Hz] and 129.82 [dd, P *trans* P ^1J(RhP) 162 Hz, ^2J(PP) 37 Hz]. Electron impact (FAB) mass spectrum: *m/z* 1891 [(M - Cl)⁺]. Found: C, 44.39; H, 2.07. Calc. for RhCl{Ph₂P(OC₆H₄C₆F₁₃)}₃: C, 44.87; H, 2.20%.

6.6.7.2 *Preparation of RhCl{PhP(OC₆H₄-4-C₆F₁₃)₂}₃ (3.49)*

RhCl{PhP(OC₆H₄-4-C₆F₁₃)₂}₃ was prepared as for (3.48) using [Rh(η^2-C₂H₄)₂Cl]₂ (0.020 g, 0.05 mmol) and PhP(OC₆H₄-4-C₆F₁₃)₂ (0.314 g, 0.34 mmol) to afford product as a yellow solid. Yield 0.164 g, 54 %. δ ¹H NMR (CDCl₃) 7.40 - 7.05 [27 H, d, *ortho* C₆H₅], 6.94 [8 H, d, *meta* OC₆H₄ ^3J(HH) 8.6 Hz], and 6.71 [4 H, d, *meta* OC₆H₄ ^3J(HH) 8.6 Hz]. δ ¹⁹F{¹H} NMR (CDCl₃) -81.33 [3 F, tt, CF₃, ^3J(FF) 2.4 Hz, ^4J(FF) 10.0 Hz], -110.56 [2 F, tm, $^\alpha$CF₂, ^4J(FF) 14.1 Hz], -121.98 [2 F, m, $^\beta$CF₂], -122.28 [2 F, m, $^\delta$CF₂], -123.33 [2 F, m, $^\epsilon$CF₂], -126.66 [2 F, m, $^\gamma$CF₂]. δ ³¹P{¹H} NMR (CDCl₃) 151.78 [dt, P *trans* Cl ^1J(RhP) 245 Hz, ^2J(PP) 44 Hz] and 146.79 [dd, P *trans* P ^1J(RhP) 187 Hz, ^2J(PP) 44 Hz]. FAB mass spectrum: *m/z* 2929 [(M + H)⁺], 2893 [(M - Cl + H)⁺]. Found: C, 36.86; H, 1.29; Cl, 3.02. Calc. for RhCl{PhP(OC₆H₄C₆F₁₃)₂}₃: C, 36.90; H, 1.34; Cl, 1.21 %.

6.6.7.3   Preparation of RhCl{P(OC₆H₄-4-C₆F₁₃)₃}₃ (3.50)

$RhCl\{P(OC_6H_4\text{-}4\text{-}C_6F_{13})_3\}_3$ was prepared by the addition of a solution of $P(OC_6H_4\text{-}4\text{-}C_6F_{13})_3$ (0.406 g, 0.32 mmol) in dry PP3 (40 cm^3) to a solution of $[Rh(\eta^2\text{-}C_2H_4)_2Cl]_2$ (0.020 g, 0.05 mmol) in dry dichloromethane (40 cm^3). The fluorous phase was transferred to a   Schlenk flask and the solvent removed *in vacuo* to yield a yellow solid which was recrystallised from ethanol and dried *in vacuo*. Yield 0.287 g, 71%. δ ^{1}H NMR (CDCl₃) 7.68 [4 H, d, *ortho* OC₆H₄C₆F₁₃ ^3J(HH) 8.7 Hz], 7.61 [2 H, d, *ortho* OC₆H₄C₆F₁₃ ^3J(HH) 8.6 Hz], 7.42 [2 H, d, *meta* OC₆H₄C₆F₁₃ ^3J(HH) 8.6 Hz] and 7.37 [2 H, d, *meta* OC₆H₄C₆F₁₃ ^3J(HH) 8.7 Hz]. δ ^{19}F{^{1}H} NMR (CDCl₃) -82.13 [3 F, bt, CF₃, ^4J(FF) 10.0 Hz], -110.53 [2 F, tm, ^{α}CF₂, ^4J(FF) 14.0 Hz], -122.03 [2 F, m, ^{β}CF₂], -122.63 [2 F, m, ^{δ}CF₂], -123.59 [2 F, m, ^{ε}CF₂], -126.66 [2 F, m, ^{γ}CF₂]. δ ^{31}P{^{1}H} NMR (CDCl₃) 121.23 [dt, P *trans* Cl ^1J(RhP) 286 Hz, ^2J(PP) 53 Hz] and 113.56 [dd, P *trans* P ^1J(RhP) 225 Hz, ^2J(PP) 53 Hz]. FAB mass spectrum: *m/z* 3896 [(M – Cl + H)$^+$]. Found: C, 32.83; H, 0.83; Cl, 1.11. Calc. for RhCl{PhP(OC₆H₄C₆F₁₃)₂}₃: C, 32.97; H, 0.92; Cl, 0.90 %.

6.6.7.4   Preparation of RhCl{P(OC₆H₄-4-C₈F₁₇)₃}₃ (3.51)

$RhCl\{P(OC_6H_4\text{-}4\text{-}C_8F_{17})_3\}_3$ was prepared similarly to (3.50) using $[Rh(\eta^2\text{-}C_2H_4)_2Cl]_2$ (0.016 g, 0.04 mmol) and $P(OC_6H_4\text{-}4\text{-}C_8F_{17})_3$ (0.438 g, 0.28 mmol) to afford product as a yellow solid. Yield 0.126 g, 32%. δ ^{1}H NMR (CDCl₃) 7.60 [4 H, d, *ortho* OC₆H₄C₆F₁₃ ^3J(HH) 8.7 Hz], 7.51 [2 H, d, *ortho* OC₆H₄C₆F₁₃ ^3J(HH) 8.6 Hz], 7.32 [2 H, d, *meta* OC₆H₄C₆F₁₃ ^3J(HH) 8.6 Hz] and 7.29 [2 H, d, *meta* OC₆H₄C₆F₁₃ ^3J(HH) 8.7 Hz]. δ ^{19}F{^{1}H} NMR (CDCl₃) -82.13 [3 F, t, CF₃, ^4J(FF) 10.0 Hz], -110.53 [2 F, tm, ^{α}CF₂, ^4J(FF) 14.0 Hz], -122.03 [2 F, m, ^{β}CF₂], -122.63 [2 F, m, ^{δ}CF₂], -123.59 [2 F, m, ^{ε}CF₂], -126.66 [2 F, m, ^{γ}CF₂]. δ ^{31}P{^{1}H} NMR (CDCl₃) 120.26 [dt, P *trans* P ^1J(RhP) 283 Hz, ^2J(PP) 53 Hz] and 112.78 [dd, P *trans* P ^1J(RhP) 225 Hz, ^2J(PP) 53 Hz]. FAB mass spectrum: *m/z* 4795 [(M – Cl)$^+$].

6.6.7.5 *Preparation of RhCl{P(OC₆H₄-4-C₁₀F₂₁)₃}₃* (3.52)

RhCl{P(OC$_6$H$_4$-4-C$_{10}$F$_{21}$)$_3$}$_3$ was prepared similarly to (3.50) using [Rh(η^2-C$_2$H$_4$)$_2$Cl]$_2$ (0.500 g, 0.27 mmol) and P(OC$_6$H$_4$-4-C$_{10}$F$_{21}$)$_3$ (0.017 g, 0.04 mmol) to afford product as a yellow solid. Yield 0.374 g, 75%. δ ^{1}H NMR (CDCl$_3$) 7.60 [4 H, d, *ortho* OC$_6$H$_4$C$_6$F$_{13}$ ^3J(HH) 8.7 Hz], 7.51 [2 H, d, *ortho* OC$_6$H$_4$C$_6$F$_{13}$ ^3J(HH) 8.6 Hz], 7.32 [2 H, d, *meta* OC$_6$H$_4$C$_6$F$_{13}$ ^3J(HH) 8.6 Hz] and 7.29 [2 H, d, *meta* OC$_6$H$_4$C$_6$F$_{13}$ ^3J(HH) 8.7 Hz]. δ ^{19}F{^{1}H} NMR (CDCl$_3$) -82.13 [3 F, t, CF$_3$, ^4J(FF) 10.0 Hz], -110.53 [2 F, m, $^\alpha$CF$_2$], -122.03 [2 F, m, $^\beta$CF$_2$], -122.63 [2 F, m, $^\delta$CF$_2$], -123.59 [2 F, m, $^\epsilon$CF$_2$], -126.66 [2 F, m, $^\gamma$CF$_2$]. δ ^{31}P{^{1}H} NMR (CDCl$_3$) 123.13 [dt, P *trans* P ^1J(RhP) 287 Hz, ^2J(PP) 53 Hz] and 113.21 [dd, P *trans* P ^1J(RhP) 225 Hz, ^2J(PP) 53 Hz].

6.6.7.6 *Preparation of RhCl{P(OC₆H₄-3-C₆F₁₃)₃}₃* (3.53)

RhCl{P(OC$_6$H$_4$-3-C$_6$F$_{13}$)$_3$}$_3$ was prepared similarly to (3.50) using P(OC$_6$H$_4$-3-C$_6$F$_{13}$)$_3$ (0.406 g, 0.32 mmol) and [Rh(η^2-C$_2$H$_4$)$_2$Cl]$_2$ (0.020 g, 0.05 mmol) to yield product as a yellow solid. Yield 0.141 g, 39%. δ ^{1}H NMR (D$_2$O) 8.2 [4 H, m, *ortho, meta, para* OC$_6$H$_4$]. δ ^{31}P{^{1}H} NMR (CDCl$_3$) 119.00 [dt, P *trans* Cl ^1J(RhP) 276 Hz, ^2J(PP) 45 Hz] and 113.56 [dd, P *trans* P ^1J(RhP) 227 Hz, ^2J(PP) 45 Hz]. FAB mass spectrum: *m/z* 3896 [(M – Cl + H)$^+$].

6.6.7.7 *Preparation of [Rh(μ-Cl){P(OC₆H₄-2-C₆F₁₃)₃}₂]₂* (3.54)

[Rh(μ-Cl){P(OC$_6$H$_4$-2-C$_6$F$_{13}$)$_3$}$_2$]$_2$ was prepared similarly to (3.40) using P(OC$_6$H$_4$-2-C$_6$F$_{13}$)$_3$ (0.414 g, 0.33 mmol) and [Rh(η^2-C$_2$H$_4$)$_2$Cl]$_2$ (0.020 g, 0.05 mmol) to afford the product as a yellow solid. Yield 0.102 g, 38%. δ ^{1}H NMR (D$_2$O) 7.65 [4 H, m, *ortho, meta, para* OC$_6$H$_4$]. δ ^{19}F{^{1}H} NMR (D$_2$O) -82.22 [3 F, tm, CF$_3$ ^4J(FF) 8.5 Hz], -108.42 [2 F, m, $^\alpha$CF$_2$], -121.65 [2 F, m, $^\beta$CF$_2$], -122.60 [2 F, m, $^\delta$CF$_2$], -123.77 [2 F, m, $^\epsilon$CF$_2$] and -126.26 [2 F, m, $^\gamma$CF$_2$]. δ ^{31}P{^{1}H} NMR (D$_2$O) 108.16 [d, ^1J(RhP) 318 Hz]. Found: C, 32.22; H, 0.89; P, 3.20. Calc. for [RhCl{P(OC$_6$H$_4$-2-C$_6$F$_{13}$)$_3$}$_2$]$_2$: C, 32.42; H, 0.91; P, 2.32%.

6.6.7.8 Preparation of RhCl{Ph₂P(OC₂H₄C₆F₁₃)}₂ (3.55)

$RhCl\{Ph_2P(OC_2H_4C_6F_{13})\}_2$ was prepared similarly to (3.48) using $[Rh(\eta^2\text{-}C_2H_4)_2Cl]_2$ (0.057 g, 0.15 mmol) and $Ph_2P(OC_2H_4C_6F_{13})$ (0.510 g, 0.93 mmol) to afford product as a pale, orange solid. δ ^1H NMR (CDCl₃) 7.84 [2 H, m, *ortho* PPh], 7.71 [4 H, m, *ortho* PPh], 6.99 [6 H, m, *meta/para* PPh], 6.89 [3 H, m, *meta/para* PPh], 4.50 [2 H, m, OCH₂], 2.27 [2 H, tt, CH₂CF₂ ^3J(HH) 6.5 Hz, ^3J(FH) 19.0 Hz] and 1.53 [4 H, tt, $^\beta$CH₂ ^3J(HH) 6.5 Hz, ^3J(FH) 19.4 Hz]. δ $^{19}F\{^1H\}$ NMR (CDCl₃) -81.42 [9 F, m, CF₃], -113.54 [2 F, tm, $^\alpha$CF₂ ^4J(FF) 13.6 Hz], -113.76 [4 F, tm, $^\alpha$CF₂ ^4J(FF) 14.1 Hz], -122.15 [6 F, m, $^\beta$CF₂], -123.21 [6 F, m, $^\delta$CF₂], -123.96 [6 F, m, $^\epsilon$CF₂] and -126.54 [6 F, m, $^\gamma$CF₂]. δ $^{31}P\{^1H\}$ NMR (CDCl₃) 131.41 [dt, P *trans* Cl ^1J(RhP) 207 Hz, ^2J(PP) 41 Hz] and 124.57 [dd, P *trans* P ^1J(RhP) 160 Hz, ^2J(PP) 41 Hz].

6.6.7.9 Preparation of RhCl{PhP(OC₂H₄C₆F₁₃)}₂ (3.56)

$RhCl\{PhP(OC_2H_4C_6F_{13})\}_2$ was prepared similarly to (3.48) using $[Rh(\eta^2\text{-}C_2H_4)_2Cl]_2$ (0.005 g, 0.01 mmol) and $PhP(OC_2H_4C_6F_{13})_2$ (0.045 g, 0.05 mmol) to afford product as an orange solid. δ ^1H NMR (CDCl₃) 8.12-7.31 [5 H, m, *ortho, meta, para* PPh], 5.54 [2 H, m, OCH], 4.18 [2 H, m, OCH], 2.28 [4 H, m, CH₂CF₂]. δ $^{19}F\{^1H\}$ NMR (CDCl₃) -81.48 [3 F, m, CF₃], -113.77 [2 F, m, $^\alpha$CF₂], -122.19 [2 F, m, $^\beta$CF₂], -123.25 [2 F, m, $^\delta$CF₂], -123.97 [2 F, m, $^\epsilon$CF₂] and -126.62 [2 F, m, $^\gamma$CF₂]. δ $^{31}P\{^1H\}$ NMR (CDCl₃) 159.32 [1 P, dt, P *trans* Cl ^1J(RhP) 236 Hz, ^2J(PP) 41 Hz] and 156.69 [dd, P *trans* P ^1J(RhP) 182 Hz, ^2J(PP) 41 Hz].

6.6.7.10 Preparation of RhCl{P(OC₂H₄C₆F₁₃)₃}₃ (3.57)

$RhCl\{P(OC_2H_4C_6F_{13})_3\}_3$ was prepared similarly to (3.50) using $[Rh(\eta^2\text{-}C_2H_4)_2Cl]_2$ (0.018 g, 0.05 mmol) and $P(OC_2H_4C_6F_{13})_3$ (0.380 g, 0.34 mmol) to afford product as an air and moisture sensitive yellow oil. δ ^1H NMR (D₂O) 3.93 [6 H, m, OCH₂], and 1.98 [6 H, tm, CH₂CF₂, ^3J(HF) 18.1 Hz]. δ $^{31}P\{^1H\}$ NMR (D₂O) 140.28 [dt, P *trans* Cl ^1J(RhP) 268 Hz, ^2J(PP) 53 Hz] and 131.74 [dd, P *trans* P ^1J(RhP) 209 Hz, ^2J(PP)

53 Hz]. Found: C, 24.61; H, 1.07; P, 3.00. Calc. for RhCl{P(OC$_6$H$_4$C$_6$F$_{13}$)$_3$}$_3$: C, 24.71; H, 1.04; P, 2.66 %.

6.7 Catalytic Reactions

All hydroformylation experiments were performed in collaboration with St Andrews University using a purpose built metal hydroformylation rig, designed and constructed by St Andrews University staff. The phosphite ligand (2.4) was prepared as described in section 2.3.

6.7.1 Hydroformylation of 1-Hexene, 1-Nonene and 2-Nonene

A solution of [Rh(CO)$_2$(acac)] (0.013 g, 0.05 mmol) in dry, degassed toluene (2 cm^{-3}) was prepared in a 10 cm^3 steel autoclave under an atmosphere of argon. For reactions with PPh$_3$ and P(OPh)$_3$ the ligand was added along with PP3 (2 cm^3). In the case of reactions with ligand (2.4), a solution of P(OC$_6$H$_4$-4-C$_6$F$_{13}$)$_3$ (0.186 g, 0.15 mmol) in PP3 (2 cm^3), prepared in a glovebox under nitrogen, was transferred to the autoclave *via* a gas syringe. The stirred mixture was heated to 70 °C under 14 bar of CO/H$_2$ (1:1). The system was allowed to come to equilibrium, at which point alkene (1 cm^3) was injected and the pressure raised to 20 bar. The pressure was maintained at 20 bar throughout the reaction using a ballast tank connected to the apparatus. The reaction was allowed to proceed for 1 hr after which the autoclave was cooled and vented. The contents of the autoclave were transferred to a glass vial and samples of the organic and fluorous phases taken for GC analysis.

6.8 Synthesis of Bidentate Ligands and Complexes.

6.8.1   *Preparation of (C$_6$F$_{13}$-4-C$_6$H$_4$O)$_2$PCH$_2$CH$_2$P(OC$_6$H$_4$-4-C$_6$F$_{13}$)$_2$ (5.1)*

4-Perfluoro-*n*-hexylphenol (6.300 g, 15.3 mmol) in dry ether (50 cm^3) was added dropwise *via* cannular to a solution of Cl$_2$PC$_2$H$_4$PCl$_2$ (0.845 g, 3.6 mmol) and triethylamine (1.474 g, 14.6 mmol) in dry ether (50 cm^3) over a period of 1 hr. The

reaction mixture was stirred for a further 12 hrs, after which it was filtered through celite under nitrogen to remove the triethylammonium hydrochloride formed in the reaction. The solvent was removed *in vacuo* to yield impure product as a white solid which was recrystallized from dichloromethane. Yield 5.500 g, 87%. δ ^{1}H NMR (C_6D_6) 7.35 [8 H, d, *ortho* OC_6H_4, ^3J(HH) 8.8 Hz], 6.93 [8 H, d, *meta* OC_6H_4, ^3J(HH) 8.8 Hz], 2.11 [4 H, t, CH_2, ^2J(HP) 8.3 Hz]. δ ^{19}F$\{^1$H$\}$ NMR (C_6D_6) -81.79 [3 F, tm, CF_3 ^3J(FF) 10.1 Hz], -110.64 [2 F, tm, $^\alpha CF_2$, ^3J(FF) 14.8 Hz], -121.68 [2 F, m, $^\beta CF_2$], -122.40 [2 F, m, $^\delta CF_2$], -123.32 [2 F, m, $^\varepsilon CF_2$], -126.80 [2 F, m, $^\gamma CF_2$]. δ ^{31}P$\{^1$H$\}$ NMR (C_6D_6) 180.88 [s].

6.8.2   *Preparation of PtCl$_2${(C$_6$F$_{13}$-4-C$_6$H$_4$O)$_2$PCH$_2$CH$_2$P(OC$_6$H$_4$-4-C$_6$F$_{13}$)$_2$}* (**5.2**)

A slurry of $PtCl_2(MeCN)_2$ (0.090 g, 0.26 mmol) and (**5.1**) (0.500 g, 0.29 mmol) in dry dichloromethane was gently refluxed under nitrogen for 2 hrs. The reaction mixture was filtered and the solvent removed *in vacuo* to leave an off-white solid. Recrystallisation from dichloromethane and hexane afforded product as a fine white solid. Yield 0.183 g, 32 %. δ ^{1}H NMR $(CDCl_3)$ 7.51 [8 H, d, *ortho* OC_6H_4, ^3J(HH) 8.5 Hz], 7.33 [8 H, d, *meta* OC_6H_4, ^3J(HH) 8.5 Hz], 2.48 [4 H, t, CH_2, ^2J(HP) 8.1 Hz]. δ ^{19}F$\{^1$H$\}$ NMR $(CDCl_3)$ -81.24 [3 F, tt, CF_3, ^4J(FF) 2.3 Hz, ^3J(FF) 10.0 Hz], -110.99 [2 F, tm, $^\alpha CF_2$, ^3J(FF) 14.1 Hz], -121.99 [2 F, m, $^\beta CF_2$], -122.02 [2 F, m, $^\delta CF_2$], -123.30 [2 F, m, $^\varepsilon CF_2$], -126.58 [2 F, m, $^\gamma CF_2$]. δ ^{31}P$\{^1$H$\}$ NMR (D_2O) 135.15 [s, ^1J(PtP) 4673 Hz]. FAB mass spectrum: m/z 1965 [(M-Cl+H)$^+$], 1929 [(M-2Cl)$^+$].

6.8.3   *Preparation of Rh$_2$Cl$_2${(C$_6$F$_{13}$-4-C$_6$H$_4$O)$_2$PCH$_2$CH$_2$P(OC$_6$H$_4$-4-C$_6$F$_{13}$)$_2$}* (**5.3**)

A solution of (**5.1**) (0.500 g, 0.29 mmol) in dry dichloromethane was added to a solution of $[Rh(\eta^2-C_2H_4)_2Cl]_2$ (0.056 g, 0.14 mmol) in dry dichloromethane. The solution was cooled to afford product as a yellow precipitate which was filtered and dried *in vacuo*. Yield 0.539g, 73%. δ ^{19}F$\{^1$H$\}$ NMR (C_6D_6) -81.83 [3 F, tm, CF_3 ^3J(FF) 9.9 Hz], -110.63 [2 F, m, $^\alpha CF_2$], -121.98 [2 F, m, $^\beta CF_2$], -122.58 [2 F, m, $^\delta CF_2$], -123.36 [2 F, m, $^\varepsilon CF_2$], -126.85 [2 F, m, $^\gamma CF_2$]. δ ^{31}P$\{^1$H$\}$ NMR (C_6D_6) 190.64 [d, ^2J(RhP) 265 Hz].

6.8.4 Preparation of 1,2-(methylenedioxy)-4,5-diiodobenzene (5.5)

Red $Hg^{(II)}O$ (50.157 g, 232 mmol) and iodine (54.000 g, 213 mmol) were added to a solution of 1,2-methylenedioxy benzene (7.040 g, 58 mmol) in dichloromethane (250 cm^3) and stirred for 5 days at room temperature. The reaction mixture was then filtered and the mercury residue washed with dichloromethane (2 x 50 cm^3). The filtrate was transferred to a separating funnel and washed with 5 % sodium thiosulphate solution (200 cm^3) and water (200 cm^3). The organic phase was dried over $MgSO_4$, filtered and the solvent removed *in vacuo* to obtain crude product as a red liquid. The crude product was heated on Kugelröhr distillation apparatus at 60 °C (0.01 mmHg) to remove 1,2-(methylenedioxy)-4-iodobenzene. Recrystallisation of the resulting red solid from methanol afforded the product as a crystalline, cream coloured solid. Yield 4.785 g, 22 %. δ ^{1}H NMR (CDCl$_3$) 7.24 [2 H, s, Ar-H], 5.90 [2 H, s, CH$_2$]. Electron impact (EI) mass spectrum: *m/z* 374 ($[M]^+$), 247 ($[M - I]^+$), 120 ($[M - 2I]^+$) (Found: M^+, 373.83008. C$_7$H$_4$I$_2$O$_2$ requires M^+, 373.83004).

6.8.5 Preparation of 1,2-(methylenedioxy)-4,5-bisperfluoro-n-hexylbenzene (5.7)

A copper coupling reaction was set up following standard procedures using copper (15.292 g, 240 mmol), 2,2-bipyridine (0.658 g, 4.2 mmol), C$_6$F$_{13}$I (32.224 g, 72 mmol) and (5.5) (11.259, 30 mmol) in DMSO (25 cm^3) and C$_6$H$_5$F (150 cm^3). The reaction was stirred under nitrogen at 75 °C for 4 days. The reaction mixture was then hydrolysed with water (100 cm^3), filtered and the copper residue washed with CH$_2$Cl$_2$ (200 cm^3). The organic washings were combined, washed with water (2 x 100 cm^3), dried over $MgSO_4$ and subsequently filtered. The solution was then concentrated to *ca.* 50 cm^3 and extracted with PP3 (5 x 30 cm^3). The PP3 was removed *in vacuo* to afford crude product as a brown oil. The crude product was then Kugelröhr distilled at 100 °C (0.01 mmHg) affording product as a clear, colourless oil. Yield 9.626 g, 42 %. δ ^{1}H NMR (CDCl$_3$) 7.10 [2 H, s, Ar-H], 6.12 [2 H, s, CH$_2$]. δ ^{19}F{^{1}H} NMR (CDCl$_3$) -81.23 [3 F, bt, CF$_3$, ^{3}J(FF) 10.0 Hz], -102.67 [2 F, m, $^\alpha$CF$_2$], -118.48 [2 F, m, $^\beta$CF$_2$], -122.49 [2 F, m, $^\delta$CF$_2$], -123.24 [2 F, m, $^\epsilon$CF$_2$], -126.56 [2 F, m, $^\gamma$CF$_2$]. Electron impact

(EI) mass spectrum: m/z 758 ($[M]^+$), 489 ($[M - C_5F_{11}]^+$). Accurate mass spec. calc. for $C_{19}H_4F_{26}O_2$: 757.97967. Found 757.97961.

6.8.6 Preparation of 1,2-dihydroxy-4,5-bisperfluoro-n-hexyl benzene (5.8)

A solution of BI_3 (0.621 g, 1.58 mmol) in dry dichloromethane (50 cm^3) was added *via* cannular to a stirred solution of (**5.7**) (1.192 g, 1.46 mmol) in dry dichloromethane (50 cm^3) at 0°C. After complete addition the reaction mixture was allowed to warm to room temperature and stirred for 30 mins after which time the mixture was hydrolysed with water (30 cm^3). The organic layer was separated and the solvent removed *in vacuo* affording a brown oil which was subsequently dissolved in ethanol (50 cm^3) and refluxed for 1 hr. The resulting brown solution was concentrated to ~20 cm^3 and extracted with PP3 (3 x 15 cm^3). The extractions were combined and washed with 5% sodium thiosulphate solution (50 cm^3), dried over $MgSO_4$, filtered and the solvent removed *in vacuo* to afford product as a clear, colourless oil. Yield 1.061 g, 90%. δ ^{1}H NMR (CDCl$_3$) 7.17 [2 H, s, Ar-H], 6.17 [2 H, bs, OH]. δ ^{19}F{^{1}H} NMR (CDCl$_3$) - 81.26 [3 F, tt, CF$_3$, ^4J(FF) 2.35 Hz, ^3J(FF) 10.6 Hz], -103.13 [2 F, m, $^\alpha$CF$_2$], -118.7 [2 F, m, $^\beta$CF$_2$], -122.40 [2 F, m, $^\delta$CF$_2$], -123.19 [2 F, m, $^\epsilon$CF$_2$], -126.54 [2 F, m, $^\gamma$CF$_2$]. Electron impact (EI) mass spectrum: m/z 746 ($[M]^+$).

6.8.7 Attempted Preparation of Tris(4,5-bisperfluoro-n-hexylphenyl) bisphosphite (5.9)

A solution of 1,2-dihydroxy-4,5-bisperfluoro-*n*-hexyl benzene (2.009 g, 2.69 mmol) in dry ether (50 cm^3) was added dropwise *via* cannular to a solution of PCl$_3$ (0.215 g, 1.56 mmol) and triethylamine (0.546 g, 5.40 mmol) in dry ether (50 cm^3) over a period of 1 hr. The reaction mixture was stirred for a further 3 hrs, after which it was filtered through celite under nitrogen to remove the triethylammonium hydrochloride formed in the reaction. The solvent was removed *in vacuo* to yield impure product as an off-white solid. δ ^{1}H NMR (d^8 toluene) 7.7-6.7 [m, *ortho* OC$_6$H$_4$]. δ ^{19}F{^{1}H} NMR (d^8 toluene) -81.79 [3 F, tm, CF$_3$ ^3J(FF) 10.1 Hz], -110.64 [2 F, tm, $^\alpha$CF$_2$, ^3J(FF) 14.8 Hz], -121.68 [2 F, m, $^\beta$CF$_2$], -122.40 [2 F, m, $^\delta$CF$_2$], -123.32 [2 F, m, $^\epsilon$CF$_2$], -126.80 [2

F, m, $^YCF_2$]. δ $^{31}P\{^1H\}$ NMR (d^8 toluene) 151.31 [s]. Electron impact (EI) mass spectrum: m/z 810 ([PCl{O$_2$C$_6$H$_4$(C$_6$F$_{13}$)$_2$}]$^+$).

6.8.8 Preparation of 5,5'-dibromo-2,2'-acetoxybiphenyl (5.10)

Acetic anhydride (6.530 g, 64 mmol) was added to a stirred solution of 5,5'-dibromo-2,2'-biphenol (10.020 g, 29 mmol), Et$_3$N (17.618 g, 174 mmol) and DMAP (0.020 g, 0.16 mmol) in dichloromethane (100 cm^3) and refluxed for 1 hr. The reaction mixture was then transferred to a separating funnel and washed with HCl (1 M, 100 cm^3), 5 % sodium carbonate solution (100 cm^3) and dried over MgSO$_4$. After filtering the solvent was removed *in vacuo* to afford product as a white solid. Yield 12.195 g, 98%. δ ^{1}H NMR (CDCl$_3$) 7.46 [2 H, dd, H$_b$, H$_{b'}$, ^3J(H$_b$H$_a$) 8.5 Hz, ^4J(H$_b$H$_c$) 2.3 Hz], 7.37 [2 H, d, H$_c$, H$_{c'}$, ^4J(H$_c$H$_b$) 2.3 Hz], 6.99 [2 H, d, H$_a$, H$_{a'}$, ^3J(H$_a$H$_b$) 8.5 Hz], 2.00 [6 H, s, CH$_3$]. δ $^{13}C\{^1H\}$ NMR (CDCl$_3$) 167.79 [2 C, s], 145.99 [2 C, s], 132.68 [2 C, s], 131.32 [2 C, s], 130.01 [2 C, s], 123.39 [2 C, s], 117.91 [2 C, s], 19.64 [2 C, s]. Electron impact (EI) mass spectrum: m/z 426 ([M]$^+$), 346 ([M - Br]$^+$), 266 ([M - 2Br)$^+$].

6.8.9 Preparation of 5,5'-perfluoro-n-hexyl-2,2'-acetoxybiphenyl (5.11)

C$_6$F$_{13}$I (23.022 g, 51.6 mmol), 5,5'-dibromo-2,2'-acetoxybiphenyl (10.030 g, 23.5 mmol), copper (11.919 g, 188 mmol) and 2,2-bipyridine (0.513 g, 3.3 mmol) in hexafluorobenzene (100 cm^3) and dimethylsulphoxide (100 cm^3) were heated at 80°C and stirred under nitrogen for 4 days. After cooling to room temperature the reaction mixture was hydrolysed with water (100 cm^3), filtered and the copper residue washed with dichloromethane (2 x 100 cm^3). The filtrate was then washed with water (5 x 100 cm^3) and the organic layer separated, dried over MgSO$_4$, filtered and concentrated to *ca.* 100 cm^3 *in vacuo*. The product was extracted by shaking with perfluoro-1,3-dimethylcyclohexane (4 x 30 cm^3), the washings combined and the solvent removed *in vacuo* to leave an off-white solid. The product was purified by Kugelröhr distillation at 140 °C (0.01 mmHg) and then recrystallised from methanol to afford product as a white crystalline solid. Yield 16.974 g, 80%. δ ^{1}H NMR (CDCl$_3$) 7.61 [2

H, dd, H_b, $H_{b'}$, $^3J(H_bH_a)$ 8.5 Hz, $^4J(H_bH_c)$ 2.05 Hz], 7.49 [2 H, d, H_c, $H_{c'}$, $^4J(H_cH_b)$

2.05 Hz], 7.31 [2 H, d, H_a, $H_{a'}$, $^3J(H_aH_b)$ 8.5 Hz], 2.00 [6 H, s, CH_3]. δ $^{19}F\{^1H\}$ NMR

(CDCl$_3$) -81.28 [3 F, tm, CF_3, $^3J(FF)$ 10.0 Hz], -110.79 [2 F, tm, $^\alpha CF_2$, $^3J(FF)$ 13.8

Hz], -121.91 [2 F, m, $^\beta CF_2$], -122.04 [2 F, m, $^\delta CF_2$], -123.29 [2 F, m, $^\varepsilon CF_2$], -126.62 [2

F, m, $^\gamma CF_2$]. Electron impact (EI) mass spectrum: m/z 906 ($[M]^+$), 864 ($[M - C_2H_2O]^+$),

822 ($[M - C_4H_4O_2]^+$).

6.8.10   Preparation of 5,5'-perfluoro-n-hexyl-2,2'-biphenol (5.12)

NaH (0.531 g, 22.1 mmol) was added cautiously to a stirred solution of 5,5'-perfluoro-n-hexyl-2,2'-acetoxybiphenyl (5.000 g, 5.52 mmol) in methanol (100 cm^3). After 5 mins the reaction was quenched by the addition of HCl (2 M, 40 cm^3). The reaction mixture was concentrated to ca. 15 cm^3 and extracted with PP3 (3 x 15 cm^3). The extractions were combined, dried over MgSO$_4$, filtered and the solvent removed in $vacuo$ to yield product as a white solid which was recrystallised from hexane. Yield 4.036, 89%. δ ^1H NMR (d^4 MeOH) 7.35 [4 H, m, H_b, $H_{b'}$, H_c, $H_{c'}$], 6.97 [2 H, d, H_a, $H_{a'}$, $^3J(H_aH_b)$ 9.0 Hz], 4.80 [2 H, bs]. δ $^{19}F\{^1H\}$ NMR (d^4 MeOH) -82.96 [3 F, tm, CF$_3$, $^3J(FF)$ 10.1 Hz], -111.00 [2 F, tm, $^\alpha CF_2$, $^3J(FF)$ 14.4 Hz], -122.93 [2 F, m, $^\beta CF_2$], -123.56 [2 F, m, $^\delta CF_2$], -124.35 [2 F, m, $^\varepsilon CF_2$], -127.86 [2 F, m, $^\gamma CF_2$]. Electron impact (EI) mass spectrum: m/z 822 ($[M]^+$).

6.8.11   Attempted   Preparation   of   Tris(5,5'-perfluoro-n-hexyl-2,2'-biphenyl) bisphosphite (5.13)

5,5'-perfluoro-n-hexyl-2,2'-biphenyl (4.103 g, 5.0 mmol) in dry ether (50 cm^3) was added dropwise via cannular to a solution of PCl$_3$ (0.425 g, 3.1 mmol) and triethylamine (1.019 g, 10.1 mmol) in dry ether (50 cm^3) over a period of 1 hr. The reaction mixture was stirred for a further 2 hrs, after which it was filtered through celite under nitrogen to remove the triethylammonium hydrochloride formed in the reaction. The solvent was removed in $vacuo$ to yield impure product as a white solid. δ ^1H NMR (d^8 toluene) 7.8-7.0 [m]. δ $^{19}F\{^1H\}$ NMR (d^8 toluene) -81.85 [3 F, m,

CF$_3$], -110.66 [2 F, m, $^{\alpha}$CF$_2$], -121.96 [2 F, m, $^{\beta}$CF$_2$], -123.35 [4 F, m, $^{\delta}$CF$_2$, $^{\epsilon}$CF$_2$], -126.87 [2 F, m, $^{\gamma}$CF$_2$]. δ ^{31}P{^{1}H} NMR (d^8 toluene) 146.69 [bm].

6.8.12 Preparation of {5,5'-(C$_6$F$_{13}$)$_2$-2,2'-O$_2$C$_{12}$H$_6$}PCH$_2$CH$_2$P{2,2'-O$_2$C$_{12}$H$_6$-5,5'-(C$_6$F$_{13}$)$_2$} (5.14)

5,5'-perfluoro-n-hexyl-2,2'-biphenol (4.000 g, 4.87 mmol) in dry ether (50 cm^3) was added dropwise via cannular to a solution of Cl$_2$PC$_2$H$_4$PCl$_2$ (0.564 g, 2.43 mmol) and triethylamine (1.083 g, 10.7 mmol) in dry ether (50 cm^3) over a period of 1 hr. The reaction mixture was stirred for a further 12 hrs, after which it was filtered through celite. The solvent removed in $vacuo$ to yield impure product as a white solid which was recrystallised from dichloromethane. Yield 2.819 g, 67%. δ ^{1}H NMR (C$_6$D$_6$) 7.43 [2 H, d, H$_c$, H$_{c'}$, ^4J(H$_c$H$_b$) 2.0 Hz], 7.34 [2 H, dd, H$_b$, H$_{b'}$, ^3J(H$_b$H$_a$) 7.0 Hz, ^4J(H$_b$H$_c$) 2.0 Hz], 6.88 [2 H, d, H$_a$, H$_{a'}$, ^3J(H$_a$H$_b$) 7.0 Hz], 1.65 [2 H, t, CH$_2$ ^1J(PH) 6.8 Hz]. δ ^{19}F{^{1}H} NMR (C$_6$D$_6$) -81.69 [3 F, tm, CF$_3$, ^3J(FF) 10.0 Hz], -109.99 [2 F, tm, $^{\alpha}$CF$_2$, ^3J(FF) 14.0 Hz], -121.84 [2 F, m, $^{\beta}$CF$_2$], -122.20 [2 F, m, $^{\delta}$CF$_2$], -123.24 [2 F, m, $^{\epsilon}$CF$_2$], -126.68 [2 F, m, $^{\gamma}$CF$_2$]. δ ^{31}P{^{1}H} NMR (C$_6$D$_6$) 215.65 [s].

6.8.13 Preparation of [Rh(μ-Cl){5,5'-(C$_6$F$_{13}$)$_2$-2,2'-O$_2$C$_{12}$H$_6$}PCH$_2$CH$_2$P{2,2'-O$_2$C$_{12}$H$_6$-5,5'-(C$_6$F$_{13}$)$_2$}]$_2$ (5.15)

A solution of (5.11) (0.300 g, 0.17 mmol) in dry dichloromethane (30 cm^3) was added to a solution of [Rh(COD)Cl]$_2$ (0.042 g, 0.08 mmol) in dry dichloromethane and stirred for 1 hr. The solution was extracted with PP3 (3 x 20 cm^3) and the extractions combined and the solvent removed in $vacuo$ to yield product as a yellow solid. Yield 0.271 g, 64%. δ ^{19}F{^{1}H} NMR (C$_6$D$_6$) -81.77 [3 F, tm, CF$_3$, ^3J(FF) 10.0 Hz], -110.57 [2 F, tm, $^{\alpha}$CF$_2$], -121.87 [4 F, m, $^{\beta}$CF$_2$, $^{\delta}$CF$_2$], -123.30 [2 F, m, $^{\epsilon}$CF$_2$], -126.80 [2 F, m, $^{\gamma}$CF$_2$]. δ ^{31}P{^{1}H} NMR (C$_6$D$_6$) 212.40 [d, ^1J(RhP) 276 Hz].

References for Chapter Six

[1]   F. R. Hartley, S. G. Murray and C. A. McAuliffe, *Inorg. Chem.,* 1979, **18,** 1394.

[2]   R. J. Goodfellow and L. M. Venanzi, *J. Chem. Soc.,* 1965, 7533.

[3]   J. L. Herde, J. C. Lambert and C. V. Senoff, *Inorg. Synth.,* 1974, **15,** 18.

[4]   M. Sander, *Chem. Ber.,* 1960, **93,** 1220.

[5]   K. A. Petrov, *Zh. Obshch. Khim.,* 1962, **32,** 1954.

[6]   L. M. Venanzi, *Pure Appl. Chem.,* 1980, **52,** 1117.

Appendix

Table 7.1 Crystal data and structure refinement for cis-[PtCl$_2${Ph$_2$P(OC$_6$H$_4$-4-C$_6$F$_{13}$)}$_2$] (3.1).

Empirical formula	C$_{48}$H$_{28}$Cl$_2$F$_{26}$O$_2$P$_2$Pt
Formula weight	1578.00
Temperature	150 (2) K
Wavelength	0.71073 Å
Crystal system	Triclinic
Space group	P-1
Unit cell dimensions	a = 8.962 (2) Å alpha = 97.65 (3)°
	b = 10.943 (2) Å beta = 91.85 (3)°
	c = 29.025 (6) Å gamma = 104.19 (3)°
Volume, Z	2728.9 (9) Å^3, 2
Density (calculated)	1.920 Mg/m^3
Absorption coefficient	3.005 mm^{-1}
F(000)	1532
Crystal size	0.18 × 0.14 × 0.10 mm
θ range for data collection	1.94 to 24.99°
Limiting indices	-7 ≤ h ≤ 9, -12 ≤ k ≤ 6, -32 ≤ l ≤ 32
Reflections collected	9472
Independent reflections	7221 (R$_{int}$ = 0.0522)
Absorption correction	None
Max. and min. transmission	0.807 and 0.685
Refinement method	Full-matrix least-squares on F^2
Data / restraints / parameters	7221 / 0 / 766
Goodness-of-fit on F^2	1.002
Final R indices [I>2σ(I)]	R1 = 0.0443, wR2 = 0.1125
R indices (all data)	R1 = 0.0488, wR2 = 0.1141
Largest diff. peak and hole	1.527 and -1.046 eÅ^{-3}

Table 7.2   Crystal data and structure refinement for cis-[PtCl$_2${Ph$_2$P(OC$_2$H$_4$C$_6$F$_{13}$)}$_2$] (3.6).

Empirical formula	C$_{40}$H$_{28}$Cl$_2$F$_{26}$O$_2$P$_2$Pt	
Formula weight	1362.55	
Temperature	200 (2) K	
Wavelength	0.71073 Å	
Crystal system	Triclinic	
Space group	P-1	
Unit cell dimensions	a = 11.770 (3) Å	alpha = 98.848 (3)°
	b = 18.464 (2) Å	beta = 90.97 (3)°
	c = 22.659 (4) Å	gamma = 102.78 (3)°
Volume, Z	4738 (2) Å^3, 2	
Density (calculated)	1.910 Mg/m^3	
Absorption coefficient	3.280 mm^{-1}	
F(000)	2640	
Crystal size	0.64 × 0.53 × 0.09 mm	
θ range for data collection	2.56 to 27.00°	
Limiting indices	-1 ≤ h ≤ 14, -23 ≤ k ≤ 22, -28 ≤ 1 ≤ 28	
Reflections collected	19926	
Independent reflections	18381 (R$_{int}$ = 0.0220)	
Absorption correction	None	
Max. and min. transmission	0.807 and 0.685	
Refinement method	Full-matrix least-squares on F^2	
Data / restraints / parameters	18379 / 37 / 898	
Goodness-of-fit on F^2	1.011	
Final R indices [I>2σ(I)]	R1 = 0.0815, wR2 = 0.2027	
R indices (all data)	R1 = 0.1275, wR2 = 0.2367	
Largest diff. peak and hole	2.356 and -4.262 eÅ^{-3}	

Table 7.3 Crystal data and structure refinement for cis-[PtCl$_2$(PEt$_3$){P(OC$_6$H$_4$-4-C$_6$F$_{13}$)$_3$}] (3.11).

Empirical formula	C$_{42}$H$_{27}$Cl$_2$F$_{39}$O$_3$P$_2$Pt
Formula weight	1648.57
Temperature	293 (2) K
Wavelength	0.71073 Å
Crystal system	Monoclinic
Space group	P2 (1)/n
Unit cell dimensions	a = 10.474 (2) Å alpha = 90°
	b = 47.370 (10) Å beta = 101.48 (3)°
	c = 11.141 (2) Å gamma = 90°
Volume, Z	5417 (2) Å^3, 4
Density (calculated)	2.021 Mg/m^3
Absorption coefficient	2.923 mm^{-1}
F(000)	3184
Crystal size	0.10 × 0.08 × 0.08 mm
θ range for data collection	1.91 to 25.04°
Limiting indices	-11 ≤ h ≤ 11, -52 ≤ k ≤ 50, -13 ≤ l ≤ 12
Reflections collected	15315
Independent reflections	7095 (R$_{int}$ = 0.1174)
Refinement method	Full-matrix least-squares on F^2
Data / restraints / parameters	7095 / 0 / 722
Goodness-of-fit on F^2	1.056
Final R indices [I>2σ(I)]	R1 = 0.0975, wR2 = 0.3151
R indices (all data)	R1 = 0.1361, wR2 = 0.3243
Largest diff. peak and hole	1.946 and -3.074 eÅ^{-3}

Table 7.4   Crystal data and structure refinement for $[RhCl_2(\eta^5\text{-}C_5Me_5)\{PhP(OC_6H_4\text{-}4\text{-}C_6F_{13})_2\}]$ (3.25).

Empirical formula	$C_{40}H_{29}Cl_2F_{26}O_2PRh$
Formula weight	1297.48
Temperature	190 (2) K
Wavelength	0.71073 Å
Crystal system	Monoclinic
Space group	$P2_1/c$
Unit cell dimensions	a = 20.437 (5) Å alpha = 90°
	b = 15.669 (5) Å beta = 96.66 (2)°
	c = 15.875 (4) Å gamma = 90°
Volume, Z	5050 (2) $Å^3$, 4
Density (calculated)	1.707 Mg/m^3
Absorption coefficient	0.611 mm^{-1}
F(000)	2576
Crystal size	$0.63 \times 0.40 \times 0.13$ mm
θ range for data collection	2.58 to 26.00°
Limiting indices	$-25 \le h \le 25, -19 \le k \le 1, -1 \le l \le 18$
Reflections collected	9957
Independent reflections	8633 (R_{int} = 0.0619)
Absorption correction	Semi empirical based on psi scan data
Max. and min. transmission	0.743 and 0.637
Refinement method	Full-matrix least-squares on F^2
Data / restraints / parameters	8631 / 47 / 623
Goodness-of-fit on F^2	1.025
Final R indices [I>2σ(I)]	R1 = 0.1063, wR2 = 0.2469
R indices (all data)	R1 = 0.1668, wR2 = 0.2951
Largest diff. peak and hole	1.049 and -0.914 $eÅ^{-3}$

Table 7.5 Crystal data and structure refinement for [RhCl$_2$(η^5-C$_5$Me$_5$){P(OC$_6$H$_4$-4-C$_6$F$_{13}$)$_3$}] (3.26).

Empirical formula	C$_{46}$H$_{28}$Cl$_2$F$_{39}$O$_3$PRh
Formula weight	1631.53
Temperature	293 (2) K
Wavelength	0.71073 Å
Crystal system	Monoclinic
Space group	C2/c
Unit cell dimensions	a = 38.221 (4) Å alpha = 90°
	b = 15.676 (2) Å beta = 119.640 (8)°
	c = 22.579 (2) Å gamma = 90°
Volume, Z	11758 (3) Å^3, 8
Density (calculated)	1.843 Mg/m^3
Absorption coefficient	0.577 mm^{-1}
F(000)	6432
Crystal size	0.48 × 0.38 × 0.38 mm
θ range for data collection	2.60 to 25.00°
Limiting indices	-1 ≤ h ≤ 45, -1 ≤ k ≤ 18, -26 ≤ 1 ≤ 23
Reflections collected	10247
Independent reflections	9429 (R$_{int}$ = 0.0336)
Absorption correction	Analytical
Max. and min. transmission	0.831 and 0.807
Refinement method	Full-matrix least-squares on F^2
Data / restraints / parameters	9427 / 0 / 829
Goodness-of-fit on F^2	1.038
Final R indices [I>2σ(I)]	R1 = 0.0993, wR2 = 0.2716
R indices (all data)	R1 = 0.1598, wR2 = 0.3583
Largest diff. peak and hole	1.947 and −1.653 eÅ^{-3}

Table 7.6   Crystal data and structure refinement for [IrCl$_2$(η^5-C$_5$Me$_5$){PhP(OC$_6$H$_4$-4-C$_6$F$_{13}$)$_2$}] (3.33).

Empirical formula	C$_{40}$H$_{28}$Cl$_2$F$_{26}$IrO$_2$P
Formula weight	1328.69
Temperature	180 (2) K
Wavelength	0.71073 Å
Crystal system	Orthorhombic
Space group	P2$_1$2$_1$2$_1$
Unit cell dimensions	a = 10.530 (4) Å alpha = 90°
	b = 13.061 (2) Å beta = 90°
	c = 33.821 (6) Å gamma = 90°
Volume, Z	4651 (2) Å^3, 4
Density (calculated)	1.897 Mg/m^3
Absorption coefficient	3.160 mm^{-1}
F(000)	2576
Crystal size	0.62 × 0.46 × 0.08 mm
θ range for data collection	2.65 to 27.00°
Limiting indices	-1 ≤ h ≤ 13, -1 ≤ k ≤ 16, -1 ≤ l ≤ 43
Reflections collected	6179
Independent reflections	5997 (R$_{int}$ = 0.0414)
Absorption correction	Semi-empirical based on psi scan data
Max. and min. transmission	0.831 and 0.807
Refinement method	Full-matrix least-squares on F^2
Data / restraints / parameters	5997 / 0 / 649
Goodness-of-fit on F^2	1.060
Final R indices [I>2σ(I)]	R1 = 0.0409, wR2 = 0.0956
R indices (all data)	R1 = 0.0526, wR2 = 0.1023
Largest diff. peak and hole	1.395 and −1.502 eÅ^{-3}

Table 7.7   Crystal data and structure refinement for $[IrCl_2(\eta^5-C_5Me_5)\{Ph_2P(OC_2H_4C_6F_{13})\}]$ (3.35).

Empirical formula	$C_{30}H_{29}Cl_2F_{13}IrOP$
Formula weight	946.60
Temperature	200 (2) K
Wavelength	0.71073 Å
Crystal system	Monoclinic
Space group	$P2_1/c$
Unit cell dimensions	$a = 22.828$ (3) Å alpha = 90°
	$b = 9.997$ (2) Å beta = 97.49 (2)°
	$c = 14.961$ (4) Å gamma = 90°
Volume, Z	3385.2 (11) $Å^3$, 4
Density (calculated)	1.857 Mg/m^3
Absorption coefficient	4.246 mm^{-1}
F(000)	1840
Crystal size	$0.36 \times 0.29 \times 0.16$ mm
θ range for data collection	2.23 to 27.00°
Limiting indices	$-29 \leq h \leq 28, -12 \leq k \leq 1, 0 \leq l \leq 19$
Reflections collected	7179
Independent reflections	6280 ($R_{int} = 0.0438$)
Absorption correction	Analytical
Max. and min. transmission	0.777 and 0.353
Refinement method	Full-matrix least-squares on F^2
Data / restraints / parameters	6279 / 86 / 183
Goodness-of-fit on F^2	1.021
Final R indices [I>2σ(I)]	R1 = 0.1029, wR2 = 0.2646
R indices (all data)	R1 = 0.1606, wR2 = 0.3239
Largest diff. peak and hole	2.518 and -1.675 $eÅ^{-3}$